Lower Hunter Particle Characterisation Study

Mark F. Hibberd (CSIRO), Melita D. Keywood (CSIRO), Paul W. Selleck (CSIRO), David D. Cohen (ANSTO), Ed Stelcer (ANSTO), Yvonne Scorgie (OEH) and Lisa Chang (OEH)

Final report to the NSW Environment Protection Authority

April 2016

The NSW Environment Protection Authority (NSW EPA) commissioned this report from the Office of Environment and Heritage (OEH), CSIRO and the Australian Nuclear Science and Technology Organisation (ANSTO).

This report was prepared by OEH, CSIRO and ANSTO in good faith exercising all due care and attention, but no representation or warranty, express or implied, is made as to the relevance, accuracy, completeness or fitness for purpose of this document in respect of any particular user's circumstances. Users of this document should satisfy themselves concerning its application to, and where necessary seek expert advice in respect of, their situation. The views expressed within are not necessarily the views of the NSW EPA and may not represent NSW EPA policy.

Citation:
Hibberd MF, Keywood MD, Selleck PW, Cohen DD, Stelcer E, Scorgie Y & Chang L 2016, *Lower Hunter Particle Characterisation Study, Final Report*, Report prepared by CSIRO, ANSTO and the NSW Office of Environment and Heritage on behalf of the NSW Environment Protection Authority, April 2016.

Cover photograph: courtesy of the Hunter Development Corporation

© 2016 CSIRO, ANSTO and State of NSW and OEH

With the exception of photographs, the State of NSW, OEH, CSIRO and ANSTO are pleased to allow this material to be reproduced in whole or in part for educational and non-commercial use, provided the meaning is unchanged and its source, publisher and authorship are acknowledged. Specific permission is required for the reproduction of photographs.

CSIRO advises that the information contained in this publication comprises general statements based on scientific research. The reader is advised and needs to be aware that such information may be incomplete or unable to be used in any specific situation. No reliance or actions must therefore be made on that information without seeking prior expert professional, scientific and technical advice. To the extent permitted by law, CSIRO (including its employees and consultants) excludes all liability to any person for any consequences, including but not limited to all losses, damages, costs, expenses and any other compensation, arising directly or indirectly from using this publication (in part or in whole) and any information or material contained in it.

OEH has compiled this technical report in good faith, exercising all due care and attention. No representation is made about the accuracy, completeness or suitability of the information in this publication for any particular purpose. OEH shall not be liable for any damage which may occur to any person or organisation taking action or not on the basis of this publication. Readers should seek appropriate advice when applying the information to their specific needs.

Published by:
Office of Environment and Heritage NSW on behalf of OEH, CSIRO and ANSTO
59 Goulburn Street, Sydney NSW 2000
PO Box A290, Sydney South NSW 1232; Phone: (02) 9995 5000 (switchboard)
Phone: 131 555 (environment information and publications requests)
Phone: 1300 361 967 (national parks, climate change and energy efficiency information, and publications requests); Fax: (02) 9995 5999; TTY: (02) 9211 4723
Email: info@environment.nsw.gov.au; Website: www.environment.nsw.gov.au

ISBN: 978 1 76039 341 0
OEH 2016/0243
April 2016

Contents

Glossary ..... **vi**

Acknowledgments ..... **xii**

Summary ..... **xiii**

Key results at a glance xiii

Why study particles in the air in the lower Hunter region? xiv

What were the aims of the study? xv

Who was involved in the study? xv

How was the study conducted? xv

What did the study find? xvi

Detailed results xviii

Contributing to the evidence base and further work xxiv

1 Introduction **1**

1.1 Study objectives 1

1.2 Regional context 1

1.3 Study overview 6

2 Data collection **9**

2.1 Measurement sites 9

2.2 Sampling program 14

2.3 Ambient particulate matter (PM) during sampling period 17

2.4 Sample collection rates 22

2.5 Wind roses 23

2.6 Pollution roses 27

2.7 Rainfall 27

2.8 Events log 31

2.9 Summary 31

3 Methodology **32**

3.1 Filter analysis 32

3.2 Receptor modelling (PMF) 37

3.3 Wind sector analysis (CPF technique) 38

3.4 Trajectory modelling 39

3.5 Chemical transport modelling 39

4 Particle composition **41**

4.1 Particle concentrations 41

4.2 Particle composition 44

4.3 Main components of $PM_{2.5}$ 49
4.4 Main components of $PM_{2.5-10}$ 51
5 Data analysis by PMF (positive matrix factorisation) 52
5.1 Selection of species 52
5.2 PMF configuration 55
5.3 PMF mass closure 56
5.4 Species correlations 58
6 Receptor modelling results – $PM_{2.5}$ factors 65
6.1 $PM_{2.5}$ Factor 1 – Fresh sea salt 66
6.2 $PM_{2.5}$ Factor 2 – Pollutant-aged sea salt 69
6.3 $PM_{2.5}$ Factor 3 – Secondary ammonium sulfate 72
6.4 $PM_{2.5}$ Factor 4 – Wood smoke 76
6.5 $PM_{2.5}$ Factor 5 – Soil 81
6.6 $PM_{2.5}$ Factor 6 – Vehicles 84
6.7 $PM_{2.5}$ Factor 7 – Primary or secondary nitrate 88
6.8 $PM_{2.5}$ Factor 8 – Mixed shipping/industry 92
6.9 $PM_{2.5}$ Factor 9 – Mixed industry/vehicle 96
7 Summary of fine particle results ($PM_{2.5}$) 99
7.1 Seasonal variability 102
8 Receptor modelling results – $PM_{2.5-10}$ factors 106
8.1 $PM_{2.5-10}$ Factor 1 – Fresh sea salt 106
8.2 $PM_{2.5-10}$ Factor 2 – Light-absorbing carbon (LAC) 108
8.3 $PM_{2.5-10}$ Factor 3 – Pollutant-aged sea salt 110
8.4 $PM_{2.5-10}$ Factor 4 – Soil 112
8.5 $PM_{2.5-10}$ Factor 5 – Industry 114
8.6 $PM_{2.5-10}$ Factor 6 – Bioaerosol 116
9 Summary of coarse particle results ($PM_{2.5-10}$) 118
9.1 Seasonal variability 120
10 Modelling results 122
10.1 Fresh sea salt case study 122
10.2 Wood smoke (residential wood heating) and ammonium nitrate 125
10.3 Wood smoke (vegetation fires) 129
10.4 Shipping influence at Beresfield 131
11 Discussion 135
11.1 General 135
11.2 Secondary particles 138

11.3 Contribution of human activities to PM levels 140
11.4 Coal particle contributions in $PM_{2.5-10}$ 141
11.5 Ammonium nitrate at Stockton 142
11.6 Comparison with earlier PMF results 145
11.7 Summary of results from supplementary modelling study 150
12 Conclusions 151
References 157

Glossary

Definitions of acronyms and various technical terms used in this report are given here to assist the reader. If required, the reader should look to other sources for more formal and technical definitions.

Term	Meaning
ABL	Atmospheric boundary layer. The atmospheric boundary layer is the lowest 100 to 3000m of the atmosphere modified by the Earth's surface, e.g. by heating, cooling, roughness, etc. Its extent is deeper in the daytime and shallower in the night-time. It is often turbulent and capped by a temperature inversion (see definition below).
Aerosol	A suspension of fine solid, liquid or mixed-phase particles in air
Aethalometer	An instrument measuring light adsorption that uses light wavelength to detect black carbon
Al	Aluminium
Anion	A negatively charged atom or molecule
ANSTO	Australian Nuclear Science and Technology Organisation
AQM	Air quality monitoring
AQMN	Air quality monitoring network
AQMS	Air quality monitoring station
Arabitol	Naturally occurring sugar alcohols, a biomarker for fungal spores (see also mannitol)
AS/NZS	Australian Standard / New Zealand Standard
ASP	ANSTO's Aerosol Sampling Program which collects particles on sample filters over 24 hours for subsequent analysis using a range of nuclear methods
BAM	Beta attenuation monitor – a method of measuring ambient particle concentrations based on absorption of beta radiation by solid particles. In NSW, OEH currently uses BAMs to measure $PM_{2.5}$. www.environment.nsw.gov.au/AQMS/sampling.htm
BC	Black carbon (BC) is formally defined as a term to describe a light-absorbing substance composed of carbon, i.e. it is defined with reference to an optical measurement method. The term BC is also widely used to describe particulate matter emitted mainly during the combustion of fossil fuels (e.g. motor vehicles, power stations, industrial boilers, non-road diesel equipment and transport including diesel-electric locomotives) and biomass burning (e.g. bushfires and domestic wood-burning heaters). These definitions are not necessarily equivalent, one describing a measurement method, the other a type of particle. Note that the fine particles from combustion are often described

Term	Meaning
	as soot (see the description in Section 3.1.4), but this is not necessarily the same as what is measured as black carbon. Coal particles from non-combustion sources, which are typically larger than 2.5 micrometres (µm) in diameter, may contribute to light-absorbing carbon in the coarse $PM_{2.5-10}$ fraction, but are not described as black carbon.
Boundary layer	See definition of ABL (Atmospheric Boundary Layer) above
Br	Bromine
$C_2O_4^{2-}$	Oxalate
Ca, Ca^{2+}	Calcium, calcium cation
Cation	A positively charge atom or molecule
Cl^-	Chloride
Co	Cobalt
CO	Carbon monoxide
CPF	Conditional probability function. In this study, it refers to a type of pollution rose that only considers factor contributions that exceed a given condition (e.g. it only includes the top 25% of values). A CPF plot shows the likelihood of a measured factor contribution arriving at the sample site from a particular direction.
Cr	Chromium
CSIRO	Commonwealth Scientific and Industrial Research Organisation
Cu	Copper
Dispersion	Dispersion refers to the movement of pollutants horizontally and/or vertically by the wind and their dilution by mixing due to atmospheric turbulence
EBC	Equivalent black carbon; see also Section 3.1.5
EC	Elemental carbon (EC) is principally emitted during the combustion of fossil fuels as small, sooty particles often with other chemicals attached to their surface
EDT	Eastern daylight time (daylight saving time)
EPA	NSW Environment Protection Authority
EST	Eastern Standard Time
F, F^-	Flourine, fluorine anion
Fe	Iron
GENT	A type of air sampler developed at the University of Gent. It is a stacked filter unit, i.e. it contains more than one filter with the unit designed so that each filter collects particles in a different size fraction. In this study, the filters collect the $PM_{2.5-10}$ and $PM_{2.5}$ size fractions.

Term	Meaning
GMA	The Greater Metropolitan Area including Newcastle, Sydney and Wollongong, defined by local government area.
GMR	The Greater Metropolitan Region including Newcastle, Sydney and Wollongong, but defined by a geometric grid, to aid air modelling.
HYSPLIT - NOAA	HYSPLIT is a computer model that calculates air parcel trajectories as well as complex dispersion and deposition simulations. It is publically provided by the National Oceanic and Atmospheric Administration, US Department of Commerce.
IBA	Ion beam analysis. A range of nuclear techniques using high energy ion beams to determine the elemental composition of samples.
IC	Ion chromatography. A chromatography technique used for water chemistry analysis and able to measure concentrations of major ions and cations down to very low concentrations. It separates charged particles (ions) and polar molecules based on their affinity to an ion exchanger.
Inversion	An atmospheric layer in which (potential) temperature increases with altitude (e.g. the layer above the atmospheric boundary layer). These layers are stable and resistant to vertical mixing and hence may restrict the dispersion of pollutants. Properly described as a temperature inversion.
Ion	An atom or molecule that is electrically charged, usually as a result of normal chemical processes. The charge may be negative or positive.
K, K+	Potassium, potassium cation
L, L^{-1}	Litres, per litre
Levo	Levoglucosan
Levoglucosan	An organic compound used as a chemical tracer for biomass burning. It is formed by the pyrolysis of carbohydrates such as cellulose and starch. The levoglucosan/mannosan ratio depends on the types of biomass burnt.
LHAQMN	Lower Hunter Air Quality Monitoring Network
LHPCS	Lower Hunter Particle Characterisation Study
LIPM	Laser integrated plate method. The light adsorption of the sample provides an indication of some chemical components, particularly light-absorbing black carbon.
Mannitol	Naturally occurring sugar alcohols, a biomarker for fungal spores (see also arabitol)
Mannosan	An organic compound used a chemical tracer for biomass burning. It is formed by the pyrolysis of carbohydrates such as cellulose and starch. The levoglucosan/mannosan ratio depends on the types of biomass burnt.
MDL	Method detection limit – the lowest mass of a particular element that can be detected with a given method
Mg, Mg^{2+}	Magnesium, magnesium cation

Term	Meaning
Micron	Micrometre, see µm
Mn	Manganese
MSA	Methane sulfonic acid
MSA^-	Methanosulfonate
MSLP	Mean sea level pressure
Na, Na^+	Sodium, sodium cation
NCCCE	Newcastle Community Consultative Committee on the Environment
Neutral	A term describing a type of atmospheric boundary layer (ABL) that forms when winds are strong and/or when there is negligible heating/cooling of the ground (e.g. overcast conditions). The turbulence responsible for mixing (dispersion) under these conditions is generated by wind.
ng	Nanogram (1 ng = 0.000 000 001 gram = 10^{-9} gram). One billionth of a gram. One thousandth of a microgram (µg)
NH_3, NH_4^+	Ammonia, ammonium
Ni	Nickel
NLAQMN	Newcastle Local Air Quality Monitoring Network
NO	Nitric oxide
NO_2	Nitrogen dioxide
NO_3^-	Nitrate
NO_x	Oxides of nitrogen (commonly $NO_x = NO + NO_2$)
nss SO_4^{2-}	Non-sea-salt sulfate. In the atmosphere, sea salt can be a significant source of sulfate. Non-sea-salt sulfate represents the sulfate produced by other sources.
O_3	Ozone – good in the upper atmosphere (stratospheric ozone) but harmful to people and vegetation at ground level
OC	Organic carbon. Organic carbon (OC) includes compounds that contain carbon, excluding particles that are elemental carbon. Sources of organic carbon include traffic, industrial, residential and non-road diesel equipment combustion.
OEH	NSW Office of Environment and Heritage
P	Phosphorous
Pb	Lead
PESA	Proton elastic scattering analysis. An ion beam analysis method that can identify elemental hydrogen at concentrations down to 20 ng m^{-3}
PIGA	Proton induced gamma-ray emission. An ion beam analysis method that quantifies light elements such as fluorine and sodium in concentrations above 100 ng m^{-3}

Term	Meaning
PIXE	Proton induced X-ray emission. An ion beam analysis method that can determine mass of elements with atomic weights from aluminium to lead in concentrations from as low as a few ng m^{-3}
PM_{10}	All particles 10 micrometres or less in equivalent aerodynamic diameter
$PM_{2.5}$	All particles 2.5 micrometres or less in equivalent aerodynamic diameter
$PM_{2.5-10}$	Particles sized between 2.5 and 10 micrometres in equivalent aerodynamic diameter
PMF	Positive matrix factorisation – a technique that considers a range of chemical analysis in a matrix to identify and quantify recurring 'factors' which are combinations of elements and compounds that commonly occur together
Pollution rose	A diagram like a wind rose but showing pollution concentration instead of wind speed, and its variation with wind direction. See Wind Rose
S	Sulfur
Sea salt	Sea salt is the salt produced from the evaporation of sea water. It contains mainly sodium chloride (colloquially referred to as sea salt) but also other salts such as magnesium and calcium chloride and sulfates. The main ionic constituents are listed in Table 7.
S/N	Signal-to-noise ratio. It compares the level of a signal to the level of background noise. In this study, the signal is typically the concentration being measured and noise arises from uncertainties in the sampling, measurement or analysis technique. A ratio greater than 1:1 indicates more signal than noise.
SFU	Stacked filter unit. A unit that simultaneously collects specific sized particles on different filters. See GENT
Si	Silicon
SO_2^-	Sulfur dioxide
SO_4^{2-}	Sulfate
Stable	A term describing a type of atmospheric boundary layer (ABL) that develops during the night when the ground is substantially cooler than the air above it, thus forming a stable temperature gradient with height in the air; this inhibits vertical motion of the air and results in little ambient turbulence and so little dispersion.
TEOM	Tapered element oscillating microbalance. An instrument for continuous measurement of particulate concentration in the atmosphere. Particles are collected on a filter held on the end of a tapered tube. Filter mass change is detected as a frequency change in the oscillation of the tapered tube. In NSW, OEH currently uses TEOMs to measure PM_{10}. www.environment.nsw.gov.au/AQMS/sampling.htm
Ti	Titanium

Term	Meaning
TSP	Total suspended particulates – all particles smaller than about 50µm in diameter suspended in the atmosphere
Unstable	A term describing a type of atmospheric boundary layer (ABL) characterised by vigorous turbulence, generated by solar heating of the ground which is very effective at mixing pollutants, particularly in the vertical.
UHFPCS	Upper Hunter Fine Particle Characterisation Study
UTC	Coordinated universal time
V	Vanadium
WHO	World Health Organization
Wind rose	A diagram that shows the distribution of wind direction experienced at a particular site. It is often used to show the prevailing wind direction(s). It commonly consists of a circle with lines (or sectors) radiating for the centre speed; the total length of each line is proportional to the frequency of wind, and the range of wind speeds from each direction is also usually shown.
WRF	Weather Research and Forecasting Model. An open-access computer model used to forecast weather and for other atmospheric research; pronounced ‘wharf’. www.wrf-model.org/
WRF-ARF	Advanced Research WRF. A version of WRF supported by the NCAR (US National Center for Atmospheric Research) Mesoscale and Microscale Meteorology Division
Zn	Zinc
µm	Micrometer (1 µm = 0.000001 metre = 10^{-6} metre). One millionth of a metre. Also called a micron
µg	Microgram (1 µg = 0.000001 gram = 10^{-6} gram). One millionth of a gram
µg m^{-3}	Microgram per cubic metre. A unit for the concentration of a gas or particulate matter in the atmosphere based in the density approach, i.e. mass per unit volume of air

Acknowledgments

This project was funded by

- NSW Environment Protection Authority (EPA)
- NSW Office of Environment and Heritage (OEH)
- NSW Ministry of Health
- CSIRO Oceans & Atmosphere (O&A)
- ANSTO.

The project was supported by the Project Management Team of Matt Riley, Yvonne Scorgie, Judy Greenwood, Ann Louise Crotty, Leanne Graham, Wayne Smith, John Kirkwood, Keith Craig, Mark Hibberd, Melita Keywood, David Cohen, and Ed Stelcer.

We acknowledge the contributions of the CSIRO project support team of Kate Boast and Paul Selleck, the ANSTO project support team of David Garton and Armand Atanacio, and OEH project support and field staff Peter Crabbe, Scott Thompson, Gareth James, Upma Dutt and Stuart Masson. We also acknowledge inputs by Ben Scalley of NSW Ministry of Health.

Support provided by Orica Limited for the study by facilitating sampling at Stockton Air Quality Monitoring Site and making available monitoring records from this site is gratefully acknowledged.

Support extended by CSIRO Energy Centre for the establishment of study samplers on the grounds of the centre in Mayfield is gratefully acknowledged.

Summary

Key results at a glance

The Lower Hunter Particle Characterisation Study (LHPCS) provides details about the **composition and major sources of $PM_{2.5}$ (fine airborne particles) and $PM_{2.5-10}$ (coarse airborne particles).**

Measurements were made for **one year** from March 2014 to February 2015 at two air quality monitoring stations representative of **regional population exposures** (Newcastle and Beresfield) and two stations **near the Port of Newcastle** (Mayfield and Stockton).

Annual average $PM_{2.5}$ concentrations were very similar at Newcastle, Mayfield and Beresfield (6.4–6.7 µg m^{-3}) but about **40% higher at Stockton** (9.1 µg m^{-3}). The higher levels at Stockton were mainly due to both more sea salt and to the **primary ammonium nitrate, which was only detected at Stockton**. The ammonium nitrate, which contributed on average 19% of the $PM_{2.5}$ mass (and ~40% in winter), was identified as **very likely** to be due to primary emissions from **Orica's ammonium nitrate manufacturing facility** on Kooragang Island.

Other than the ammonium nitrate, **$PM_{2.5}$ composition and sources** were found to be fairly similar across the four sites. Key results on the sources and their contributions are:

- fresh sea salt particles: 24% at Newcastle, decreasing to 13% at Beresfield
- pollutant-aged sea salt: ~23% at all sites; this is sea salt reacted with industrial, commercial, road and non-road transport emissions from local and regional sources
- wood smoke: 15% at Beresfield, decreasing to 6% at Stockton
- secondary ammonium sulfate: ~10% at all sites
- soil dust: ~10% at all sites
- vehicles: ~10% at three sites, but only 5% at Stockton
- industry factors: ~12% at three sites but 24% at Stockton
- mixed shipping/industry: ~3% at all sites
- nitrate: 19% ammonium nitrate at Stockton and secondary nitrate at other sites (6-11%).

On an annual average basis, there is an approximately 50:50 split between primary and secondary particles at three sites (Newcastle, Beresfield and Mayfield) and a 65:35 split at Stockton because of the significant contribution from the primary ammonium nitrate.

$PM_{2.5-10}$ composition and sources were only determined at the stations near the Port of Newcastle. The 2½ times higher annual average $PM_{2.5-10}$ concentration at Stockton (21.5 µg m^{-3}) than at Mayfield (8.3 µg m^{-3}) was found to be mainly due to a **much higher contribution by fresh sea salt particles at Stockton**.

The $PM_{2.5-10}$ factors and their contributions were identified as:

- fresh sea salt: 13.6 µg m^{-3} at Stockton, 3.3 µg m^{-3} at Mayfield
- industry plus pollutant-aged sea salt: 2.4 µg m^{-3} at both sites
- light-absorbing carbon: 2.2 µg m^{-3} at Stockton, 0.9 µg m^{-3} at Mayfield
- soil: 2.3 µg m^{-3} at Stockton, 1.2 µg m^{-3} at Mayfield
- bioaerosol: 1.1 µg m^{-3} at Stockton, 0.5 µg m^{-3} at Mayfield.

Most $PM_{2.5-10}$ particles are **primary particles** or physical combinations of primary emissions, but there is evidence of chemical reactions in the pollutant-aged sea salt factor.

Coal particles could contribute up to 10% of the $PM_{2.5-10}$ particles. Further investigations are needed to clarify the contribution of coal.

Why study particles in the air in the lower Hunter region?

The Lower Hunter Particle Characterisation Study was initiated by the NSW Environment Protection Authority (EPA) in 2013 in response to community concerns about particle pollution in the lower Hunter region of New South Wales. This region is located along the NSW east coast and includes the city of Newcastle, located about 120 km north-north-east of Sydney. The region includes the Port of Newcastle, the largest bulk shipping port on the east coast of Australia and one of largest coal export ports in the world.

Exposure to airborne particles is a health concern with inhaled particles known to cause respiratory and circulation problems, particularly in elderly people, children and people with existing health conditions. According to the World Health Organisation (WHO 2013), particulate matter affects more people than any other air pollutant and its effects on health occur at levels of exposure currently being experienced by most urban and rural populations in developed countries.

Particle pollution in the air can come directly from human activities and natural sources (**primary particles**), or be produced in the air by chemical reactions between gases or between gases and other particles (**secondary particles**). Particles in the atmosphere vary in size, with particles less than 10 microns (µm) in diameter (PM_{10}) and fine particles less than 2.5 microns in diameter ($PM_{2.5}$) being the focus of air quality monitoring and management. PM_{10} comprises **fine particles** (smaller than 2.5 microns, termed $PM_{2.5}$) and **coarse particles** (ranging in size from 2.5 to 10 microns, termed $PM_{2.5\text{-}10}$).

PM_{10} and $PM_{2.5}$ levels measured at regional air quality monitoring stations in the lower Hunter are comparable to levels measured in Sydney and the Illawarra with national air quality standards occasionally exceeded. Health effects due to exposures to ambient particle concentrations are, however, known to occur at levels which are below national standards. Higher levels of particle pollution have also been measured to occur in the vicinity of the Port of Newcastle resulting in concerns by members of the local community and environmental groups about the effects of particle pollution on the health and wellbeing of local residents.

WHO recommends reducing fine particle pollution ($PM_{2.5}$) as the focus for policies to improve air quality (WHO 2013). Both long- and short-term exposures to fine particulate air pollution increase mortality and ill health. Longer term exposure to $PM_{2.5}$ has a larger health effect than short-term exposures and exposures to coarse particles, indicating that strategies that provide long-term reductions in fine particle pollution are likely to produce the greatest health benefit (EPA 2013; US EPA 2011; WHO 2013). Assessing source contributions to average $PM_{2.5}$ concentrations therefore represented a focus of the study to better understand air quality issues in the lower Hunter and inform policies and programs to improve air quality.

There is also emerging evidence that **short term exposure to coarse particulate air pollution** ($PM_{2.5\text{-}10}$) may cause an increase in mortality, and increase cardiovascular and respiratory health effects. (US EPA, 2009; WHO, 2013). The Newcastle community also requested that the LHPCS address both fine and coarse particles. The study therefore also addressed coarse particles in the vicinity of the Port of Newcastle. Throughout this study, results will be presented for these two particle size ranges ($PM_{2.5}$ and $PM_{2.5\text{-}10}$).

What were the aims of the study?

The study aimed to address community information needs and enhance the evidence base for policies targeting particle pollution in the lower Hunter region. The specific aims were to:

- determine the composition and major sources contributing to $PM_{2.5}$ concentrations at sites representative of regional population exposures (Newcastle and Beresfield)
- determine the composition and major sources contributing to $PM_{2.5}$ and $PM_{2.5\text{-}10}$ concentrations at sites indicative of population exposures in areas near to the Port of Newcastle (Mayfield and Stockton).

Who was involved in the study?

Following consultation with the local community about their information needs, the EPA developed the study as a research collaboration with the Office of Environment and Heritage (OEH), the NSW Ministry of Health, the Commonwealth Scientific and Industrial Research Organisation (CSIRO) and the Australian Nuclear Science and Technology Organisation (ANSTO). The management team established to oversee the study included representatives from these organisations and a representative from the local community nominated by the Newcastle Community Consultative Committee on the Environment (NCCCE).

How was the study conducted?

The Lower Hunter Particle Characterisation Study provides details of the composition and sources of fine ($PM_{2.5}$) and coarse ($PM_{2.5\text{-}10}$) air particles in the lower Hunter region based on sampling and analysis for four locations. In addition to providing the local community with trustworthy information, study findings are intended to expand the evidence for air quality management to improve air quality in the region. Two monitoring sites were representative of regional population exposures (Newcastle and Beresfield) and two were indicative of population exposures in areas near to the Port of Newcastle (Mayfield and Stockton), as shown in the Figure S1.

Samples were collected for 24 hours every third day for the 12-month sampling period from 1 March 2014 to 28 February 2015. $PM_{2.5}$ samples were collected at all four sites and $PM_{2.5\text{-}10}$ was also collected at Mayfield and Stockton. Almost all planned samples were able to be collected (a small number were missed due to power outages, instrument problems, etc.) and an overall collection rate of 99–100% was achieved.

Chemical analysis was undertaken using a range of techniques to provide a comprehensive picture of the particle composition. Techniques included ion beam analysis for 20 elements, ion chromatography for 14 soluble ions, levoglucosan and mannosan (wood smoke tracers), organic carbon, elemental carbon, black carbon, and light-absorbing carbon, as well as gravimetric analysis (weighing the samples) to determine the mass collected.

The chemical composition of the samples was analysed using a mathematical technique called positive matrix factorisation (PMF), which is widely used in air pollution source apportionment studies. PMF was used to identify likely source groupings, called factors. Each factor has a ‘fingerprint’ which represents a mix of chemical components that generally occur together. For example, on days when there are fine sea salt particles in the $PM_{2.5}$, the chemical analysis of the filters show the main elements in sea water (sodium, chlorine, magnesium, calcium) in similar proportions to those present in sea water. On some days, the concentrations will all be higher and on other days lower but the proportions will stay the

same. An advantage of PMF is that in some cases it is able to identify the presence of specific secondary particles by the ratio of chemical species in the factor.

Figure S1: Sampling sites for Lower Hunter Particle Characterisation Study

Once the factors were obtained, further analysis was undertaken to identify the sources in each factor. Information about known sources and other knowledge of atmospheric chemistry as well as wind sector and seasonal analysis was used to identify the most likely source of emissions for each factor and hence the contribution that each source makes to the total $PM_{2.5}$ or $PM_{2.5-10}$ concentrations. In many cases, there is a single dominant source in a factor and this has been used to name the factors. However, if sources are co-located or otherwise correlated, they can appear together in a single factor or across several factors.

What did the study find?

Key results

Over the one year of sampling, annual average $PM_{2.5}$ concentrations were measured to be 6.6 µg m^{-3} at Newcastle, 6.4 µg m^{-3} at Beresfield, 6.7 µg m^{-3} at Mayfield and 9.1 µg m^{-3} at Stockton. Annual average $PM_{2.5-10}$ concentrations were measured to be 8.3 µg m^{-3} at Mayfield and 21.5 µg m^{-3} at Stockton.

The PMF analysis identified 9 factors in the $PM_{2.5}$ and 6 factors in $PM_{2.5-10}$ chemical species data.

$PM_{2.5}$

A fairly consistent picture of the $PM_{2.5}$ composition and sources was found across the four sites. One major factor was only present at one site – ammonium nitrate at Stockton where it contributed on average 19% of the $PM_{2.5}$ mass. This was identified as very likely to be due to primary ammonium nitrate emissions from Orica's ammonium nitrate manufacturing facility on Kooragang Island.

The factors that contribute a similar percentage to $PM_{2.5}$ at all sites were:

- pollutant-aged sea salt[1] (~23%)
- secondary ammonium sulfate (~10%)
- soil dust (~10%)
- mixed shipping/industry (~3%).

The factors for $PM_{2.5}$ showing significant variations in contributions across the sites are:

- fresh sea salt: this decreased from 24% at Newcastle to 13% at Beresfield, which can be explained by the increasing distance from the coast, the source of the fresh sea salt
- wood smoke, which increased from 6% at Stockton to 15% at Beresfield. This can be explained by better dispersion (more wind) at Stockton and poorer dispersion (lighter night time winds) at Beresfield as well as higher local wood smoke emissions at Beresfield than at Stockton
- vehicles: this factor was ~10% at three sites but only 5% at Stockton, which can be explained by less traffic in Stockton
- secondary nitrate: increased from 6% at Beresfield to 11% at Mayfield. As noted above, at Stockton there was 19% of primary ammonium nitrate
- mixed industry/vehicle factor: increased from 1% at Mayfield to 9% at Beresfield. However, combining the contributions from primary and secondary nitrates and industry as generally being from industry, this 'industry' contribution was on average 13% at three of the sites and 24% at Stockton.

Some of the particles are primary particles (those emitted directly as particles from a source) and some are secondary particles (those formed by chemical reactions in the atmosphere and by gas-to-particle conversions).

- Primary particles: fresh sea salt, soil, some wood smoke, vehicle, shipping and industry emissions, and ammonium nitrate at Stockton.
- Secondary particles: Secondary sulfates and nitrates (such as ammonium sulfate and sodium nitrate), and organic carbon compounds contributed by emissions from combustion sources such as vehicles, wood heaters, non-road diesel equipment and transport (including diesel-electric locomotives), shipping, and industry. The pollutant-aged sea salt is included here as it undergoes chemical reactions between source and receptor.

[1] Pollutant-aged sea salt refers to sea salt reacted with industrial, commercial, road and non-road transport emissions from local and regional sources, in particular with sulfur dioxide and oxides of nitrogen through a series of chemical reactions.

On an annual average basis, there is an approximately 50:50 split between primary and secondary particles at three sites (Newcastle, Beresfield and Mayfield) and a 65:35 split at Stockton because of the significant contribution from the primary ammonium nitrate.

Fine particles are able to travel long distances, with $PM_{2.5}$ particles being transported a thousand or more kilometres from the sources of their particle or precursor gas emissions (Cope & Ischtwan 1996; Nelson et al. 2002; Cohen et al. 2012; Cope et al. 2014). This means that local and regional sources contribute to fine particle concentrations in the lower Hunter.

The seasonal variation in the contributions of the factors are shown at the end of this summary.

$PM_{2.5-10}$

For $PM_{2.5-10}$, the differences between the two sites are more significant. The annual average concentration at Stockton is 2½ times higher than at Mayfield with most of this due to the higher fresh sea salt contribution.

Because of the large differences in total $PM_{2.5-10}$ concentrations, it is more useful when comparing the sites to consider the absolute contributions rather than percentages. The factors contributing approximately equally are:

- industry and pollutant-aged sea salt: together 2.4 µg m^{-3} at both sites.

Those with a larger contribution at Stockton are:

- fresh sea salt: 13.6 µg m^{-3} at Stockton vs 3.3 µg m^{-3} at Mayfield
- light-absorbing carbon: 2.2 µg m^{-3} at Stockton vs 0.8 µg m^{-3} at Mayfield
- soil: 2.3 µg m^{-3} at Stockton vs 1.2 µg m^{-3} at Mayfield
- bioaerosol: 1.1 µg m^{-3} at Stockton vs 0.5 µg m^{-3} at Mayfield.

Secondary particle formation primarily occurs in the $PM_{2.5}$ fraction. An exception to this is the pollutant-aged sea salt factor in the $PM_{2.5-10}$ fraction which provides evidence of chemical reactions occurring in this size range. These chemical reactions transform the $PM_{2.5-10}$ at a slower rate than for $PM_{2.5}$ due to their relatively smaller surface-area-to-volume ratio and their shorter lifetime in the atmosphere before being deposited (due to their greater mass). Thus most $PM_{2.5-10}$ particles are primary particles or physical combinations of primary emissions.

Detailed results

The following figures and tables show in detail the percentage contributions of each factor to annual averages and list probable sources. Results are given for $PM_{2.5}$ and then for $PM_{2.5-10}$ as pie graphs and summary tables. This is followed by bar graphs showing the seasonal variability in the absolute contribution of each factor.

PM2.5 – Fine particles

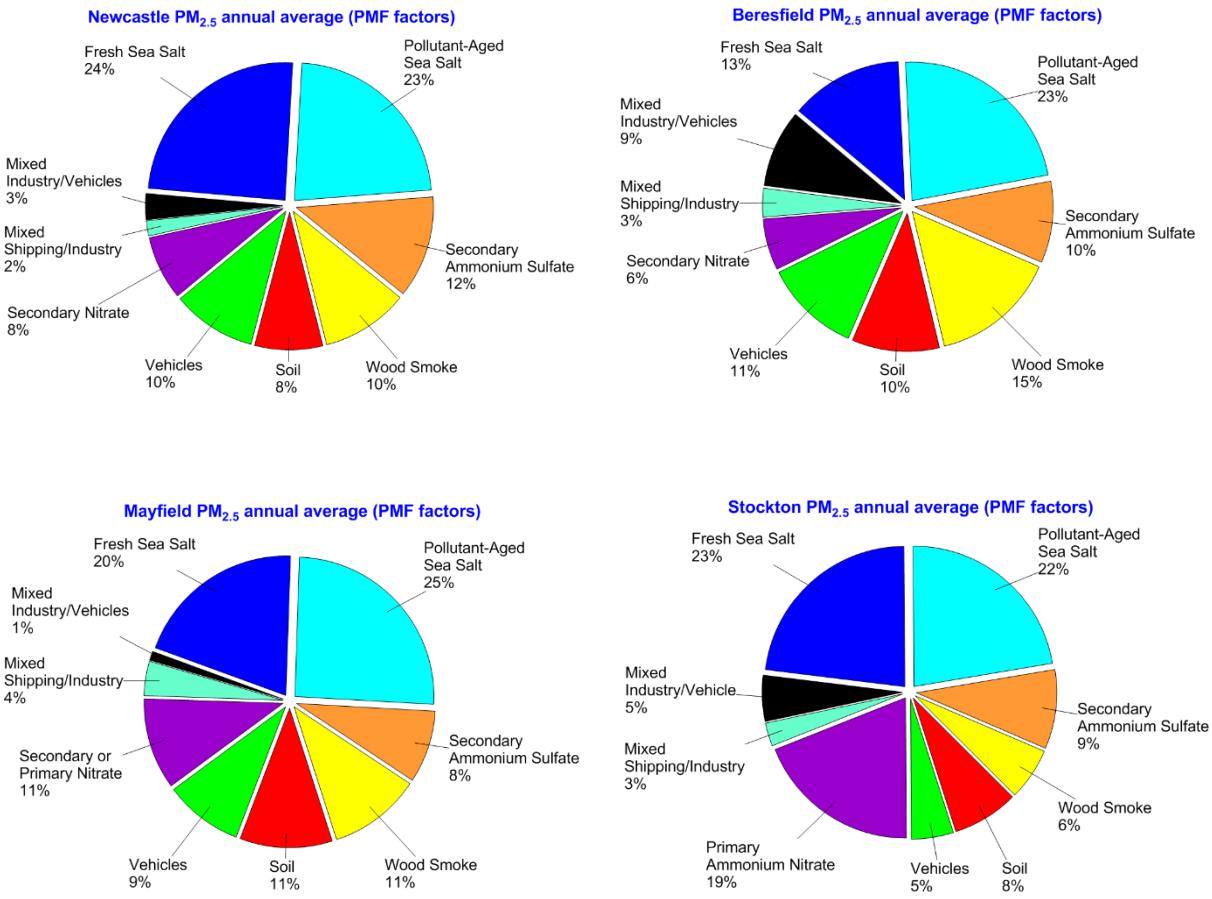

Figure S2: Percentage annual average contributions to total $PM_{2.5}$ mass at the four study sites during the study

Table S1: Summary of PMF factors for $PM_{2.5}$ listing main species, contributions and potential sources

Factor	Main species (drivers bold)	Contribution of the factor to total annual $PM_{2.5}$ mass (with uncertainty range) at:				Potential sources (primary/secondary)
		New-castle	Beres-field	Mayfield	Stock-ton	
Factor 1 Fresh sea salt	**Cl^-:Na^+:SO_4^{2-}:Mg^{2+}**	24% (20-27%)	13% (12-16%)	20% (18-22%)	23% (19-25%)	Primary particles. Fresh sea salt aerosol from wave-breaking
Factor 2 Pollutant-aged sea salt	Non-sea-salt SO_4, **Na^+:Mg^{2+}**, OC, EC, almost no Cl^-	23% (9-38%)	23% (15-34%)	25% (15-40%)	22% (13-28%)	Sea salt reacted with industrial, commercial, road & non-road transport emission from local & regional sources, esp. SO_2
Factor 3 Secondary ammonium sulfate	**NH_4^+:nssSO_4^{2-}**, OC, EC	12% (6-16%)	10% (9-17%)	8% (7-16%)	9% (7-13%)	Secondary aerosol – ammonium sulfate. Local & regional sources of SO_2 (e.g. fossil fuel burning) and ammonia (agriculture, industry, vehicles, non-road diesel equipment, soils, ocean)
Factor 4 Wood smoke	**Levo**, OC, EC, NO_3^-, SO_4^{2-}, Cl^- K^+, **Mannosan**	10% (6-18%)	15% (8-24%)	11% (7-15%)	6% (5-9%)	Primary aerosol. Domestic wood heaters, bushfires, hazard reduction burns
Factor 5 Soil	**Si:Al:Ti**, Fe, Ca^{2+}, OC, EC	8% (2-14%)	10% (9-14%)	11% (5-16%)	8% (5-10%)	Primary particles. Soil dust. Potential industrial contributions of organic & black carbon at Mayfield & Stockton. Possibly coal particles and/or soot contribute.
Factor 6 Vehicle	**EC, OC, Fe**, NO_3^-, SO_4^{2-}, **Cu, Mn, Cr, Pb**	10% (3-15%)	11% (6-13%)	9% (5-15%)	5% (4-7%)	Primary (EC, metals, OC) & secondary (NO_3-, OC) particles. Vehicles, non-road diesel equipment
Factor 7 Primary or secondary nitrate	**NO_3^-, Na^+**, SO_4^{2-}, Cl^-, OC **NH_4, NO_3** at Stockton	8% (5-14%)	6% (4-13%)	11% (7-16%)	19% (17-22%)	Secondary sodium nitrate at Mayfield, Newcastle and Beresfield. Primary ammonium nitrate at Stockton – industry. NO_x from vehicles, non-road diesel equipment, industry
Factor 8 Mixed shipping/ industry	SO_4^{2-}, NH_4^-, EC OC, NO_3^-, **V:Ni**	2% (1-6%)	3% (3-10%)	4% (3-7%)	3% (2-9%)	Secondary & primary (V, Ni) particles. Shipping, sulfate, ammonium
Factor 9 Mixed industry/ vehicle (a)	**Zn**, Fe, **Mn**, Cu, Cr, SO_4^{2-}, NH_4^+, NO_3	3% (2-9%)	9% (3-13%)	1% (1-3%)	5% (4-10%)	Primary (metals) & secondary particles. Industry, vehicles, non-road diesel equipment

(a) Emissions from industrial premises are likely to contribute to factors other than the mixed industry/vehicle factor, such as the pollutant-aged sea salt, secondary sulfate and nitrate factors, and maybe also the vehicle and soil factors.

$PM_{2.5-10}$ – Coarse particles

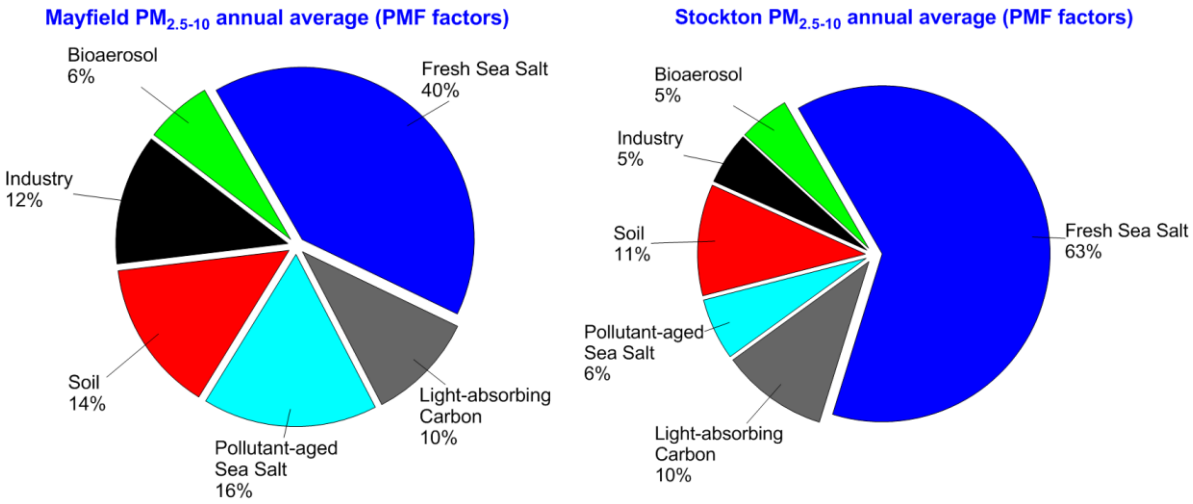

Figure S3: Percentage annual average contributions to total $PM_{2.5-10}$ mass at Mayfield and Stockton during the study

Table S2: Summary of PMF factors for $PM_{2.5-10}$ listing main species present, contributions and potential sources

Factor	Main species in factor (drivers in bold)	Contribution of the factor to total annual $PM_{2.5-10}$ mass (with uncertainty range) at:		Potential sources
		Mayfield (a)	Stockton	
Factor 1 Fresh sea salt	**Cl^-:Na^+:SO_4^{2-}:Mg^{2+}**	40% (33-45%)	63% (50-66%)	Primary particles. Generated by wave-breaking on ocean
Factor 2 Light-absorbing carbon	**Cl^-:Na^+, BC, SO_4^{2-}, Mg^{2+}**	10% (8-26%)	10% (7-19%)	Light-absorbing carbon (LAC) with some sea salt. Coal particles are conjectured to contribute to this factor.
Factor 3 Pollutant-aged sea salt	**NO_3^-, SO_4^{2-}, Na^+:Mg^{2+}**, Reduced Cl-, enhanced SO_4^{2-} cf. fresh sea salt	16% (7-17%)	6% (4-11%)	Sea salt reacted with industry emissions, particularly NO_2 and SO_2
Factor 4 Soil	**Si:Al**, Fe, **Ti**, Ca^{2+}, SO_4^{2-}	14% (10-27%)	11% (6-14%)	Primary particles. Soil dust
Factor 5 Industry	**F^-**, Si, **Fe**, Cl^-, Al, **SO_4^{2-}**	12% (3-19%)	5% (3-10%)	Industry
Factor 6 Bioaerosol	Cl^-, SO_4^{2-}, **arabitol, mannitol**, Fe, Mg^{2+}	6% (5-15%)	5% (2-9%)	Bioaerosol such as fungal spores and pollens combined with industrial emissions and sea salt

(a) Factor contributions do not sum to 100% due to rounding of values.

Seasonal variability

The seasonal variation in the contributions of the various $PM_{2.5}$ factors are similar at Newcastle, Beresfield and Mayfield. The most significant features are:

- Fresh sea salt and pollutant-aged sea salt contribute most from October to February. This is due to the predominance of on-shore flows during these months whereas during autumn and winter the winds are mostly from the north-west (offshore).
- Wood smoke and vehicles contribute most in the cool months of May to August. There are two reasons for this. One is the meteorology with lower inversion heights and poor dispersion leading to higher concentrations. A second is the higher emissions, such as more cold starts by vehicles, and wood smoke emissions mainly occur during the cooler months (although there were occasional bushfire emissions at other times during the LHPCS).
- Shipping contributes least during winter because most winds are offshore at this time of year.

The seasonal $PM_{2.5}$ trends at Stockton are significantly different. The large contribution from ammonium nitrate of 19% as an annual average makes up 40% of the mass from May to July.

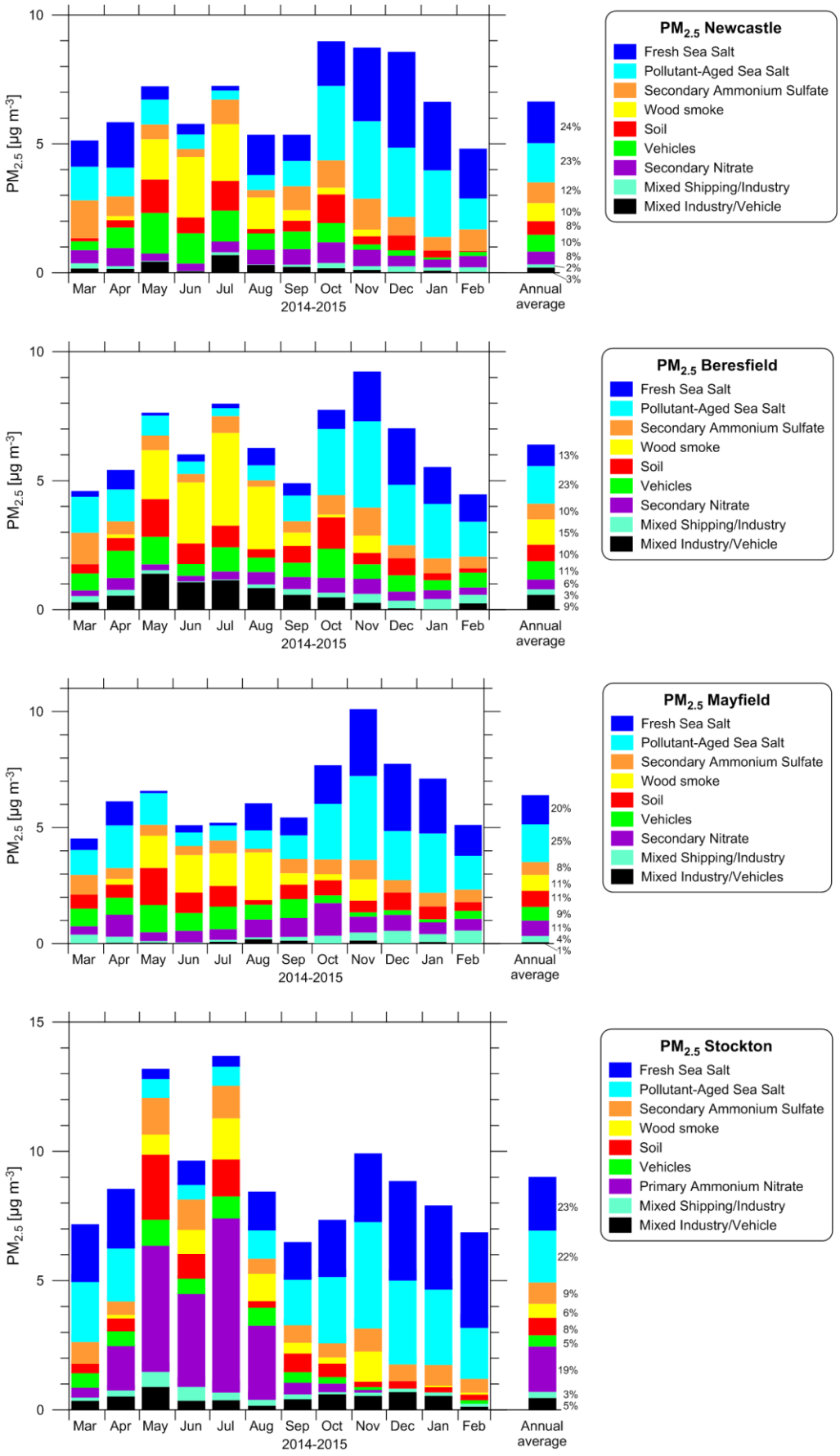

Figure S4: Monthly and annual factor contributions to $PM_{2.5}$ at the four study sites

(Note: the concentration range differs for the Stockton graph.)

The seasonal variations in the absolute values of $PM_{2.5-10}$ are much larger than for $PM_{2.5}$. The pattern is similar at both sites but with an overall larger contribution at Stockton than at Mayfield.

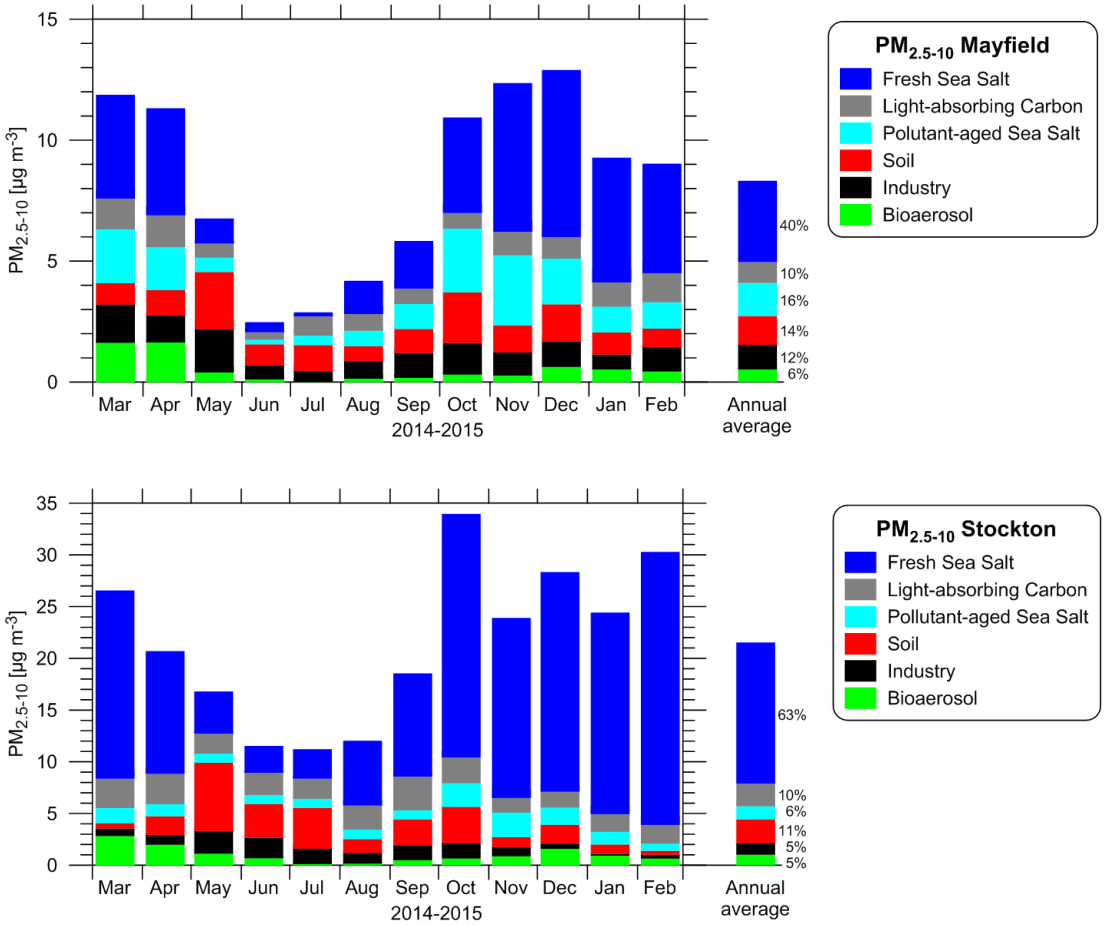

Figure S5: Monthly and annual factor contributions to $PM_{2.5-10}$ at Mayfield and Stockton

Contributing to the evidence base and further work

Based on the results from this study, emissions from

- human activities are estimated to account for 45–54% of the annual $PM_{2.5}$ mass, and 15–22% of the annual $PM_{2.5-10}$ mass
- mixed human and natural sources for 30–36% of the annual $PM_{2.5}$ mass and 17–30% of the annual $PM_{2.5-10}$ mass
- fresh sea salt 13–24% of the annual $PM_{2.5}$ mass, and 46–68% of the annual $PM_{2.5-10}$ mass across the study sites.

Sources associated with human activities which potentially contribute to the factors identified in the study include industrial and commercial sources, vehicles, wood heating, bushfires and hazard reduction burns, non-road diesel equipment and transport (including diesel-electric locomotives), shipping and agriculture as shown in the summary tables for $PM_{2.5}$ and $PM_{2.5-10}$.

In some cases the study identified mixed source factors and secondary particle factors where further evidence is needed to assess the contributions of individual types of sources.

Chemical transport modelling accounts for processes associated with the formation of secondary particles and can be used to refine these estimates. Such modelling can confirm the contribution of emissions from human activities to sulfate and nitrate and determine their contribution to the pollutant-aged sea salt and soil factors. Such modelling can also be used to assess inter-regional transport of pollution, spatially localised source contributions and determine how reducing specific sources may affect total PM concentrations.

Light-absorbing carbon was found through the species analysis of the components of $PM_{2.5-10}$ to account for about 10% of the coarse particle mass at Mayfield and Stockton. Coal particles are conjectured to contribute to this factor, contributing at most 10% of $PM_{2.5-10}$. Further analysis is needed to quantify the contribution of coal particles to the light-absorbing carbon in this factor.

The findings of the LHPCS provide the region's communities and the NSW Government with new, reliable scientific information about the chemical composition of fine and coarse particles and insight into sources contributing to particle pollution in the region. The results from this research add to the evidence base the NSW Government relies on to inform policies and programs to improve air quality, public health and the understanding of air quality issues in the lower Hunter region.

1 Introduction

The Lower Hunter Particle Characterisation Study (LHPCS) was initiated in 2013 to provide the NSW Environment Protection Authority (EPA) and communities in the lower Hunter region of New South Wales with scientific information about the composition and likely sources of airborne particles in their local environment. The study was initiated in response to community concerns about particle pollution in the region.

The study represents a collaboration between the NSW EPA, the NSW Office of Environment and Heritage (OEH), NSW Ministry of Health, the Commonwealth Scientific and Industrial Research Organisation (CSIRO) and the Australian Nuclear Science and Technology Organisation (ANSTO). The management team established to oversee the study design and delivery included representatives from these organisations and a representative from the local community nominated by the Newcastle Community Consultative Committee on the Environment (NCCCE).

Following the establishment of governance arrangements and an independently peer-reviewed study design, a one-year airborne particle study program was undertaken during the period 1 March 2014 to 28 February 2015. Four progress reports were published on the project website (www.environment.nsw.gov.au/aqms/lowhunterparticle.htm) at the completion of the autumn, winter, spring and summer sampling periods. Major sources contributing to airborne particles were then identified and their contributions quantified based on chemical speciation of particles collected, source apportionment modelling and supplementary analysis. This final report documents the overall study and presents the findings.

1.1 Study objectives

The Lower Hunter Particle Characterisation Study determined the composition of fine ($PM_{2.5}$) and coarse ($PM_{2.5-10}$) air particles, and identified major sources contributing to $PM_{2.5}$ and $PM_{2.5-10}$ concentrations in the lower Hunter region to address community information needs and enhance the evidence base for policies targeting particle pollution.

Specific objectives were to:

- determine the composition and major sources contributing to $PM_{2.5}$ concentrations at sites representative of regional population exposures
- determine the composition and major sources contributing to $PM_{2.5}$ and $PM_{2.5-10}$ concentrations at sites indicative of population exposures in areas near to the Port of Newcastle.

1.2 Regional context

1.2.1 Geographical setting

The lower Hunter is the region where the Hunter River valley opens out to a coastal plain along the NSW east coast. The region is made up of five local government areas (LGAs): Newcastle, Cessnock, Maitland, Port Stephens and Lake Macquarie (Figure 1). Major urban areas include the city of Newcastle and the Maitland regional centre. The Newcastle–Maitland urban area has a population of 430,000, with the highest population density in the city of Newcastle (ABS 2015). The Port of Newcastle is the largest bulk shipping port on the east coast of Australia and an internationally significant coal export port.

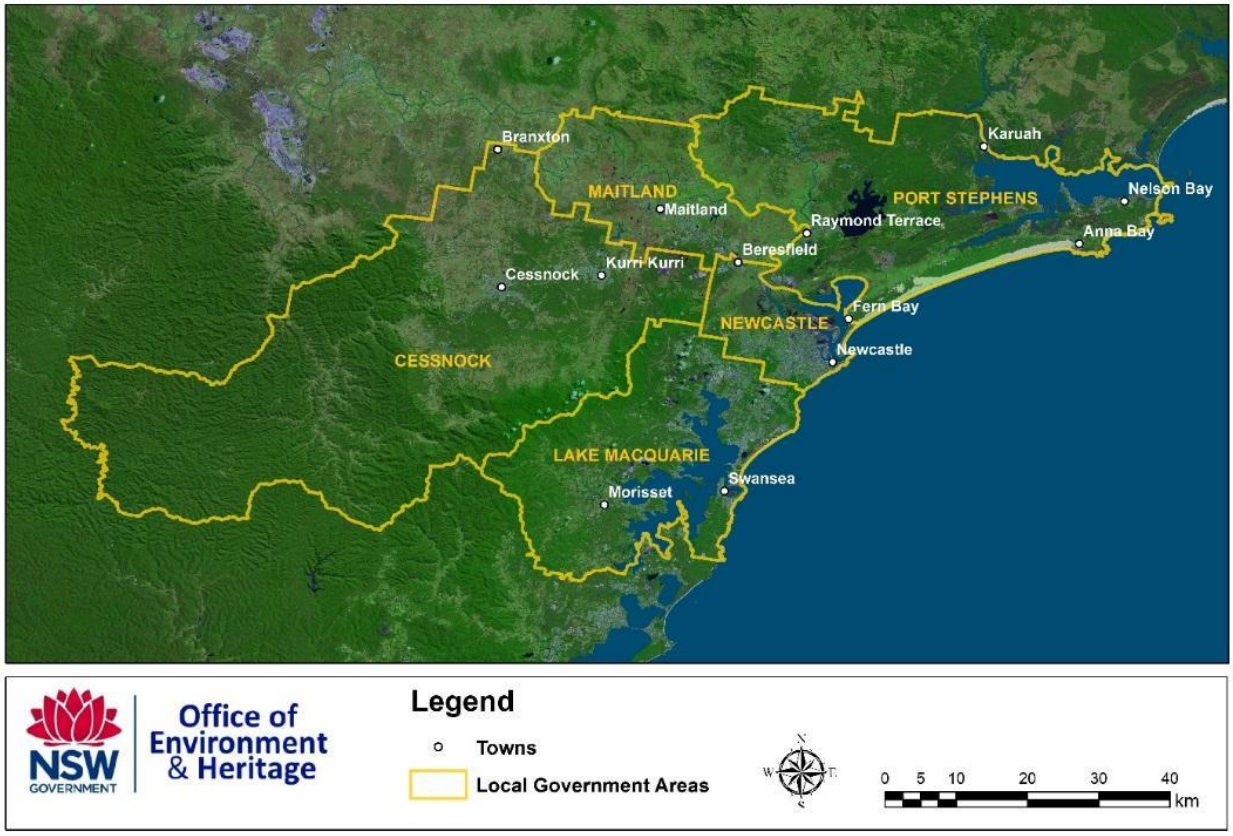

Figure 1: The lower Hunter region of New South Wales

1.2.2 Ambient air quality

Air quality monitoring has been undertaken by NSW environmental agencies in the lower Hunter since 1992, with nitrogen dioxide (NO_2), sulfur dioxide (SO_2), particulate matter (PM_{10}, $PM_{2.5}$), ozone (O_3), and carbon monoxide (CO) measured to assess regional air quality affecting the general population. The OEH-operated Lower Hunter Air Quality Monitoring Network (LHAQMN) comprises regional air quality monitoring stations at Beresfield, Newcastle and Wallsend (Figure 3). The industry-funded, OEH-operated Newcastle Local Air Quality Monitoring Network (NLAQMN) comprising three stations near the Port of Newcastle (Stockton, Mayfield and Carrington) was established in the latter half of 2014, during the LHPCS (Figure 3). This network was established to monitoring local air quality within the vicinity of the port.

Gaseous air pollutant concentrations are generally measured to be within national air quality standards in the region. PM_{10} and $PM_{2.5}$ levels measured at regional air quality monitoring stations in the lower Hunter are comparable to levels measured in Sydney and the Illawarra (OEH 2012, 2014; EPA 2013). At such stations, 24-hour average $PM_{2.5}$ concentrations are observed to be below the National Advisory Reporting Standard of 25 µg m^{-3} much of the time, with the infrequent exceedances of this standard often attributable to regional bushfire or dust storm events (OEH 2014, 2015)[2]. Annual average $PM_{2.5}$ concentrations measured in the

[2] At the meeting of Environment Ministers in December 2015 it was agreed to strengthen national ambient air quality reporting standards for airborne fine particles. Ministers agreed to adopt reporting standards for annual average and 24-hour $PM_{2.5}$ particles of 8 µg m^{-3} and 25 µg m^{-3} respectively, aiming to move to 7 µg $m^{-3}$and 20 µg m^{-3} respectively by 2025. Ministers also agreed to establish an annual average standard for PM_{10} particles of 25 µg m^{-3}. (www.environment.gov.au/system/files/pages/4f59b654-53aa-43df-b9d1-b21f9caa500c/files/mem-meeting4-statement.pdf)

region are generally within or marginally exceed the National Advisory Reporting Standard of 8 µg m^{-3}.

The maximum, minimum, average and range of 24-hour average $PM_{2.5}$ and PM_{10} concentrations recorded at LHAQMN and NLAQMN stations during the 1 November 2014 to 31 October 2015 period are illustrated in Figure 2.The grey box shows the most typical range in daily averages with 80% of days recording levels in this range; the box is bounded by the 10th and 90th percentile values with the medium concentrations shown. Higher PM_{10} levels are recorded near the Port of Newcastle with localised peaks not evident at regional air quality monitoring stations. Higher $PM_{2.5}$ and PM_{10} concentrations are measured at the Stockton monitoring station, with a greater number of elevated PM days measured for this station as discussed further in Section 2. Possible reasons for this include greater sea salt contribution due to the coastal location of the site and the likely influence of industrial emissions.

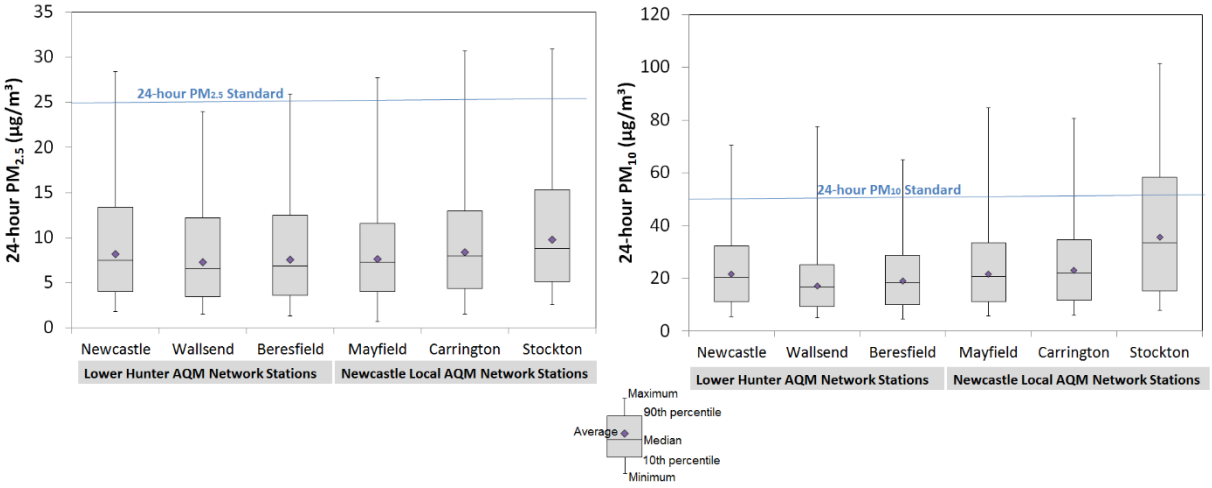

Figure 2: 24-hour average $PM_{2.5}$ and PM_{10} concentrations measured at Lower Hunter and Newcastle Local AQMN stations (maximum, minimum, median, 90th and 10th percentile)

Data range: 1 November 2014 to 31 October 2015 for all stations.

The commissioning of the Orica-operated Stockton Air Quality Monitoring Station and online reporting of data from this station from October 2012 prompted concerns by members of the local community and environmental groups when PM_{10} levels were measured to more frequently exceed 50 µg m^{-3} when compared to regional air quality stations. The LHPCS was initiated in response to this and other community concerns about particle pollution in the region.

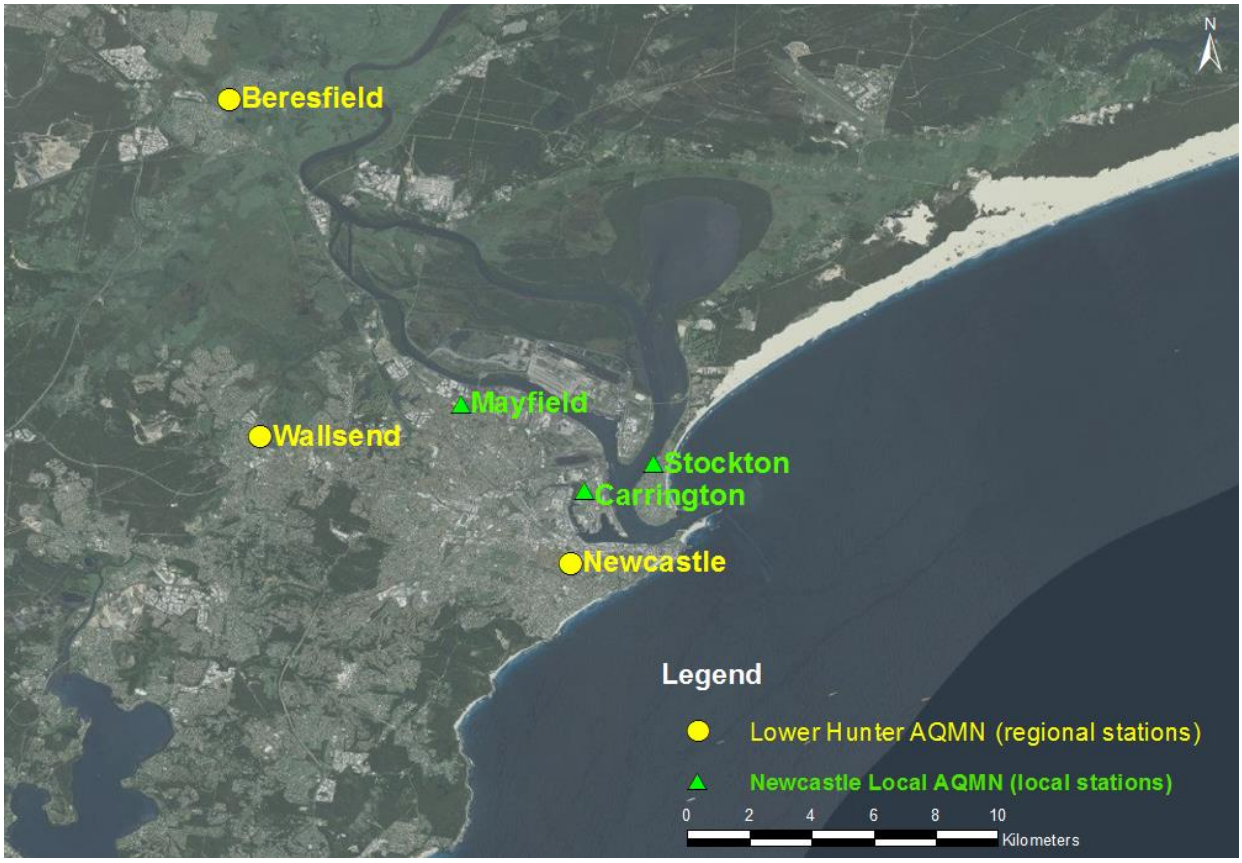

Figure 3: The Lower Hunter Air Quality Monitoring Network and Newcastle Local Air Quality Monitoring Network

1.2.3 Air pollution sources and emissions

Particle pollution includes primary particles released directly from sources, and secondary particles produced by chemical reactions between gases or between gases and other particles in the air. The spatial distribution of primary $PM_{2.5}$ and PM_{10} emissions in the region is shown in Figure 4 and Figure 5, based on the EPA's Greater Metropolitan Region air emissions inventory for the 2008 base year (EPA 2012). Sources of particle emissions include industry (bulk coal handling associated with the port[3], explosives manufacturing, electricity generation by coal and mining), residential wood heating[4], vegetation burning[5], vehicle[6], non-road diesel equipment and transport (including locomotives) and shipping emissions[7].

A large proportion of primary $PM_{2.5}$ emissions occur near ground level near the Port of Newcastle. Particle precursor gases, such as sulfur dioxide (SO_2), oxides of nitrogen (NO_x),

[3] Coal operation facilities at the Port of Newcastle are Newcastle Coal Infrastructure Group (NCIG) operations on Kooragang Island, Port Waratah Coal Service Ltd (PWCS) Kooragang Coal Terminal and PWCS Carrington Coal Terminal. They were estimated to emit 93 tonnes/year of $PM_{2.5}$ and 750 tonnes/year of PM_{10}.

[4] Residential wood heater emissions emitted 900 tonnes of $PM_{2.5}$ and about 35 tonnes of $PM_{2.5\text{-}10}$ in 2008 across the five local lower Hunter LGAs (EPA 2012).

[5] Bushfire and prescribed burning emissions are highly variable from year to year. The 2008 estimates were 245 tonnes of $PM_{2.5}$ and about 45 tonnes of $PM_{2.5\text{-}10}$.

[6] On-road vehicles emissions of $PM_{2.5}$ were 230 tonnes in 2008 and comprised of exhaust emissions from diesel (55.2%), petrol (8.3%) and other vehicles (0.4%), and non-exhaust emissions from brake, tyre and road surface wear (36.1%) (EPA 2012).

[7] $PM_{2.5}$ emissions from shipping (main engines, auxiliary engines and boilers) within the Port of Newcastle were estimated to be 60 tonnes/year based on 2013 activity data (DNV 2015). The largest proportions were from bulk carriers (60%), oil tankers (18%), and general cargo vessels (13%).

volatile organic compounds (VOCs) and ammonia (NH_3) are emitted by industry, vehicles, commercial businesses, household activities, road transport, non-road diesel equipment and transport (including locomotives) and natural sources (EPA 2012).

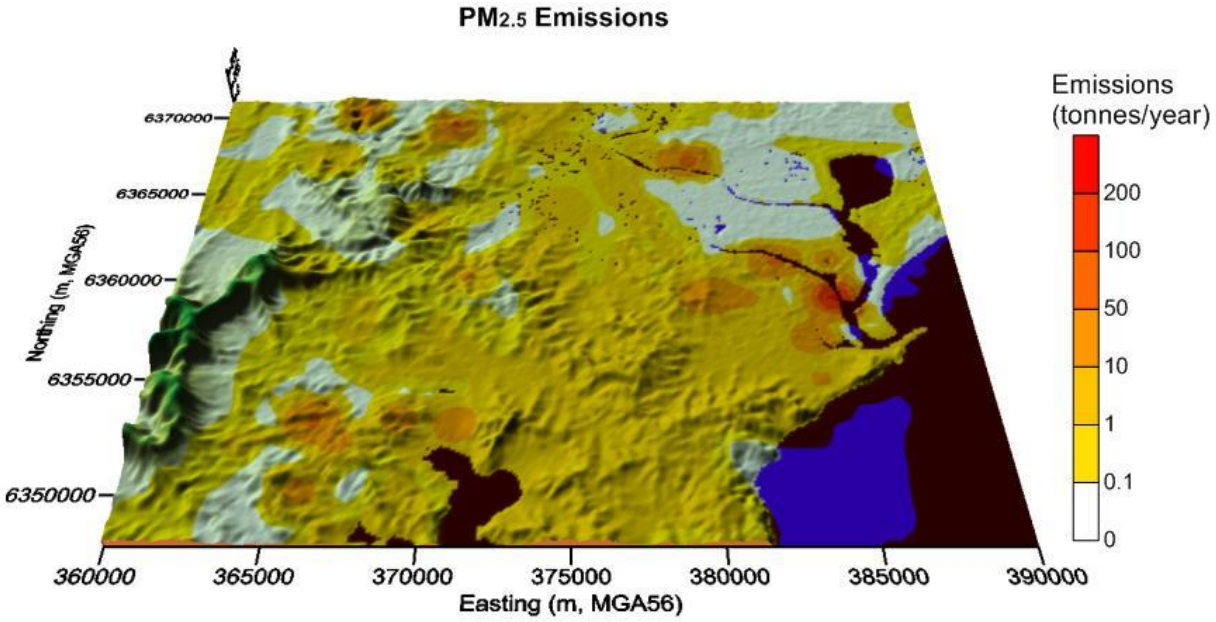

Figure 4: Spatial distribution of primary $PM_{2.5}$ emissions for the 2008 calendar year

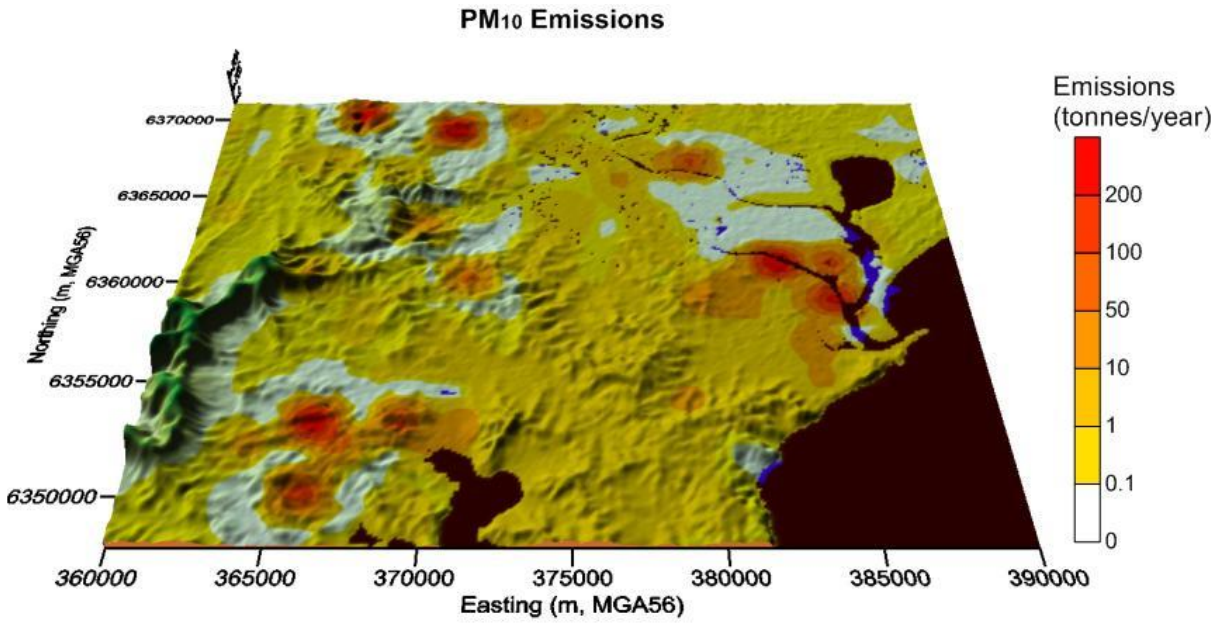

Figure 5: Spatial distribution of primary PM_{10} emissions for the 2008 calendar year

1.2.4 Health effects of particulate matter

There is little evidence of a threshold below which exposure to particulate air pollution is not associated with health effects. Therefore, any increase in exposure should be assumed to have a negative impact on health and any reduction in exposure can be assumed to have a health benefit.

There is a substantial body of evidence from which to conclude that exposure to fine particulate air pollution, also known as $PM_{2.5}$, has an impact on health. Both long- and short-term exposures to fine particulate air pollution increase mortality and ill health in general. Evidence for the effects of this type of air pollution specifically on respiratory and cardiovascular disease is now well-established. It has also been suggested that other specific diseases such as diabetes, neurological development in children and neurological disorders in adults may also be associated with fine particulate air pollution (WHO 2013).

There is emerging evidence that exposure to coarse particulate air pollution ($PM_{2.5-10}$) may cause an increase in mortality, and increase cardiovascular and respiratory health effects (US EPA 2009). While the evidence for the health effects for short-term exposure to coarse particulate air continues to strengthen, there is continuing uncertainty about the significance of long-term exposure. There is an increasing body of evidence that indicates a specific association of coarse particulate air pollution with adverse respiratory and cardiovascular health effects (WHO 2013).

Particles can comprise a range of chemical species, and a number of sources contribute to airborne particle concentrations. There is ongoing research to assess whether different particle chemical compositions and different sources of particulate matter produce different health outcomes. Assessing the overall impact of particulate matter on health requires large populations to accurately characterise the relationship between exposure to particle pollution and health effects. Thus even larger populations are required to determine the effects of subcomponents of particles based on composition or source, making these studies difficult to undertake. Some studies suggest that certain components, such as combustion-related sources and black carbon particles emitted during combustion, may have a greater health impact than other sources and particle compositions (WHO 2013). It is still considered, however, that there is not yet sufficient evidence to differentiate between particle chemical composition and particle sources by their health effects (WHO 2013; US EPA 2009).

1.3 Study overview

The study comprised $PM_{2.5}$ sampling at four sites in the lower Hunter region over a one-year period, including two sites representative of wider community exposures in the region (Newcastle and Beresfield) and two sites indicative of public exposures in areas neighbouring the Port of Newcastle (Stockton and Mayfield). $PM_{2.5-10}$ sampling and analysis was also undertaken for the Stockton and Mayfield sites in response to community requests that PM_{10} be addressed. Because PM_{10} includes $PM_{2.5}$ particles as a subset, better information about PM is obtained by separate sampling and analysis of $PM_{2.5-10}$ and $PM_{2.5}$. The sampling site locations are shown in Figure 6.

In 2013 when the study was initiated, existing or planned ambient air quality monitoring sites were preferred locations for sampling since they allowed timely establishment of study sampling sites. Air quality monitoring stations also have continuous particulate matter and gaseous monitoring records and meteorological data available for use in the study. Selected study sites coincided with the existing OEH Beresfield Air Quality Monitoring (AQM) Station, the OEH Newcastle AQM Station, the Orica Fullerton Street Stockton AQM Station, and CSIRO Energy Centre in Mayfield West. Sampling was conducted over the period 1 March 2014 to 28 February 2015. Following the commencement of sampling, OEH-operated AQM Stations were commissioned at CSIRO Energy Centre in July 2014 and at the Orica Fullerton Street Stockton site in October 2014, as part of the Newcastle Local Air Quality Monitoring Network.

Figure 6: Sampling sites for the Lower Hunter Particle Characterisation Study

A summary of the LHPCS sampling sites, equipment and filter types and sampling schedules for the study is given in Table 1.

Sample analysis for the $PM_{2.5}$ component included ion beam analysis (IBA) techniques and ion chromatography (IC) on the Teflon filters and organic and elemental carbon (OC/EC) analysis using a DRI Model 2001A thermal-optical carbon analyser for the quartz filters. Equivalent black carbon (EBC) was determined through the use of the laser integrated plate method (LIPM). The use of ANSTO Aerosol Sampling Program (ASP) $PM_{2.5}$ cyclone samplers at each of the four sites provides the basis for gravimetric analysis to determine $PM_{2.5}$ concentrations.

Chemical analysis of the $PM_{2.5\text{-}10}$ component included IBA and IC on the Nuclepore filters in addition to light-absorbing carbon (LAC) being determined through the use of the LIPM, which is a light absorption technique. The use of quartz filters to support OC/EC analysis of the coarse fraction was not possible because duplicate GENT samplers were not available, which would have been needed for the quartz filters.

The chemical composition of all the samples was used as input into receptor modelling using a mathematical technique called positive matrix factorisation (PMF) to identify factors and the contribution of each factor to the total $PM_{2.5}$ and $PM_{2.5\text{-}10}$ concentration. The key source(s) of emissions in each factor were identified using a range of information including source characteristics, wind data and the pattern of seasonal variation in the factor. Supporting analysis undertaken to inform the study included backward trajectory analysis and chemical transport modelling.

A project website (www.environment.nsw.gov.au/aqms/lowhunterparticle.htm) was established to provide further information about the project and includes copies of the four progress reports.

Table 1: LHPCS monitoring sites, equipment, filter types and sampling schedule

Monitoring site	Equipment, size fraction and filter type	Sampling schedule
OEH Newcastle AQM Station	Two ANSTO Aerosol Sampling Program (ASP) $PM_{2.5}$ cyclone samplers – one collecting on a Teflon filter and one on a quartz filter. AQM station includes continuous monitoring of PM_{10} using a tapered elemental oscillating microbalance or TEOM (with an operating temperature of 50°C), $PM_{2.5}$ using a beta attenuation monitor (BAM), ozone (O_3), nitrogen oxide (NO, NO_2, NO_x), sulfur dioxide (SO_2) and carbon monoxide (CO).	1-in-3 days
OEH Beresfield AQM Station	Two ANSTO ASP $PM_{2.5}$ samplers – one collecting on a Teflon filter and one on a quartz filter. AQM station includes continuous monitoring of air temperature, wind speed and direction, relative humidity, PM_{10} (TEOM, operating temperature of 50°C), $PM_{2.5}$ (BAM), O_3, NO, NO_2, NO_x and SO_2.	1-in-3 days
OEH Mayfield AQM Station (at CSIRO Energy Centre)	One GENT stacked filter unit (SFU) sampling 'coarse' ($PM_{2.5-10}$) particles on a Nuclepore filter and 'fine' ($PM_{2.5}$) particles on a quartz filter. One ANSTO ASP $PM_{2.5}$ sampler collecting fine particles on a Teflon filter (this sampler was relocated to this site from the nearby former Steel River AQM station). AQM station includes continuous monitoring of air temperature, wind speed and direction, relative humidity, PM_{10} (TEOM, operating temperature of 50°C), $PM_{2.5}$ (BAM), NO, NO_2, NO_x and SO_2.	1-in-3 days
OEH Stockton AQM Station (formerly Orica Fullerton Street Stockton AQM Station)	One GENT SFU sampling 'coarse' ($PM_{2.5-10}$) particles on a Nuclepore filter and 'fine' ($PM_{2.5}$) particles on a quartz filter. One ANSTO ASP $PM_{2.5}$ cyclone sampler collecting fine particles on a Teflon filter. (This sampler was already in operation at this site, funded by Orica with sampling and analysis undertaken by ANSTO.) AQM Station includes continuous monitoring of air temperature, wind speed and direction, relative humidity, PM_{10} (TEOM, operating temperature of 50°C), $PM_{2.5}$ (BAM), NO, NO_2, NO_x, SO_2 and ammonia.	1-in-3 days

2 Data collection

This section provides more detailed information on the measurement sites (Section 2.1) and one-year sampling program (Section 2.2). Airborne particle concentrations recorded at ambient air quality monitoring stations in the region during the study sampling period are compared to longer term monitoring records to determine the representativeness of the sampling period (Section 2.3). The sample collection rate achieved is documented (Section 2.4) and additional information collected noted (Sections 2.5 to 2.8).

2.1 Measurement sites

Site selection is an important component of the design of the study with emphasis placed on representative sampling locations with characteristics that match the study objectives. Reference was made to information from emissions inventories, meteorological data, and available air quality monitoring and airborne particle speciation data to determine candidate locations for sampling. This information was used in conjunction with the program objectives to determine appropriate site selection. Furthermore, sampling sites identified to meet the study objectives were selected to coincide with existing ambient air quality monitoring sites where possible to ensure timely establishment of sites and enable reference to longer term, continuous particulate matter and gaseous monitoring records and to detailed meteorological monitoring records from such sites.

The study sampling sites selected are as follows (Figure 6):

- OEH Newcastle AQM Station (hereafter the ‘Newcastle site’)
- OEH Beresfield AQM Monitoring Station (the ‘Beresfield site’)
- Orica Fullerton Street Stockton AQM Station (the ‘Stockton site’)
- CSIRO Energy Park Meteorological Monitoring Station in Mayfield (the ‘Mayfield site’).

The manner in which each site contributed to the study objectives being met is explained below and further contextual information on each site provided.

The Newcastle and Beresfield sites were selected as sampling sites representative of more general population exposures within the lower Hunter. The Newcastle site is located in the Newcastle Sportsground, off Dumaresq Street, Newcastle (Figure 7, Figure 8). It is situated in a residential area, next to a school, close to the commercial centre of Newcastle, 500m from a major road (Stewart Avenue) and is at an elevation of 5m. The site is not located in the immediate vicinity of major roads, nor any other significant local emission sources. The air quality monitoring at this site was commissioned in November 1992, with PM_{10}, NO, NO_2, NO_x, SO_2, CO and O_3 being continuously measured, in addition to wind speed and direction, air temperature and relative humidity. PM_{10} is measured using a tapered element oscillating microbalance (TEOM). Although $PM_{2.5}$ has not been historically measured at this site, a continuous beta attenuation monitor (BAM) was installed at the site prior to the particle characterisation study commencing. (BAMs are in use for $PM_{2.5}$ monitoring across the OEH NSW Air Quality Monitoring Network.)

The TEOMs are operated with the inlet heated to 50°C to dry out the particles before they land on the filter. The BAMs also include heating with the amount of heating determined by the humidity levels of the incoming sample stream.

Figure 7: Newcastle Air Quality Monitoring Station during the site visit from the project team

Figure 8: A 360° panorama from the roof of the Newcastle Air Quality Monitoring Station located next to an athletics field (vertically stretched to aid identification of features)

The Beresfield site is located in Francis Greenway High School, on Lawson Avenue, Beresfield (Figure 9, Figure 10). It is situated in a residential area north-west of Newcastle and is at an elevation of 14m. Air quality monitoring was commissioned at this site in May 1993, with PM_{10}, $PM_{2.5}$, NO, NO_2, NO_x, CO and O_3 being continuously measured, in addition to wind speed and direction, air temperature and relative humidity. SO_2 is not measured at this site. PM_{10} is measured using a TEOM, with $PM_{2.5}$ measured with a BAM. The Beresfield site is located about 300m from the main railway line along which diesel-electric trains are in use, including passenger and freight trains and coal trains transporting coal from mines in the Hunter to the Newcastle Port for shipping (Figure 11). It is also located next to a school parking area that is frequented by buses on school days.

The Newcastle and Beresfield sites were selected over the OEH Wallsend Air Quality Monitoring Station for a number of reasons. Higher PM_{10} concentrations are recorded at Newcastle and Beresfield, with higher $PM_{2.5}$ concentrations also observed at Beresfield when compared to Wallsend (Figure 2). Airflow patterns at Newcastle and Beresfield are more representative of the greater lower Hunter region, whereas airflow at Wallsend is significantly influenced by the local terrain. The Newcastle site is in an area characterised by greater population densities compared to Wallsend. The location of the Beresfield site relative to the

Newcastle site supported the evaluation of the change in contribution of the sea salt component of $PM_{2.5}$ with increasing distance from the coast.

Figure 9: Beresfield Air Quality Monitoring Station located adjacent to Francis Greenway High School

Figure 10: A 360° panorama from the roof of the Beresfield Air Quality Monitoring Station (vertically stretched to aid identification of features)

Figure 11: The location of the Beresfield site with respect to the railway line (indicated by dashed black line)

The Stockton and Mayfield sites were selected to represent residential areas situated in proximity to the Port of Newcastle.

The Mayfield site at CSIRO Energy Park is situated within the Steel River Estate at 10 Murray Dwyer Circuit, Mayfield West (Figure 12, Figure 13). The site is located south of the south arm of the Hunter River in close proximity to the Mayfield West residential areas and industrial operations at the Port of Newcastle including the coal terminals on Kooragang Island. (Figure 13 does not include the view south because of poor visibility due to it raining at the time the photos were taken.) Residences are located to the south of the Mayfield site. Although no air quality monitoring was undertaken at the site when sampling commenced, a meteorological station was in operation and the site was situated near to the Steel River Air Quality Monitoring Station at which total suspended particulates (TSP) and PM_{10} are sampled on a 1-in-6 day schedule and SO_2 and NO_x continuously monitored. The ANSTO ASP $PM_{2.5}$ sampler located at the Steel River monitoring station was relocated to the CSIRO Energy Park site for inclusion in the study. The CSIRO Energy Park site was also the preferred location for sampling since it was earmarked to be a Newcastle Air Quality Monitoring Network station. In July 2014, during the LHPCS sampling period, the Mayfield AQM station was established as part of this network, with the LHPCS samplers moved to the roof of the new monitoring shed.

Figure 12: Mayfield Air Quality Monitoring Station located in the grounds of the CSIRO Energy Park

Figure 13: A 270° panorama in the vicinity of the Mayfield Air Quality Monitoring Station

The Stockton site is situated between the Stockton residential area and the northern arm of the Hunter River, and across the river from industries situated on Kooragang Island (Figure 14, Figure 15). Being situated on a peninsula, the Stockton site is also in close proximity to the ocean (Figure 6). Orica commissioned air quality monitoring at this site in October 2012, with PM_{10}, $PM_{2.5}$, NO_2, NO_x and NH_3 being continuously measured, in addition to wind speed and direction. PM_{10} was continuously measured using a TEOM, with $PM_{2.5}$ measured with a BAM. There was also an existing ANSTO ASP $PM_{2.5}$ sampler located at the site, with sampling and analysis undertaken by ANSTO (and soluble ion chemistry by CSIRO) and funded by Orica. The Stockton site was earmarked to be a Newcastle Air Quality Monitoring Network station. In October 2014, during the LHPCS sampling period, the Stockton AQM station was established as part of this network, with the LHPCS samplers moved to the roof of the new monitoring shed.

Figure 14: View from the Stockton Air Quality Monitoring Station looking west, across the river to Kooragang Island

Figure 15: A 360° panorama from the roof of the Stockton Air Quality Monitoring Station (vertically stretched to aid identification of features; residences are located to the east and south of the site)

2.2 Sampling program

2.2.1 Sampling equipment

Two types of samplers were selected for use in the study:

- ANSTO's low volume Aerosol Sampling Program (ASP) $PM_{2.5}$ cyclone samplers
- GENT stacked filter units (SFUs) sampling 'coarse' ($PM_{2.5-10}$) and 'fine' ($PM_{2.5}$) particles.

ASP $PM_{2.5}$ sampler

The ANSTO-built ASP sampling unit is a $PM_{2.5}$ cyclone-type sampler based on the US EPA IMPROVE system used across North America in their National Parks air monitoring program (Cohen et al. 1996; Malm et al. 1994). The unit was specifically designed for use with multi-elemental ion bean analysis methods. The cyclone operates at a flow rate of 22 L min^{-1} using a mass flow controller which results in a 2.5µm particle size cut-off. The particles are most typically collected on a 25mm-diameter thin-stretched Teflon filter masked to 17mm diameter to increase sample thickness and improve deposit uniformity.

ANSTO ASP $PM_{2.5}$ samplers are currently being used by ANSTO for the ongoing Australian East Coast Particle Sampling and Characterisation Project and were successfully used in the Upper Hunter Fine Particle Characterisation Study (Hibberd et al. 2013).

GENT stacked filter units

The GENT stacked filter unit (SFU) sampler is capable of collecting air particulate matter samples in coarse (2.2–10µm) and fine (<2.2µm) size fractions (Hopke et al. 1997). The GENT SFU uses a nominal flow rate of 16 L min^{-1} to simultaneously collect these particle size fractions on different filters. These sampler types have been used to support ion beam analysis and particle characterisation in a number of published studies (Cohen et al. 2004, 2012; Santoso et al. 2008). The cut point of 2.2µm between the two size fractions in the GENT sampler differs slightly from the standard 2.5µm used to separate fine ($PM_{2.5}$) from coarse ($PM_{2.5-10}$) particles. In addition the slope of the cut-off is sharper in the ASP than for the GENT (John & Reischl 1980; John et al. 1983), so that the GENT $PM_{2.5}$ samples probably contain a larger fraction of $PM_{2.5-10}$ than the ASP samples.

2.2.2 Sampler deployment and sampling schedule

Appropriate filter types were selected for the samplers to support the range of analytical techniques applied in the study as discussed further in the next section. Two purposely installed ANSTO ASP $PM_{2.5}$ cyclone samplers were deployed at the Newcastle site, one collecting particles on a Teflon filter and the other on a quartz filter (Figure 16, Figure 17). The reason for using different filter materials is outlined in Section 3.1. The same sampler configuration was deployed at the Beresfield site.

At the Stockton site, one GENT SFU was deployed collecting $PM_{2.5-10}$ particles on Nuclepore filters and $PM_{2.5}$ particles on quartz filters, with an ANSTO ASP $PM_{2.5}$ sampler used to collect fine particles on Teflon filters (Figure 18, Figure 19). The same sampler configuration was deployed at the Mayfield site.

Figure 16: ASP samplers (Teflon filters on left and quartz filters on right) installed at the OEH Newcastle Air Quality Monitoring Station

Figure 17: Details of the ASP Sampler at the Newcastle site being inspected by David Cohen

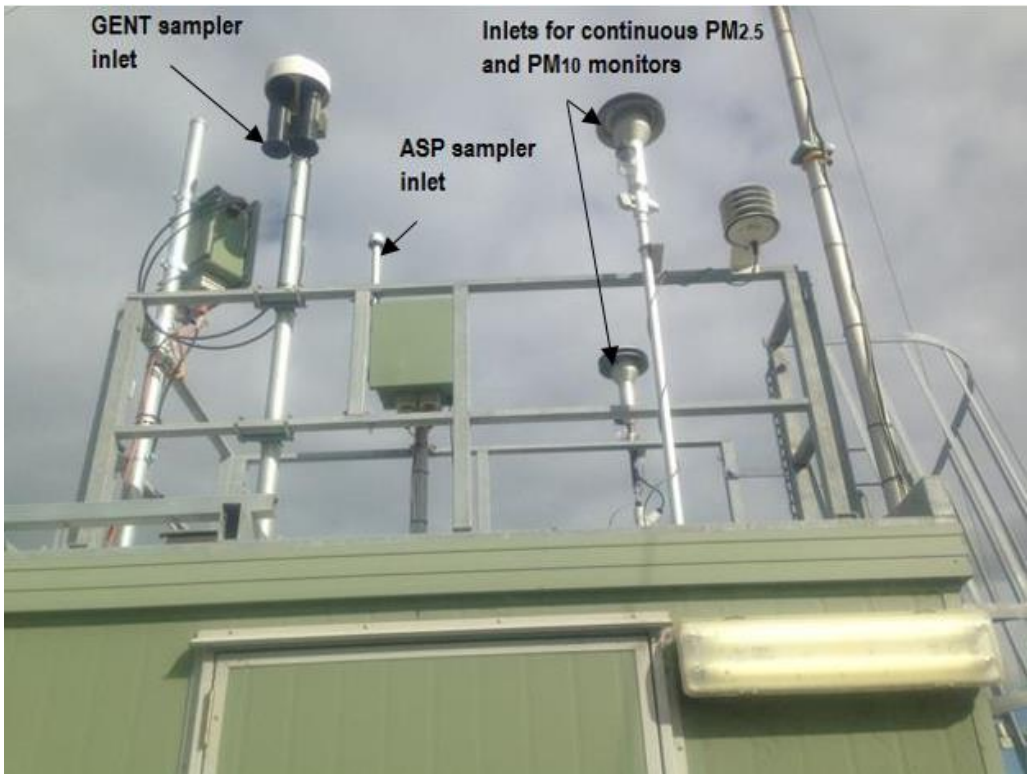

Figure 18: Identification of ASP and GENT samplers and inlets of OEH's continuous particle monitoring instruments on the roof of the Stockton Air Quality Monitoring Station

Figure 19: Details of the GENT sampler at the Stockton site being inspected by Peter Crabbe

Samplers were installed in February 2014, with the one-year sampling program starting on 2 March 2014 and ending on 28 February 2015. Samples were collected every third day over 24 hours from midnight to midnight Eastern Standard Time (with no adjustments made for Daylight Saving). The 1-in-3 day schedule was preferred over a two-day-per-week schedule to increase the representativeness and number of samples available for source apportionment.

2.2.3 Quality assurance

Procedures for sampling were trialled and tested prior to the official start of the one-year sampling program, and the procedures audited by an OEH Senior Air Quality Monitoring Officer. OEH conducted site audits at all four of the LHPCS sampling sites to confirm that samplers conformed to *AS/NZS 3580.1.1:2007 Methods for sampling and analysis of ambient air – Part 1.1: Guide to siting air monitoring equipment.* Overall it was concluded that the procedures reviewed were fit for purpose with minor amendments to sampler placement recommended in some cases to ensure compliance with Australian Standards. The recommendations from the audit report were implemented.

Control filters were routinely included with filters for sampling to identify any contamination in the sampling process. These filters were conditioned, unexposed filters that were transported to and from the site but were not exposed (i.e. they were not placed in the sampler) while at the site. Control Teflon filters were included in one batch per month while control quartz filters were included with every batch of filters.

Quartz field blanks were used every six days for the ASP $PM_{2.5}$ samplers and every 12 days for the GENT stacked filters, with the blanked values propagated in the analysis.

Field log sheets were maintained with a number of parameters recorded for each sample for use in data quality assurance, analysis and interpretation. These field log sheets were completed at each sampling site for each filter as the filters were being changed by OEH field staff. Completed log sheets were returned to the laboratory with the exposed filters.

Parameters recorded included:

- initial sample installation date and time
- final sample removal date and time
- sample run dates
- operator's name
- initial vacuum pressure (with pinch test)
- initial start flow rate
- initial vacuum pressure
- initial mass volume
- final vacuum pressure
- final mass volume
- final finish flow rate
- elapsed sampling time
- maximum and minimum temperature
- additional comments.

2.3 Ambient particulate matter (PM) during sampling period

OEH-operated air quality monitoring stations at Beresfield, Newcastle and Wallsend characterise regional air quality and provide a framework for the detailed particle characterisation study. Long-term time series of PM_{10} and $PM_{2.5}$ continuously monitored at ambient air quality stations in the region for the period October 2012 – October 2015 are shown in Figure 20 and Figure 21. Data are included from the OEH-operated monitoring stations; the Stockton station was run by Orica until 14 October 2014 following which the industry-funded, OEH-operated Stockton station was established as part of the Newcastle

Local Air Quality Monitoring Network. Table 2 lists some key statistics of the 2013 and 2014 PM_{10} and $PM_{2.5}$ results – average, median, maximum, and number of days exceeding the criteria.

The figures show much stronger regional variations in PM_{10} than $PM_{2.5}$ concentrations. The PM_{10} levels recorded at Stockton are almost always significantly higher than at the other sites and include many peaks above 50 µg m^{-3} during October to February of the study. This pattern is similar to that seen in 2012–13 and 2013–14, and as shown in Figure 31 is mainly associated with winds in the easterly sector. $PM_{2.5}$ levels measured at the Stockton monitoring station are comparable to levels measured at the OEH Beresfield and Wallsend stations for much of the year, with average and median levels only marginally higher. LHPCS sampling included days on which higher concentrations of PM_{10} occurred at Stockton.

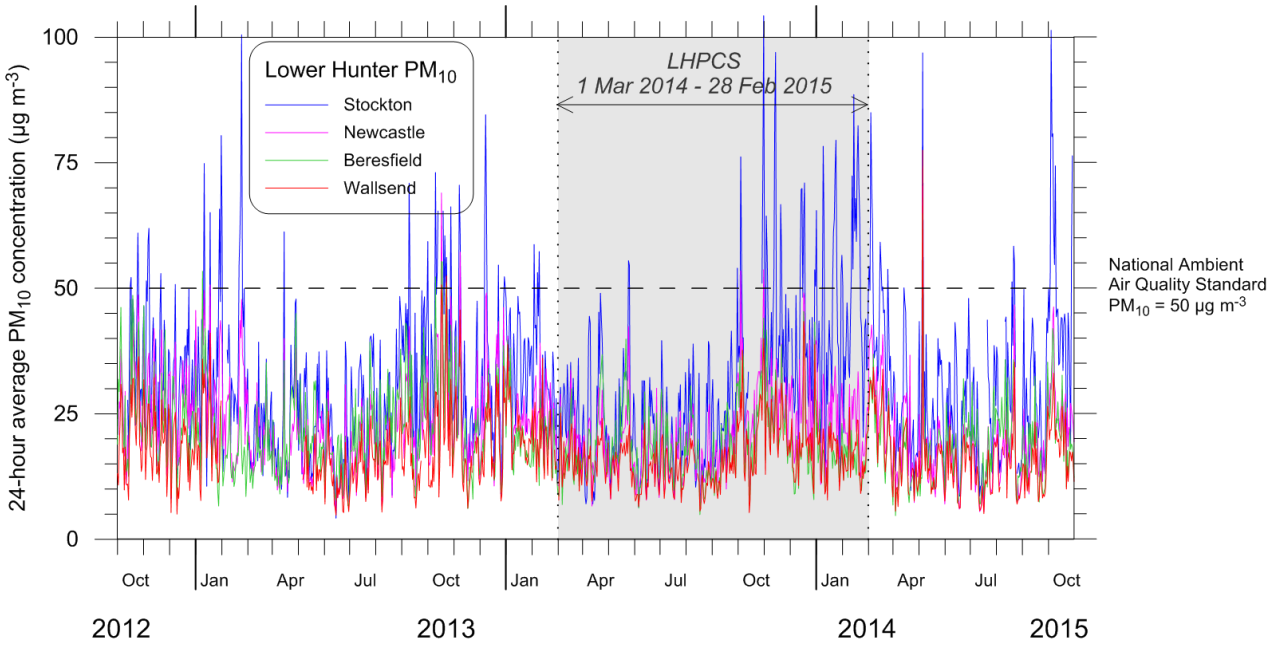

Figure 20: Long-term (Oct 2012 – Oct 2015) time series of 24-hour average PM_{10} (TEOM) concentrations recorded at the OEH lower Hunter monitoring stations

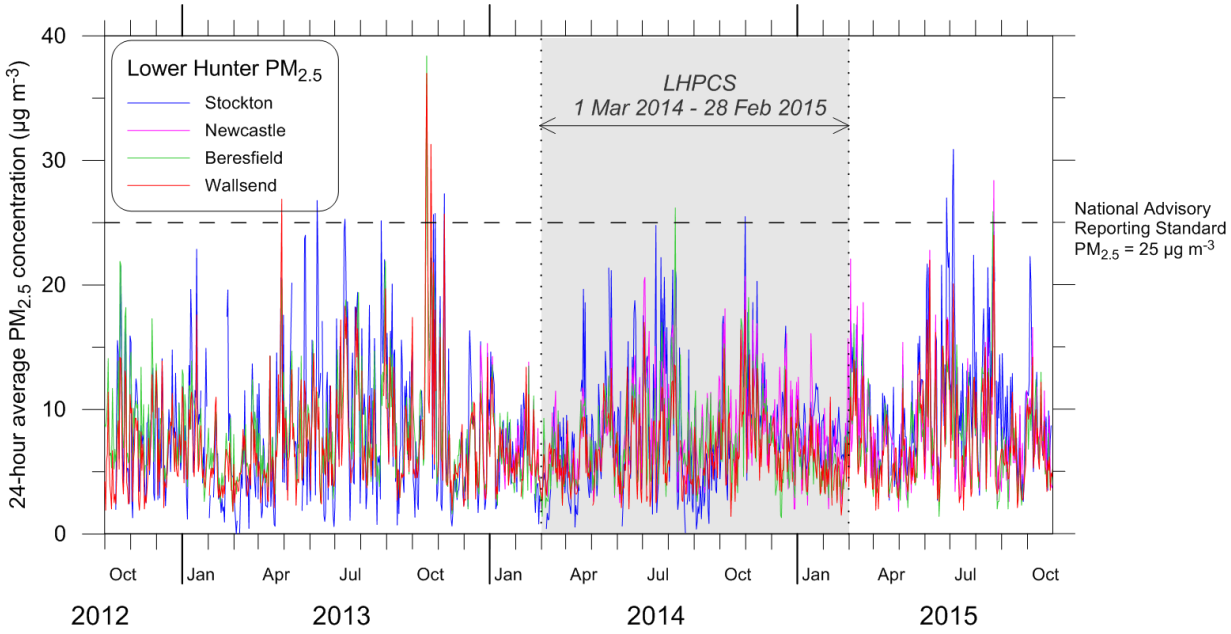

Figure 21: Long-term (Oct 2012 – Oct 2015) time series of 24-hour average $PM_{2.5}$ (BAM) concentrations recorded at the OEH lower Hunter monitoring stations

Figure 20 shows that the PM_{10} values are lowest during both March to August periods, whereas $PM_{2.5}$ are lowest in January to April (Figure 21). A clearer picture of the relative importance of the fine and coarse fractions of PM_{10} is provided by Figure 22, which shows the smoothed 31-day running average of the $PM_{2.5}/PM_{10}$ ratio at the four sites and since August 2014 for the new Mayfield site. The three years of data shows an annual trend of the $PM_{2.5}/PM_{10}$ ratio being highest in winter and lowest in summer, indicating an influence from seasonal meteorological factors such as more persistent and shallower surface inversions in winter, as well as from seasonal changes in emissions such as more domestic wood heating and more cold starts in winter. Reasons for this are explored further in subsequent sections in relation to source apportionment modelling results.

Table 2: Key statistics of the 2013 and 2014 PM_{10} and $PM_{2.5}$ OEH monitoring results

Monitoring site	Beresfield		Newcastle		Stockton		Wallsend	
	2013	2014	2013	2014	2013	2014	2013	2014
PM_{10} (µg m^{-3})								
Average	21.4	19.4	22.7	21.4	29.6	29.1	17.4	16.9
Median	19.1	18.3	20.5	20.5	26.6	27.0	15.5	16.1
Maximum	55.3	45.4	69.0	53.7	100.5	104.3	52.5	43.4
Days>50 µg m^{-3}	5	0	4	2	28	26	2	0
$PM_{2.5}$ (µg m^{-3})								
Average	8.2	7.5		8.1	8.6	8.0	7.7	6.7
Median	7.2	6.9		7.3	7.3	7.3	6.2	6.3
Maximum	38.4	26.2		20.7	32.6	25.5	37.0	18.0
Days>25 µg m^{-3}	1	1		0	7	1	6	0

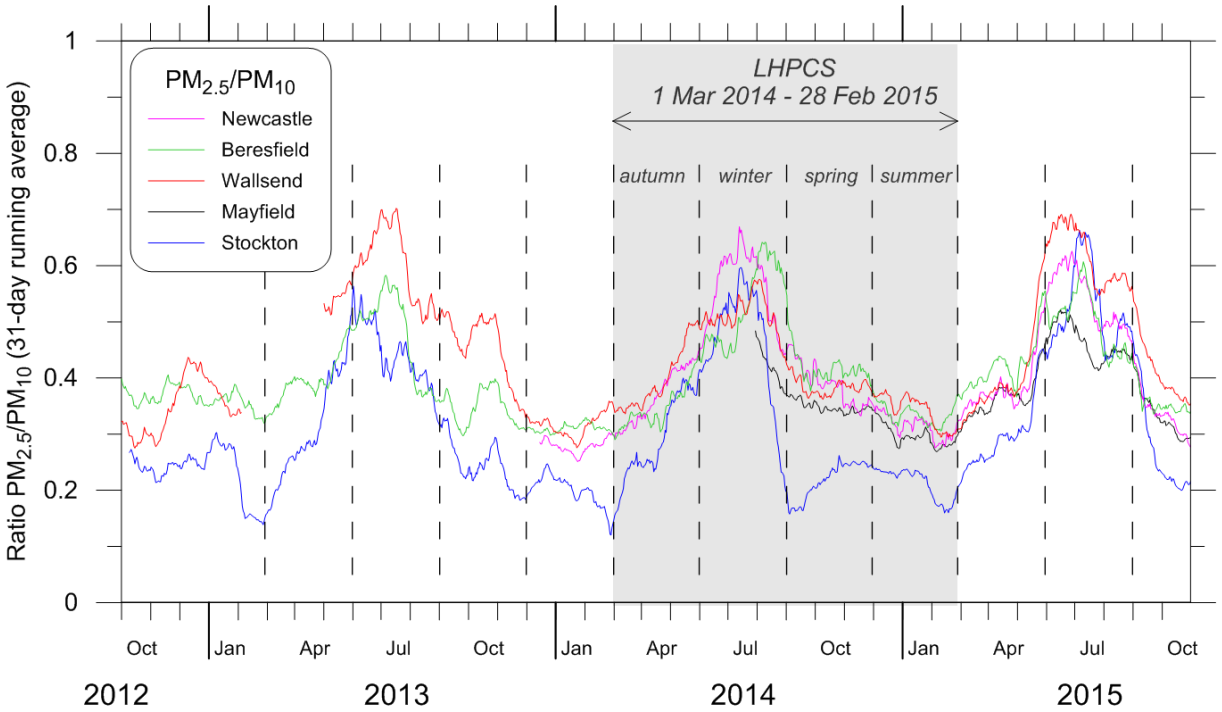

Figure 22: Long-term time series of $PM_{2.5}/PM_{10}$ ratio (31-day running average) recorded at OEH and Newcastle local air quality monitoring stations (Oct 2012 – Oct 2015)

The Stockton station was run by Orica until 14 October 2014.

Figure 23 shows the time series of 24-hour average $PM_{2.5}$ concentrations measured at the Newcastle, Beresfield, Stockton and Mayfield monitoring sites using the standard TEOM and BAM equipment during the study sampling year. The green bars highlight the days when 1-in-3-day sampling was carried out for the current study. It shows these are representative of the

full period, including days with both low and high concentrations, including the days with the highest concentrations.

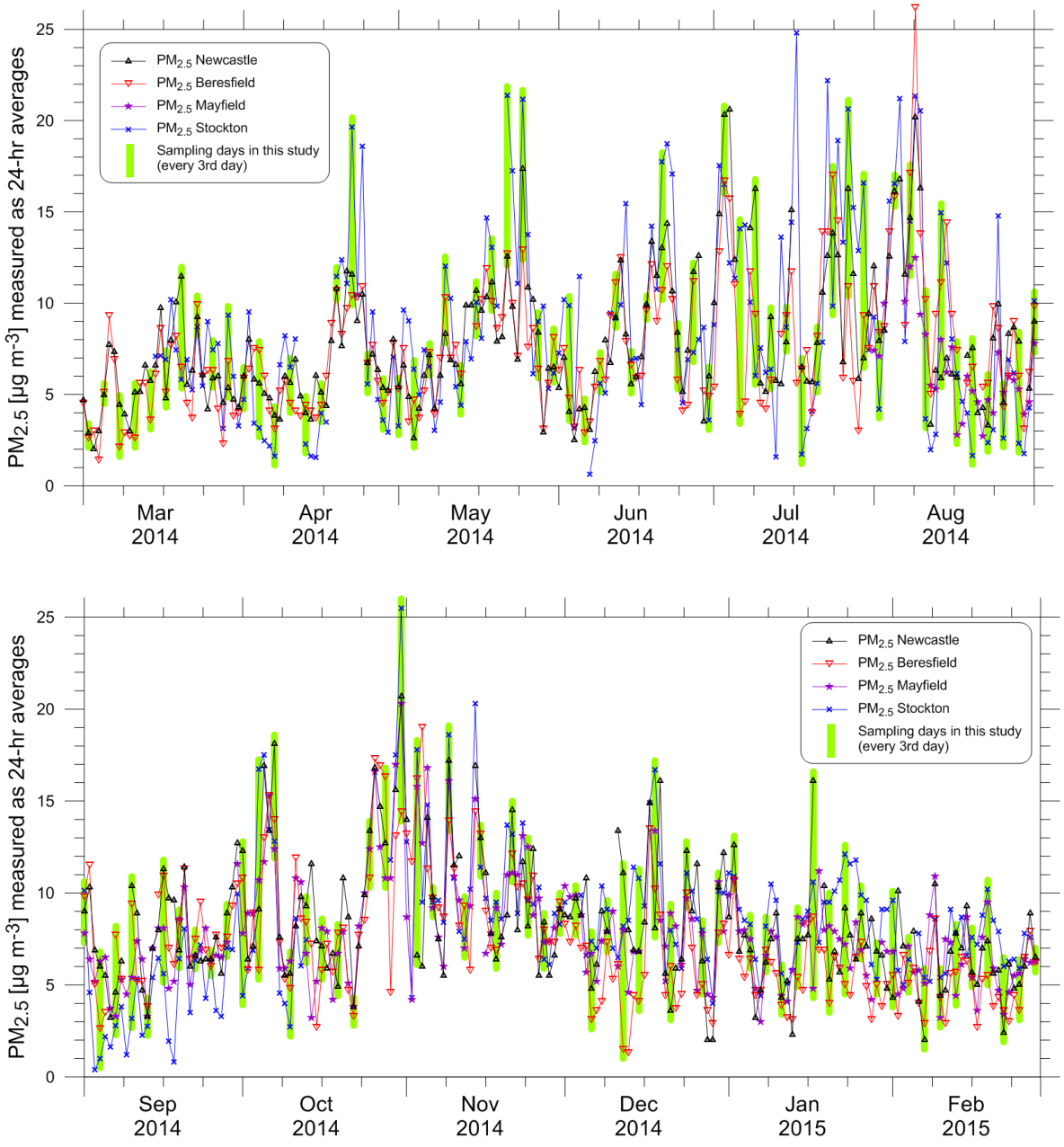

Figure 23: Time series of 24-hour average $PM_{2.5}$ concentrations measured at the Newcastle, Beresfield, Mayfield and Stockton sites using the standard BAM equipment

Figure 24 shows the equivalent results for PM_{10} concentrations. As above, the green bars highlight the days when 1-in-3-day sampling was carried out for the current study, and show these are generally representative of the full period, including days with both high and low concentrations. The most striking feature is the much higher concentrations at Stockton than at other sites, particularly during late spring and summer months.

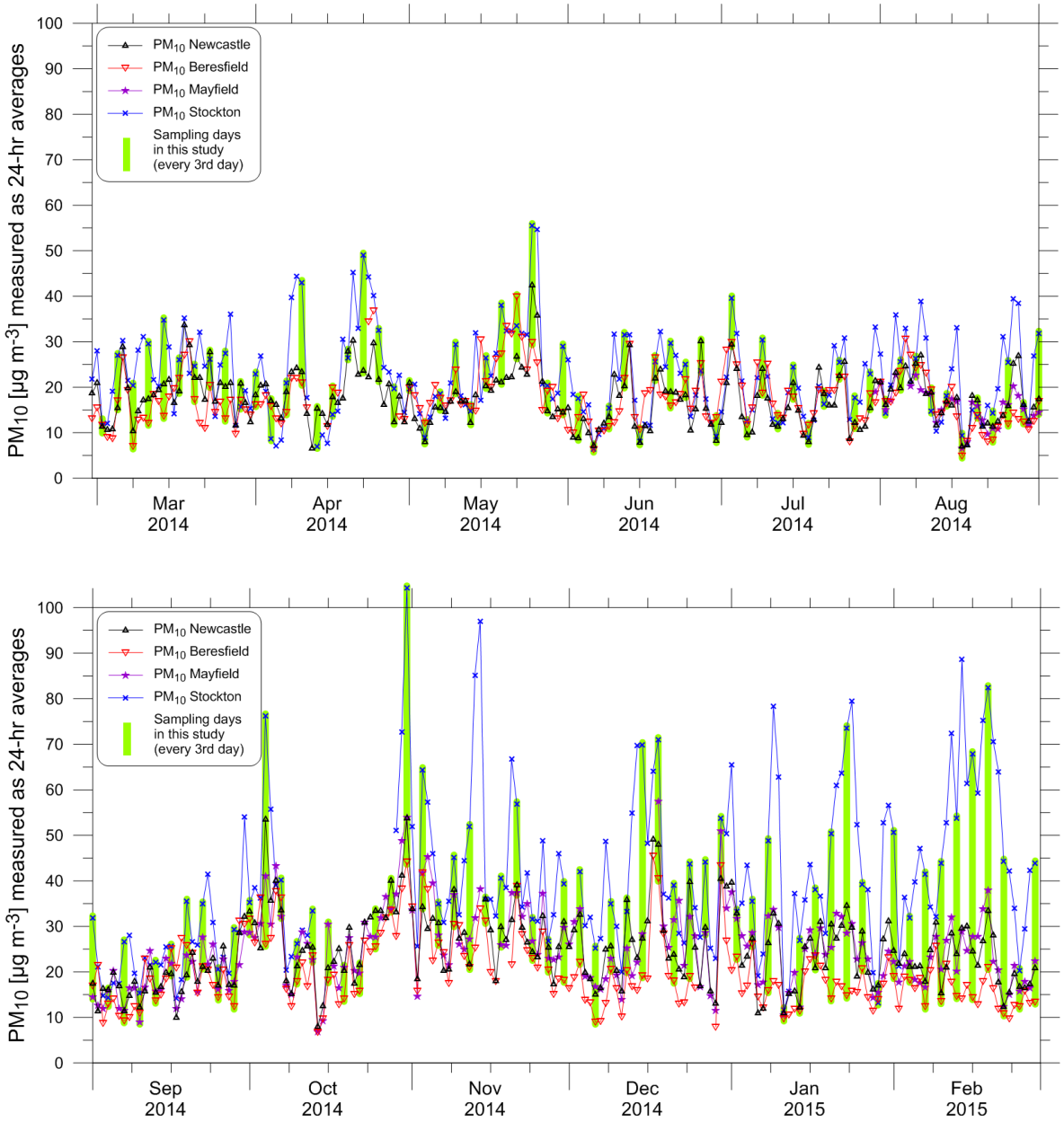

Figure 24: Time series of 24-hour average PM_{10} concentrations measured at the Newcastle, Beresfield, Mayfield, and Stockton sites using the standard TEOM equipment

2.4 Sample collection rates

The overall collection rate for each sampler at each site for the whole study was excellent – the values are listed in Table 3. At Beresfield and Newcastle, where samplers were located at existing OEH AQM stations, no samples were missed so the collection the rate was 100%. During the first quarter of the sampling year, some issues were experienced at the Mayfield site resulting in a loss of samples during the first quarter. These issues were addressed resulting in the annual collection rate being higher than 97% at Mayfield. Similarly at Stockton, there was a problem with the ASP sampler in the first quarter giving a 94% return, but the annual collection rate was 98.5% for the ASP sampler and 100% for the GENT sampler.

Table 3: Overall annual sample collection rate for the one-year study

Beresfield $PM_{2.5}$		Newcastle $PM_{2.5}$		Mayfield $PM_{2.5-10}$ & $PM_{2.5}$			Stockton $PM_{2.5-10}$ & $PM_{2.5}$		
ASP14 TEFLON	ASP15 QUARTZ	ASP12 TEFLON	ASP13 QUARTZ	ASP10 TEFLON $PM_{2.5}$	GAS44C NUCLEPORE $PM_{2.5-10}$	GAS44Q QUARTZ $PM_{2.5}$	ASP89 TEFLON $PM_{2.5}$	GAS43C NUCLEPORE $PM_{2.5-10}$	GAS43Q QUARTZ $PM_{2.5}$
100%	100%	100%	100%	97%	99%	99%	98.5%	100%	100%

2.5 Wind roses

Meteorological measurements are available for the Newcastle, Beresfield and Stockton sites for the entire sampling year, and for the Mayfield site for the latter half of the sampling year. All measurements were undertaken by OEH, with the exception of meteorological measurements for the Stockton site prior to 14 October 2014 when the site belonged to Orica.

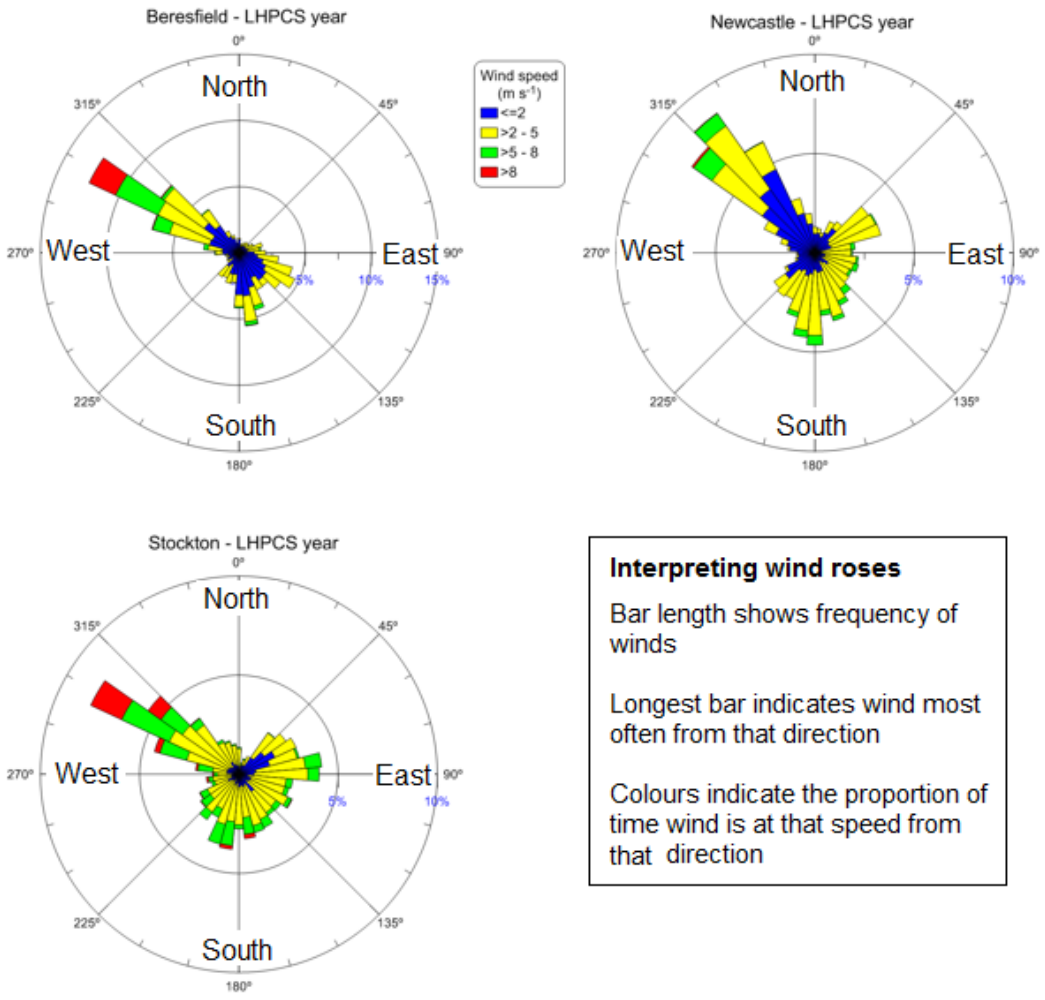

Figure 25: Annual wind roses from the study sites including data from the sample days only

Mayfield not shown because wind data was only collected there for the second half of the year.

Wind patterns are depicted as wind roses, which show the distribution of wind direction experienced at a particular site. The direction of each sector radiating from the centre is the

wind direction (the direction the wind is blowing from). Its total length is proportional to the frequency of the wind from that direction, and the proportion of each wind speed range is shown by the coloured sectors. For comparison with the sampling results, wind data were included from sampling days only.

Note there are only very minor differences between these wind roses and those computed using data from all days in the year (not shown). The prevailing wind field results from the combined influence of synoptic-scale circulation patterns and thermo-topographically induced circulation due to the coastline and local terrain. Annually, at Beresfield the prevailing winds are from the north-west and south-east quadrants (Figure 25). North-westerly quadrant wind is also prominent at Newcastle and Stockton, but the easterly component winds are more varied, ranging from north-easterly to south-easterly, and south-south-westerly winds are also apparent.

Seasonal wind roses are presented in Figure 26 (Beresfield), Figure 27 (Newcastle), Figure 28 (Mayfield), and Figure 29 (Stockton).

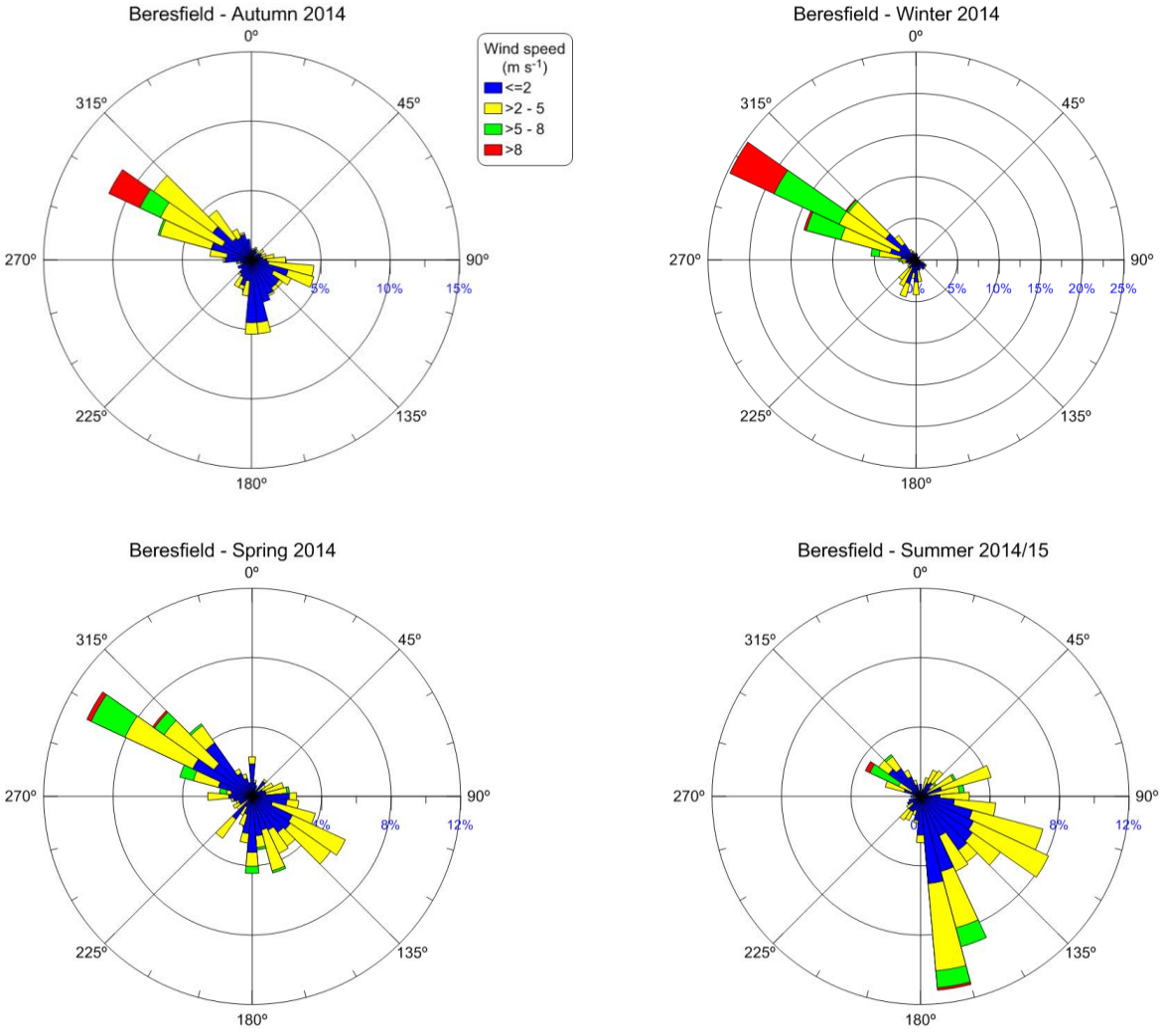

Figure 26: Seasonal wind roses from the Beresfield site (including wind data from the study sample days only)

During the winter off-shore, westerly to west-north-westerly airflow prevails over the region. The passage of disturbances such as frontal systems, cyclonic disturbances and troughs result in daily flow variations and the occasional occurrence of south-westerly airflows. During

the summer, easterly (on-shore) airflow dominates the region. Spring and autumn seasons are characterised by more varied airflow patterns, with wind from the north-western and south-eastern quadrants prevalent across much of the region.

Daily variations in airflow occur as a result of land-sea breeze circulation which is driven by differential heating and cooling of land and water surfaces. During the day, the land is heated more rapidly than the sea surface, with pressure differences resulting in surface convergence and ascent over the land and descent and surface divergence over the sea.

This results in the prevalence of on-shore (easterly component) sea breezes during the daytime, with return currents prevalent in the upper airflow. At night, more rapid cooling of the land results in a reversal of the daytime sea breeze and upper air return currents and the onset of off-shore, land breezes at the surface. Lower wind velocities and more frequent calm wind conditions occur at night-time, whereas unstable conditions and more frequent strong wind occur during the daytime. During the winter, the regional westerlies reinforce the land breezes, whereas during the late spring and summer the on-shore sea breezes are strengthened.

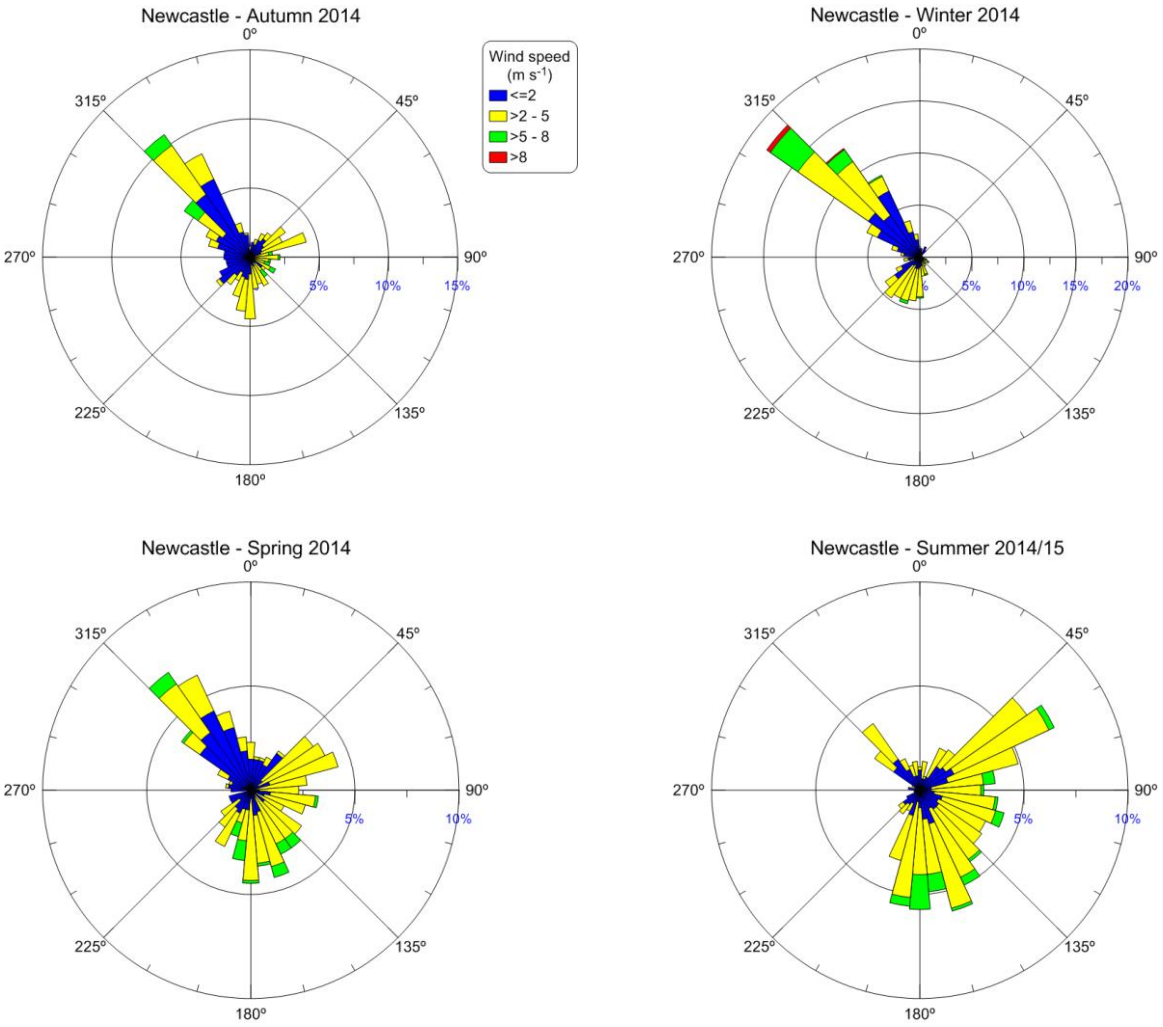

Figure 27: Seasonal wind roses from the Newcastle site (including wind data from the study sample days only)

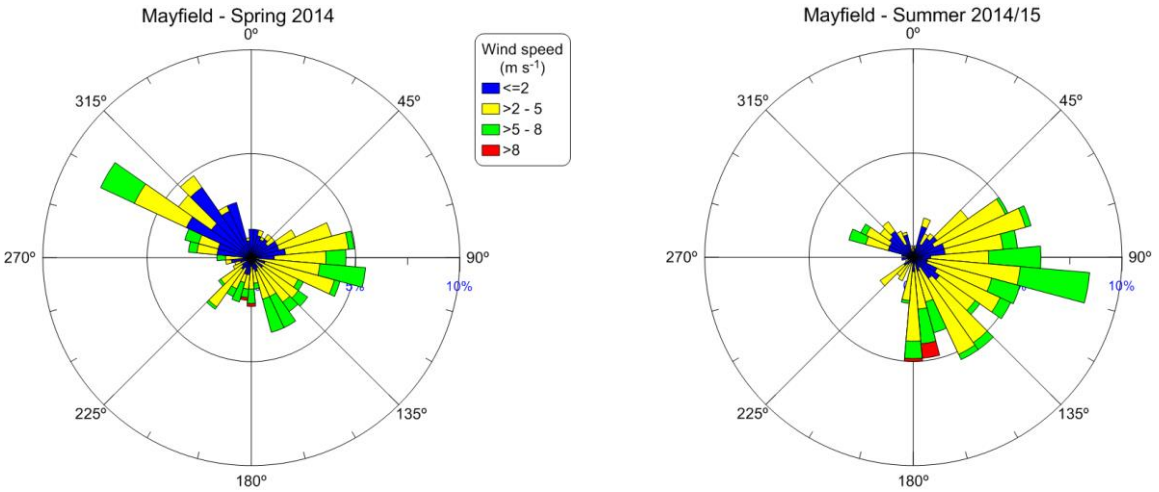

Figure 28: Seasonal wind roses from the Mayfield site (including wind data from the sample days only; data available for the second half of the study period only)

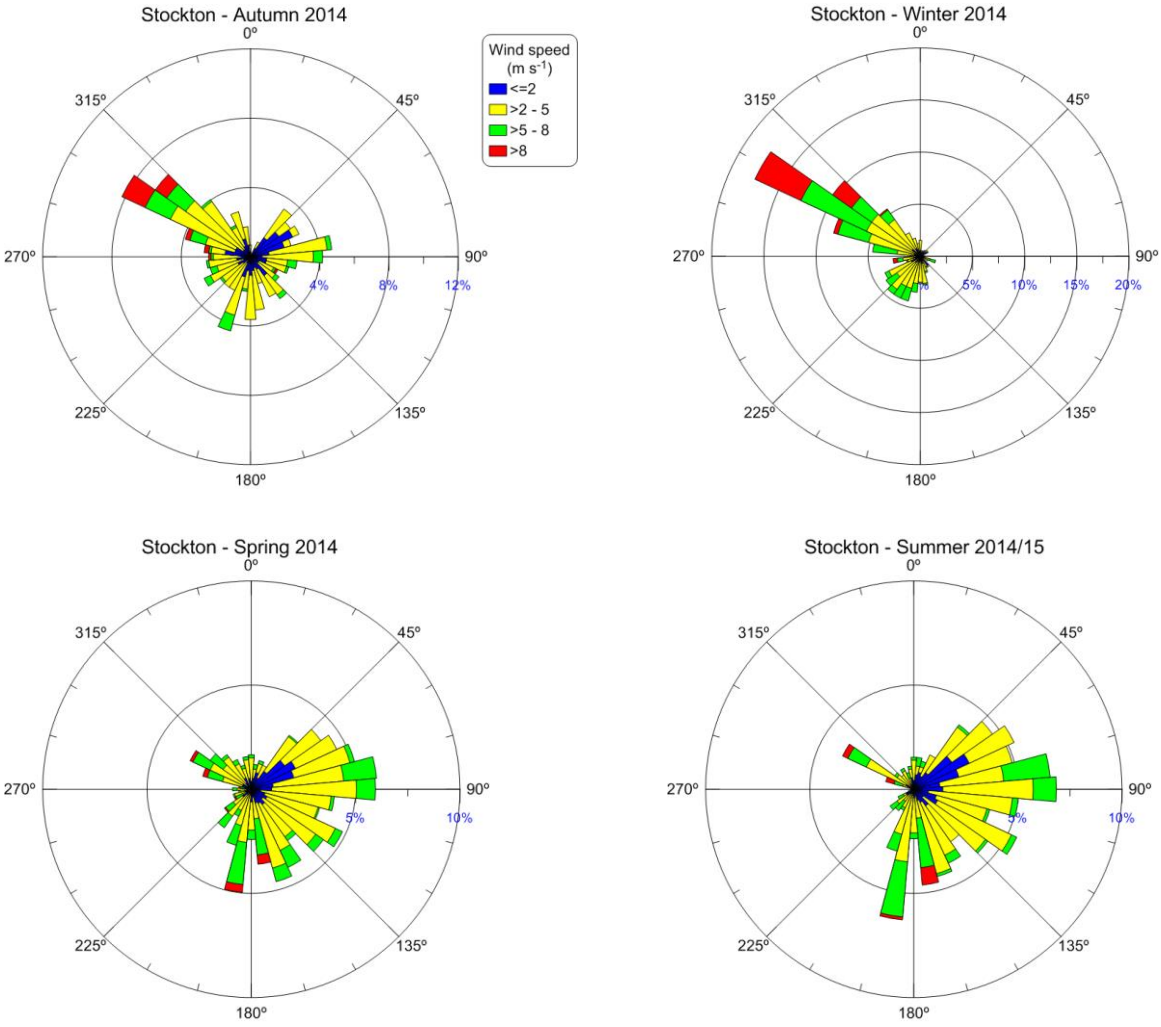

Figure 29: Seasonal wind roses from the Stockton site (including wind data from the sample days only).

2.6 Pollution roses

Pollution roses are like wind roses but they show pollution concentration instead of wind speed, and its variation with wind direction. They show the wind directions associated with the highest pollution concentrations.

Figure 31 and Figure 32 show the PM_{10} and $PM_{2.5}$ pollution roses computed using the hourly-averaged continuous monitoring data from the sampling sites but restricted to above-average concentrations, namely PM_{10} > 20 µg m^{-3} and $PM_{2.5}$ > 10 µg m^{-3}. This shows the high concentration results more clearly.

For PM_{10}, the Newcastle site shows some elevated levels for almost all wind directions. In contrast, at the Beresfield site almost all of the elevated concentrations occur with north-westerly winds, whereas at Mayfield this is the case for easterlies. At Stockton the highest proportion of elevated concentrations coincide with easterly to north-easterly winds (i.e. onshore), with some occurring with north-westerly winds.

At most sites, the $PM_{2.5}$ pollution roses show similar patterns. The biggest differences are at Stockton where most of the highest $PM_{2.5}$ concentrations are for north-westerly winds compared to easterlies for PM_{10}. Similarly at Newcastle, the highest $PM_{2.5}$ concentrations occur in north-westerly wind conditions.

In all case, there is suitably close agreement between the results for the 1-day-in-3 sampling days (right-hand side of each pair) and those for the full year (left-hand side), which confirms the representativeness of the sampling days.

2.7 Rainfall

Reference was made to rainfall records from the Bureau of Meteorology's station at Newcastle University (station number 61390) to show the extent of rainfall experienced during the study period relative to rainfall statistics for the 2001 to 2015 period (Figure 30, no rainfall data available for March 2014 for this station). Above-average rainfall was recorded in August, December and January during the study period, with below-average rainfall occurring in February, May, June, July and November. The remaining months (April, September and October) experienced rainfall amounts similar to the longer term average. Overall rainfall during the study period was marginally lower than the long-term average annual rainfall.

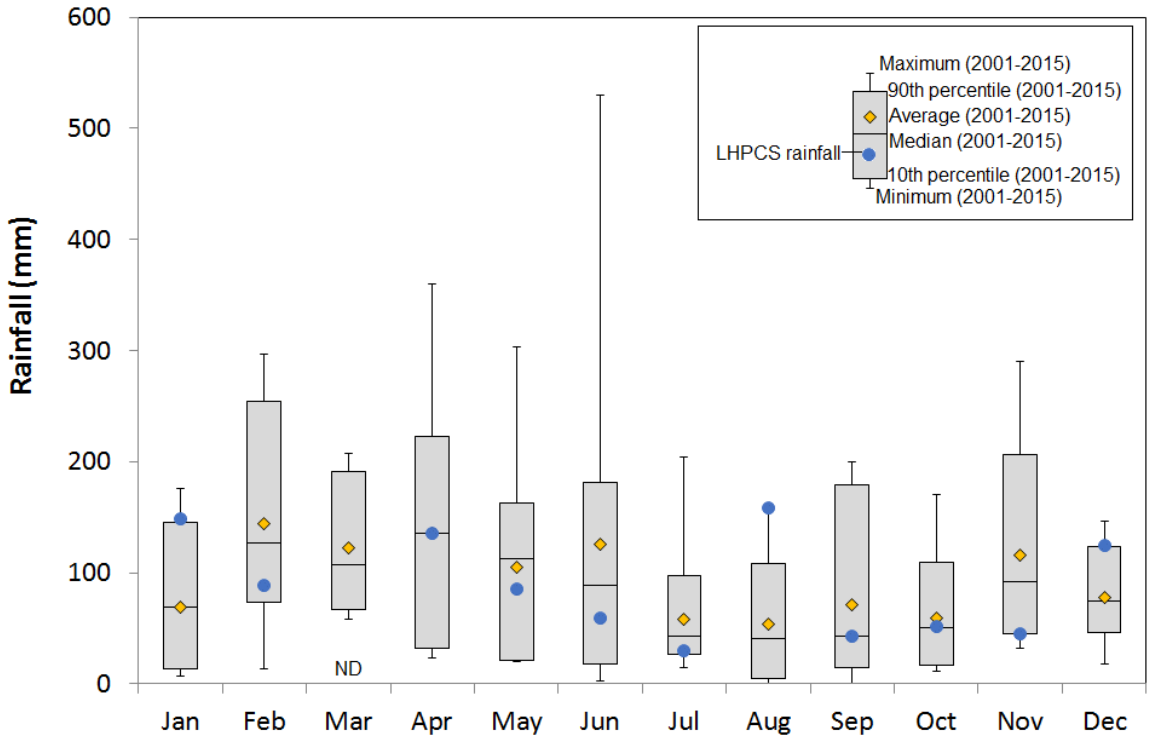

Figure 30: Comparison of rainfall recorded during the study period (March 2014 to February 2015) with rainfall statistics for the January 2001 to December 2015 period, as recorded at the Bureau of Meteorology's Newcastle University station

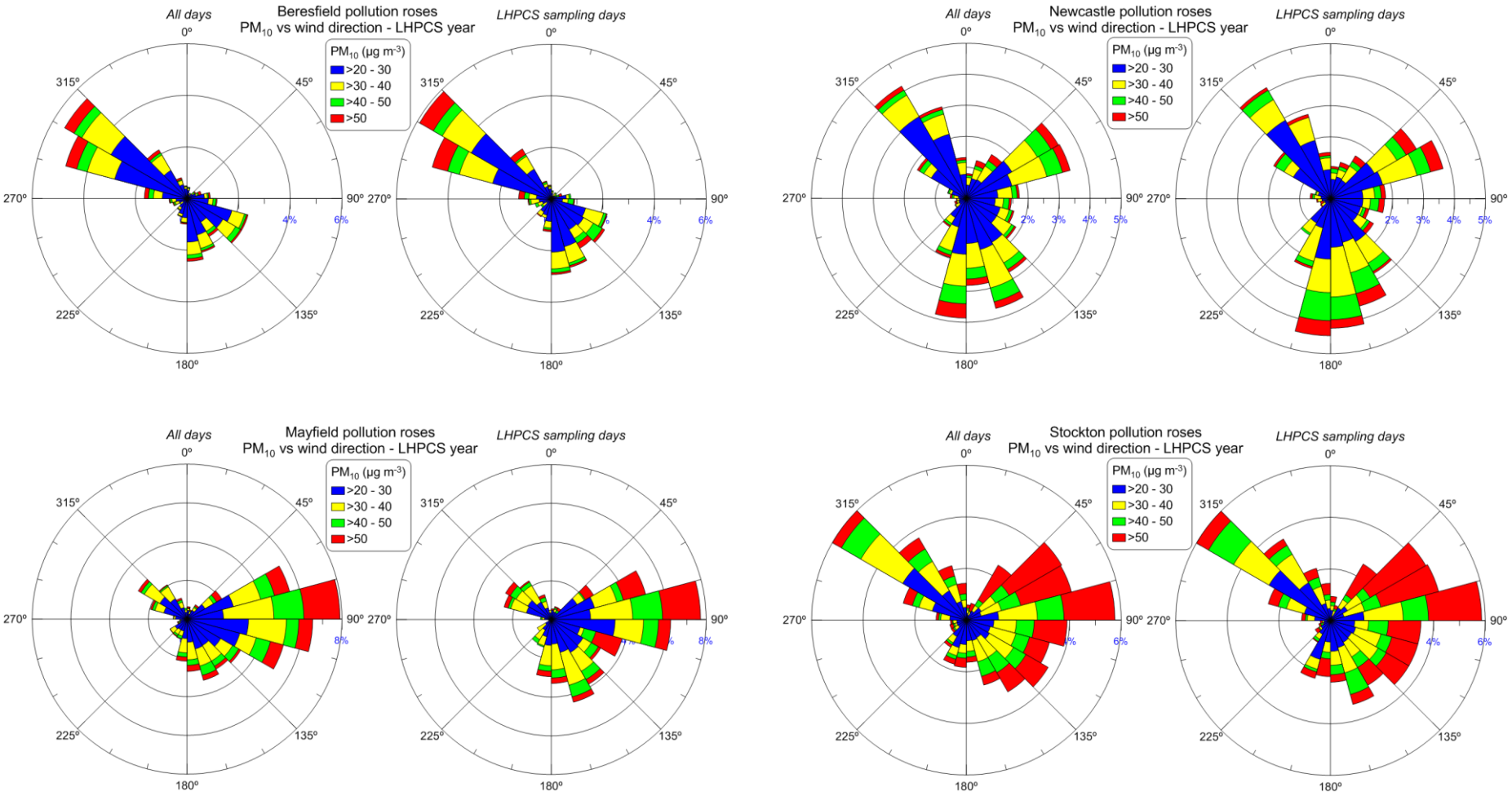

Figure 31: PM_{10} pollution roses for PM_{10} > 20 µg m^{-3} for the study period at Newcastle, Beresfield and Stockton showing close agreement between all days (left-hand side) and the 1-day-in-3 sampling days (right-hand side)

Note: these pollution roses depict the distribution of PM_{10} concentrations at each wind direction.

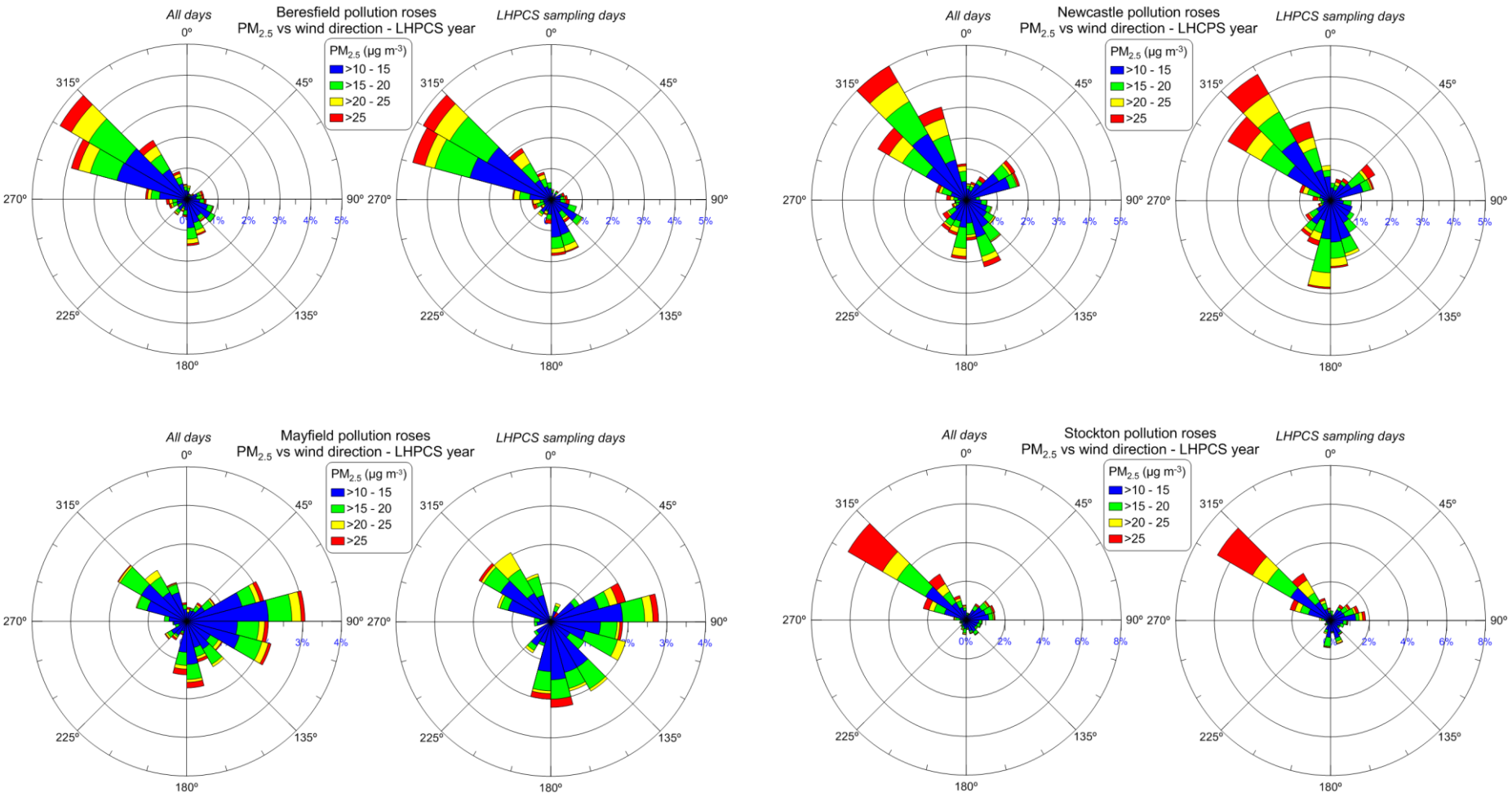

Figure 32: $PM_{2.5}$ pollution roses for $PM_{2.5}$ > 10 µg m^{-3} for the study period at Newcastle, Beresfield and Stockton showing close agreement between all days (left-hand side) and the 1-day-in-3 sampling days (right-hand side)

Note: these pollution roses depict the distribution of $PM_{2.5}$ concentrations at each wind direction.

2.8 Events log

Information on air pollution events such as bushfires, hazard reduction burns and anomalous industrial emissions occurring during the LHPCS sampling year were logged to assist data analysis and result interpretation. Information on time periods when regular air pollution emissions are absent is also useful. To capture information on air pollution events that could impact on the LHPCS, an events register was maintained. This register includes information from a variety of sources including the EPA's Environment Line, the NSW Rural Fire Service (RFS) ICON fire incident database and eye witness reports.

2.9 Summary

The sampling program was completed successfully. An overall sample collection rate of 99–100% was achieved, and sampling days generally coinciding with low, high and average ambient particle concentration measurements across all sampling sites. There were no significant issues with filter shipping or analysis of the filter samples. Supplementary information collected included continuous air pollution and meteorological measurements from OEH air quality monitoring stations and information on air pollution events.

3 Methodology

This section provides an overview of the sample analysis undertaken for the fine ($PM_{2.5}$) and coarse ($PM_{2.5-10}$) samples (Section 3.1), a brief description of the receptor modelling method applied to the chemical composition of all samples, which was used to identify factors and their contributions to the total fine and coarse particle concentrations (Section 3.2). The key source of emissions in each factor was identified using a range of information including wind sector analysis using a conditional probability function approach outlined in Section 3.3. The trajectory modelling method applied for case study periods to investigate air mass movements on days when certain factors had higher contributions is described briefly in Section 3.4. The section finishes with an overview of the chemical transport modelling method (Section 3.5) used to model chemical transport and particle dynamics, with details of the method and results presented in a supplementary report (Emmerson et al. 2016).

3.1 Filter analysis

3.1.1 Filter types

Appropriate filter types were selected based on the analytical techniques to be applied in the study, which include ion beam analysis (IBA) techniques, ion chromatography (IC), organic and elemental carbon (OC/EC) analysis using a DRI Model 2001A thermal-optical carbon analyser, and the laser integrated plate method (LIPM) for measuring equivalent black carbon (EBC). Teflon and Nuclepore filters are appropriate for IBA, LIPM and IC analysis, whereas quartz filters are required for OC/EC analysis with the DRI analyser.

The overall sampling program was described in the previous section. Samplers and types of filters used in the study to support chemical analysis and source apportionment were as follows:

- two purposely installed ANSTO ASP $PM_{2.5}$ cyclone samplers at the **Newcastle site**, one collecting particles on a Teflon filter (for IBA, LIPM and IC analysis) and the other on a quartz filter (for EC/OC analysis)
- two purposely installed ANSTO ASP $PM_{2.5}$ cyclone samplers at the **Beresfield site**, one collecting particles on a Teflon filter (for IBA, LIPM and IC analysis) and the other on a quartz filter (for EC/OC analysis)
- one GENT SFU at the **Mayfield site**, collecting $PM_{2.5-10}$ particles on a Nuclepore filter (for IBA, LIPM and IC analysis) and $PM_{2.5}$ particles on a quartz filter (for EC/OC analysis)
- relocation of the existing ANSTO ASP $PM_{2.5}$ sampler collecting particles on Teflon filters from the Steel River monitoring station to the **Mayfield site**. Results from the IBA conducted on these filters by ANSTO (funded by EPA) was integrated into the study, with further (IC) analysis conducted on the filters by CSIRO
- one GENT SFU at the **Stockton site**, collecting $PM_{2.5-10}$ particles on a Nuclepore filter (for IBA, LIPM and IC analysis) and $PM_{2.5}$ particles on a quartz filter (for EC/OC analysis)
- integration of results from the IBA conducted on the ASP $PM_{2.5}$ sampler Teflon filters from the **Stockton site** by ANSTO (funded by Orica) into the study, with further (IC) analysis conducted on the filters by CSIRO.

As mentioned in Section 2.2.1, the cut point for the GENT sampler of 2.2µm between the two size fractions differs slightly from the standard 2.5µm used to separate fine ($PM_{2.5}$) from

coarse ($PM_{2.5-10}$) particles. As this point is located in the dip in the size distribution between the fine and coarse modes (e.g. Figure 33), it is not expected to have a significant impact on the results. Thus although the coarse fraction reported in this study is actually $PM_{2.2-10}$, for consistency with common terminology, we refer to it here as $PM_{2.5-10}$. The typical cut-off curves for $PM_{2.5}$ and PM_{10} size-selective inlets are also shown in Figure 33.

For the fine fraction, most of the speciation is from the ASP filters which have a 2.5µm cut-off, but the EC/OC measurements are from the fine GENT filter with the 2.2µm cut-off. This is not expected to affect these results because most OC and EC in $PM_{2.5}$ is usually in the submicron size range. Thus we also use the common terminology and refer to all the fine fraction results as $PM_{2.5}$.

In this report we have not added results for the fine and coarse fractions to present PM_{10} results, both because of this difference in cut-points but more importantly because the processes associated with emissions, chemical transformations and dispersion of PM_{10} are much easier to understand when the fine and coarse fractions are considered separately. (The one exception is in a brief comparison of the LHPCS concentration measurements with those from the OEH Air Quality Monitoring Network in Section 4.1.3.)

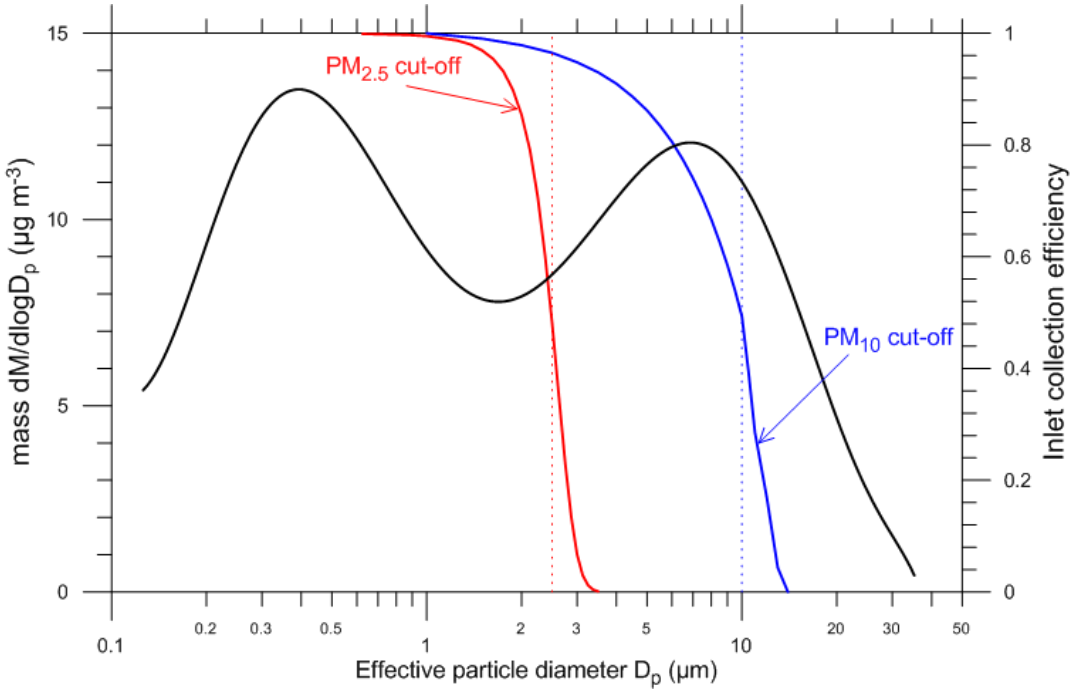

Figure 33: Size distribution measured at Liverpool in Sydney during the Australian Fine Particle Study (Keywood, pers. comm.) with size-selective inlet cut-offs for $PM_{2.5}$ and PM_{10}

3.1.2 Ion beam analysis (IBA)

The Teflon and Nuclepore filters were analysed non-destructively on the ANSTO STAR 2MV accelerator using nuclear IBA techniques.

The simultaneous IBA techniques applied were:

- proton induced X-ray emission (PIXE) – for analysis of elements from aluminium to lead in concentrations from a few ng m^{-3} upwards, as described in Cohen (1993)
- proton induced gamma-ray emission (PIGE) – for analysis of light elements such as fluorine and sodium in concentrations above 100 ng m^{-3}, as described in Cohen (1998)

- proton elastic scattering analysis (PESA) – for analysis of hydrogen at levels down to 20 ng m^{-3}, as described in Cohen (1996).

A full description of these methods and how they are used can be found on the ANSTO webpage at www.ansto.gov.au/ResearchHub/IER/Capabilities/IBA/index.htm together with key publications describing other fine particle studies at ANSTO.

The elements whose concentrations were determined are:

- hydrogen (H)
- sodium (Na)
- aluminium (Al)
- silicon (Si)
- phosphorous (P)
- sulfur (S)
- chlorine (Cl)
- potassium (K)
- calcium (Ca)
- titanium (Ti)
- vanadium (V)
- chromium (Cr)
- manganese (Mn)
- iron (Fe)
- cobalt (Co)
- nickel (Ni)
- copper (Cu)
- zinc (Zn)
- bromine (Br)
- lead (Pb).

3.1.3 Ion chromatography (IC)

The Teflon and Nuclepore filters were analysed for major water-soluble ions by suppressed ion chromatography (IC) and carbohydrates, including levoglucosan, by high-performance anion-exchange chromatography with pulsed amperometric detection (HPAEC-PAD). The Nuclepore filters were extracted in 10ml of 18.2mΩ de-ionized water and the sample was then preserved using 1% chloroform. The Teflon filter was first wetted with 100µl of methanol, extracted in 5ml of 18.2mΩ de-ionized water and then preserved with 1% chloroform.

Anion and cation concentrations were determined with a Dionex ICS-3000 reagent free ion chromatograph. Anions were separated using a Dionex AS17c analytical column (2 x 250mm), an AERS-500 suppressor and a gradient eluent of 0.75mM to 35mM potassium hydroxide. Cations were separated using a Dionex CS12a column (2 x 250mm), a CERS-500 suppressor and an isocratic eluent of 20 mM methanesulfonic acid.

Carbohydrate concentrations were determined by HPAEC-PAD with a Dionex ICS-3000 chromatograph with electrochemical detection. The electrochemical detector utilises disposable gold electrodes and is operated in the integrating (pulsed) amperometric mode using the carbohydrate (standard quad) waveform. Carbohydrates were separated using a Dionex CarboPac MA 1 analytical column (4 x 250mm) with a gradient eluent of 300mM to 550mM sodium hydroxide.

The species whose concentrations were determined are:

- chloride (Cl^-)
- nitrate (NO_3^-)
- sulfate (SO_4^{2-})
- oxalate ($C_2O_4^-$)
- formate ($HCOO^-$)
- acetate (CH_3COO^-)
- phosphate (PO_4^{3-})
- methanosulfonate (MSA^-)
- sodium (Na^+)
- ammonium (NH_4^+)
- magnesium (Mg^{2+})
- calcium ($Ca^{2+)}$
- potassium (K^+)
- levoglucosan ($C_6H_{10}O_5$, an anhydrous sugar–woodsmoke tracer)
- mannosan ($C_6H_{10}O_5$, an anhydrous sugar–woodsmoke tracer)
- arabitol
- mannitol.

3.1.4 Organic and elemental carbon (OC, EC)

The carbon in $PM_{2.5}$ is analysed to obtain two separate components – organic carbon and elemental carbon – because different sources emit different types of carbon.

Organic carbon (OC) is the carbon in organic compounds in $PM_{2.5}$. In practice this includes most compounds that contain carbon, excluding particles that are just elemental carbon. Coal particles are primarily organic carbon but with most particles larger than 1µm. Organic carbon can be emitted directly by sources as primary particles or formed in the air by chemical reactions and referred to as secondary particles or secondary organic aerosols (SOA). Sources of organic carbon include traffic and industrial combustion, non-road diesel equipment and transport (including locomotives), biomass burning, cooking, biogenic sources of secondary organic aerosols and primary organics from sea spray. Some of these sources also emit elemental carbon.

Elemental carbon (EC) is formally defined as a substance containing only carbon, not bound to other elements. It is principally emitted during the combustion of fossil fuels (e.g. motor vehicles, power stations, industrial boilers, non-road diesel equipment and transport including diesel-electric locomotives) and biomass burning (e.g. bushfires and domestic wood-burning heaters). Although elemental carbon is emitted as primary particles from incomplete combustion, these small, sooty particles absorb organic vapours when combustion products cool down, and often occur in air as particles with other chemicals attached to their surface. Soot therefore includes a mixture of elemental and organic carbon. Some sources emit both organic and elemental carbon, with the ratio of these components varying by source type. This can be used to provide further information for source identification.

Elemental and organic carbon analysis was performed using a DRI Model 2001A thermal-optical carbon analyser following the IMPROVE-A temperature protocol (Chow et al. 2007). Laser reflectance is used to correct for charring, since reflectance has been shown to be less sensitive to the composition and extent of primary organic carbon. Prior to analysis of filter samples, the sample was baked in an oven to 910°C for 10 minutes to remove residual carbon. System blank levels were then tested until < 0.20 $\mu g\ C\ cm^{-2}$ was reported (with repeat oven baking if necessary). Twice daily calibration checks were performed to monitor possible catalyst degeneration. The analyser was reported to effectively measure carbon concentrations between 0.05–750 $\mu g\ C\ cm^{-2}$, with uncertainties in OC and EC of ± 10%.

The IMPROVE-A carbon method measures four OC fractions at four non-oxidizing heat ramps (OC1 at 140°C, OC2 at 280°C, OC3 at 480°C, OC4 at 580°C) and three EC fractions at three oxidizing heat ramps (EC1 at 580°C, EC2 at 740°C, EC3 at 840°C). The quartz filter sample was held at the target temperature until all carbon was desorbed at that fraction. During the non-oxidizing heat ramps some of the OC can be pyrolyzed and will not desorb until the oxidized stages. The quantity of OC that was pyrolyzed (OCpyro) during the non-oxidizing heat ramps was determined based on the time the reflectance of the filter rises back up to its initial value. Total OC was then calculated from the addition of all the OC fractions plus OCpyro. Total EC was calculated from the addition of all the EC fractions minus OCpyro.

3.1.5 Black carbon (BC) and light-absorbing carbon (LAC)

Black carbon (BC) is formally defined as a term to describe a light-absorbing substance composed of carbon (Petzold et al. 2013), i.e. it is defined with reference to an optical measurement method. The term BC is also widely used to describe PM emitted mainly during the combustion of fossil fuels (e.g. motor vehicles, power stations, industrial boilers, non-road diesel equipment and transport including diesel-electric locomotives) and biomass burning (e.g. bushfires and domestic wood-burning heaters) (EEA 2013). These definitions are not necessarily equivalent, one describing a measurement method, the other a type of particle. Note that the fine particles from combustion are often described as soot (see the description in Section 3.1.4), but this is not necessarily the same as what is measured as black carbon.

In a recent review to clarify terminology, Petzold et al. (2013) describe the confusion arising from differing uses of terminology and recommend that the term **equivalent black carbon (EBC)** be used instead of black carbon when the measurement is based on an optical absorption method. This is because the mass absorption coefficient needed to convert the measured light absorption to mass concentration depends on particle size, shape and the presence of other non-carbonaceous material.

Equivalent black carbon measured by the optical method is often used as a surrogate measure for EC, which is usually measured with thermal-optical methods as described above, but it is important to also note that the measurement techniques are not strictly equivalent. In the $PM_{2.5}$ fraction, the correspondence is often reasonable, but in the coarser $PM_{2.5\text{-}10}$ fraction, it is much better to refer to the measurement from the light absorption technique as **light-absorbing carbon (LAC)** to avoid any confusion with black carbon or soot.

ANSTO measured equivalent black carbon (EBC) on the 25mm Teflon filters using a light-absorption technique called the laser integrated plate method (LIPM). For LIPM measurements, light from a HeNe laser (wavelength 633nm) is diffused and collimated to give a uniform beam across the Teflon filter. The transmitted signal intensity is measured using a photodiode detector on each filter before and after exposure. The EBC concentration is estimated from these two transmission measurements assuming a mass absorption coefficient value for carbon particles of 7 $m^2\ g^{-1}$ for $PM_{2.5}$, which has been well-established for Australian conditions, see also Figure 34. Full details can be found in a publication by Taha et al. (2007).

Equivalent black carbon concentrations generally agree well with elemental carbon concentrations (US EPA 2012) but differences arise because the two techniques each measure different but related properties of the carbon. A scatter plot of the EBC and EC measurements from this study is shown in Figure 134 in Appendix B. The offset of non-zero EBC probably indicates contributions from other constituents such as soil dust, which also absorbs light. For the $PM_{2.5}$ source apportionment purposes in this study, the EC measurements rather than the EBC data have been used.

There is much more uncertainty in the value of the mass absorption coefficient for $PM_{2.5-10}$ with the theoretical value for spherical particles showing strong size dependence but on average they are an order of magnitude smaller. Figure 34 shows the dependence reported by Taha et al. (2007). The established value of ε = 7 for $PM_{2.5}$ is due to most of the particles being in the submicron range. For $PM_{2.5-10}$, the curve indicates a range for ε of 0.2–0.8 with the mid-point at about 0.35. However, Cohen et al. (2000) reported a value of 1.4 $m^2\ g^{-1}$ for graphite dust with an average diameter of 3µm, which is double the value on the curve. Thus, a value of 0.7 $m^2\ g^{-1}$ was used for $PM_{2.5-10}$. But note there is considerable uncertainty in this value, possibly up to a factor of 2.

Coal particles from non-combustion sources, which are typically larger than 2.5µm in diameter, would contribute to light-absorbing carbon measured in the coarse $PM_{2.5-10}$.

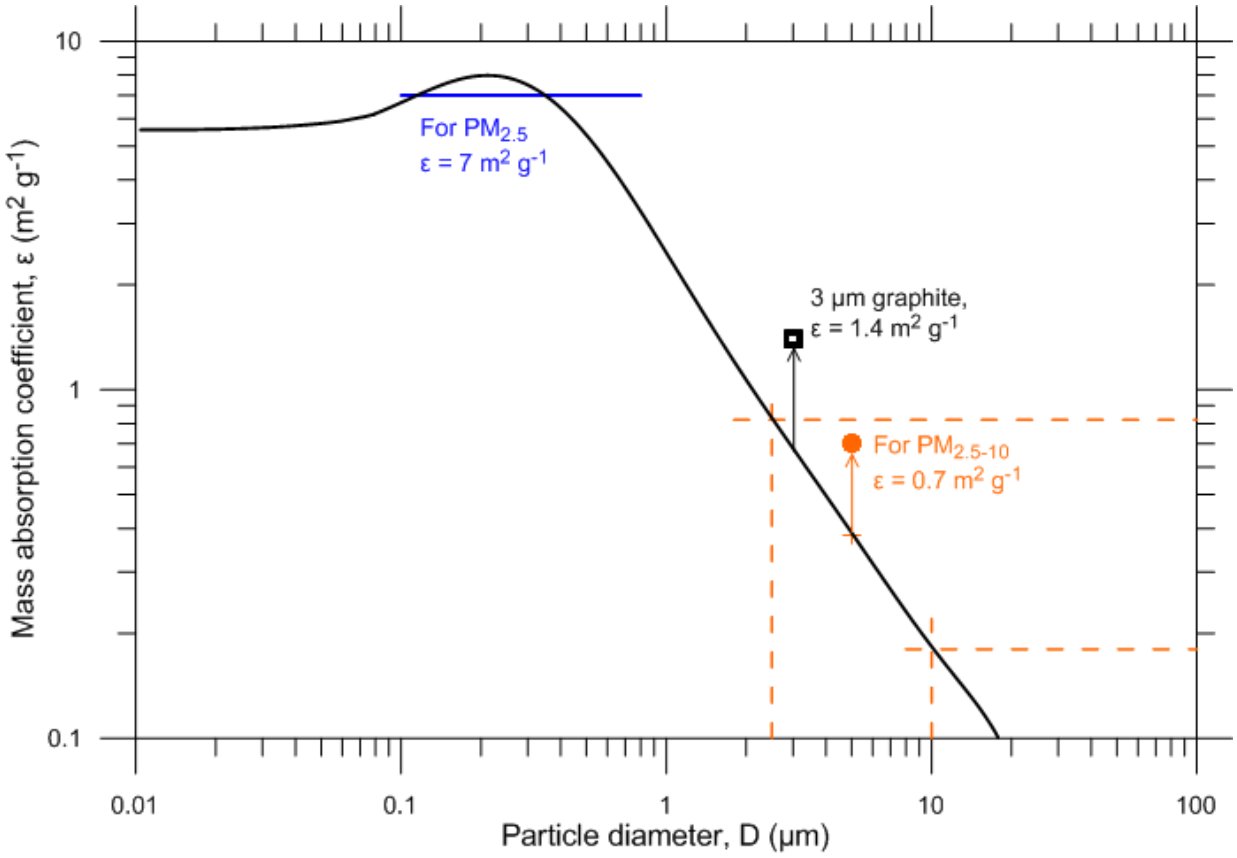

Figure 34: Mass absorption coefficient, *ε*, as a function of particle diameter at wavelength of 630nm (adapted from Taha et al. 2007). See text for description

3.2 Receptor modelling (PMF)

Positive matrix factorisation (PMF) is a type of receptor modelling. It uses observations at a monitoring site (receptor) as the input data to a mathematical model to determine the factors (similar to sources) contributing to the pollution. It is also referred to as a source apportionment technique because its goal is to resolve a mixture of sources that contribute to the sample and to apportion the relative contribution of each. The method is described in greater detail by Paatero (1997).

PMF requires large numbers of samples with variations in the relative contributions from each source to produce reliable results. This study collected over 100 samples at each site over a full year to satisfy this requirement and to be able to discern seasonal variations.

PMF is widely used in air pollution studies for source apportionment, including in Australia (e.g. Chan et al. 2008; Cohen et al. 2011; Cohen et al. 2012; Hibberd et al. 2013). The US EPA has developed a software package to implement this technique and EPA PMF 5.0 (Norris & Duvall 2014) was used for this study. Analysis was also undertaken by ANSTO using PMF2 DOS in order to assist in confirming the analysis.

In the main analysis for this study, the chemical composition data of all the samples from each site was analysed using the EPA PMF software. This identified a number of factors. Each factor has a 'fingerprint' which represent a mix of components that generally occur together in the data. To understand what this means, consider a simplified example of fine particles of sea salt in the air formed from sea spray. The ratio of the concentrations of the main elements in sea water is well known – the ratio of [Na:Cl:Mg:Ca] is equal to [1.0:1.8:0.12:0.04]. Thus on days when there are fine sea salt particles in the $PM_{2.5}$, the chemical analysis of the filters will show these elements occurring together in the above proportions. On some days, the concentrations will all be higher and on other days lower but the proportions will stay the same. It is this principal that underlies PMF.

PMF is a mathematical technique to identify the factors. Once the factors are obtained, further analysis is undertaken to identify the source(s) in each factor. This is done using information about the species in the factor and any seasonal variation, measured source profile information, wind direction analysis, emissions inventories, and knowledge of atmospheric chemistry and dispersion, etc. (e.g. Norris & Duvall 2014). In some cases, there is a single dominant source in a factor and this is used to name the factor. However, sometimes a factor will represent a mixture of sources, especially if they are co-located or otherwise correlated. Sources identified can include those directly emitting the particles (primary particles) or those formed by chemical reactions in the atmosphere and gas-to-particle conversions (secondary particles). In the current study where the samples are 24-hour averages, information about the diurnal variation in emissions (e.g. from vehicles) is not resolved, and this can reduce the ability of PMF to separate all sources into unique factors.

3.3 Wind sector analysis (CPF technique)

To provide information about the directions from the sampling site which are likely to include the locations of the source(s) in each factor, the conditional probability function (CPF) technique was used. This couples the source contribution estimates from PMF with the wind directions measured at the sampling site (e.g. Kim & Hopke 2004). The CPF estimates the probability that a given source contribution from a given wind direction will exceed a pre-determined criterion. It is defined as

$$CPF = m_{\Delta\theta}/n_{\Delta\theta}$$

where $m_{\Delta\theta}$ is the number of occurrences from wind sector $\Delta\theta$ that exceed the criterion and $n_{\Delta\theta}$ is the total number of data from the same wind sector.

In this study, the optimum value of the size of the wind sector $\Delta\theta$ was found to be 20°. Very light winds when the wind direction is often highly variable were excluded from the analysis by excluding wind speeds below 0.5 m s^{-1}.

Daily fractional mass contribution from each source was used rather than the absolute source contribution. This is to avoid the CPF being dominated by occasional days with unusually high absolute concentrations. The criterion was set as the upper 25th percentile of the fractional contribution from each source. This is found to be a good level for obtaining useful CPF plots.

A complicating factor is the selection of the wind direction data. The study samples and PMF gives 24-hour average contributions. If 24-hour average wind directions are used, then much of the variability in wind directions is lost and the average can be quite unrepresentative of hourly winds.

One solution is to use hourly-average wind directions and in the above formula, assume that the factor contribution is constant throughout the day and equal to the 24-hour average contributions for that day. This was the solution adopted in the analysis for the Upper Hunter Fine Particle Characterisation Study (Hibberd et al. 2013), and the CPFs were found to have limited use in helping to identify sources of the factors.

A modified technique used for this study was found to provide more useful CPF information. In addition to using the hourly wind direction data, the daily mass fraction for each factor was scaled each hour by the ratio of the PM ($PM_{2.5}$ or PM_{10}) concentration for that hour to the daily average PM concentration. The PM data used for this was the continuous monitoring data from the OEH network measured using BAMs or TEOMs.

Both these methods suffer from assumptions that are rarely, if ever, fully satisfied. In general, the contribution from each source will vary during the day and the contribution from each source will vary differently depending on its direction from the sampling site and the wind directions during the day. Deviations from the assumptions will likely be greater for variable emissions such as wood heaters or vehicles, and for sea breeze flows. In spite of this, the CPFs often provide useful information, as described in Sections 6 and 8. However, in some cases, they do little to assist in understanding the sources, and the limitations discussed above must be borne in mind when using the CPFs.

3.4 Trajectory modelling

Back trajectory modelling was undertaken for selected periods to assess the movement of air masses prior to their moving over the study area. Case study periods selected for analysis included periods with elevated particle concentrations and periods when certain factors had higher contributions. The back trajectory analysis was undertaken using the National Oceanic and Atmospheric Administration (NOAA) Hybrid Single-Particle Lagrangian Integrated Trajectory (HYSPLIT) model. HYSPLIT has been widely used identify the source–receptor relationship for air pollutants using backward trajectories analysis. It has been used for a range of events including wildfire smoke transport, dust storm episodes, nuclear incidents and volcanic eruptions (Draxler & Rolph 2015). An outline of the method is provided in Appendix E.

3.5 Chemical transport modelling

Computer modelling of chemical transport and particle dynamics was undertaken as part of the study using the CSIRO Chemical Transport Model (CTM) (Cope et al. 2014). The CTM is a three-dimensional Eulerian chemical transport model with the capability of modelling the emission, transport, chemical transformation, wet and dry deposition of a coupled gas and aerosol phase atmospheric system. CTM is able to predict ambient concentrations of particulate matter, including primary and secondary particles, occurring due to particle and precursor gas emissions from the range of natural and human sources.

The CTM modelling documented in the supplementary report (Emmerson et al. 2016) focused on predicting aerosol components of fine particles ($PM_{2.5}$) for July and November 2014 case study periods. These periods encompass the high wood smoke found in the measurements

during winter and the high sea salt measured in late spring/summer. Predicted $PM_{2.5}$ component concentrations were compared to the measurements made at the four LHPCS sampling sites: Newcastle, Stockton, Mayfield and Beresfield. Spatial patterns of predicted $PM_{2.5}$ components are illustrated in the supplementary report and the usefulness of the modelling in predicting $PM_{2.5}$ composition at sites for which no measurements are available demonstrated for Toronto and Maitland.

4 Particle composition

Particle concentrations measured during the study are presented in Section 4.1, with particle composition results discussed in Section 4.2, and summarised for $PM_{2.5}$ in Section 0 and for $PM_{2.5-10}$ in Section 4.4.

4.1 Particle concentrations

4.1.1 $PM_{2.5}$ time series

The time series of 24-hour average $PM_{2.5}$ concentrations determined from the filter samples collected at the four sites are shown in Figure 35. $PM_{2.5}$ concentrations at the three sites other than Stockton tend to trend together with very similar concentrations on most days illustrating that the regional transport and dispersion of fine particles significantly influences concentration levels at each site. The values are similar at Stockton in the last four months of the study period, whereas in earlier months although the regional trends are similar at Stockton, the concentrations are higher, at times significantly higher.

The regional trend shows that $PM_{2.5}$ peaks in late October to early November with levels at Stockton being similar to other sites. Significantly higher $PM_{2.5}$ levels were recorded at Stockton on many occasions from mid-April to mid-August. Levels at Newcastle, Beresfield and Mayfield were most similar during autumn and spring months, with differences apparent in winter and summer. In winter slightly higher levels were measured at Beresfield compared to levels at Mayfield, with the reverse occurring in summer.

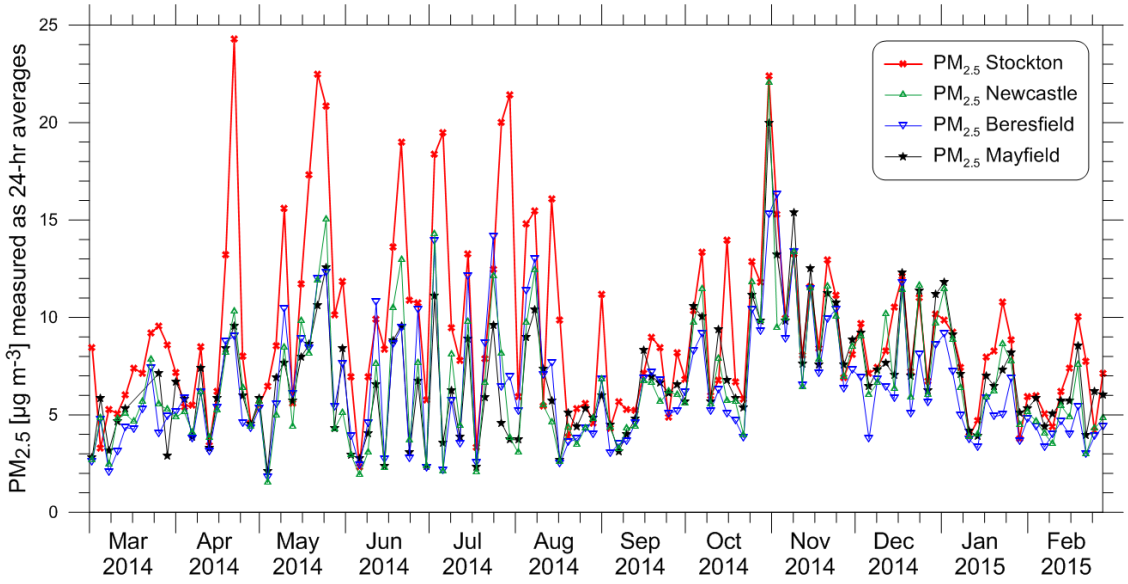

Figure 35: Time series of 24-hour average $PM_{2.5}$ concentrations from gravimetric analysis of LHPCS samples

4.1.2 $PM_{2.5-10}$ time series

The time series of 24-hour average $PM_{2.5-10}$ concentrations sampled at Stockton and Mayfield are shown in Figure 36. Notably higher coarse particle concentrations were measured at Stockton, as compared to Mayfield, throughout the sampling year. The lowest levels were measured during winter at both sites. Compared to winter-time levels, Mayfield experienced

more than a threefold increase in coarse particle levels during autumn, spring and summer. Similarly at Stockton, a twofold increase in levels was measured in autumn, spring and summer.

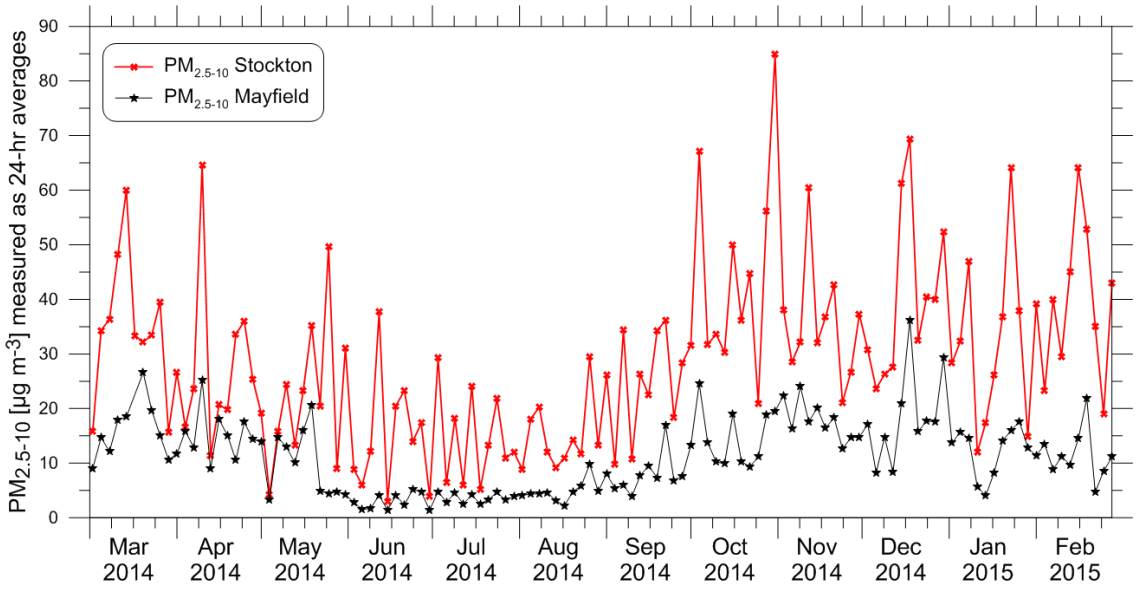

Figure 36: Time series of 24-hour average $PM_{2.5-10}$ levels from gravimetric analysis of LHPCS samples at Stockton and Mayfield

4.1.3 Comparison of LHPCS and OEH network data

For completeness, PM concentrations determined from the gravimetric determinations on the LHPCS filters are compared with data from the OEH Air Quality Monitoring Network. In comparing these measurements, it is important to note that the OEH instruments report concentrations at standard NEPM conditions of 0°C and 1013.25hPa whereas the LHPCS instruments (ASP and GENT) report air volumes at ambient pressures and temperatures. The LHPCS instruments are configured to support chemical analysis and source apportionment, and not to assess compliance with air quality standards. The pressure correction is small but with ambient temperatures typically between 15°C and 25°C, the adjustment to ambient conditions increases the OEH volumes by 5–10% and so reduces the OEH concentrations by 5–10%. In the following, the OEH daily average temperatures at the Newcastle monitoring site have been used, and the average of the 9am and 3pm atmospheric pressures at the Williamtown Bureau of Meteorology site, to adjust the LHPCS measurements so as to support an approximate comparison with OEH station measurements.

Figure 37 compares the $PM_{2.5}$ results. The LHPCS results were obtained from gravimetric determination of the mass of particles on the filters of the ASP samplers (Section 2.2.1). The Air Quality Monitoring Network uses BAMs, which rely on the attenuation of beta radiation through the filter to determine mass and hence concentration. The overall correlation is good with an r^2 of 0.94 but there is considerable scatter, although most points are within the wide band bounded by the dashed lines, which are at ± 4 µg m^{-3} from the 1:1 line.

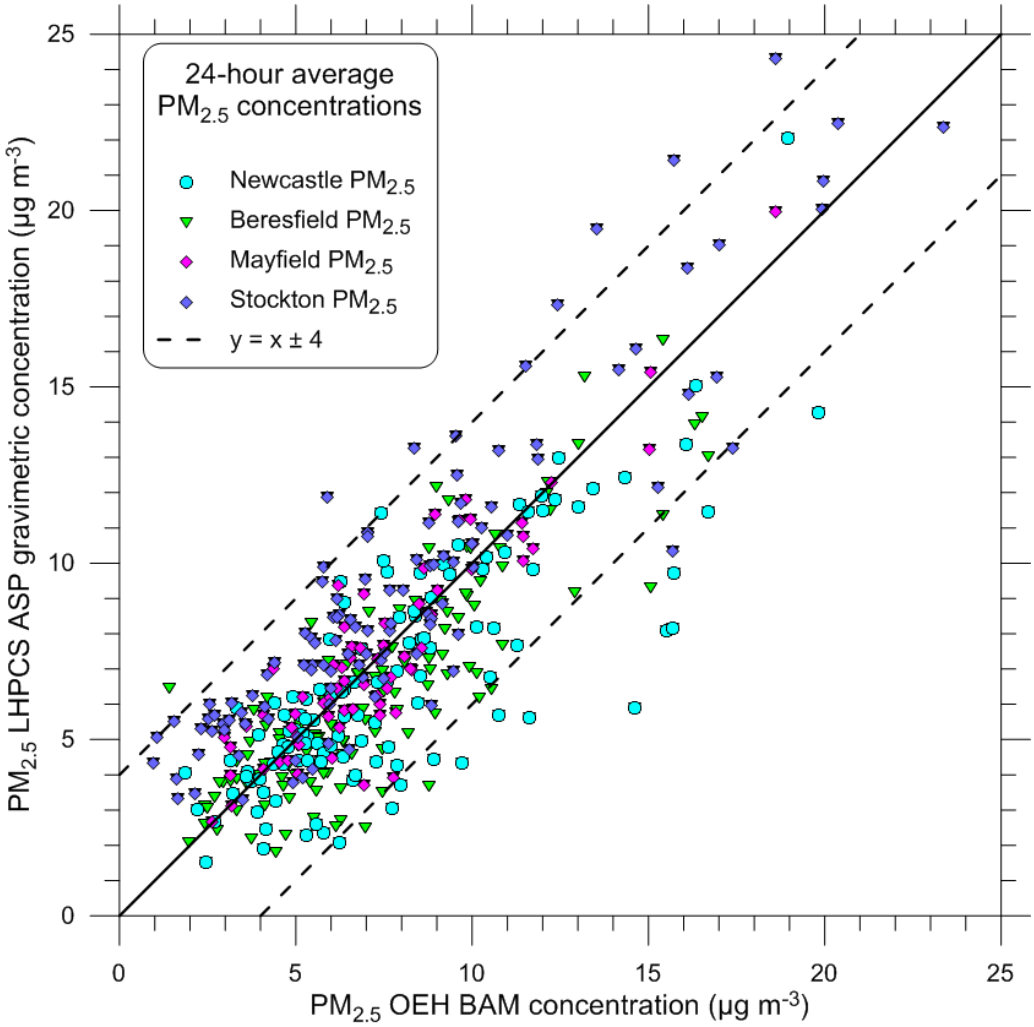

Figure 37: Comparison of $PM_{2.5}$ concentrations measured on the LHPCS filters with the regular results from the OEH Air Quality Monitoring Network using BAM instruments

Reasons for the large day-to-day differences between LHPCS gravimetric mass measurements and AQMN measurements include:

- *Instrument differences*. Different instruments have slightly different characteristics such as differences in the cut points or cut characteristics of the inlets, so that differences of 10% between masses are not unusual from co-located instruments.
- *Humidity*. Both the OEH-operated $PM_{2.5}$ BAMs and PM_{10} TEOMs have heated inlets whereas the ASP and GEN filters are unheated and they are weighed at 40–50% relative humidity. This would increase the masses measured on the LHPCS filters, and especially on filters with a higher fresh sea salt loading such as at Stockton.
- *Daily differences*. The role played by the above factors varies depending on the size distribution and chemical composition of the particles, which probably contributes to the large day-to-day differences because there is a good average fit to the 1:1 line.

The equivalent figure for PM_{10} is shown in Figure 38. The LHPCS results were obtained from gravimetric determination of the sum of the masses of particles on filters from two separate instruments – the coarse filters in GENT samplers providing $PM_{2.2\text{-}10}$, and the $PM_{2.5}$ filters in the ASP samplers (Sections 2.2.1, 3.1). No adjustment for the 'double counting' of the 2.2–2.5µm range was made. Based on Figure 33, the significance of such double counting is likely

to be negligible when comparing PM_{10} results. The Air Quality Monitoring Network uses TEOMs, which rely on mass measurement using resonant frequency of the oscillating filter. The overall correlation is slightly better than for $PM_{2.5}$ at $r^2 = 0.96$ but the scatter is still large, some of which can be explained by the reasons listed above.

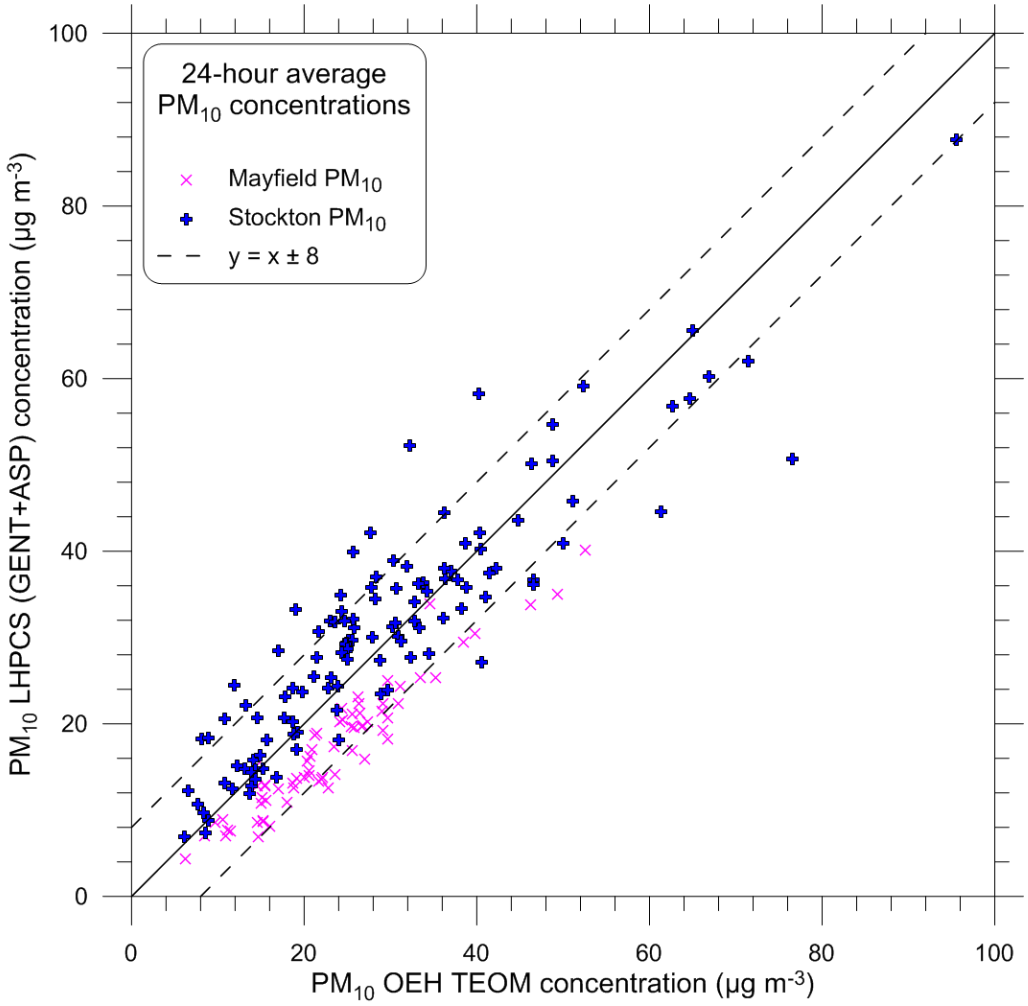

Figure 38: Comparison of PM_{10} concentrations measured on the LHPCS filters with the regular results from the OEH Air Quality Monitoring Network using TEOM instruments

4.2 Particle composition

4.2.1 Speciation of $PM_{2.5}$

The species measured in the Newcastle $PM_{2.5}$ samples are shown in Figure 39 (all sites are shown in Figure 122 to Figure 125 in Appendix A), with the minimum, 25th percentile, median, 75th percentile and maximum concentration of each species detected shown to illustrate the range of concentrations. A logarithmic scale is used given that the concentrations of individual species range over several orders of magnitude, from a few µg m^{-3} to less than 0.01 ng m^{-3}. The averages, standard deviations and maxima for all sites are also listed in Table 22 in Appendix A.

$PM_{2.5}$ species include sea salt constituents (such as chloride, sodium and magnesium), secondary particle constituents (such as sulfate and ammonium), organic and elemental carbon, wood smoke tracers (levoglucosan, mannosan), and metals and other species

associated with industrial and vehicle emissions as well as crustal dust (such as aluminium, silicon, titanium, iron and zinc). Elemental carbon in the fine fraction is likely to be directly emitted during the combustion of fossil fuels (e.g. motor vehicles, power stations, industrial boilers, non-road diesel equipment and transport including diesel-electric locomotives) and biomass burning (e.g. bushfires and domestic wood-burning heaters). Organic carbon includes primary OC emitted directly by sources and secondary organic aerosols formed in the air by chemical reactions. Sources of organic carbon include traffic and industrial combustion, biomass burning, cooking, biogenic sources of secondary organic aerosols and primary organics from sea spray.

The $PM_{2.5}$ species measured at all LHPCS sites are given in Appendix A. The same species in similar ranges are evident across the four sites in most cases. Some differences are apparent. For example, higher nitrate and ammonium concentrations are evident in Stockton $PM_{2.5}$ samples compared to other sites.

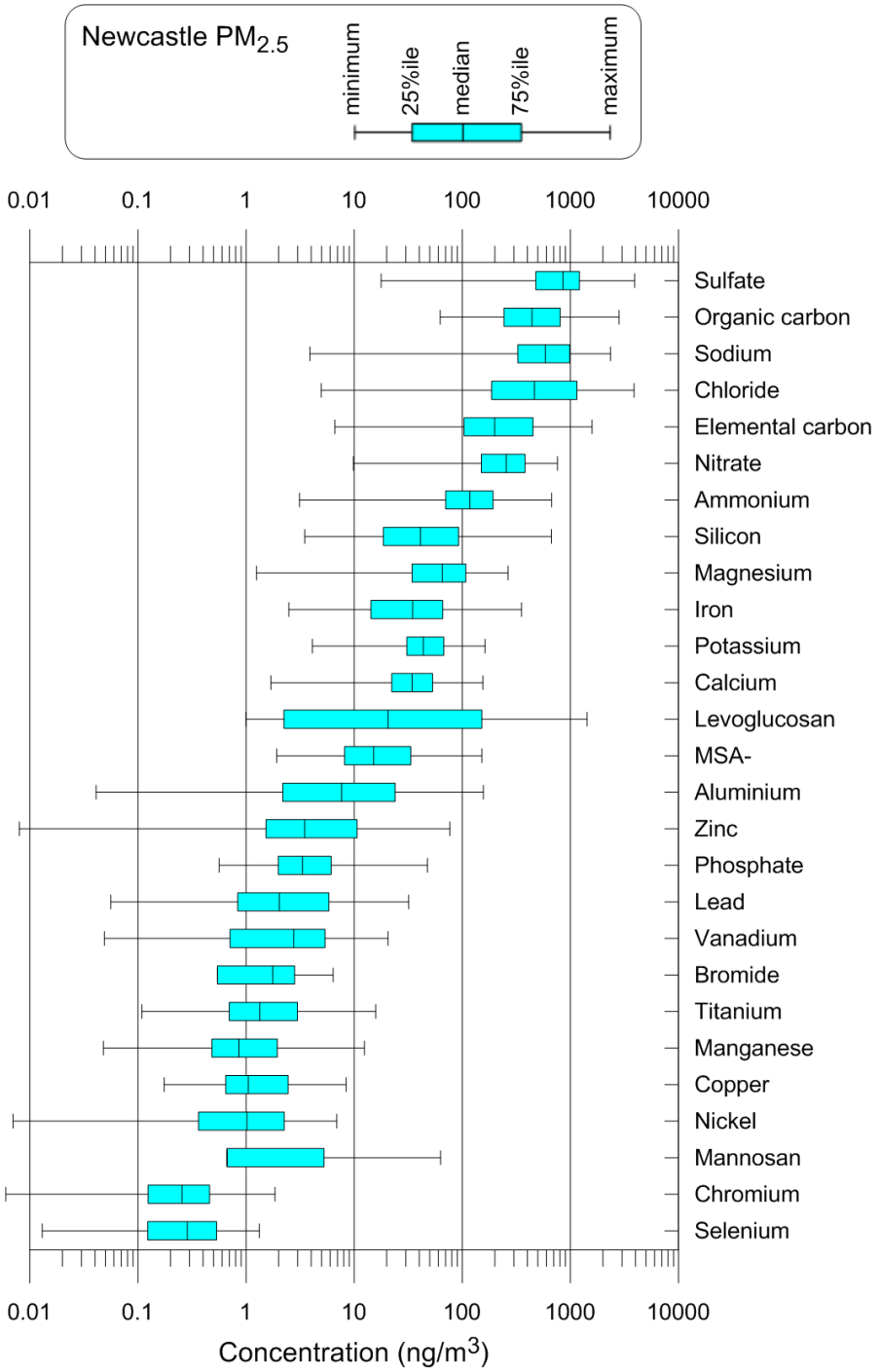

Figure 39: Box and whisker plot of the $PM_{2.5}$ species concentrations measured in the year of filter samples from Newcastle

4.2.2 Speciation of $PM_{2.5-10}$

The species measured in the Stockton $PM_{2.5-10}$ samples are shown in Figure 40, with the minimum, 25th percentile, median, 75th percentile and maximum concentration of each species detected shown. A logarithmic scale is used given that the concentrations of individual species range over several orders of magnitude, from tens of µg m^{-3} to less than 0.01 ng m^{-3}. The $PM_{2.5-10}$ species measured at Mayfield are given in Figure 126 in Appendix A. The averages, standard deviations and maxima are also listed in Table 23 in Appendix A.

$PM_{2.5-10}$ species include sea salt constituents (such as chloride, sodium, and magnesium), black carbon, species associated with crustal dust (e.g. aluminium, silicon, titanium, and iron), species emitted by industry, vehicles and non-road diesel equipment (e.g. zinc, iron, manganese, chromium, calcium, fluoride) and trace species or biomarkers for fungal spores (arabitol and mannitol) to assess the abundance of biogenic aerosols. Coal particles from non-combustion sources, which are typically larger than 2.5µm in diameter, may contribute to light-absorbing carbon in the $PM_{2.5-10}$.

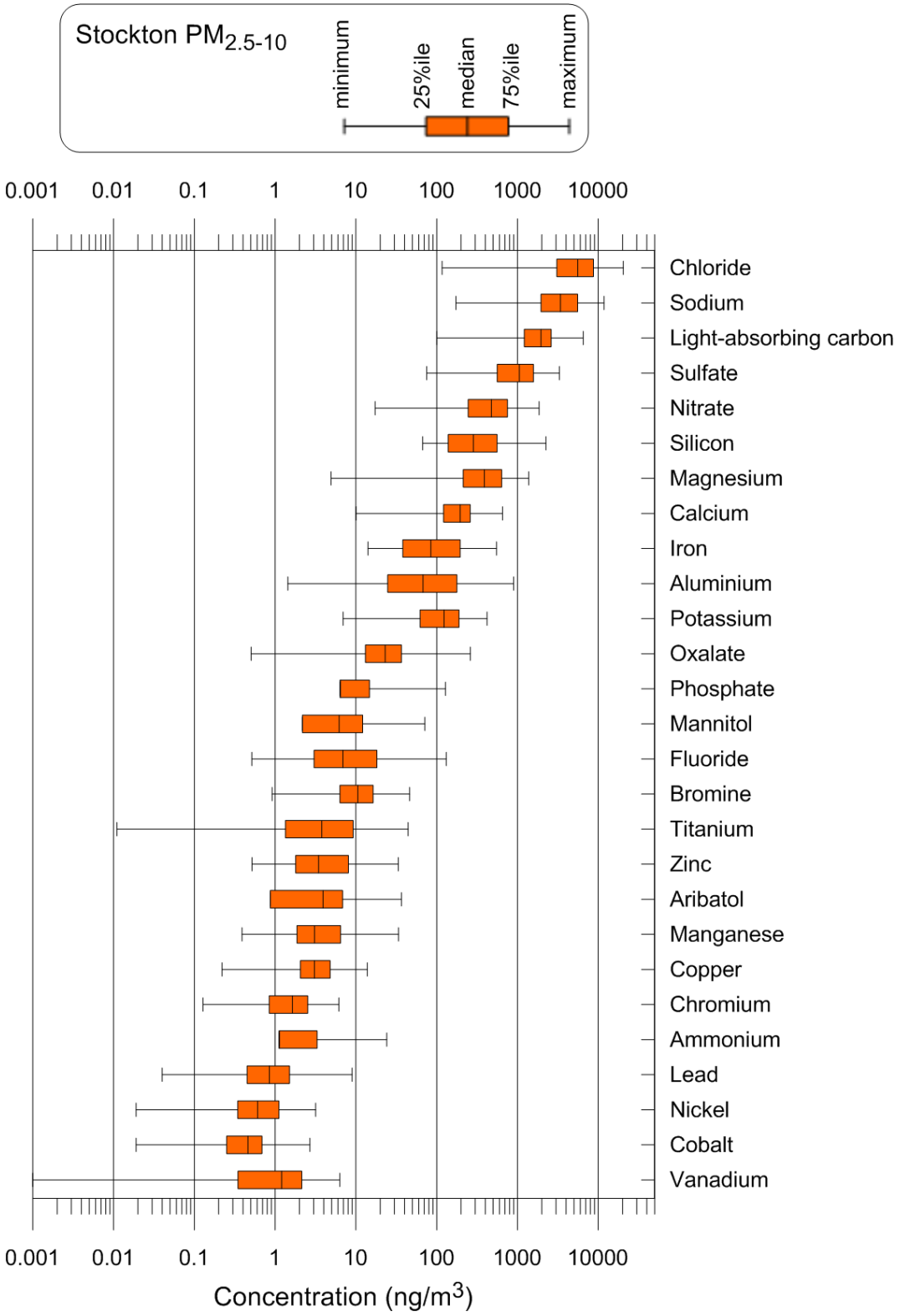

Figure 40: Box and whisker plot of the $PM_{2.5-10}$ species concentrations measured in the year of filter samples from Stockton

4.3 Main components of $PM_{2.5}$

A clearer overview of the main constituents of the particles can be obtained by estimating some key components as follows:

Sea salt = 3.27 x Na^+

Organic matter = 1.4 x OC

Non-sea-salt sulfate = SO_4^{2-} - (2.71/35.17) x sea salt]

Soil = 2.20 x Al + 2.49 x Si + 1.63 x Ca + 1.94 x Ti + 2.42 x Fe.

where the estimate for soil was based on the widely used results from Malm et al. (1994).The sea salt calculation is based on the composition of standard sea water given by Millero et al. (2008) with the total mass of sea salt being (35.17/10.77) times the mass of Na^+. This reference also gives the proportion of sulfate in standard sea water as (2.71/35.17). In the third equation above, this is multiplied by the sea salt concentration and then subtracted from the measured sulfate concentration to compute the non-sea-salt sulfate. The factor 1.4 for converting organic carbon to organic matter was based on Bae et al. (2006) and Russell (2003). A constant value was used for the whole year although it is known to vary depending on the number of functional groups in the organic compounds, generally being higher in winter. It is likely that at least some of the component labelled ‘other’ in the pie charts is other organic matter because an analysis of the seasonal variation showed that ‘other’ contributed more in winter. The moisture was calculated as (0.26 x sea salt) based on the uptake of sea salt particles at 40% humidity reported by McInnes et al. (1996).

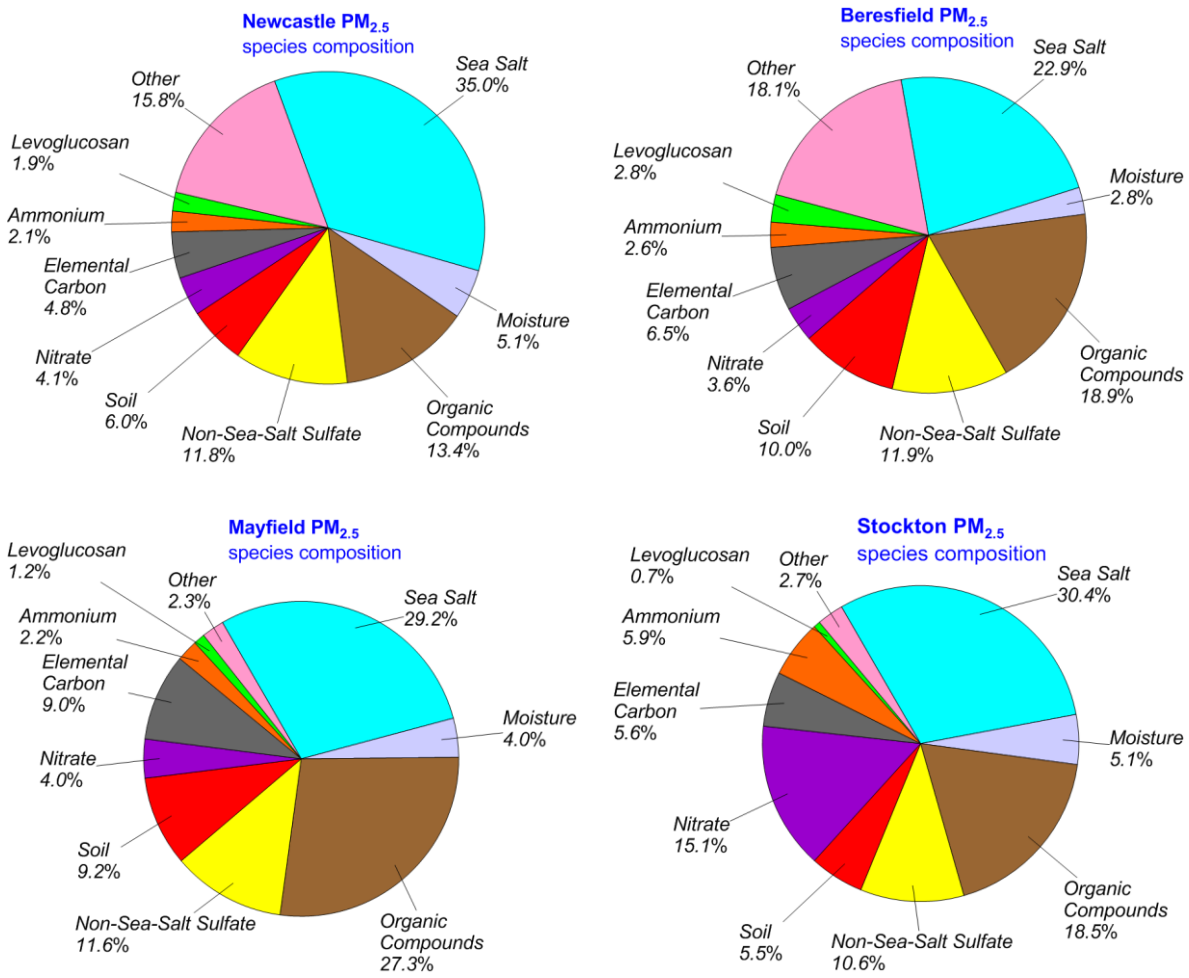

Figure 41: Main components of $PM_{2.5}$ based on the chemical speciation (annual averages)

The main components of $PM_{2.5}$ measured over the sampling year at each of the four sites are shown in Figure 41. The most abundant $PM_{2.5}$ components across all sites are sea salt, organic matter, non-sea-salt sulfate, soil, nitrate and elemental carbon. The non-sea-salt sulfate component is described as such because sea salt also contains sulfate (about 7.7% by mass).

Sea salt is the largest component at the three more coastal sites comprising about 30–35% of the annual mass, with the concentration of sea salt reducing to about 23% at the Beresfield site which is located about 16km from the coast. Organic matter constitutes the next most abundant species, comprising 13–27% of the annual mass, with elemental carbon comprising a further 5–9%.

Non-sea-salt sulfate accounts for 10–12% of the mass annually. The contribution of nitrate is notably higher for the Stockton site where it accounts for about 15% of the annual mass, compared to about 4% at Newcastle, Beresfield and Mayfield. The ammonium component is similarly greater at the Stockton site being about 6%, compared to 2–3% at other sites.

Soil accounts for 6% of the mass at Newcastle and Stockton sites, and 9–10% of the annual mass at Mayfield and Beresfield. Levoglucosan, a wood smoke tracer, is evident at all four sites, but is highest at Beresfield, comprising about 3% of the annual mass.

Due to the seasonal nature of certain sources, such as wood burning, and seasonal variations in meteorology, significant differences in seasonal $PM_{2.5}$ composition occur. This is reflected in the range of $PM_{2.5}$ concentrations in Appendix A and in the seasonal variation in factor contributions determined through receptor modelling presented in Section 5.

4.4 Main components of $PM_{2.5-10}$

The main components of $PM_{2.5-10}$ measured over the sampling year at Stockton and Mayfield sites are shown in Figure 42. Sea salt makes up a significant component of the coarse fraction, accounting for 62% of the annual mass at Stockton and 47% at Mayfield. Soil and light-absorbing carbon comprise the next most significant contributions to annual $PM_{2.5-10}$ mass, followed by nitrate and non-sea-salt sulfate. As discussed in Section 3.1.5, the light-absorbing carbon fraction could include a contribution from soil because it affects light transmittance.

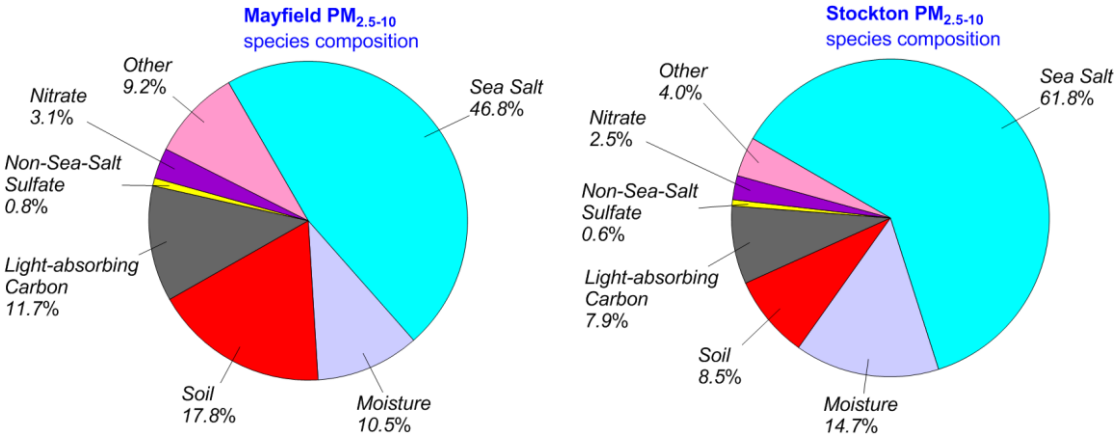

Figure 42: Main components of $PM_{2.5-10}$ based on the chemical speciation (annual averages)

5 Data analysis by PMF (positive matrix factorisation)

As outlined in Section 3.2, positive matrix factorisation (PMF) is a type of receptor modelling for analysing data collected at receptors. It is a mathematical method that relies on internal correlations between species in the data set to identify both the factors contributing to the samples and calculates the amount that each factor contributes.

Once the factors are obtained, further analysis is undertaken to identify the source(s) in each factor. This uses the species information in the factor and other knowledge of atmospheric chemistry as well as wind sector and seasonal analysis to identify the most likely source(s) of emissions for each factor. In many cases, there is a single dominant source in a factor and this is used to name the factor. However, if sources are co-located or otherwise correlated, they can appear together in a single factor or across several factors. It is important to note that the sources identified by PMF are not necessarily the same as the sources listed in an emissions inventory.

An advantage of PMF is that it is often able to identify factors representing species or groups of species which are not directly emitted as particles (primary particles) but form by chemical reactions in the atmosphere and gas-to-particle conversions (secondary particles), such as secondary ammonium sulfate which is not directly emitted from a source, and will not be listed in a source emissions inventory.

In the main analysis for this study, the chemical composition data of all the samples from each site was analysed using the EPA PMF 5.0 software (Norris & Duvall 2014).

5.1 Selection of species

The selection of species for inclusion in PMF analysis requires some discussion. The analytical methods used for the analysis of samples in this project have produced data sets for 45 species. In a number of cases different methods have measured the same or similar species (e.g. SO_4^{2-} by IC and S by PIXE, EC by thermal desorption and BC by laser integrated plate method). In these cases one of these species has been selected for PMF. The IBA data for Na, S, Cl, K and Ca were excluded because of the negative bias at high concentrations discussed in Appendix B. Species where the PMF does not fit the observations well ($r^2 < 0.4$) were excluded because they act as ‘noise’ in the PMF and can worsen the factor fit for other species. It is worth noting that PMF determines the principal factors that determine most of the variance in the data set. In so doing, it does not describe unusual episodes such as, for example, once-a-year fireworks. The species not included in the PMF analysis are listed in Table 4.

Table 4: Species excluded from the PMF analysis

Species excluded	Reason
Na by PIXE	High concentration bias, so used Na^+ by IC
S by PIXE	High concentration bias, so used SO_4^{2-} by IC
Cl by PIXE	High concentration bias, so used Cl^- by IC
BC ($PM_{2.5}$)	EC data better defined. LAC (light-absorbing carbon) data used for $PM_{2.5-10}$ because EC not measured
K by PIXE	High concentration bias, so used K^+ by IC
Ca by PIXE	High concentration bias, so used Ca^{2+} by IC
$PM_{2.5}$ P, Co, Se, Br by PIXE PO_4 , F^-, acetate, formate, arabitol, mannitol, glactosan, glucose by IC	Low S/N or poorly fitted by PMF model (correlation between observed and modelled $r^2 < 0.4$)
PM_{10} P, V, Co, Ni, Cu, Se by PIXE Br, PO_4, acetate, formate, MSA, levogluocsan, mannosan, glactosan, glucose by IC	Low S/N or poor model fit ($r^2 < 0.4$)

S/N: signal-to-noise (ratio)

In a number of cases a large proportion of the concentrations were below the method detection limit (MDL). The EPA PMF 5.0 User Guide (Norris & Duvall 2014) recommends the exclusion of species if more than 95% of samples have concentrations less than the MDL. In addition, species with more than 75% of samples less than the MDL were examined closely and their inclusion was dependent on how well the modelled time series fit the observational data.

We also used the criteria of the signal-to-noise (S/N) ratios as calculated by EPA PMF to assign an uncertainty weighting to the species. Variables were initially defined to be strong, weak or bad depending on their S/N ratio. Species with S/N ratios less than 0.5 were excluded. Species with S/N ratios between 0.5 and 1 were considered weak variables and by flagging them as such their estimated uncertainties were increased by a factor of 3 to reduce their weight in the solution. We also set the mass variable to weak by assigning it as a totalising variable. Finally, we evaluated the ability of PMF to model each species. This mainly led to species being downgraded from strong to weak, which prevented outliers from driving the PMF solution.

Table 5 and Table 6 list the strength of the various species used in the PMF analysis for the fine and coarse fractions. There was a total of 122 samples from each site, each with 30 species for the $PM_{2.5}$ and 22 species for the $PM_{2.5-10}$ analysis.

Table 5: Species included in PMF analysis of $PM_{2.5}$ data listing PMF category, and the median concentration and signal-to-noise ratio calculated by EPA PMF at each site

Species	PMF strength	Newcastle		Beresfield		Mayfield		Stockton	
		Median (ng m^{-3})	S/N	Median (ng m^{-3})	S/N	Median (ng m^{-3})	S/N	Median (ng m^{-3})	S/N
Mass	Weak	5801.0	-	5485.0	-	6364.5	-	8095.0	-
H	Weak	132.3	10.00	158.5	10.00	148.9	10.00	169.7	9.99
Al	Strong	6.8	4.66	19.6	7.27	22.8	7.10	12.4	5.35
Si	Strong	40.1	9.56	73.1	9.99	72.6	9.90	50.5	9.54
Ti	Strong	1.3	4.20	1.9	5.25	2.2	5.66	1.3	3.68
V	Strong	2.3	5.20	0.6	1.64	1.7	4.66	5.0	7.30
Cr	Weak	0.1	0.36	0.3	1.60	0.3	0.98	0.1	0.25
Mn	Weak	0.8	3.98	1.5	5.44	2.2	6.30	1.0	4.16
Fe	Strong	33.7	9.95	77.8	10.00	71.8	10.00	31.8	9.85
Ni	Strong	1.0	3.30	0.3	0.85	0.8	2.37	1.9	4.81
Cu	Weak	1.0	3.89	1.0	3.17	1.7	4.81	0.7	2.44
Zn	Weak	3.2	6.22	5.0	7.33	7.9	7.89	4.7	6.52
Pb	Weak	1.7	1.21	1.8	1.10	2.5	1.29	1.7	1.00
Na^+	Strong	589.7	9.83	333.8	9.91	488.5	9.93	709.6	9.97
NH_4^+	Strong	117.8	9.97	132.2	10.00	122.4	10.00	198.2	10.00
K^+	Strong	43.3	5.77	38.6	6.24	41.7	6.13	51.9	7.09
Mg^{2+}	Strong	66.6	9.55	36.3	9.22	55.4	9.56	77.1	9.67
Ca^{2+}	Weak	34.1	8.62	30.1	6.64	43.3	7.50	44.0	9.05
Cl^-	Strong	471.6	9.31	203.5	8.60	359.6	8.92	718.5	9.86
Br	Weak	1.8	2.29	1.2	1.42	1.2	1.75	3.6	4.91
NO_3^-	Strong	252.8	10.00	199.0	10.00	232.2	10.00	464.5	10.00
SO_4^{2-}	Strong	852.3	9.97	713.3	10.00	765.8	10.00	1126.9	10.00
$C_2O_4^{2-}$	Weak	51.7	9.33	44.1	9.58	49.0	9.34	62.8	9.56
MSA^-	Strong	15.5	8.02	15.3	7.99	17.2	8.13	16.2	8.03
Levoglucosan	Strong	19.4	5.61	36.2	6.23	18.0	5.77	16.5	6.05
Mannosan	Strong	0.7	2.01	0.7	2.53	0.7	1.67	0.7	1.40
OC1	Weak	26.0	0.90	76.4	1.56	122.6	1.56	63.6	0.94
OC2	Weak	90.0	2.97	138.5	3.36	248.9	2.33	244.1	2.55
OC3	Weak	184.8	2.33	227.7	3.64	421.1	2.19	348.2	1.39

Species	PMF strength	Newcastle		Beresfield		Mayfield		Stockton	
		Median (ng m^{-3})	S/N	Median (ng m^{-3})	S/N	Median (ng m^{-3})	S/N	Median (ng m^{-3})	S/N
OC4	Weak	124.3	3.54	130.7	3.90	153.5	3.15	170.4	2.68
EC	Weak	194.7	3.66	290.3	3.93	463.2	3.36	374.2	3.01

Table 6: Species included in PMF analysis of $PM_{2.5-10}$ data listing PMF category, and the median concentration and signal-to-noise ratio calculated by EPA PMF at each site

Species	PMF strength	Mayfield		Stockton	
		Median (ng m^{-3})	S/N	Median (ng m^{-3})	S/N
Mass	Weak	8136.5	-	20981.0	-
Al	Strong	86.4	7.17	58.2	5.69
Si	Strong	228.3	7.90	283.1	7.89
Ti	Strong	4.3	3.60	3.2	3.05
Mn	Weak	3.7	4.98	3.1	3.98
Fe	Strong	112.9	7.88	82.1	7.83
Cu	Weak	3.6	5.38	3.0	4.24
Zn	Weak	3.9	5.38	3.3	4.82
Br	Weak	2.4	2.44	10.9	5.11
Pb	Weak	0.7	0.33	0.7	0.36
BC	Strong	825.5	6.05	1854.2	6.70
Na^+	Strong	1130.4	9.32	3870.2	10.00
NH_4^+	Weak	1.3	1.89	1.1	1.28
K^+	Strong	38.1	3.34	136.2	6.53
Mg^{2+}	Strong	122.9	8.04	450.7	9.49
Ca^{2+}	Strong	91.1	5.94	211.4	8.52
Cl^-	Strong	1646.6	9.39	6075.7	10.00
NO_3^-	Strong	183.4	8.18	451.6	10.00
SO_4^{2-}	Strong	364.9	9.54	1148.6	10.00
$C_2O_4^{2-}$	Weak	14.3	7.37	23.3	8.95
F^-	Weak	4.8	5.14	6.7	6.17
Arabitol	Strong	3.2	3.21	3.9	3.17
Mannitol	Strong	5.6	2.50	6.2	2.42

5.2 PMF configuration

The PMF model was run separately for each data set, i.e. for each site and separately for $PM_{2.5}$ and $PM_{2.5-10}$. The model was executed with 100 base runs, a random seed until the final

solution was found, with various numbers of factors and an extra modelling uncertainty of 10% to account for errors not considered in calculating measurement or analytical errors.

Examination of the ability to model the observed time series of the species concentrations was used in arriving at the final solution, along with the desire for physically sensible interpretations of the factors. The best fit with factors that could be explained physically was obtained using 10 factors for the $PM_{2.5}$ and 6 factors for $PM_{2.5\text{-}10}$. There were two aged-sea salt factors in the ten-factor solution for $PM_{2.5}$, so these have been combined in the results presented in this report to present nine factors.

The G-space plots showed little rotation and F_{peak} was not used. All runs converged and the Q values were stable.

The uncertainty in the factor contributions is derived from the bootstrapping and displacement methods in the EPA PMF 5.0 software (Norris & Duvall 2014) and are reported in Appendix D.

5.3 PMF mass closure

Figure 43 compares the daily $PM_{2.5}$ concentrations during the study from the gravimetric measurement on the Teflon filter against the reconstructed mass from the PMF analysis. The figure combines results for all four sites. The solid line represents perfect agreement with the dashed lines either side at ±10% showing that almost all points lie within this range.

A similar result was obtained for the $PM_{2.5\text{-}10}$ fraction, as shown in Figure 44.

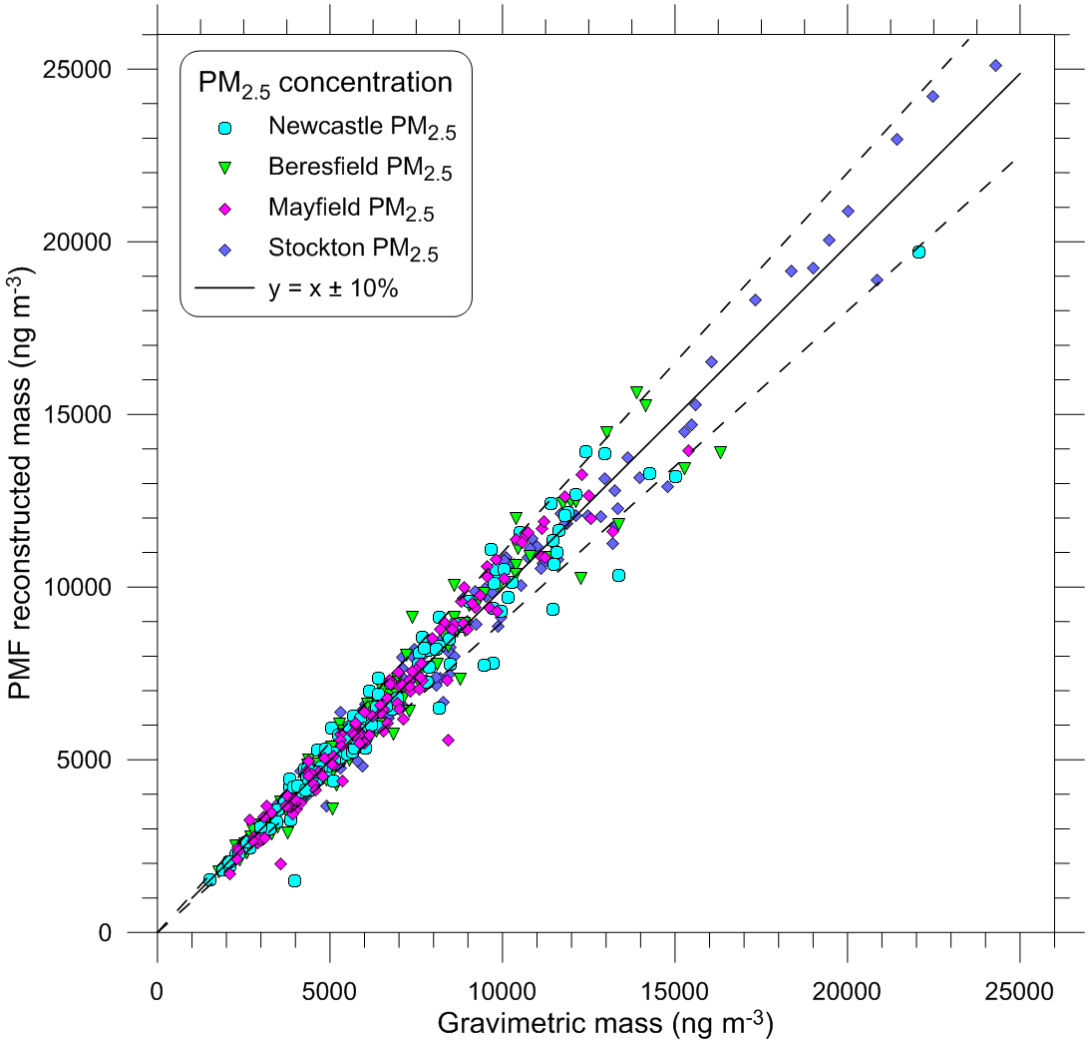

Figure 43: Scatter plot of daily $PM_{2.5}$ concentrations from the gravimetric mass determination and the reconstructed mass from the PMF solution

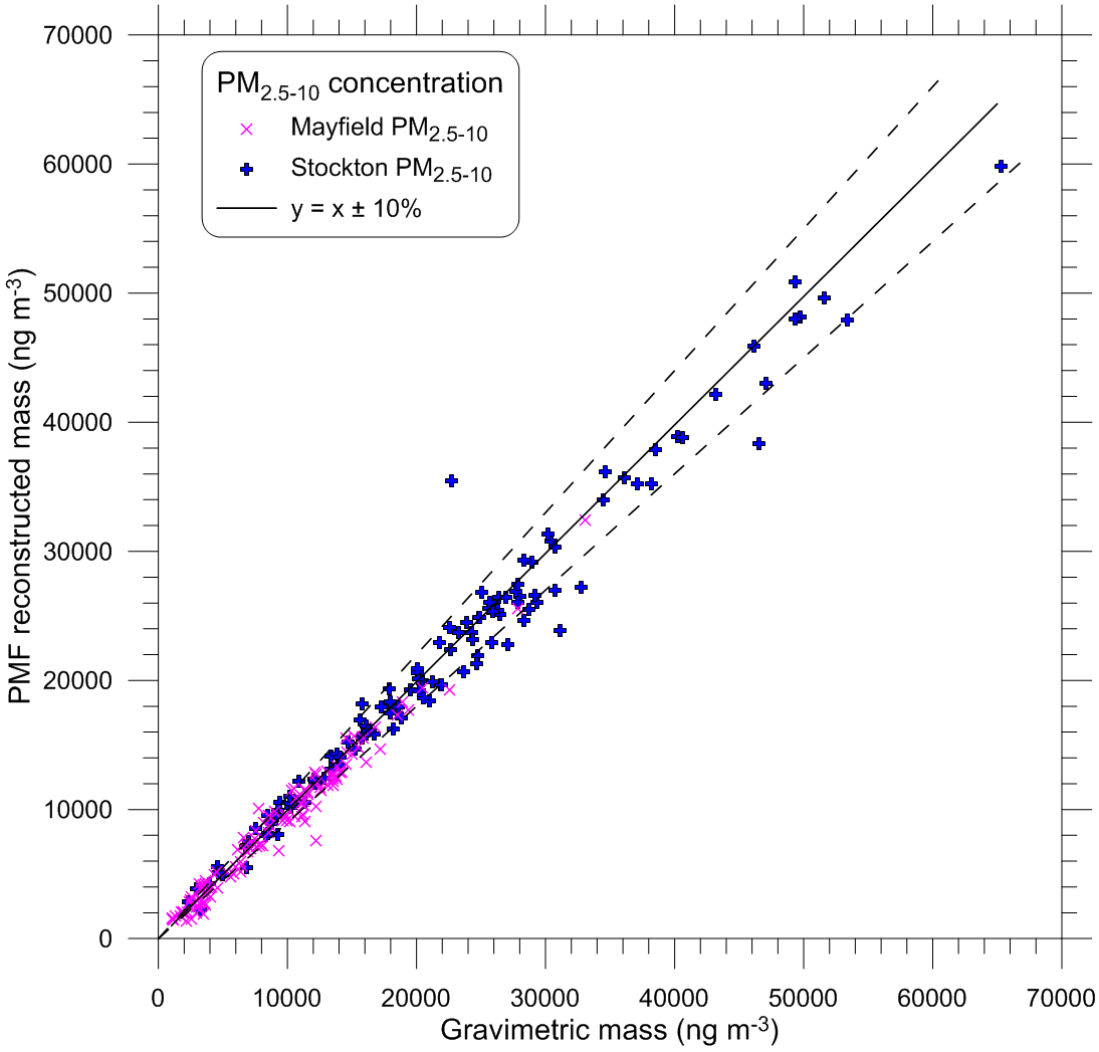

Figure 44: Scatter plot of daily $PM_{2.5-10}$ concentrations from the gravimetric mass determination and the reconstructed mass from the PMF solution

5.4 Species correlations

The analysis using EPA PMF 5.0 is an iterative process requiring a physical interpretation of the results in order to select the appropriate number of factors, and to identify and name them. Correlations between species in the collected data provide a useful indication of the key species in the PMF factors and also indicate the extent to which markers from different source types may show up in the same factor. In the following we examine some of these correlations, which provide a good introduction to the discussion of the individual factors in Sections 6 and 8.

Figure 45 displays the linear relationships between magnesium and sodium with the Mg^{2+}/Na^{+} ratio of 0.116 being that for standard sea salt (Millero et al. 2008). This provides strong evidence that all the sodium and magnesium in the samples has its origin as sea salt. The evidence is convincing because it is very unlikely that any anthropogenic or other source would emit these two species in exactly the same ratio. Millero et al. (2008) lists the key components of sea salt as Cl^{-} (55%), Na^{+} (31%), SO_4^{2-} (7.7%), Mg^{2+} (3.7%), Ca^{2+} (1.2%) and K^{+} (1.1%).

Unlike the magnesium component of sea salt which remains present in the particles, the chloride can be displaced by sulfate and nitrate ions (e.g. Seinfeld & Pandis 2006) but this

only occurs to any significant extent for fine particles ($PM_{2.5}$). Figure 46 shows the scatter plot of $PM_{2.5}$ concentrations of chloride versus sodium with all points lying below the line for fresh sea salt (Cl^-/Na^+ = 1.80). That is, for a given sodium concentration, the observed chloride concentration is always lower by varying amounts depending on the amount of loss. This displacement of chloride is referred to as 'aging' of the sea salt and is discussed in more detail in Section 6.2.

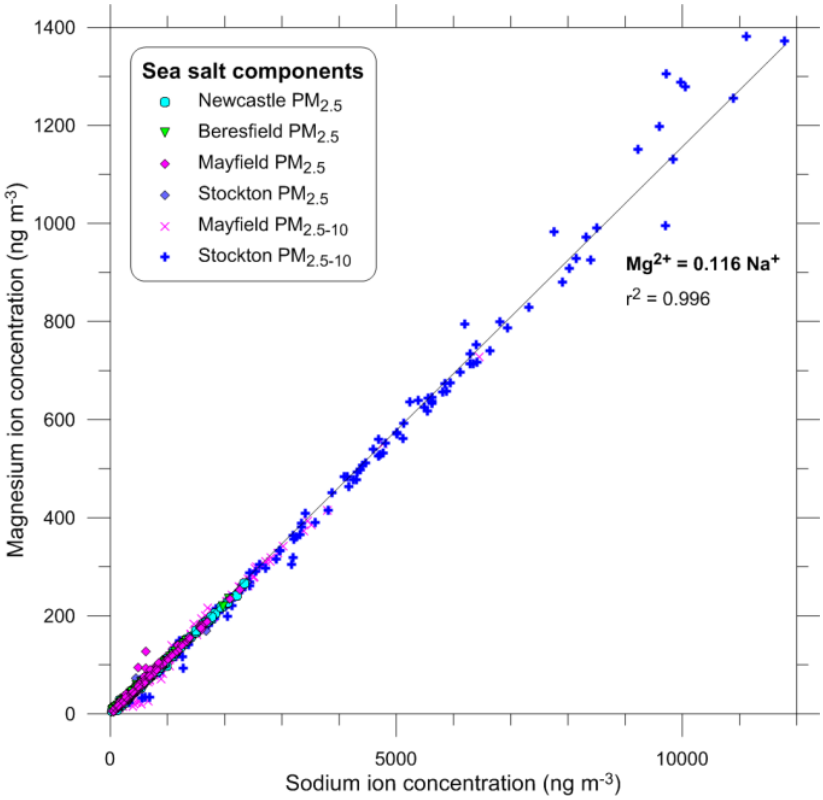

Figure 45: Scatter plot showing the strong linear relationship between magnesium and sodium concentrations in the LHPCS dataset

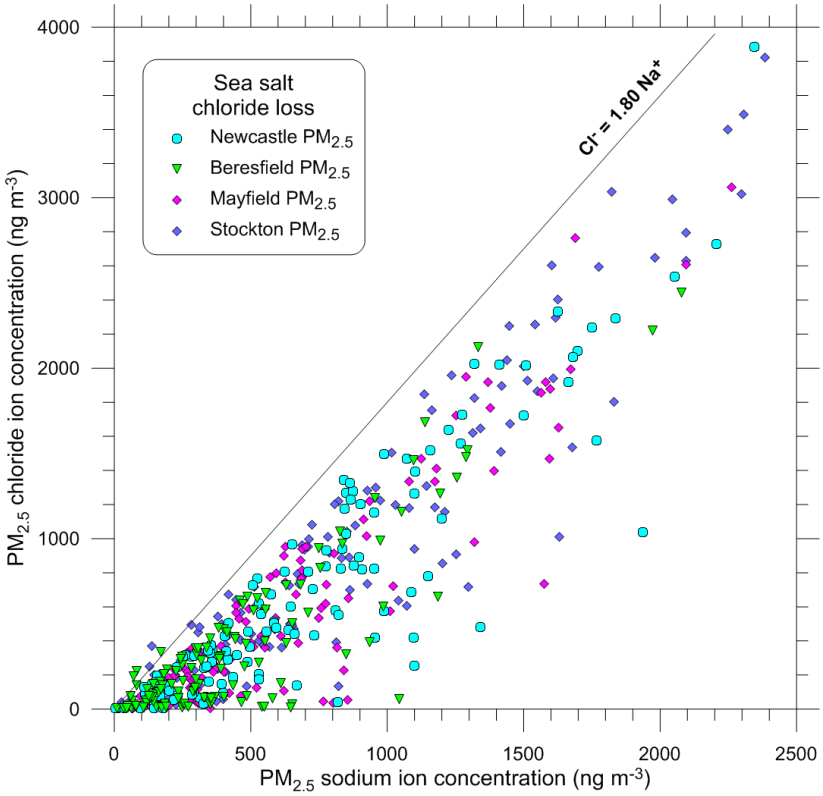

Figure 46: Scatter plot for $PM_{2.5}$ showing that for a given sodium concentration, the observed chloride concentrations are always lower than for fresh sea salt (Cl^-/Na^+ = 1.80) due to the presence of 'aged' sea salt in the atmosphere for these 24-hour averages

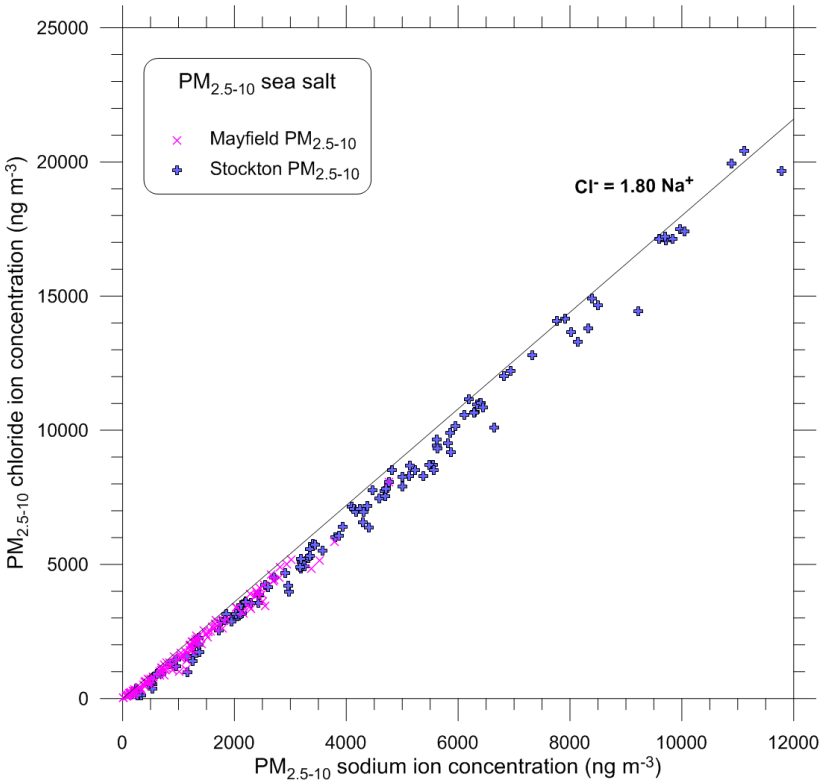

Figure 47: Scatter plot for $PM_{2.5-10}$ showing that, unlike for $PM_{2.5}$, there is a strong correlation between chloride and sodium concentration with the ratio (Cl^-/Na^+ = 1.80) matching that for fresh sea salt

In Figure 47, the equivalent scatter plot for $PM_{2.5-10}$, there is a strong correlation between chloride and sodium matching the ratio for fresh sea salt, i.e. there is no evidence of aging of the coarse fraction. (Note that although not discernible in the figure, for sodium concentrations below 1000 ng m^{-3}, there is actually chloride loss of up to 30%.) This general absence of aging is because the reactions displacing chloride occur on the surface of the particle and the larger particles have much smaller surface-area-to-volume ratios. The coarser particles also have less opportunity for aging because they are larger and so are deposited more quickly than $PM_{2.5}$.

Since sulfate in particulate matter has several sources including from the combustion of fossil fuels as well as sea salt, it is useful to identify the non-sea-salt component of the sulfate (nss SO_4^{2-}). This can be done in Figure 48, which is a scatter plot of sulfate versus sodium with the solid line representing the SO_4^{2-}/Na^+ ratio in fresh sea salt. All the points above the line indicate the presence of more sulfate than in fresh sea salt and the part above the line is termed nss SO_4^{2-}. For $PM_{2.5-10}$, most of the points lie just above the line indicating a minor nss SO_4^{2-} component, whereas there is a major nss SO_4^{2-} component in $PM_{2.5}$. The reasons for the difference between the fine and coarse fractions are different from those discussed above – most of the nss sulfate in the atmosphere is in the fine fraction, being produced from emissions of, for example, sulfur dioxide.

Levoglucosan and mannosan are unique tracers for the combustion of cellulose found in trees and plants (Iinuma et al. 2007). Figure 49 shows a good correlation between these species with the levoglucosan ratio between 20 and 40 representative of wood smoke from the combustion of hardwood (Goncalves et al. 2010).

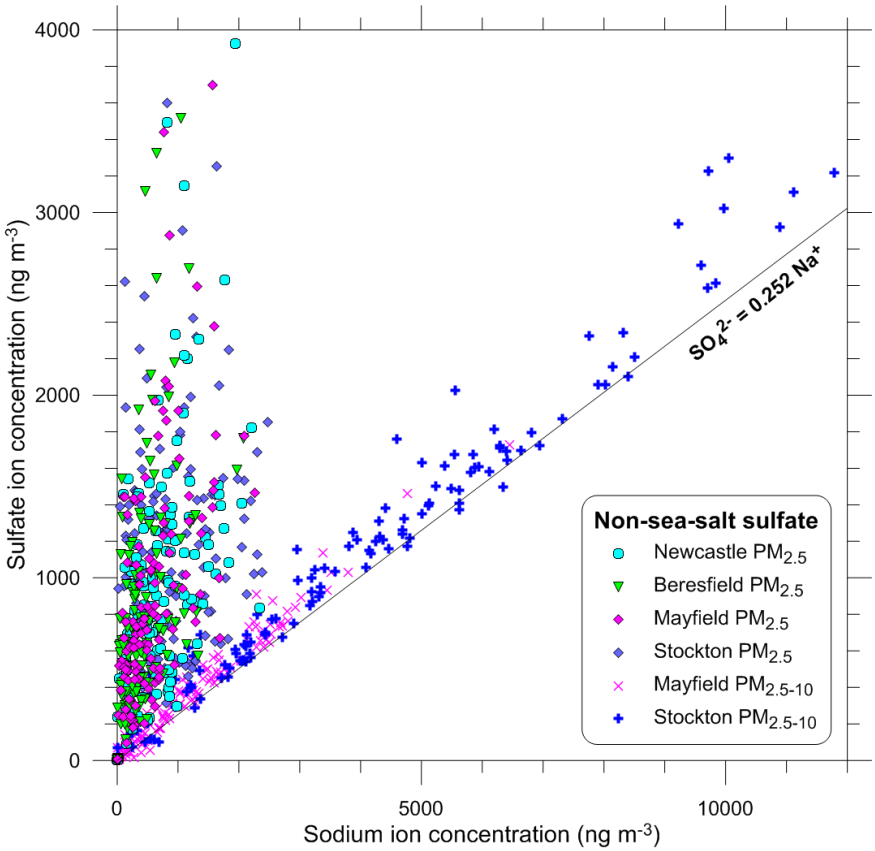

Figure 48: Scatter plot of sulfate versus sodium in fine and coarse fractions

Points above the line indicate the presence of non-sea-salt sulfate.

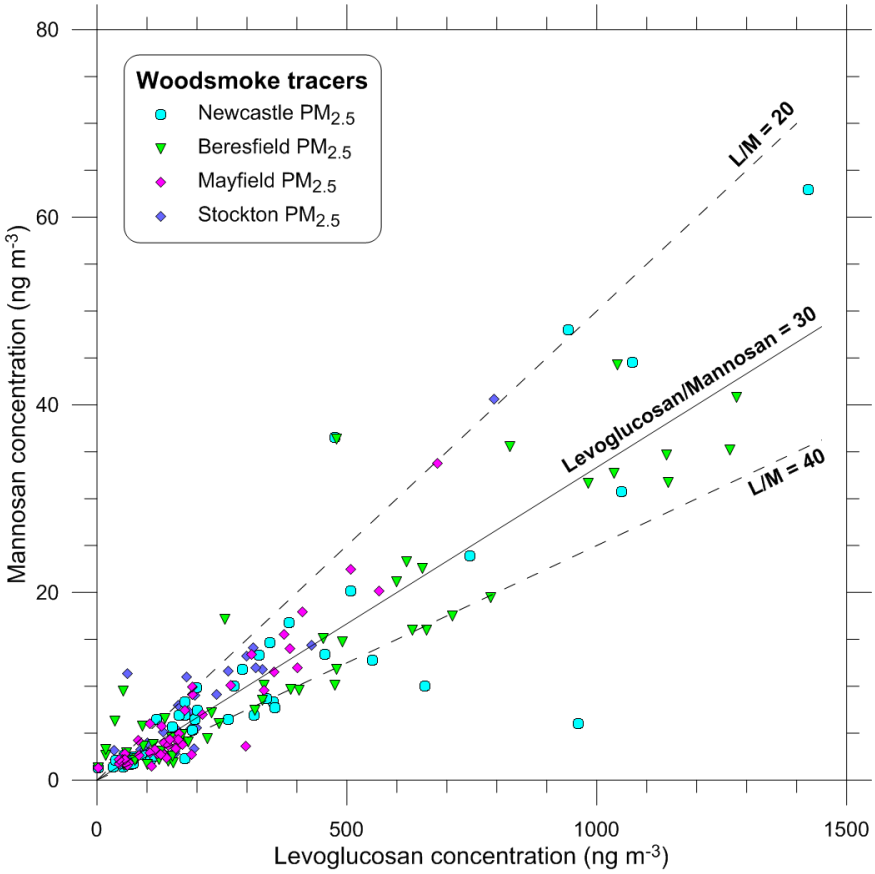

Figure 49: Scatter plot of mannosan versus levoglucosan in the $PM_{2.5}$ measured during the study

The identification of soil dust relies on the presence of aluminium, silicon, titanium, iron and calcium. The first three have few other sources and are the most useful identifiers. Figure 50 shows a scatter plot of titanium against aluminium with the line representing the typical value for crustal dust (Lide 1997). For the $PM_{2.5}$ at Newcastle, Beresfield, and Mayfield the Al/Ti ratio is closer to 10, whereas it is closer to 18 at Stockton for $PM_{2.5}$ and at both Stockton and Mayfield for $PM_{2.5\text{-}10}$, probably indicating a slightly different origin of the soil dust. For most sites, the correlation is stronger for silicon versus aluminium in Figure 51 with a Si/Al ratio of 3.3. However the $PM_{2.5\text{-}10}$ fraction at Stockton shows many points with an excess of either silicon or aluminium compared to the line. This indicates other sources than just soil dust, possibly sand for Si and industry for Al.

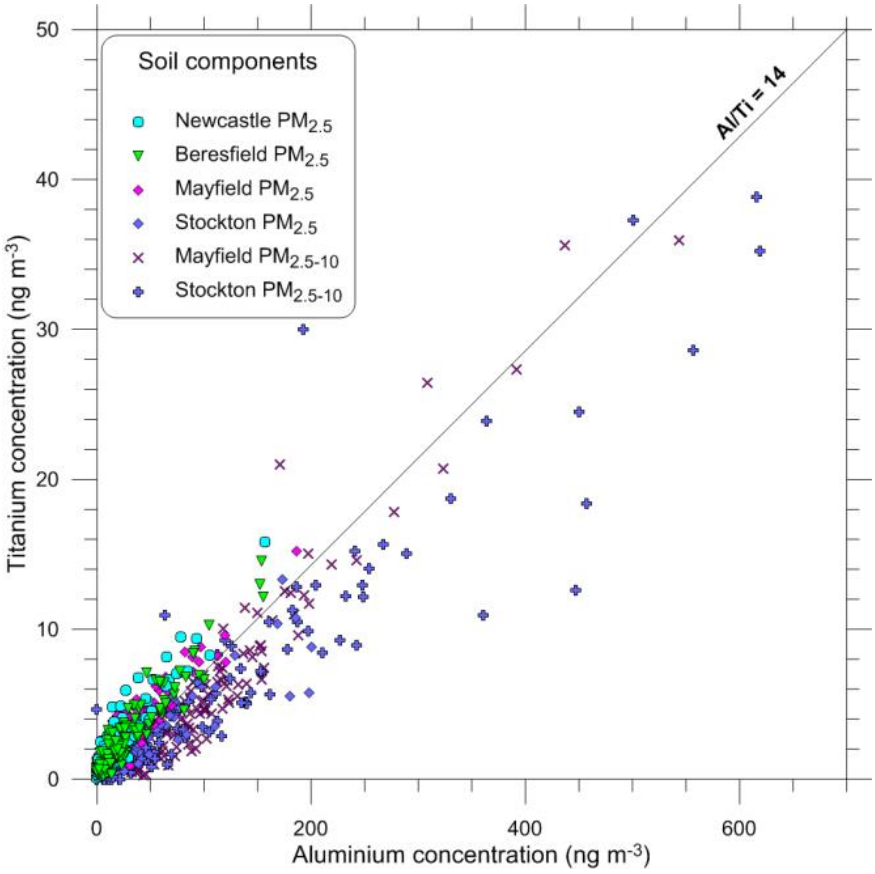

Figure 50: Scatter plot of titanium versus aluminium in $PM_{2.5}$ and $PM_{2.5-10}$

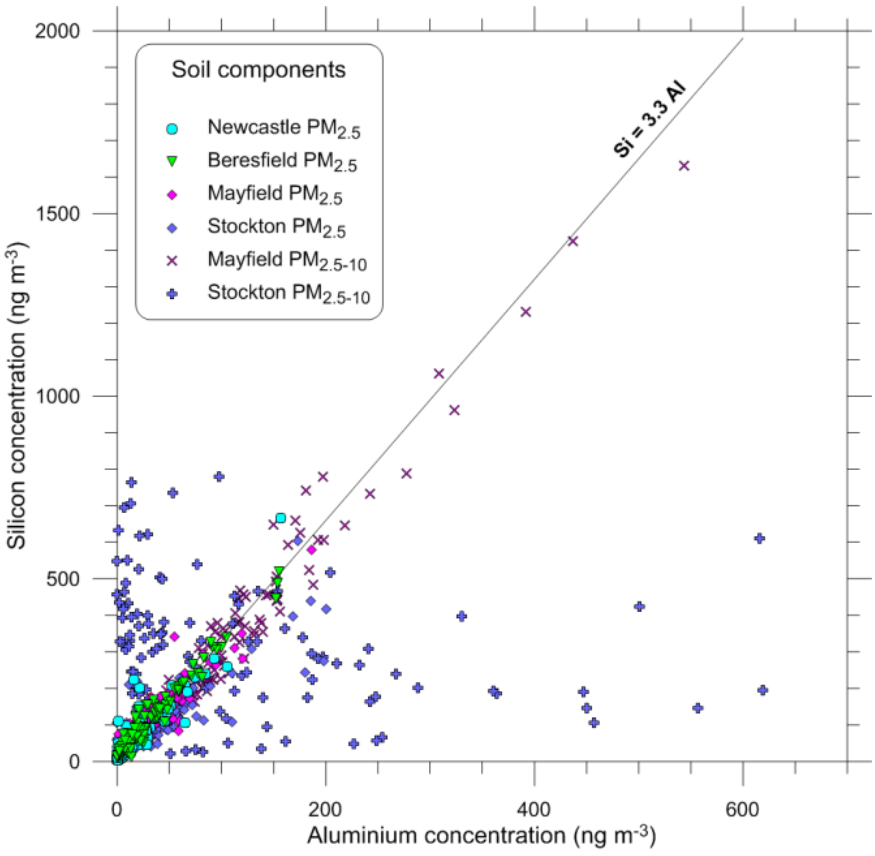

Figure 51: Scatter plot of silicon versus aluminium in $PM_{2.5}$ and $PM_{2.5-10}$

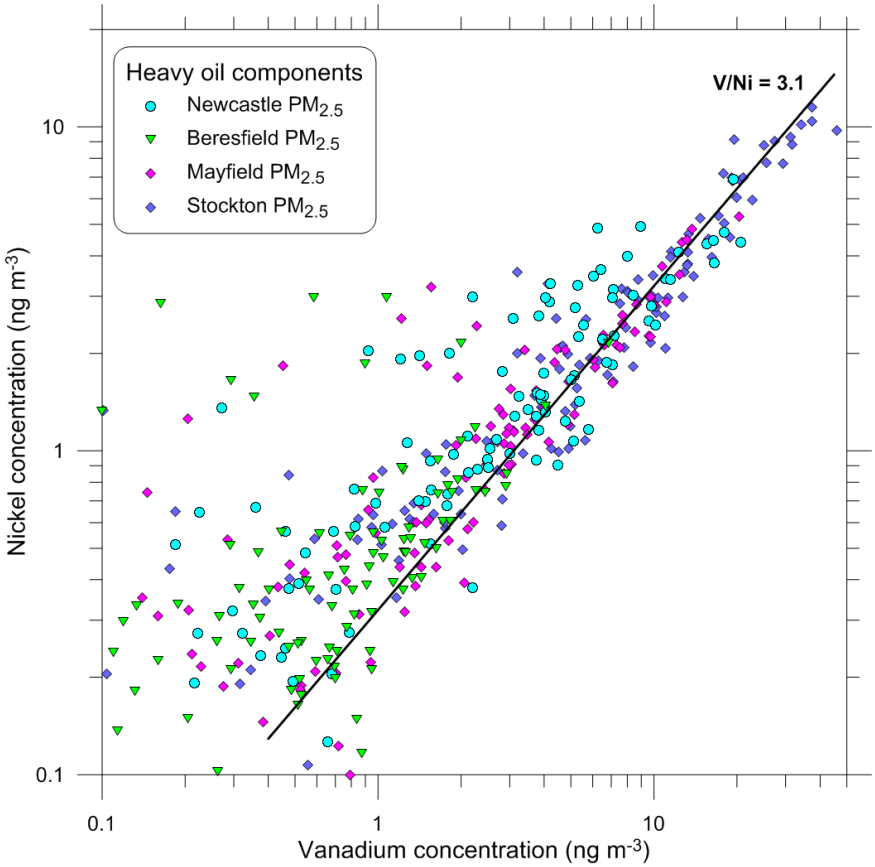

Figure 52: Scatter plot of nickel versus vanadium in $PM_{2.5}$.

Note the log-log scale, used to show the distribution at low concentrations more clearly.

The final species correlation is nickel versus vanadium in Figure 52, which is plotted as a log-log scale to show the range more clearly. These are species in heavy fuel oil commonly used in shipping. The points are reasonably well correlated with the V/Ni ratio of 3.1 typical of shipping (Viana et al. 2009, 2014). Most of the larger deviations from the line are for an excess of nickel (at concentrations below about 4 ng m^{-3}), indicating an additional source(s) of nickel in the airshed. The National Pollutant Inventory (NPI 2014) lists total emissions to air of 90kg nickel from facilities (including two steel product manufacturers) in the Mayfield–Kooragang Island area in 2013–14, but, although not known, it is unlikely that much of this is in the $PM_{2.5}$ fraction.

6 Receptor modelling results – $PM_{2.5}$ factors

Nine factors were identified in the positive matrix factorisation (PMF) analysis of the $PM_{2.5}$ data at each site. These are discussed in detail in the following sections by factor. They are also presented by site in Figure 136 to Figure 143 in Appendix C.

Each of the factors is characterised by a chemical 'fingerprint' which is a pattern of chemical species and their concentrations. Before considering each factor in turn, we describe here the interpretation of the three types of figures presented for each factor – the fingerprints, the time series and the conditional probability function (CPF) plots, using the figures for Factor 1.

Figure 53 shows the 'fingerprint' of the factor, so called because it shows a pattern of species concentrations. The fingerprint shows the relative amounts of the various species in the factor. It does this in two ways. Firstly, the vertical blue bars show the species concentrations, e.g. in Factor 1 at Newcastle, the chloride concentration is 650 ng m^{-3}. Secondly, the dark red squares show the percentage of the species that occurs in the factor, e.g. Factor 1 at Newcastle includes 90% of the chloride measured in the samples and 24% of the total $PM_{2.5}$ mass. Both of these pieces of information (concentrations and percentages) are shown because both are important in analysing and interpreting the factors.

The right-hand part of Figure 53 shows how the contribution of the factor to total $PM_{2.5}$ varies during the year at each of the four sites. Factor 1 contributes most strongly in spring/summer and is very little during winter. This corresponds with the dominance of onshore winds during spring/summer.

Figure 54 shows the wind sector plot from the CPF analysis described in Section 3.3. In simple terms, the distance of the yellow line from the central red dot shows the probability that the wind from that direction includes a contribution to the factor, indicating that sources in that direction contribute to the factor. Because of limitations of the analysis discussed in Section 3.3, attention should focus on the gross features and not the fine detail. The CPF plots in Figure 54 all point towards the coast with the back of the semi-circular lobe aligned parallel to the coast indicating that the factor is only detected for onshore flows, consistent with this factor being fresh sea salt aerosol.

Factor contributions are expressed in µg m^{-3} and in percentage contributions to the total $PM_{2.5}$ or $PM_{2.5\text{-}10}$ mass, with reference made to the so-called reconstructed mass (i.e. the mass derived from summing the factor contributions), not the gravimetric mass. As shown in Figure 43 and Figure 44, there is close agreement between gravimetric mass and PMF reconstructed mass; the latter was used for consistency through the report.

6.1 $PM_{2.5}$ Factor 1 – Fresh sea salt

The annual average contribution of this factor to $PM_{2.5}$ is: Newcastle 1.6 µg m^{-3} (24%); Beresfield 0.8 µg m^{-3} (13%); Mayfield 1.3 µg m^{-3} (20%); Stockton 2.1 µg m^{-3} (23%).

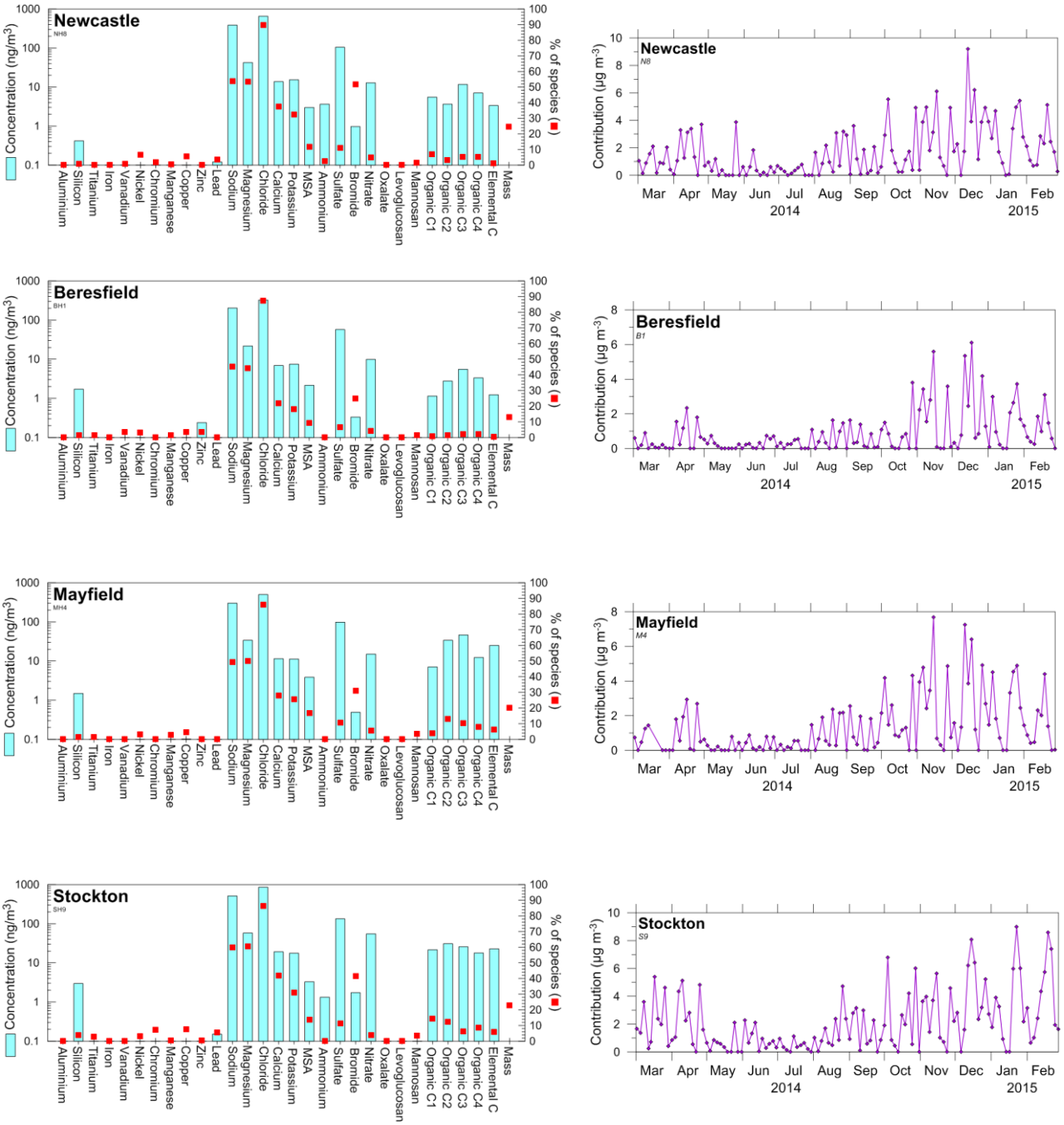

Figure 53: Fingerprints and time series plots of $PM_{2.5}$ Factor 1 (fresh sea salt) at the four study sites

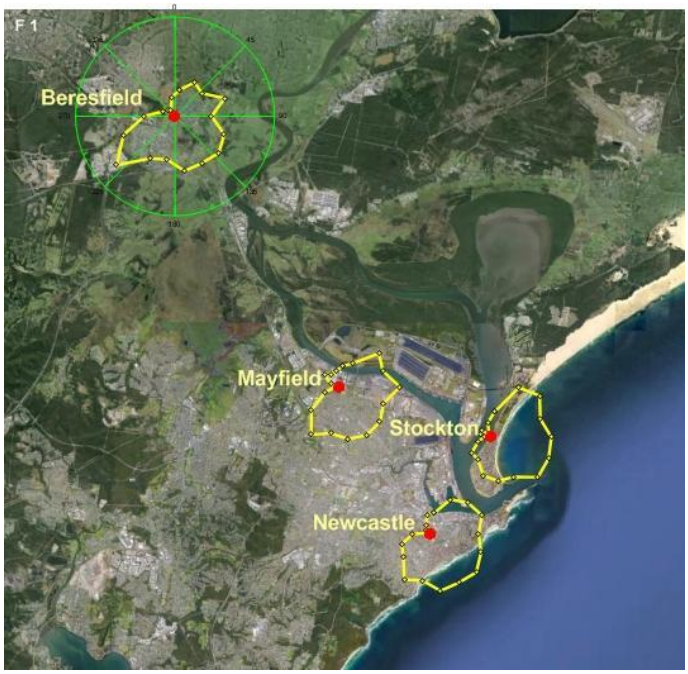

Figure 54: CPF of $PM_{2.5}$ Factor 1 (fresh sea salt) at the four study sites

The source of Factor 1 is clearly identifiable as fresh sea salt aerosol because, as Figure 53 shows, it is dominated by the sea water elements sodium, chloride, magnesium, and sulfate and their ratios (Table 7) closely match those for standard sea water (Millero et al. 2008) – mostly within 10%. This factor includes 85–90% of the chloride and about 50% of the sodium and magnesium in the samples. The fingerprints also include small contributions from nitrate and organic and elemental carbon, generally less than 1% of the factor. The nitrate contributes to the slight chloride loss, which is highest at Stockton.

Table 7: Comparison of the constituents of the fresh sea salt factor with standard sea water (Millero et al. 2008)

Species ratio to Na	Standard sea water	Newcastle	Beresfield	Mayfield	Stockton
Mg/Na	**0.120**	0.110	0.108	0.112	0.112
Cl/Na	**1.80**	1.69	1.60	1.66	1.67
Ca/Na	**0.038**	0.036	0.034	0.038	0.037
K/Na	**0.037**	0.040	0.037	0.037	0.034
SO_4/Na	**0.252**	0.27	0.28	0.33	0.26

The CPF plots in Figure 54 all point towards the coast (south-east) with the back of the semi-circular lobe aligned parallel with the coast, which runs south-west to north-east. This is consistent with the composition of this factor being fresh sea salt aerosol. At Beresfield, which is 16km from the coast, this factor contributes an average of 0.8 µg m^{-3} compared to 2.1 µg m^{-3} at Stockton, which is on the coast. Figure 55 shows the annual average decreases with the logarithm of the distance from the coast. It includes results for Singleton and Muswellbrook from Hibberd et al. (2013). A similar trend (not shown) is present in winter

although average concentrations are lower. In summer, average concentrations are higher and the fall-off faster for the sites inland from Mayfield. The time series plots in Figure 53 show this factor is strongest in spring and summer and weakest in winter. This corresponds with the dominance of onshore winds during spring and summer and their absence during winter (e.g. Figure 27).

As a proportion of total $PM_{2.5}$ mass, the annual average contribution of fresh sea salt aerosol to $PM_{2.5}$ mass decreases from 23% at Stockton to 13% at Beresfield. However, the proportions are much higher in summer, varying from 46% (3.6 µg m^{-3}) at Stockton to 27% (1.6 µg m^{-3}) at Beresfield, and much lower in May to July – 5% (0.6 µg m^{-3}) at Stockton and 3% (0.2 µg m^{-3}) at Beresfield.

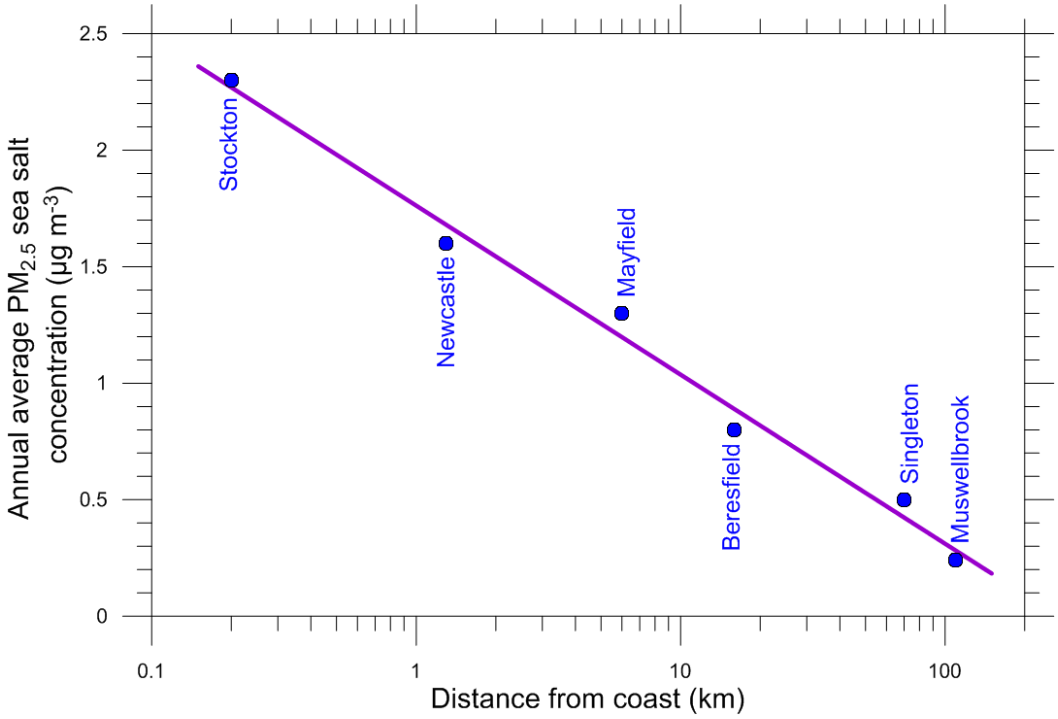

Figure 55: Variation in annual average $PM_{2.5}$ fresh sea salt concentration with distance from coast

6.2 $PM_{2.5}$ Factor 2 – Pollutant-aged sea salt

This factor is fresh sea salt aerosol that has 'aged' and changed composition through mixing and reacting with industrial, commercial, road and non-road transport and residential emissions from both local and regional sources. The contribution of inter-regional transport to airborne particle concentrations within NSW metropolitan areas has been addressed in several studies (Cope & Ischtwan 1996; Nelson et al. 2002; Cohen et al. 2012; Cope et al. 2014). It contains a complex mix of species and cannot be ascribed to a single source. The annual average contribution of this factor to $PM_{2.5}$ is: Newcastle 1.5 µg m^{-3} (23%); Beresfield 1.4 µg m^{-3} (23%); Mayfield 1.7 µg m^{-3} (25%); Stockton 2.0 µg m^{-3} (22%).

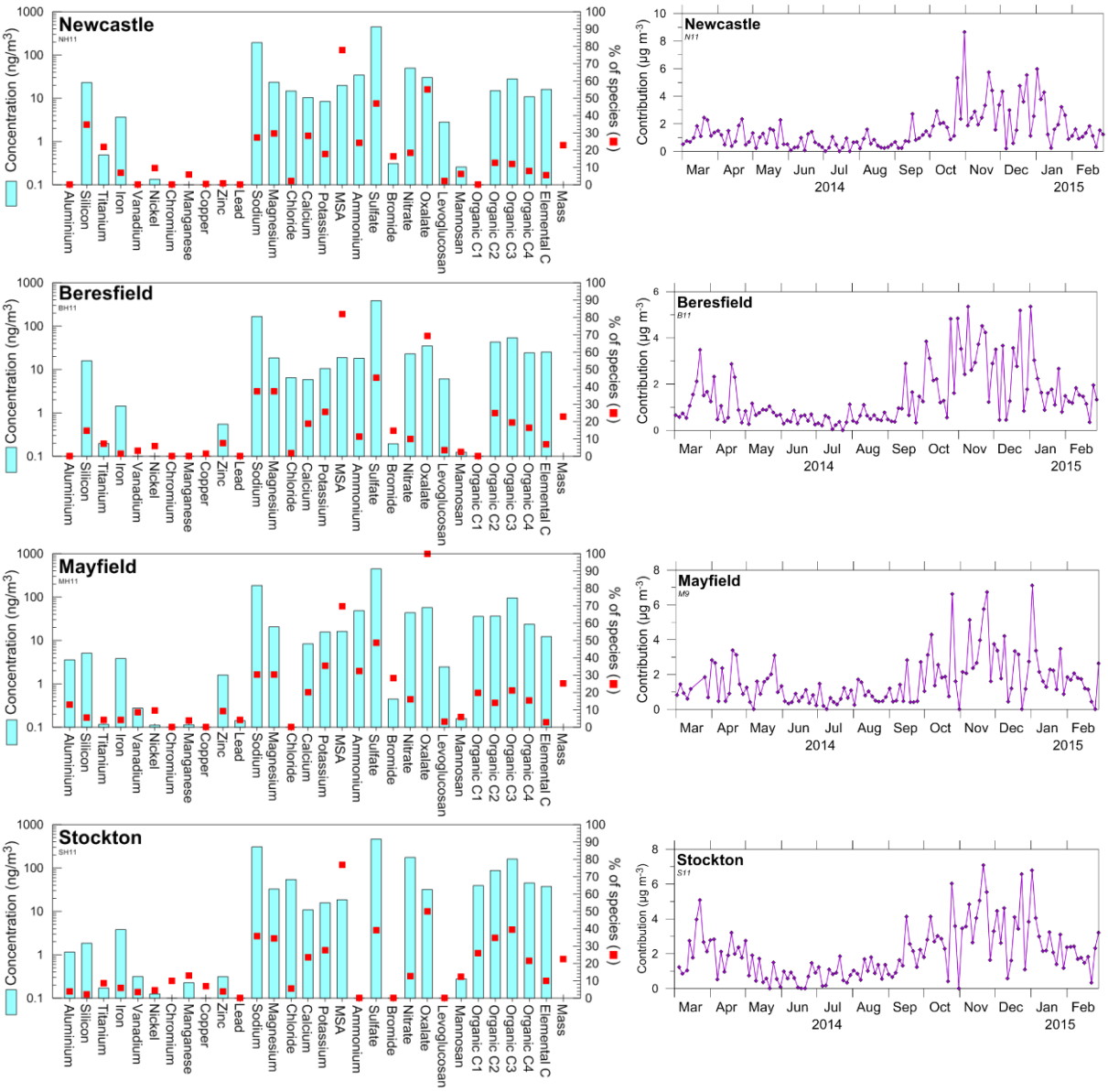

Figure 56: Fingerprints and time series plots of $PM_{2.5}$ Factor 2 (pollutant-aged sea salt) for each of the four study sites

Figure 57: CPF of $PM_{2.5}$ Factor 2 (pollutant-aged sea salt) at the four study sites

The Factor 2 fingerprints are dominated by sulfate (SO_4) and sodium (Na). The source is identified as pollutant-aged sea salt because the Mg/Na ratio is almost the same as that of sea water (0.11–0.12), and the Ca/Na and K/Na ratios are also very close to those of sea water (Table 8) but there is almost no chloride. It includes 20–35% of the Na and Mg. There is almost no chloride (Cl^-) because it has been displaced (e.g. Seinfeld & Pandis 2006), mostly by sulfuric acid (H_2SO_4) and to some extent nitric acid (HNO_3) and possibly oxalic acid ($H_2C_2O_4$) (Yu et al. 2005). Table 8 shows that the proportion of sulfate in the aged sea salt is ten times the level in fresh sea salt, and that the proportion of nitrate, and oxalate are similar across the sites. The sources of these acids are industrial and transport emissions. Sulfuric and nitric acids are produced from the oxidation of sulfur and nitrogen oxides from fossil fuel combustion. Oxalate can be produced through the oxidation of oxygenated volatile organic compounds (e.g. Warneck 2003; Carlton et al. 2007).

This aged sea salt factor includes about 50% of the sulfate in the $PM_{2.5}$ samples, 60% of the oxalate, and 70% of the MSA^- (methanosulfonate), a secondary organic marine aerosol (Rinaldi et al. 2010). It also includes 10–20% of the organic carbon and the nitrate.

Given the presence of sulfate, nitrate and ammonium in this factor at all sites (except there is no NH_4 in this factor at Stockton), it is possible this factor also includes some secondary sulfate and nitrate particles (see Section 6.3 and 6.7).

Compared to the CPF plots for fresh sea salt (Figure 54), those for aged sea salt (Figure 57) show the factor is detected approximately equally for all wind directions. This reflects the fact that the aging process requires time for the fresh sea salt aerosol to mix and react with the industrial and transport pollutants from both local and regional sources. That is, the aged sea salt is well mixed in the airshed, so there is no preferred wind direction in the CPF plots.

The time series plots in Figure 57 are very similar to those for fresh sea salt due both to the reduced presence of fresh sea salt aerosol and the much weaker photochemical reactions in winter. The annual average contribution of this factor to $PM_{2.5}$ mass is about 1.5 µg m^{-3} but

over the four months October to January, this almost doubles to 2.5–2.8 µg m^{-3} (about a third of the mass at most sites), whereas during winter it drops to about 0.5 µg m^{-3}.

Table 8: Comparison of constituents of Factor 2 with standard sea water

Species ratio to Na	Sea water	Newcastle	Beresfield	Mayfield	Stockton	
Mg/Na	**0.120**	0.121	0.110	0.111	0.106	
Ca/Na	**0.038**	0.053	0.035	0.045	0.035	
K/Na	**0.037**	0.043	0.063	0.084	0.051	
Cl/Na	***1.80***	***0.08***	***0.04***	***0.00***	***0.18***	
SO_4/Na	***0.252***	***2.32***	***2.32***	***2.41***	***1.51***	
NO_3/Na		0.26	0.14	0.24	0.57	Ratio for $NaNO_3$ = 2.70
C_2O_4/Na		0.16	0.21	0.31	0.10	
EC/Na		0.08	0.15	0.07	0.12	
(OC1-4)/Na		0.28	0.72	1.03	1.08	
MSA/Na		0.10	0.11	0.09	0.06	

6.3 $PM_{2.5}$ Factor 3 – Secondary ammonium sulfate

The annual average contribution of this secondary ammonium sulfate factor to $PM_{2.5}$ is: Newcastle 0.8 µg m^{-3} (12%); Beresfield 0.6 µg m^{-3} (10%); Mayfield 0.6 µg m^{-3} (8%); Stockton 0.8 µg m^{-3} (9%). Note that at Newcastle this is a mixed factor with about one-quarter of the sulfate present as secondary sodium nitrate.

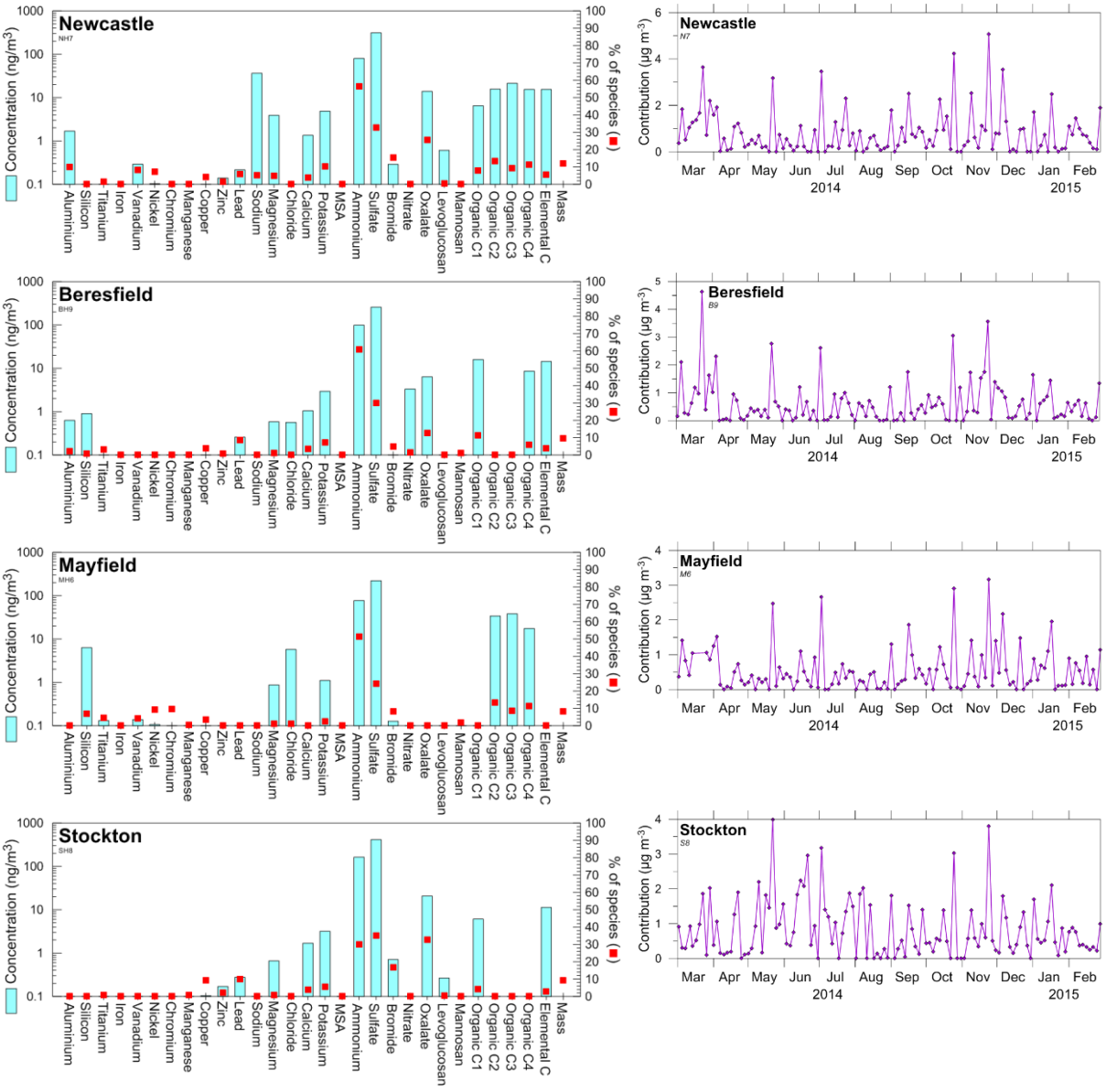

Figure 58: Fingerprints and time series plots of $PM_{2.5}$ Factor 3 (secondary ammonium sulfate) at the four study sites

Figure 59: CPF of $PM_{2.5}$ Factor 3 (secondary ammonium sulfate) at the four study sites

The fingerprints in Figure 58 show this factor is dominated by ammonium sulfate ($(NH_4)_2SO_4$), which forms as a secondary inorganic aerosol in the atmosphere. This factor accounts for about 30% of the sulfate at all sites and 55% of the ammonium except at Stockton, where it only accounts for 20% (see Factor 7, which includes a significant contribution from ammonium nitrate at Stockton). The oxalate to sulfate ratio is 0.025–0.05 except at Mayfield where it is 0 (Yu et al. 2005). At Newcastle, the V/Ni ratio of 2.8 is close to the mixed shipping/industry ratio (Factor 8) discussed in Section 6.8, but this factor only accounts for 8% of these elements compared to 75% in Factor 8.

The precursor sulfate is present in the atmosphere as the result of oxidation and photochemical reactions of sulfur from fossil fuel combustion. There may also be primary sources of sulfate such as fuel oil combustion from shipping or other combustion sources of sulfur-containing fuels which produce SO_3. Sources of ammonia include agriculture (mostly from animal excrement and fertiliser application), industrial processes, vehicular emissions and volatilization from soils and oceans (Behera et al. 2013). The seasonal cycle in Figure 58 shows the highest contribution of this factor to $PM_{2.5}$ mass in the warmer months from October to March but low in February, possibly because the temperatures were milder than usual.

Local and regional sources may contribute to secondary ammonium sulfate concentrations. The contribution of inter-regional transport to airborne particle concentrations within NSW metropolitan areas has been addressed in several studies (Cope & Ischtwan 1996; Nelson et al. 2002; Cohen et al. 2012; Cope et al. 2014). Cohen et al. (2012), by example, estimated the contribution of SO_2 emissions from coal-fired power stations located in the upper Hunter, Central Coast and Lithgow to secondary sulfate concentrations measured in parts of the Sydney basin.

The NH_4/SO_4 ratio for the components of this factor is 0.35 at Mayfield, 0.38 at Beresfield, and 0.39 at Stockton, all of which are very close to ratio of 0.38 for neutralised ammonium sulfate. However, the ratio is lower at Newcastle (0.26). This is because at this site, some of the sulfate is combined with sodium (from sea salt aerosol) to form sodium sulfate. If all the

sodium in this factor at Newcastle is assumed to be present as (secondary) sodium sulfate, then the NH_4/SO_4 ratio for the remaining sulfate is 0.34, close to the expected value. This calculation indicates that about three quarter of the secondary sulfate at Newcastle is ammonium sulfate with the remaining quarter being sodium sulfate.

Additional information is provided by Figure 60 which shows a scatter plot of the ammonium versus total sulfate concentrations in all the samples, not just the part identified by PMF as being in this factor. The points along the dashed black line represent the proportions in ammonium sulfate, whereas those along the solid red line represent the proportions in ammonium bisulfate (NH_4HSO_4). This demonstrates that simple analysis of the total concentrations in the samples would point to the secondary sulfate being present as ammonium bisulfate, whereas the PMF analysis identifies that most of the ammonium (other than at Stockton) is present as ammonium sulfate. Most of the rest of the sulfate is in the Factor 2 (pollutant-aged sea salt), Factor 1 (fresh sea salt) and at Stockton in Factor 8 (mixed shipping/industry).

All points well above the 0.375 line are for Stockton, which show an excess of ammonium. As discussed in Section 6.7, this is due to local sources of ammonium or its precursor ammonia, such as the Orica Australia ammonium nitrate manufacture facility situated on Kooragang Island to the west of the Stockton site.

A noteworthy point from Figure 60 is that the coarser $PM_{2.5\text{-}10}$ particles contain negligible ammonium compared to the $PM_{2.5}$ – the $PM_{2.5\text{-}10}$ points all lie along the x-axis in Figure 60 with the highest ammonium concentrations being only 20 ng m^{-3}.

The CPF plots for secondary ammonium sulfate (Figure 59) are similar to those for pollutant-aged sea salt with approximately equal probabilities for the wind in any given direction that the factor will make a significant contribution to the $PM_{2.5}$ mass. This reflects the fact that it is a secondary (inorganic) aerosol, which is produced by reactions in the well-mixed atmosphere, not directly downwind from any given source.

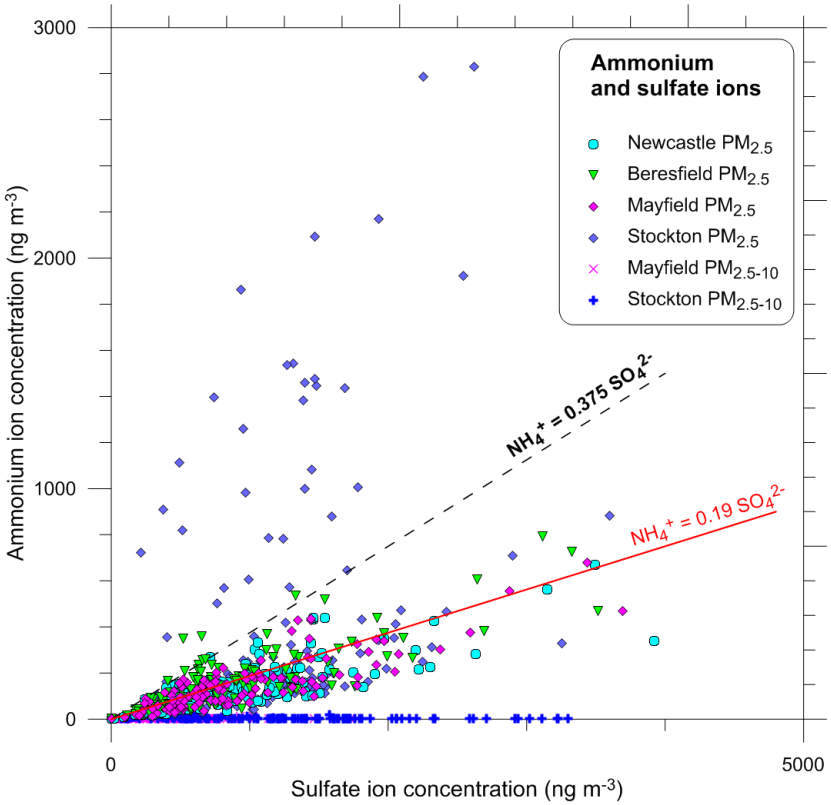

Figure 60: Scatter plot of ammonium versus total sulfate in all $PM_{2.5}$ and $PM_{2.5-10}$ samples

6.4 $PM_{2.5}$ Factor 4 – Wood smoke

The annual average contribution of this wood smoke factor to $PM_{2.5}$ is: Newcastle 0.7 µg m^{-3} (10%); Beresfield 0.9 µg m^{-3} (15%); Mayfield 0.7 µg m^{-3} (11%); Stockton 0.5 µg m^{-3} (6%).

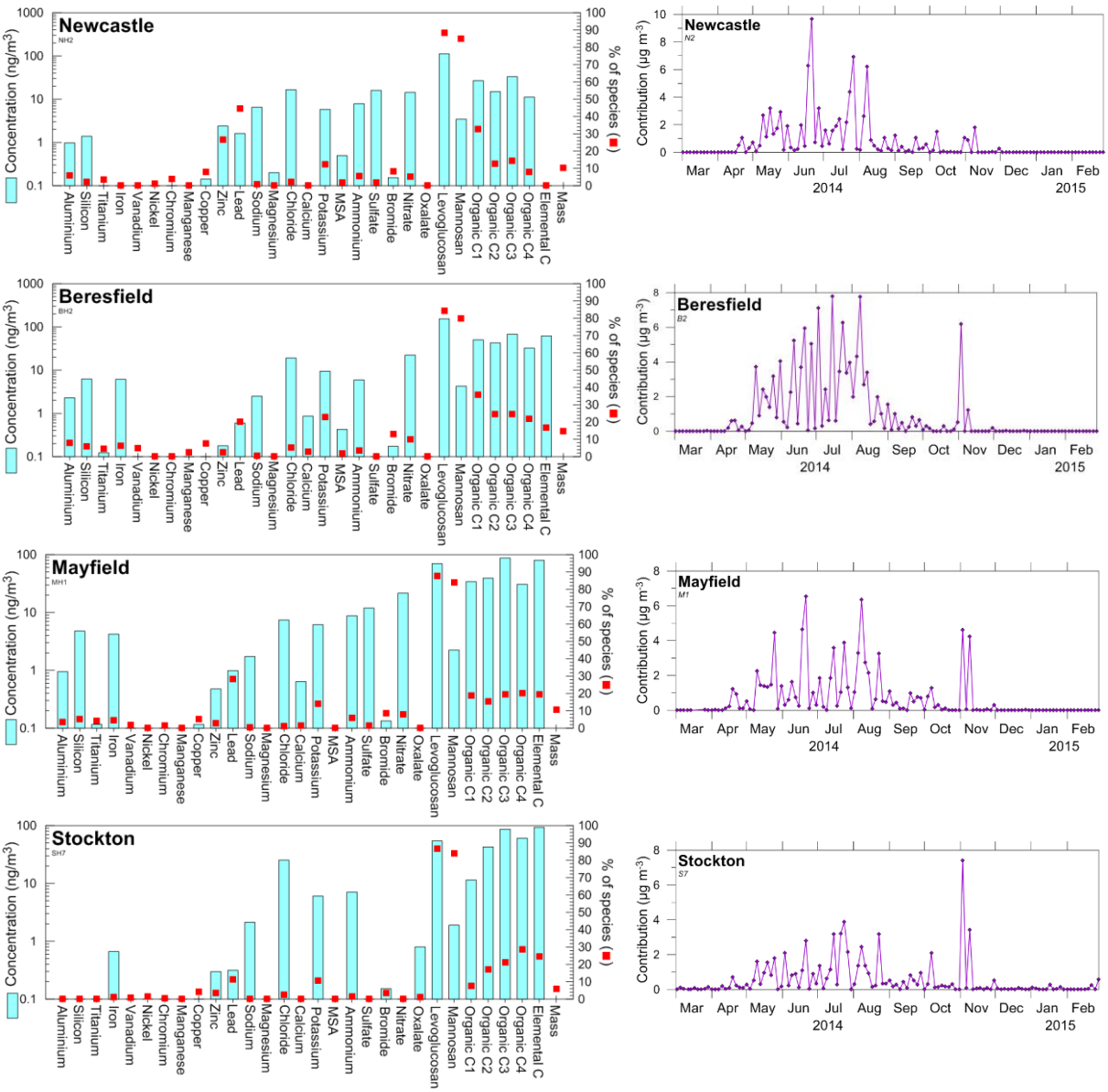

Figure 61: Fingerprints and time series plots of $PM_{2.5}$ Factor 4 (wood smoke) at the four study sites

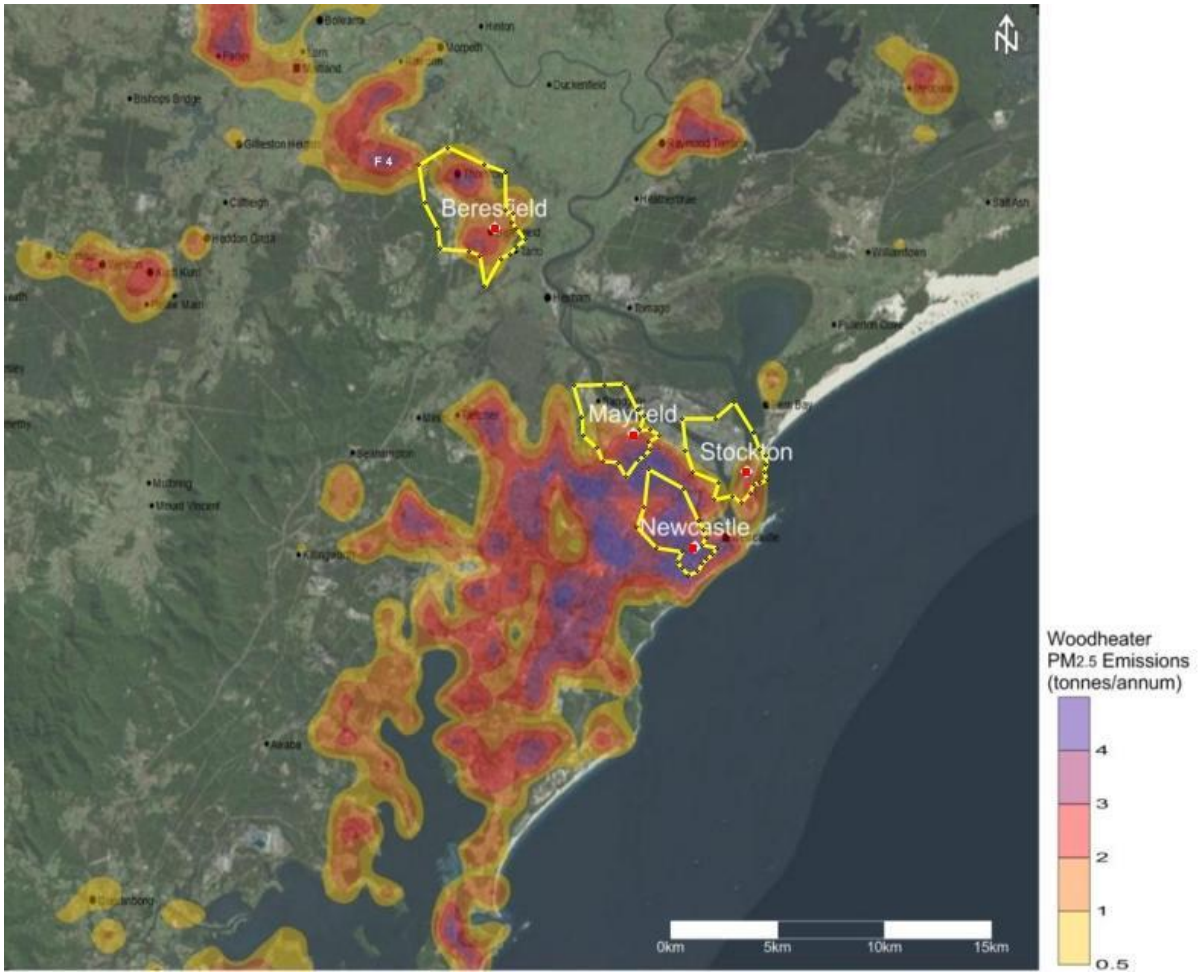

Figure 62: CPF of $PM_{2.5}$ Factor 4 (wood smoke) at the four study sites overlaid on the annual domestic wood heater $PM_{2.5}$ emissions from the Greater Metropolitan Region air emissions inventory for the 2008 calendar year (EPA 2012)

The source of Factor 4 is clearly identifiable as wood smoke because it contains 85–90% of the levoglucosan and mannosan, which are unique tracers for the combustion of cellulose found in trees and plants (Iinuma et al. 2007). These are the referred to as the 'drivers' of the factor because they ae used to identify and name the factor. However, for this factor and several others, the drivers are not the dominant species contributing most of the mass.

This factor also includes about 20% of the organic carbon (OC1-4) and elemental carbon. The ratio of levoglucosan to mannosan is an indication of the type of wood combusted. The ratio is 31 at Newcastle, 36 at Beresfield, 31 at Mayfield and 29 at Stockton. These are close to the value of 36 observed for wood smoke from domestic wood heaters in Singleton and Muswellbrook in the Upper Hunter Fine Particle Characterisation Study (Hibberd et al. 2013), and are representative of values for the combustion of eucalyptus (Goncalves et al. 2010).

When levoglucosan data are not available, potassium is often used as a tracer for wood smoke. The ratio of potassium to levoglucosan is moderately consistent across sites (factor of 2 variation) – 0.052 at Newcastle, 0.11 at Stockton, 0.088 at Mayfield, and 0.062 at Beresfield.

Residential wood heater emissions mainly comprise fine particles, with this source estimated to emit 900 tonnes of $PM_{2.5}$ and about 35 tonnes of $PM_{2.5\text{-}10}$ in 2008 across the five lower Hunter LGAs (EPA 2012). Wood heater emissions accounted for 94% of $PM_{2.5}$ emissions from the residential sector during this year.

The time series in Figure 61 shows the factor present from late autumn through to early spring, corresponding to the pattern for the use of domestic wood heaters, and with a few spikes in early November (much weaker at Newcastle) associated with bushfire/hazard reduction burns. Spatial variations in $PM_{2.5}$ emissions from wood heater emissions based on the Greater Metropolitan Region air emissions inventory for the 2008 calendar year are illustrated in Figure 62 (EPA 2012). Wood heater emissions occurring in the upper Hunter valley north-east of Maitland are not shown in the figure.

Although the annual average contribution of wood smoke to $PM_{2.5}$ mass is about 10% across all sites, it contributes much more in winter: 41% (2.8 µg m^{-3}) at Beresfield, 31% (~1.8 µg m^{-3}) at Newcastle and Mayfield, and 11% (1.2 µg m^{-3}) at Stockton.

The CPF plots in Figure 62 all show much stronger wind direction dependence than for the previous two factors. There is no smoke contribution for onshore flows. This is partly because winter winds are predominantly north-westerlies, with regional winds reinforcing the offshore land breezes characteristic of the night-time and early morning. The strong wind direction dependence also reflects the fact that the dominant species in the smoke fingerprint are primary emissions, so the wind direction plays a much larger role in determining their contribution than for the pollutant-aged sea salt or secondary ammonium sulfate factors.

This factor includes an average of 25% (range 9% at Stockton to 45% at Newcastle) of the lead detected in the samples. It should be noted that the maximum 24-hour average lead concentrations were extremely low, ranging from 21 ng m^{-3} at Stockton to 32 ng m^{-3} at the Newcastle sites. The annual averages were 3-4 ng m^{-3}, compared to the NEPM (National Environmental Protection Measure) of 500 ng m^{-3} for the annual average lead concentration. The maximum 24-hour averages are similar to those of 9.5 ng m^{-3} (at Singleton) and 20.1 ng m^{-3} (at Muswellbrook) reported by Hibberd et al. (2013) for the Upper Hunter Particle Characterisation Study. Figure 63 shows that lead concentrations are highest from May to mid-July, most closely matching the shapes of the wood smoke factor contributions in Figure 61 but with some differences, which is not surprising given this factor only explains 25% of the observed lead concentrations.

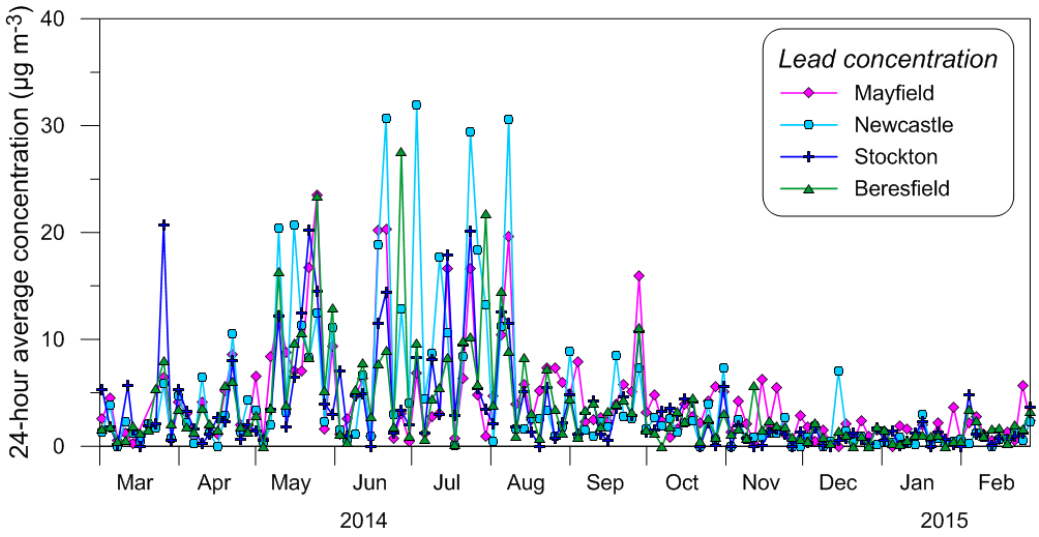

Figure 63: Time series of total lead concentrations in samples (not just in this factor)

Possible sources of lead could include (i) the burning of small amounts of old painted wood in domestic wood heaters, contrary to advice to residents by the EPA (1999), (ii) resuspension of lead in soil and dust (for example legacy lead deposited when leaded petrol was in use or due

to industrial emissions), and (iii) remobilisation by fire of historic lead in old trees (e.g. Kristensen et al. 2014).

Only a very small amount of lead needs to be released by burning to produce the observed low concentrations. For example 1g of lead released into and thoroughly mixed over an area 1km x 1km and to a depth of 100m would produce an average concentration of 10 ng m^{-3}. If the volume of air were smaller, then a smaller amount of lead would be needed to reach 10 ng m^{-3}, and vice versa. Although modern paint is restricted to a maximum of 0.1% lead, prior to 1992 the limit was 1%, and prior to 1965 it could be up to 50% lead. Based on a typical paint coverage rate of 10 m^2 $litre^{-1}$, a 1m^2 piece of 1970s painted wood could release about 1g lead when burnt.

Unlike in the Upper Hunter Particle Characterisation Study (Hibberd et al. 2013), the PMF did not produce separate wood heater and bushfire smoke factors, so an analysis of the events log was undertaken to estimate the bushfire smoke contribution.

Table 9: Analysis of possible contribution of bushfire/hazard reduction burning to the wood smoke factor

Season	Number of 'smoke affected days' at one or more sampling sites	Number of these days potentially including some contribution from bushfire/hazard reduction smoke	% of potentially smoke-affected-days	Details (back trajectories passed by the following fires' areas)
Autumn	12	3 (25, 28, 31 May 2014)	25%	3960ha hazard reduction burn (HRB) at Yengo National Park, Wollombi during 18 May to 3 June 2014
Winter	29	3 (6 June, 30 July, 2 August 2014)	10%	2ha HRB at Whitebridge on 6 June; previous day bushfire (1ha) at Kurri Kurri on 29 July; previous day bushfire (2ha) at Wyee on 1 August
Spring	10	5 (19 and 25 September, 7 October, 3 and 9 November 2014)	50%	3ha bushfire at Glendon Brook on 24 September; 7ha bushfire at Hexham on 7 October; 893ha fire at Howes Valley burning 24 October to 7 November; 38ha fire at Balickera on 9 November 2014
Summer	0	0	0%	
Annual	51	12	24%	

This was done by examining whether bushfire/hazard reduction burning smoke could have caused or contributed to smoke on sampling days when the smoke factor contributed greater than 10% of the $PM_{2.5}$ mass (hereafter referred to as smoke-affected days). This analysis included investigating bushfire incidence records and undertaking wind and air quality trend

analysis and trajectory modelling, with the results summarised in Table 9. Findings indicated that bushfire/hazard reduction burning may have contributed smoke on about a quarter of all 'smoke-affected days' during the year (10% in winter, 25% in autumn and 50% in spring). However, the overall contribution of bushfire/hazard reduction smoke to the mass of this factor is probably much smaller than 25% given that the time series in Figure 61 matches the pattern for the use of domestic wood heaters so closely. Days most likely dominated by bushfire/hazard reduction smoke are those at the end of October/early November.

The extent of bushfire and prescribed burning varies significantly from year to year, resulting in significant inter-annual variations in the emissions from these sources. Particulate matter emissions are mainly emitted as fine particles. Bushfire and prescribed burning were estimated to emit 240 tonnes of $PM_{2.5}$ and about 45 tonnes of $PM_{2.5\text{-}10}$ in 2008 across the five local lower Hunter LGAs (EPA 2012). These $PM_{2.5}$ emissions are about a quarter of those from residential wood heaters (900 tonnes) but their impact is much less because of the much greater dispersion (mixing and dilution) that occurs between the source and monitoring site than for residential wood heater emissions that commonly occur at night in light winds with shallow inversions.

6.5 $PM_{2.5}$ Factor 5 – Soil

The annual average contribution of this soil factor to $PM_{2.5}$ is: Newcastle 0.5 µg m^{-3} (8%); Beresfield 0.6 µg m^{-3} (10%); Mayfield 0.7 µg m^{-3} (11%); Stockton 0.7 µg m^{-3} (8%).

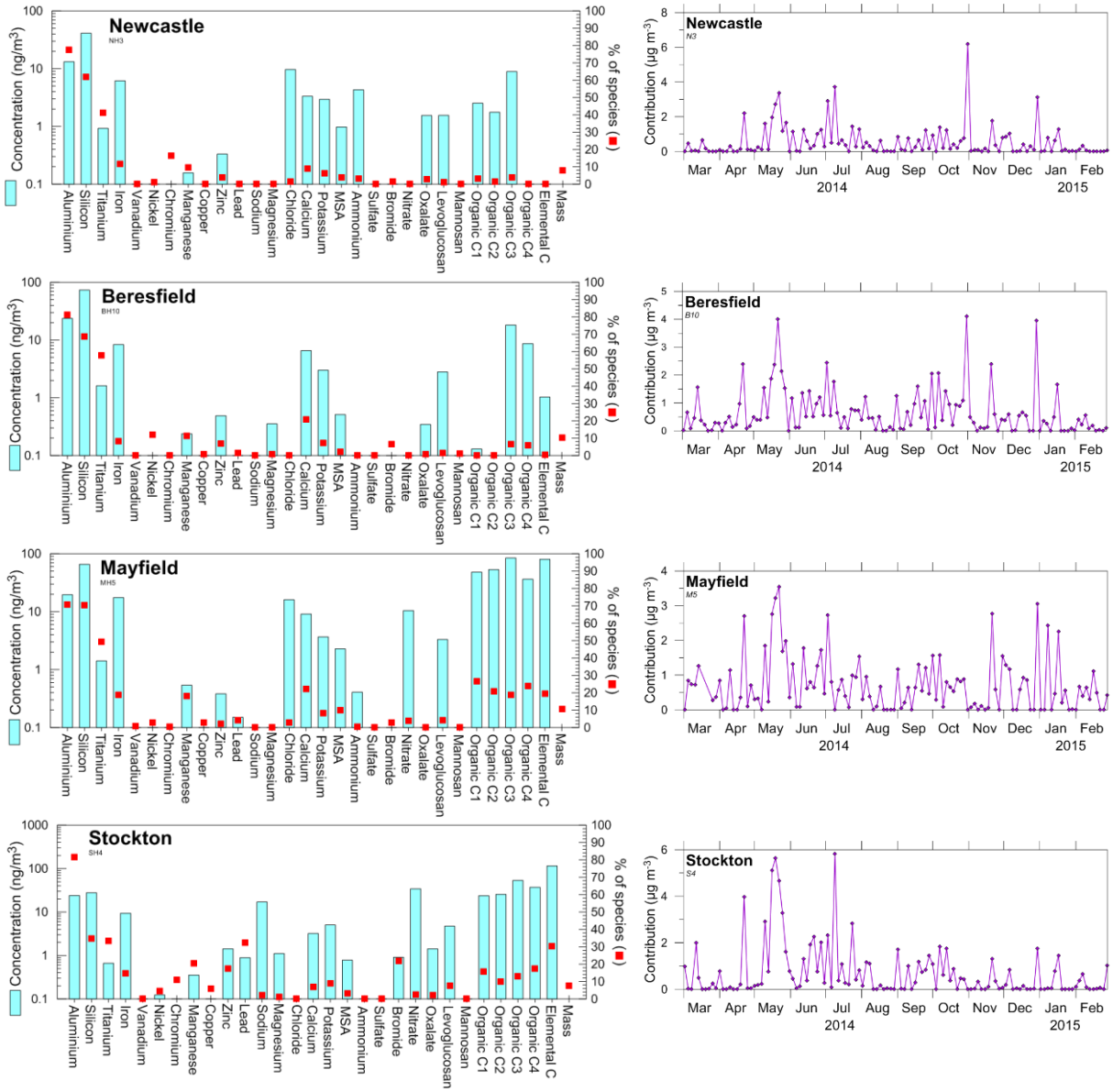

Figure 64: Fingerprints and time series plots of $PM_{2.5}$ Factor 5 (soil) at the four study sites

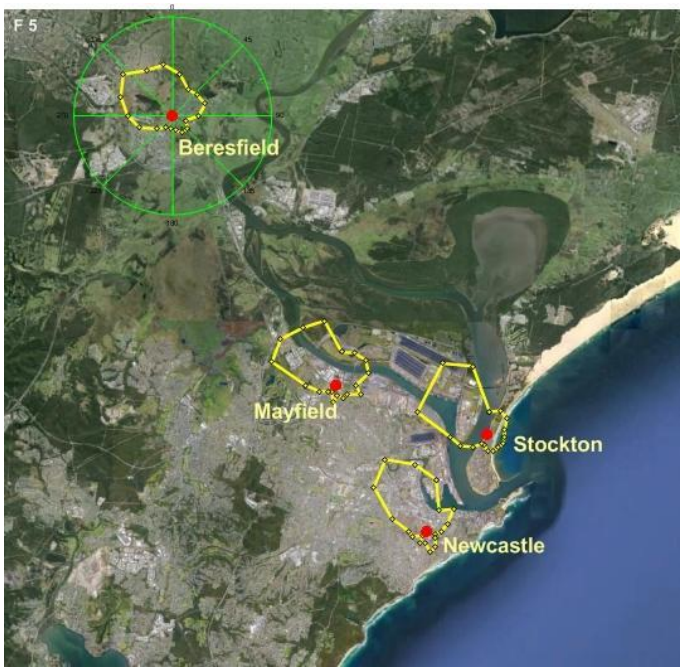

Figure 65: CPF of $PM_{2.5}$ Factor 5 (soil) at the four study sites

This factor is identified principally as soil because it includes the key elements associated with crustal dust – aluminium (Al), silicon (Si), and titanium (Ti) – and it is the factor that includes the largest proportion of these species.

A reliable indicator of soil dust is an Al/Ti ratio of 14 and an Al/Si ratio of 0.30, and Table 10 shows these values occur for this factor at three of the sites, but at Stockton the ratios are 2.5 times larger. This indicates the presence of an additional Al source in this factor at Stockton, which this analysis has not yet identified. The table also lists the ratios Ti/Si, Fe/Si and Ca/Ti and compares these against literature values for crustal composition (Lide 1997) and some inland Australian dust samples (Radhi et al. 2010). The Mayfield and Stockton sites show relatively more iron and calcium than the other two sites, possibly indicating an industrial origin for part of the dust.

Table 10: Comparison of the constituents of the soil factor with crustal composition (Lide 1997) and some typical Australian dust (Radhi et al. 2010)

Species ratio	Crustal composition (Lide 1997)	Australian dust	Newcastle	Beresfield	Mayfield	Stockton
Al/Ti	**14**	**11.5-15.1**	14.2	14.6	13.9	36
Al/Si	**0.29**	**0.27-0.29**	0.32	0.32	0.30	0.86
Ti/Si	**0.020**	**0.018-0.026**	0.022	0.022	0.021	0.023
Fe/Si	**0.200**	**0.22-0.23**	0.15	0.11	0.27	0.34
Ca/Si	**0.15**		0.08	0.09	0.14	0.12

At Mayfield and Stockton, this factor also includes varying amounts of organic and elemental carbon. At Mayfield 30% is organic carbon and 10% elemental carbon. At Stockton, organic and elemental carbon each make up 15% of the factor. These carbon components in the soil factor contribute about 0.3 µg m^{-3} (4%) of the total annual average $PM_{2.5}$ mass at Mayfield and Stockton, whereas their contribution at the other two sites is negligible. The variability between sites of the composition of this factor is consistent with soil dust being of more local origin than some other $PM_{2.5}$ factors.

This could be because there is a local source of $PM_{2.5}$ carbon at these sites or because of differences in the sampling regime. As described in Section 3.1, the EC/OC analysis for $PM_{2.5}$ at Mayfield and Stockton was conducted on quartz filters from the GENT sampler whereas at the other two sites (Newcastle and Beresfield) it was conducted on quartz filters from the ASP samplers, the ASP particle size cut-off is sharper than for the GENT, so that the GENT $PM_{2.5}$ samples probably contain a larger fraction of $PM_{2.5-10}$ particles than the ASP samples (Section 2.2.1).

The CPF plots in Figure 65 show strong lobes for north-westerly to northerly winds. At Beresfield the distribution is slightly less elongated with the dominant direction being west-north-west to north-west. Potential sources include both local and regional emissions but because this is a primary emission, we expect the lobes will generally point in the direction of the dust sources. The CPFs for the three near-coastal sites indicate contributions from local sources (potentially Kooragang Island and Mayfield and Carrington industrial areas) as well as further inland from up the Hunter Valley. Soot and/or coal particles may contribute to the carbon identified in this soil factor at Mayfield and Stockton.

The time series plots show contributions at various times through the year with the largest contribution in May, when it makes up about 20% of the $PM_{2.5}$ mass across all sites. This is likely to be due to the sampling sites being located downwind, in terms of the prevailing north-westerly quadrant winds, of potential local and regional sources of dust. The lowest concentrations are in February to March and August to September.

6.6 $PM_{2.5}$ Factor 6 – Vehicles

The annual average contribution of this vehicle factor to $PM_{2.5}$ is: Newcastle 0.7 µg m^{-3} (10%); Beresfield 0.7 µg m^{-3} (11%); Mayfield 0.6 µg m^{-3} (9%); Stockton 0.4 µg m^{-3} (5%).

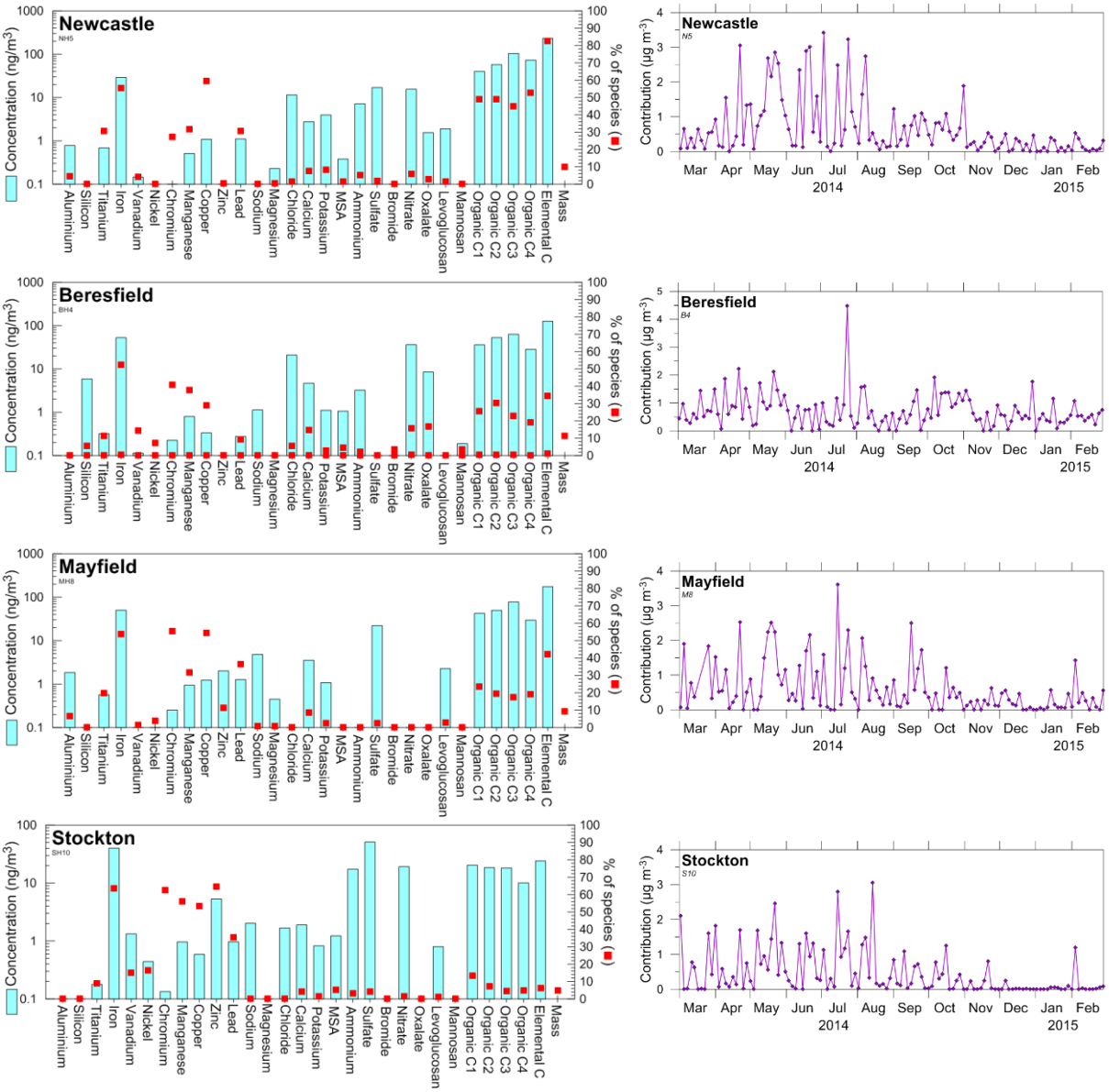

Figure 66: Fingerprints and time series plots of $PM_{2.5}$ Factor 6 (vehicle) at the four study sites

This factor includes about half the iron, manganese, chromium and copper at all sites. Scaling the concentrations of the metals to iron (Fe), all sites had 1.5–2% manganese (Mn), 0.2–0.5% chromium (Cr), 1.5–4% copper (Cu), and 5–10% calcium (Ca) (Table 11). The factor also has an OC/EC ratio of approximately 1:2, indicative of vehicles (Fujita et al. 2007; Watson et al. 1994). Non-road vehicles and equipment running on automotive petrol and diesel could also be contributing to this factor. The nature of the vehicle mix, including proportion of petrol and diesel vehicles and vehicle type and age, influences the OC/EC ratio as does the location at which measurements are done relative to the vehicle emission source. The further the monitoring site is from the source, the greater the OC/EC ratio (Fujita et al. 2007).

Copper has been identified as a marker for brake wear (Visser et al. 2015). All sites except Mayfield also include nitrate. Noteworthy is that this factor mostly includes very little or no zinc – most of the zinc (>70%) is in the mixed industry/vehicle factor (Factor 9). However, at Stockton this factor includes 60% of the zinc indicating there are probably some industry sources mixed in this factor at Stockton. The OC/EC ratio is also higher at Stockton as compared to other sites, potentially indicating that this site is further away from the main vehicle emission sources or that another source is contributing to the OC in the factor.

Table 11: Ratios of key species in the industry/vehicle factor

Species ratio	Newcastle	Beresfield	Mayfield	Stockton
Mn/Fe	0.018	0.015	0.019	0.024
Cr/Fe	0.0022	0.0043	0.0050	0.0033
Cu/Fe	0.037	0.0063	0.024	0.015
Ca/Fe	0.095	0.089	0.071	0.047
OC1/EC	0.17	0.28	0.24	0.85
OC2/EC	0.25	0.42	0.29	0.77
OC3/EC	0.45	0.50	0.45	0.76
OC4/EC	0.31	0.23	0.17	0.42
OC_{total}/EC	1.15	1.43	1.15	2.79

Although these species could indicate vehicle or industry sources, the close agreement of the ratios across all sites point to the source(s) being similar across all sites. A vehicle component could include direct vehicle emissions from the combustion of petrol and diesel, as well as emissions from brake and tyre wear.

The wear of brakes results in the emission of Fe and Cu. Manganese may be indicative of the fuel additive methylcyclopentadienyl manganese tricarbonyl (MMT), which has been used as a fuel additive in Australia since 2000 (NICNAS 2003). During combustion MMT releases inorganic Mn species (Joly et al. 2011). Cohen et al. (2005) have reported its presence due to vehicle emissions at up to 5 ng m^{-3} in $PM_{2.5}$ in Sydney. Calcium is used in lubricating oil for diesel vehicles (Cheung et al. 2010). Hence it is concluded that this is a vehicle factor.

On-road vehicles were estimated to emit 230 tonnes of $PM_{2.5}$ in 2008 across the five local lower Hunter LGAs (EPA 2012), comprising exhaust emissions from diesel (55.2%), petrol (8.3%) and other vehicles (0.4%), and non-exhaust emissions from brake, tyre and road surface wear (36.1%).

The time series in Figure 66 shows this factor is highest in winter and late autumn. This can be explained by the lower mixing heights, weaker dispersion and prevalence of offshore winds during these months, leading to higher concentrations from these local emission sources (vehicles). During the summer, easterly (onshore) airflow dominates the region as illustrated in Section 2.5, with the influence of vehicle emissions reduced at the Newcastle monitoring

station compared to winter months. This is evidenced by the significantly lower ambient nitric oxide (NO) concentrations recorded at the Newcastle site during the summer (Figure 67). Summer NO levels are lower than May to July levels by a factor of ten. The morning peak in ambient NO levels associated with vehicle emissions is substantially lower in summer and the afternoon peak largely absent due to the prevalence of onshore winds during this season.

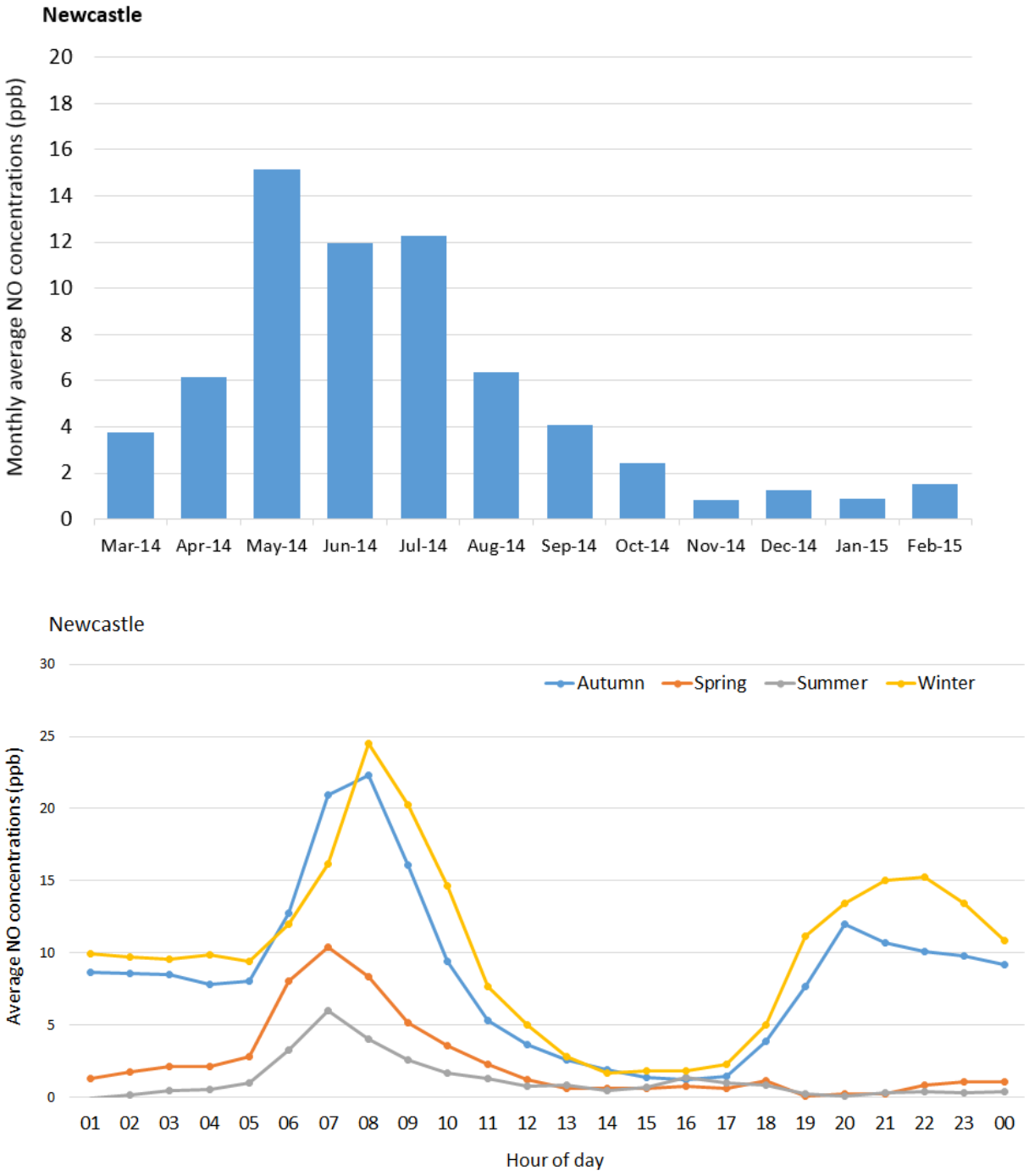

Figure 67: Monthly average nitric oxide (NO) concentrations (top) and seasonal average diurnal trends in NO concentrations (bottom) as measured at Newcastle Air Quality Monitoring Station during the study period

Figure 68 shows the excellent agreement between the wind directions to the sources given by the CPFs and the map of vehicle emissions from the EPA's Greater Metropolitan Region air

emissions inventory (EPA 2012). Note that the CPF roses only indicate the direction of the sources, not the distance from the monitoring site to the emissions source. The north-west CPF lobe points up along the highway towards Maitland.

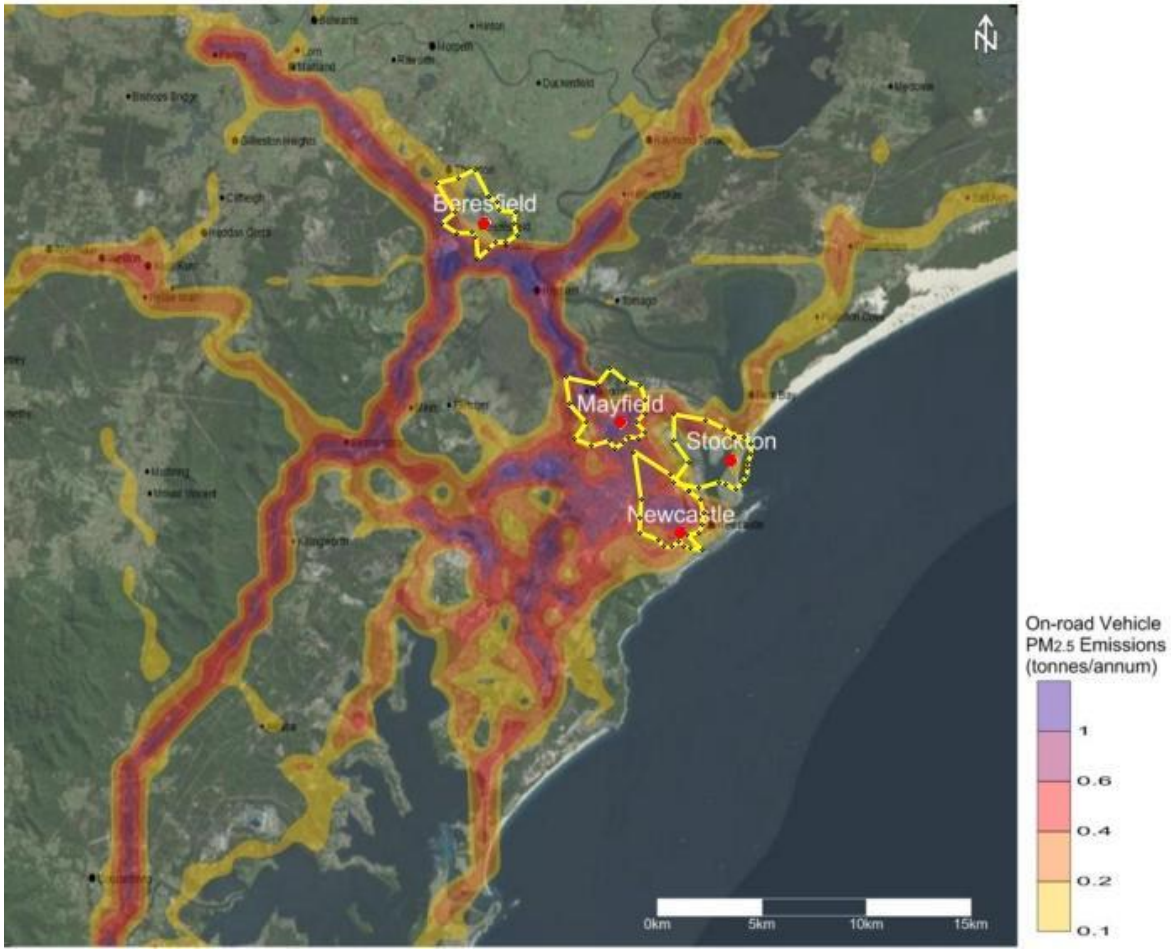

Figure 68: CPF of $PM_{2.5}$ Factor 6 (vehicle) at the four study sites overlaid on contour of $PM_{2.5}$ vehicle emissions from the Greater Metropolitan Region air emissions inventory (EPA 2012)

6.7 $PM_{2.5}$ Factor 7 – Primary or secondary nitrate

This factor is a primary emission of ammonium nitrate at Stockton but secondary nitrate (sodium nitrate) at the other three sites. The annual average contribution of this secondary nitrate factor to $PM_{2.5}$ is: Newcastle 0.5 µg m^{-3} (8%); Beresfield 0.4 µg m^{-3} (6%); Mayfield 0.7 µg m^{-3} (11%). At Stockton, this ammonium nitrate contributes 1.7 µg m^{-3} (19%) as an annual average.

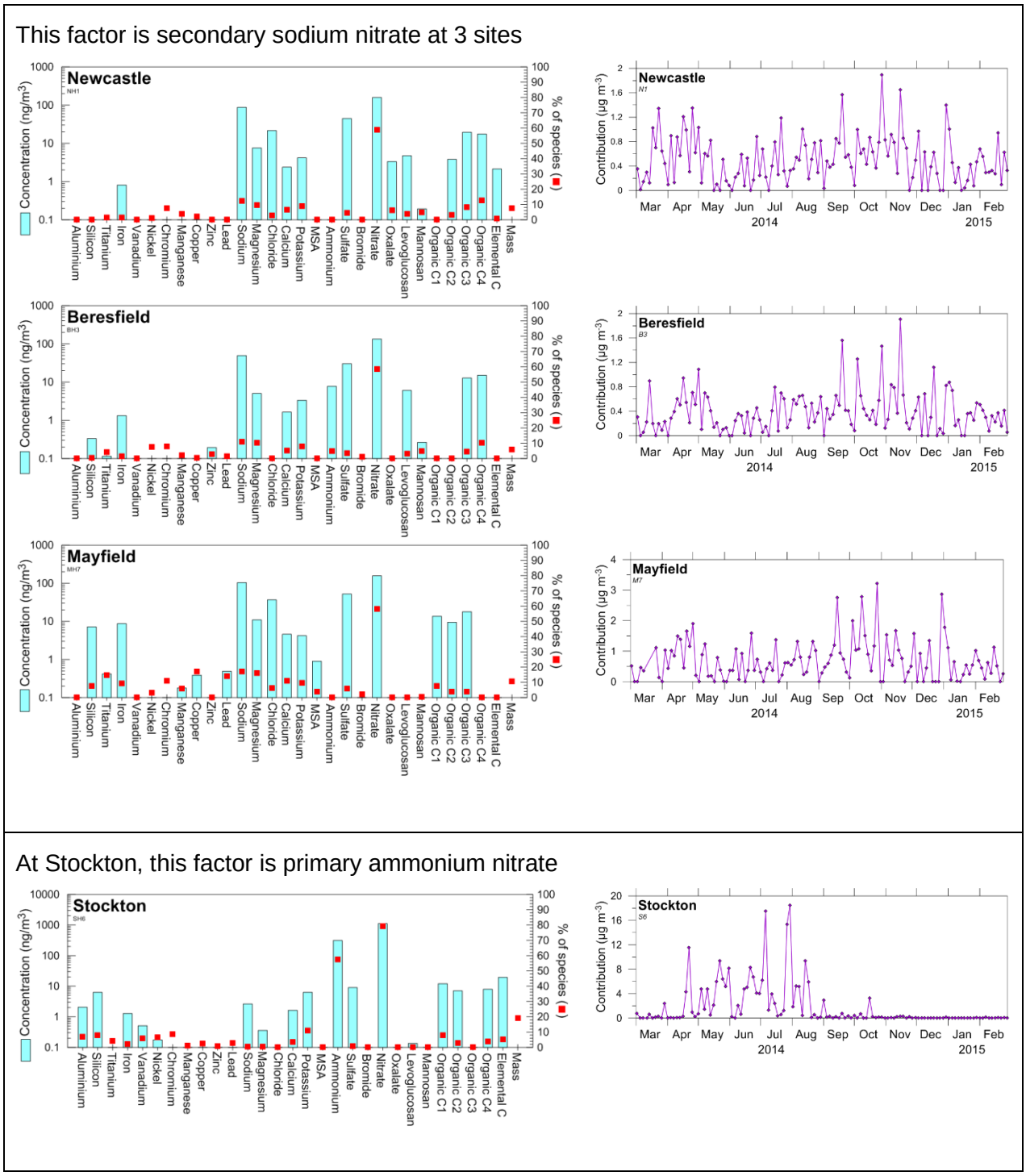

Figure 69: Fingerprints and time series plots of $PM_{2.5}$ Factor 7 (secondary sodium nitrate at three sites, primary ammonium nitrate at Stockton)

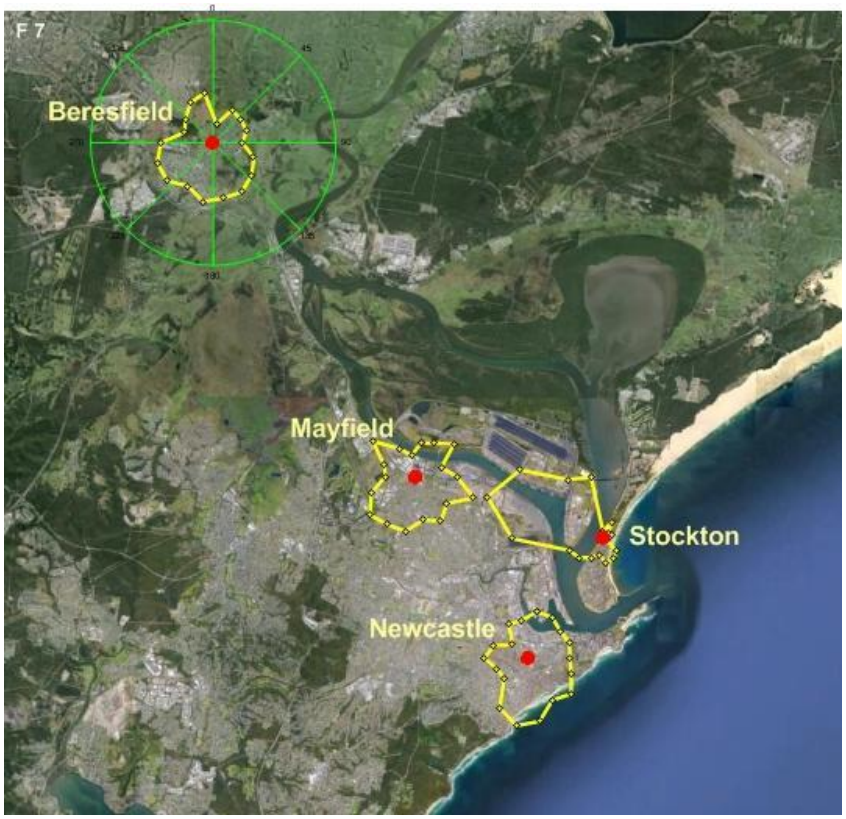

Figure 70: CPF of $PM_{2.5}$ Factor 7 (secondary sodium nitrate at three sites, primary ammonium nitrate at Stockton)

At Newcastle, Mayfield and Beresfield, the factor is mainly secondary nitrate, specifically sodium nitrate ($NaNO_3$). It includes 60% of the nitrate at these sites as well as Na^+, Cl^-, OC and about 5% of the sulfate. The sodium is predominantly from sea salt because the Mg/Na ratio in the factor at these sites is 0.09–0.10 (very close to the value for sea water) as listed in Table 12. At the Newcastle and Mayfield sites, 15–20% of the sodium is still present as sodium chloride with sufficient sodium left to neutralise all the nitrate (Gupta et al. 2015). At Beresfield, all the sodium is neutralised by nitrate with the Na/NO_3 ratio of 0.37. At Beresfield the factor also includes some ammonium and sulfate in the ratio 0.26 indicating a mix of ammonium sulfate and ammonium bisulfate, as discussed in Section 6.3. These contribute 17% of this factor.

Table 12: Ratios of key species in Factor 7 for all sites except Stockton

Species ratio	Newcastle	Beresfield	Mayfield	Reference values
Na/NO_3 (not including Na in NaCl)	0.46	**0.37**	0.51	$NaNO_3$= 0369
Mg/Na	0.087	0.102	0.104	Sea water = 0.120
Cl/Na	0.25	0	0.35	Sea water = 1.80
NH_4/SO_4	0	**0.26**	0	$(NH_4)_2SO_4$ = 0.375 NH_4HSO_4 = 0.1875

The time series in Figure 70 shows that at Newcastle, Mayfield and Beresfield it occurs throughout the year but more strongly in spring and summer, related to the photochemical reactions producing the precursor nitrate in the atmosphere. The CPF plots are similar to those for pollutant-aged sea salt (Factor 2) and secondary ammonium sulfate (Factor 3) with approximately equal probabilities for the wind in any given direction that the factor will make a significant contribution to the $PM_{2.5}$ mass. This reflects the fact that sodium nitrate is a secondary (inorganic) aerosol, which is produced by reactions in the well-mixed atmosphere, not directly downwind from any given source.

At Stockton, this factor is dominated by nitrate (80% of the nitrate is in this factor) and ammonium (60% of the ammonium is in this factor). Table 13 shows these are present as ammonium nitrate. There are negligible amounts of other species, for example the sulfate contribution is just 0.3% that of the ammonium. The Stockton site is situated about 700m to the south-east of the Orica Australia Pty Ltd (Orica) ammonium nitrate manufacturing facility on Kooragang Island. Emissions from this facility include particulate matter, ammonia, oxides of nitrogen and nitric acid (AECOM 2009), with particulate matter emissions from ammonium nitrate production (prill tower) largely comprised of $PM_{2.5}$ ammonium nitrate (NH_4NO_3), as reported in monitoring results (Orica Australia Pty Ltd 2014). Emissions from prill towers result from carry-over of fine particles and fume by the prill cooling air flowing through the tower. Emissions from low-density prill towers are documented by the US EPA as comprising predominantly small particles, 56% of which are below 2.5µm ($PM_{2.5}$), 73% below 5µm and 83% below 10µm (PM_{10}) (US EPA 1995).

Table 13: Ratios of key species at Stockton (ammonium nitrate)

Species ratio	Value for ammonium nitrate	Stockton
NH_4/NO_3	**0.290**	0.282

The direction of the source from the monitoring site is clearly indicated by the bivariate pollution rose in Figure 71. In this plot, the colour is the ammonium nitrate concentration versus wind direction (angle) and wind speed (distance from centre). The plot indicates that high ammonium nitrate concentrations at Stockton occur when the winds are from the north-west when the prill tower is directly upwind of the Stockton site. The narrowness of the red sector (‘upwind footprint’) is indicative of a direct emission of ammonium nitrate. Although ammonium and nitrate react rapidly in the atmosphere, if there were separate but nearby sources of ammonium and nitrate one would expect a broader ‘footprint’.

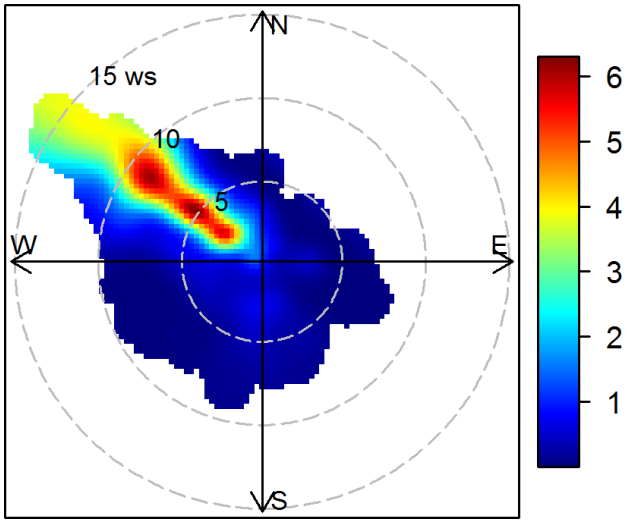

Figure 71: Bivariate pollution rose of Factor 7 (ammonium nitrate) contributions (colour scale units µg m^{-3}) versus wind direction and speed (m s^{-1}) for the LHPCS study period

The time series in Figure 70 shows that at Stockton this factor is only present in the second half of autumn and winter. This corresponds to the part of the year when north-westerly winds prevail at Stockton (see Figure 29). North-westerlies transport the emissions from Kooragang Island towards the Stockton site. The CPF in Figure 70 for this site points to this area as the location of the source.

The ammonium nitrate levels measured at Stockton are discussed further in Section 11.5.

6.8 $PM_{2.5}$ Factor 8 – Mixed shipping/industry

The annual average contribution of this mixed shipping/industry factor to $PM_{2.5}$ is: Newcastle 0.1 µg m^{-3} (2%); Beresfield 0.2 µg m^{-3} (3%); Mayfield 0.3 µg m^{-3} (4%); Stockton 0.2 µg m^{-3} (3%).

The comparative magnitude of the shipping contribution based on vanadium concentrations is a maximum at Stockton (6.1 ng m^{-3}), about half as much at Newcastle (3.0) and Mayfield (2.7), and a tenth as much at Beresfield (0.6).

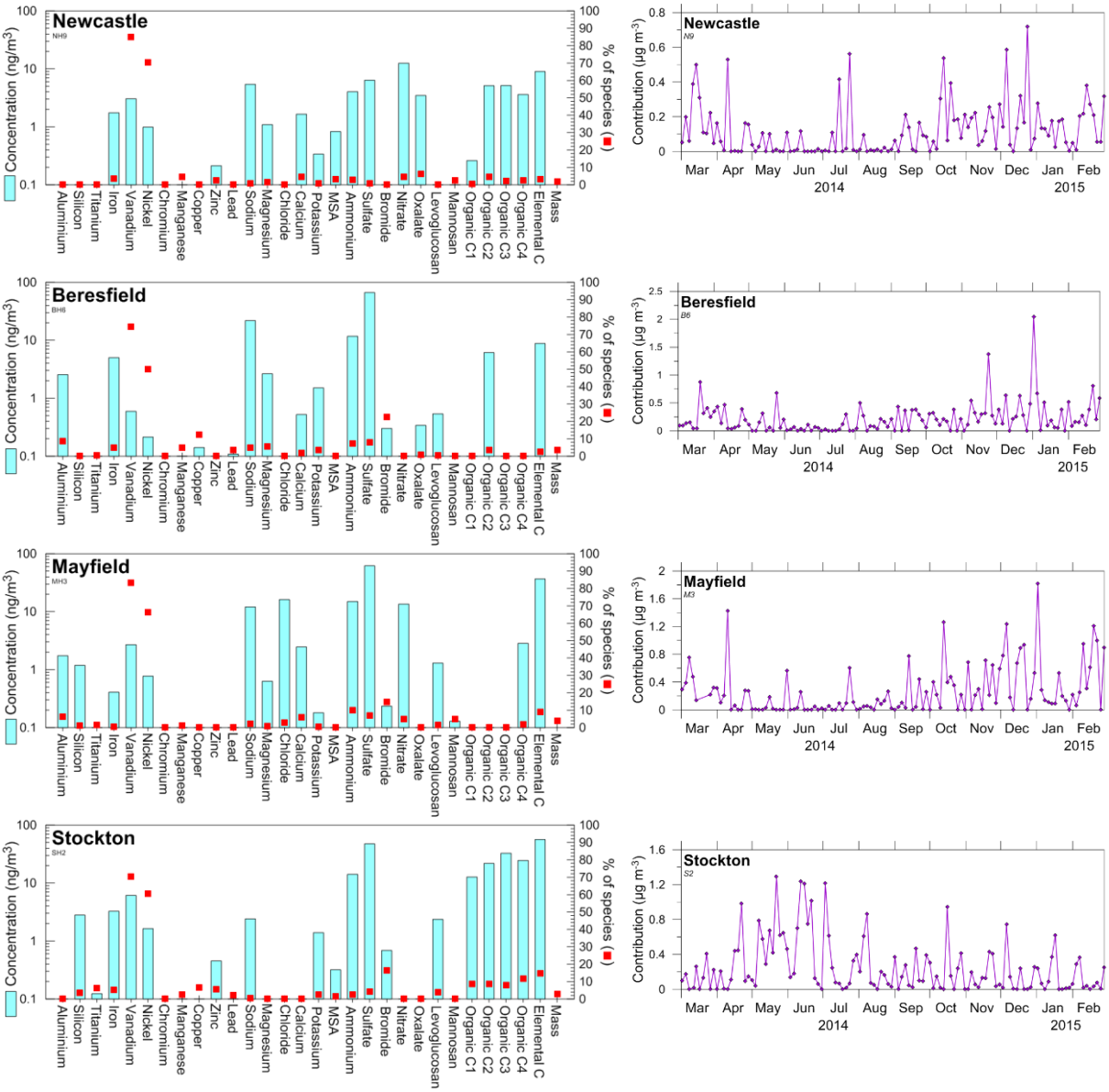

Figure 72: Fingerprints and time series plots of $PM_{2.5}$ Factor 8 (mixed shipping/industry) at the four study sites

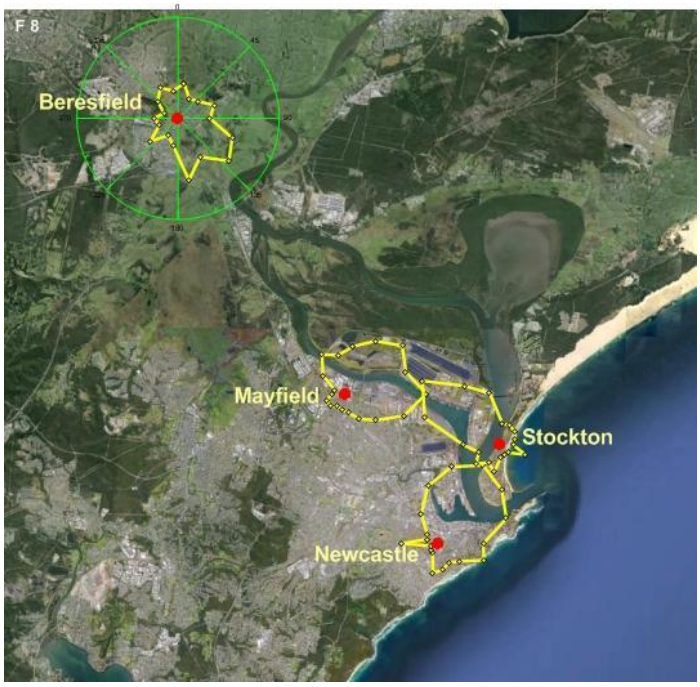

Figure 73: CPF of $PM_{2.5}$ Factor 8 (mixed shipping/industry) at the four study sites

This factor only makes a minor contribution of 2–4% to $PM_{2.5}$ mass but it appears at all sites in the PMF analysis and is identified as related to shipping because it contains most of vanadium, two-thirds of the nickel, and the V/Ni ratio of 3–3.5 is representative of heavy oil combustion from shipping (Viana et al. 2009, 2014). The first row of Table 14 lists the vanadium concentrations and reflects the direct impact of shipping emissions. The maximum is at Stockton (6.1 ng m^{-3}), about half this value at Newcastle and Mayfield, and a tenth at Beresfield (0.6 ng m^{-3}).

The factor also includes SO_4, EC, and OC with the ratios listed in Table 14. The factor also includes some secondary ammonium sulfate or ammonium bisulfate, as described more fully in Section 6.3. Shipping emissions include SO_4^{2-} and EC but whereas the V/Ni shows little variability across the sties, the SO_4^{2-}/V and EC/V ratios increase from Newcastle → Stockton → Mayfield → Beresfield indicating the increasing contribution from industry (the main source of sulfate). Thus the factor is named 'mixed shipping/industry'.

The time series in Figure 73 shows that it occurs at different times of the year at the various sites. This is related to the prevailing wind directions at the time and it occurs when shipping emissions are upwind of the site. For example, it is strongest at Stockton in autumn/winter when north-westerlies dominate, but mainly absent at this time at Mayfield and Beresfield.

This can be understood more clearly by referring to Figure 74, which shows the CPFs for the three near-coastal sites (from Figure 73) overlaid on a map of the region and with an inset of the inset of the geographical distribution of shipping fuel consumed in Newcastle in 2013 (DNV 2015). In the 'heat map' of fuel consumption, the orange/red areas show where the most fuel is consumed. The peak direction in all CPFs point to the main fuel consumption locations and confirm the contribution of shipping emissions to this factor.

Table 14: Ratios of key species in the mixed shipping/industry factor

Species ratio	Newcastle	Stockton	Mayfield	Beresfield
V (ng m^{-3})	3.0 ng m^{-3}	6.1 ng m^{-3}	2.7 ng m^{-3}	0.6 ng m^{-3}
V/Ni	3.1	3.7	3.5	2.8
SO_4^{2-}/V	2.1	8	23	112
EC/V	2.9	9	14	15
OC/V	4.6	15	1.1	10
NH_4/SO_4	0.63	0.30	0.24	0.18

Shipping emissions are not confined to within the Port of Newcastle but also occur offshore by ships approaching or leaving the port and by ships anchored off the coast. This is illustrated by reference to annual $PM_{2.5}$ emissions from shipping illustrated in Figure 75.

Note that because V and Ni are drivers of this mixed factor, it includes all almost all of the shipping contributions and the CPFs are determined by the shipping emissions. It includes increasing amounts of industry contributions at Stockton and the inland sites, but industry contributions also appear in other factors such as the pollutant-aged sea salt, secondary ammonium sulfate, and mixed industry/vehicle factors.

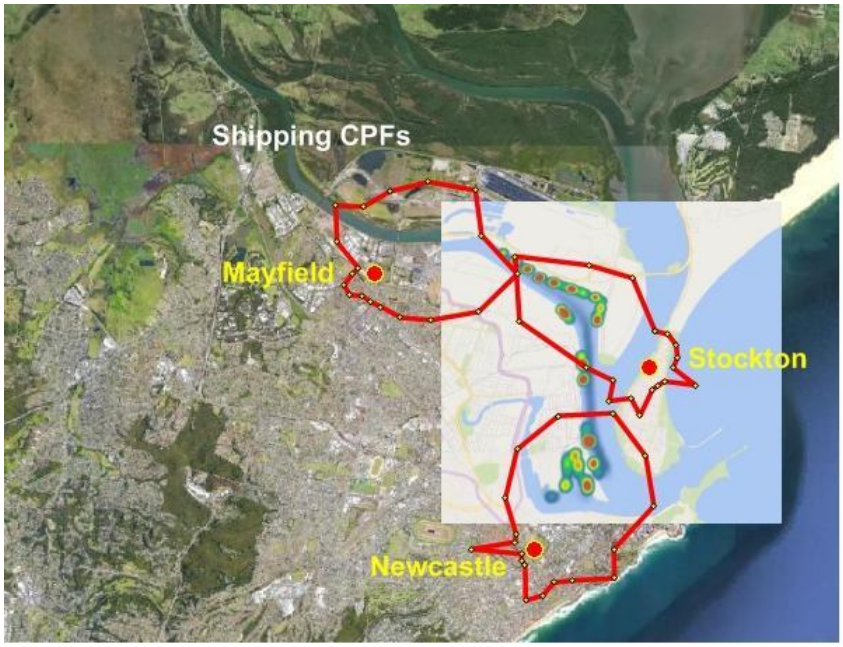

Figure 74: CPF contours overlaid on a map of the region with an inset of the geographical distribution of shipping fuel consumed in Newcastle (DNV 2015)

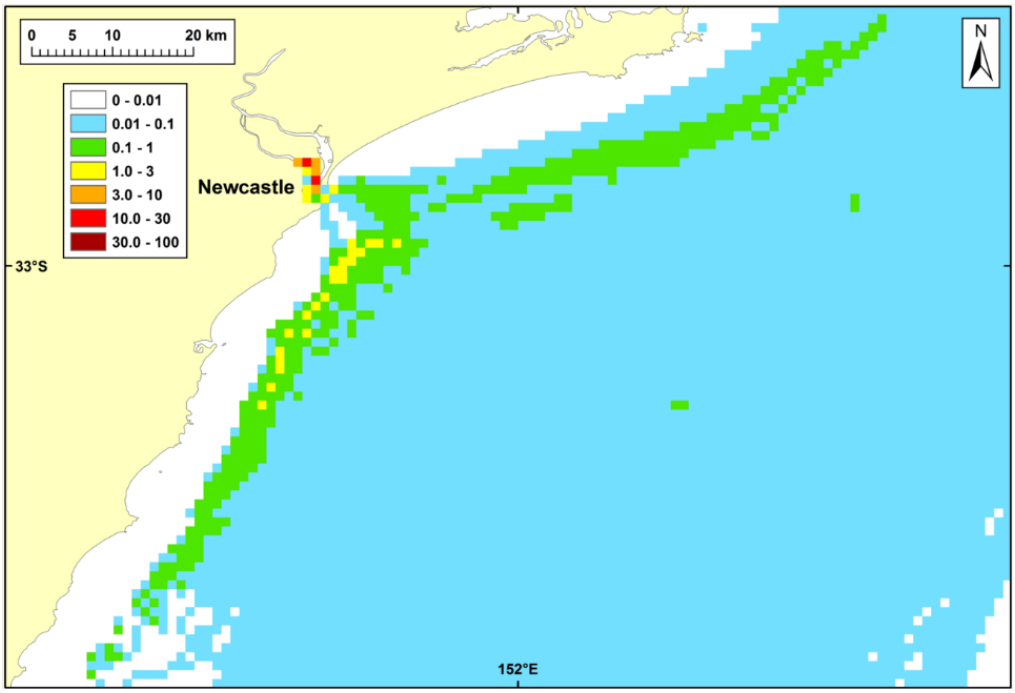

Figure 75: Annual $PM_{2.5}$ emissions from shipping for 2010–11 (given in tonnes per 1km grid cell) for the region near Newcastle (provided by Brett Goldsworthy)

Emissions data generated using the method described in Goldsworthy & Goldsworthy (2015).

DNV (2015) estimated $PM_{2.5}$ emissions from shipping (main engines, auxiliary engines and boilers) within the Port of Newcastle to be 60 tonnes per year based on 2013 activity data. This is of a similar order to $PM_{2.5}$ emissions estimated for shipping at Port Jackson (47 tonnes/year), higher than at Port Kembla (28 tonnes/year), and lower than emissions at Port Botany (140 tonnes/year). Bulk carriers accounted for 60% of the $PM_{2.5}$ emissions at the Port of Newcastle, with oil tankers (18%) and general cargo vessels (13%) being the next largest emitters of $PM_{2.5}$. Chemical/production tankers, gas tankers and container vessels each accounted for about 2% of total $PM_{2.5}$ emissions from shipping at this port, with other activities contributing the balance. Shipping emissions within Newcastle port boundaries are dominated by $PM_{2.5}$ emissions at berth from auxiliary engines and boilers, with main engine emissions during manoeuvring and transiting within the port being a further source.

In addition to primary particle emissions, shipping emits precursor pollutants with 402 tonnes/year of NOx and 612 tonnes/year of SO_2 estimated to be released at Port of Newcastle in 2013 (DNV 2015). The extent of SO_2 emissions is dependent on the sulfur content of the fuel used, with mainly heavy fuel oil (2.7% sulfur content) used including at berth (DNV 2015; AMC 2013).

6.9 $PM_{2.5}$ Factor 9 – Mixed industry/vehicle

The annual average contribution of this mixed industry/vehicle factor to $PM_{2.5}$ is: Newcastle 0.2 µg m^{-3} (3%); Beresfield 0.6 µg m^{-3} (9%); Mayfield 0.1 µg m^{-3} (1%); Stockton 0.5 µg m^{-3} (5%).

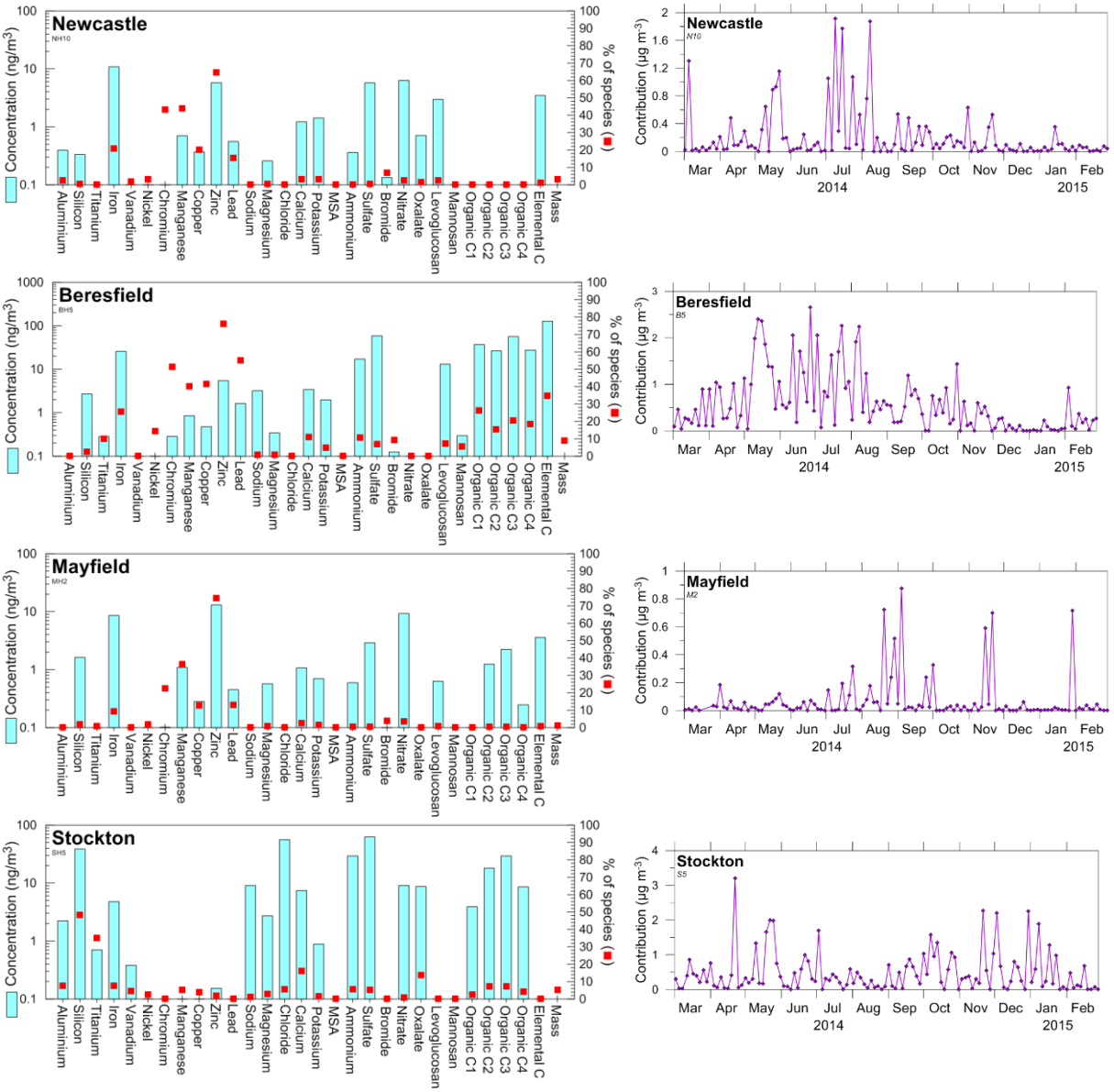

Figure 76: Fingerprints and time series plots of $PM_{2.5}$ Factor 9 (mixed industry/vehicle) at the four study sites

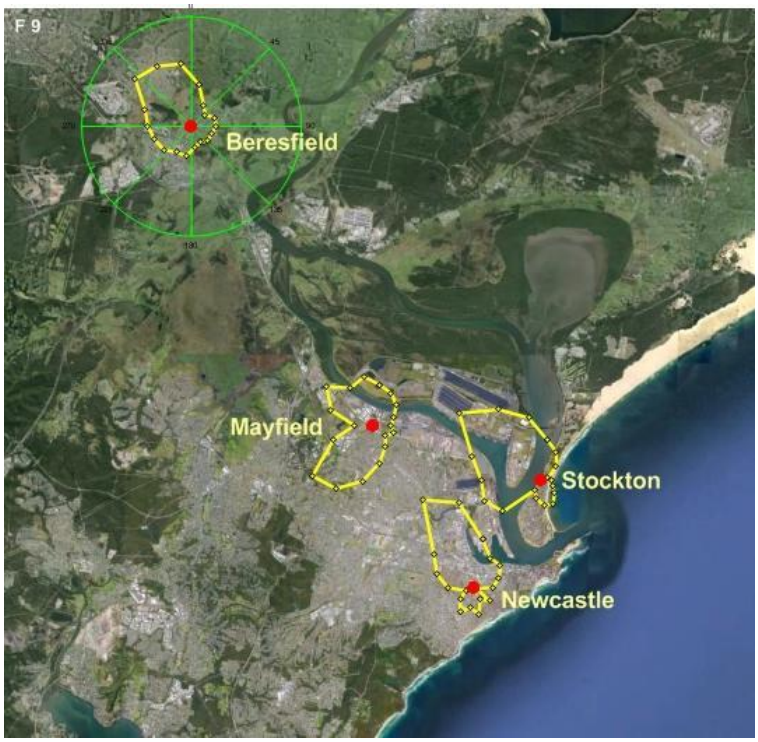

Figure 77: CPF of $PM_{2.5}$ Factor 9 (mixed industry/vehicle) at the four study sites

The key component of this factor is zinc – it includes about 70% of this species across all sites except Stockton. The National Pollutant Inventory (NPI 2014) lists the zinc sources in the region as being: 65% industry, 26% vehicles, 5% wind-blown dust and 4% other (bushfires, wood heaters).The factor also includes varying amounts of Mn, Cr, Cu, Pb and Fe, as well as SO_4, EC and a significant amount of OC at Beresfield. The ratios of the metal species to each other show more variation than for the vehicle factor and so it is concluded that this is predominantly an industry factor but mixed with vehicle contributions. There is also greater variation in the industries near each sampling site.

In contrast to the vehicle factor, the mixed industry/vehicle factor Zn/Fe ratio is 10–20 times larger and the Mn/Fe ratio 2–5 times larger. On the other hand, the Cr/Fe, Cu/Fe and Ca/Fe ratios are generally similar to those for the vehicle factor. At Stockton it includes a wider mixture of small contributions from sea salt, OC, soil-like particles and ammonium sulfate.

The time series plots in Figure 76 show this factor contributes most in late autumn through winter but with some more isolated spikes at Mayfield, which were, however, well fitted by the PMF. The prevalence of offshore winds during the late autumn and winter may contribute to higher contributions due to source areas being upwind. The Mayfield site is situated adjacent to various local sources areas, including industrial areas to the south and east of the site.

Figure 78 is an overlay of the CPFs on a map of industrial emissions from the EPAs Greater Metropolitan Region air emissions inventory (EPA 2012). The agreement between the main CPF directions and the industrial sources is very good at Stockton and Mayfield. The peak direction in the Newcastle CPF also points to the emissions around Mayfield. The map does not include emissions beyond Beresfield but it should be noted that the north-west CPF lobe points up along the highway towards the Thornton industrial area and Maitland.

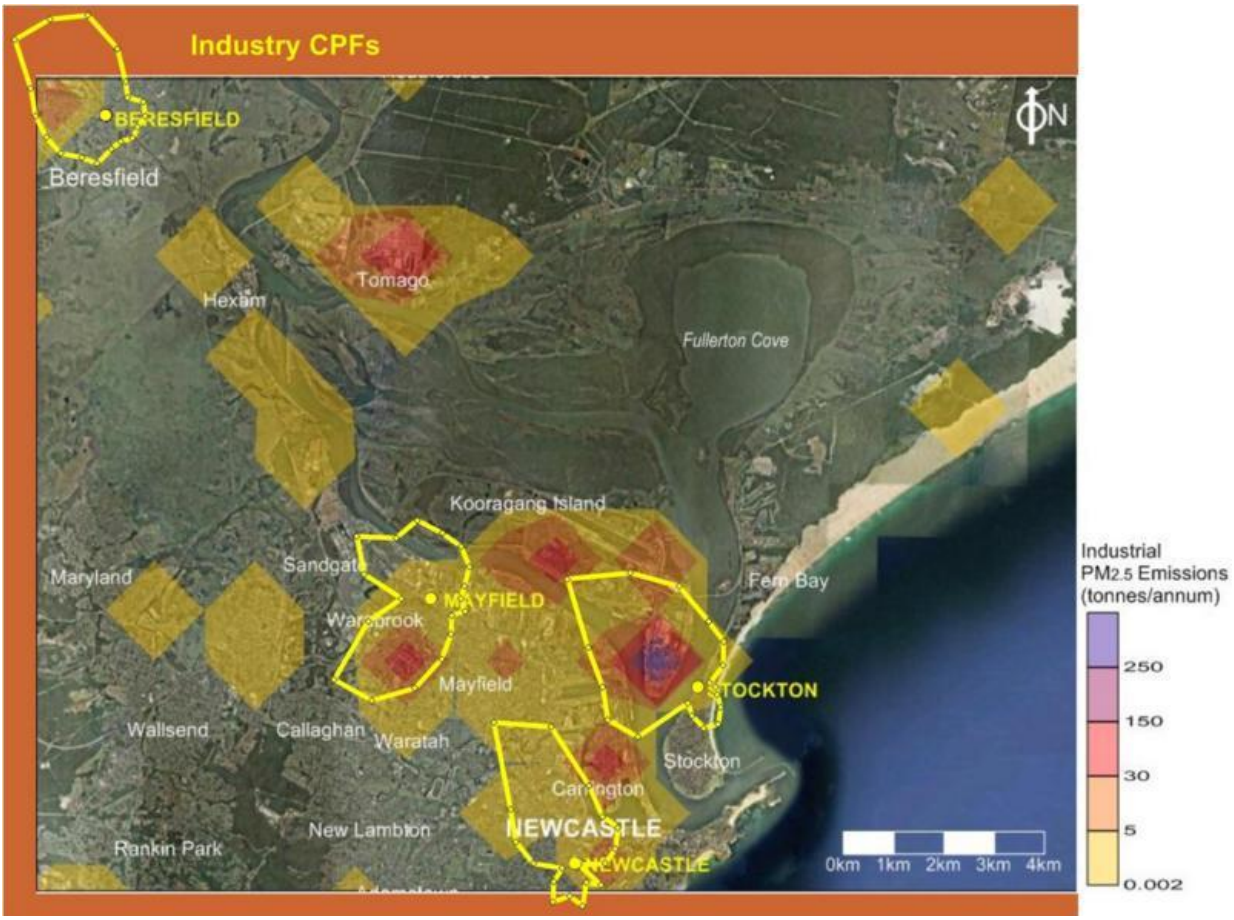

Figure 78: CPF contours overlaid on contour of $PM_{2.5}$ industrial emissions from the Greater Metropolitan Region air emissions inventory

7 Summary of fine particle results ($PM_{2.5}$)

Table 15 summarises the results for $PM_{2.5}$ from the previous section, listing the main species in each factor and the drivers, i.e. those species that are used to identify and name the factor. It also lists the percentage contribution of each factor at each site to total $PM_{2.5}$ mass, identifies the factor as a primary and/or secondary aerosol, and summarises potential sources.

Table 15: Summary of PMF factors for $PM_{2.5}$ listing main species present, contributions of these factors at each site, and potential sources

Factor	**Main species (drivers bold)**	**Contribution of the factor to total annual $PM_{2.5}$ mass (with uncertainty range) at:**				**Potential sources (primary/secondary)**
		New-castle	**Beres-field**	**Mayfield**	**Stock-ton**	
Factor 1 Fresh sea salt	**Cl^-:Na^+:SO_4^{2-} :Mg^{2+}**	24% (20-27%)	13% (12-16%)	20% (18-22%)	23% (19-25%)	Primary particles. Fresh sea salt aerosol from wave-breaking
Factor 2 Pollutant-aged sea salt	Non-sea-salt SO_4, **Na^+:Mg^{2+}**, OC, EC, almost no Cl^-	23% (9-38%)	23% (15-34%)	25% (15-40%)	22% (13-28%)	Sea salt reacted with industrial, commercial, road & non-road transport emission from local & regional sources, esp. SO_2
Factor 3 Secondary ammonium sulfate	**NH_4^+:nssSO_4^{2-}**, OC, EC	12% (6-16%)	10% (9-17%)	8% (7-16%)	9% (7-13%)	Secondary aerosol – ammonium sulfate. Local & regional sources of SO_2 (e.g. fossil fuel burning) and ammonia (agriculture, industry, vehicles, non-road diesel equipment, soils, ocean)
Factor 4 Wood smoke	**Levo**, OC, EC, NO_3^-, SO_4^{2-}, Cl^- K^+, **Mannosan**	10% (6-18%)	15% (8-24%)	11% (7-15%)	6% (5-9%)	Primary aerosol. Domestic wood heaters, bushfires, hazard reduction burns
Factor 5 Soil	**Si:Al:Ti**, Fe, Ca^{2+}, OC, EC	8% (2-14%)	10% (9-14%)	11% (5-16%)	8% (5-10%)	Primary particles. Soil dust. Potential industrial contributions of organic & black carbon at Mayfield & Stockton. Possibly coal particles and/or soot contribute.
Factor 6 Vehicle	**EC, OC, Fe**, NO_3^-, SO_4^{2-}, **Cu, Mn, Cr, Pb**	10% (3-15%)	11% (6-13%)	9% (5-15%)	5% (4-7%)	Primary (EC, metals, OC) & secondary (NO_3^-, OC) particles. Vehicles, non-diesel road equipment
Factor 7 Primary or secondary nitrate	**NO_3^-, Na^+**, SO_4^{2-}, Cl^-, OC **NH_4, NO_3** at Stockton	8% (5-14%)	6% (4-13%)	11% (7-16%)	19% (17-22%)	Secondary sodium nitrate at Mayfield, Newcastle and Beresfield. Primary ammonium nitrate at Stockton - industry. NO_x from vehicles, non-road diesel equipment, industry.

Factor	**Main species (drivers bold)**	**Contribution of the factor to total annual $PM_{2.5}$ mass (with uncertainty range) at:**				**Potential sources (primary/secondary)**
		New-castle	**Beres-field**	**Mayfield**	**Stock-ton**	
Factor 8 Mixed shipping/ industry	SO_4^{2-}, NH_4^-, EC OC, NO_3^-, **V:Ni**	2% (1-6%)	3% (3-10%)	4% (3-7%)	3% (2-9%)	Secondary & primary (V, Ni) particles. Shipping, sulfate, ammonium
Factor 9 Mixed industry/ vehicle (a)	**Zn**, Fe, **Mn**, Cu, Cr, SO_4^{2-}, NH_4^+, NO_3	3% (2-9%)	9% (3-13%)	1% (1-3%)	5% (4-10%)	Primary (metals) & secondary particles. Industry, vehicles, non-diesel road equipment

(a) Emissions from industrial premises are likely to contribute to factors other than the mixed industry/vehicle factor, such as the pollutant-aged sea salt, secondary sulfate and nitrate factors, and maybe also the vehicle and soil factors.

The uncertainty in the factor contributions is derived from the bootstrapping and displacement methods in the EPA PMF 5.0 software (Norris & Duvall 2014). Note that the uncertainties are not symmetric about the best fit. They are not standard deviations but rather represent confidence intervals that with a high probability contain the (unknown) true values. Some factor contributions have relatively little uncertainty (e.g. the fresh sea salt factor) whereas others are much more uncertain (e.g. the mixed industry/vehicle factor).

The factor profiles for each site are shown together in Figure 136 to Figure 143 in Appendix C. Also included is the distribution of the species across the factors, which summarises some of the discussion in the previous section in a different presentation format.

The annual contributions of each factor to total $PM_{2.5}$ mass at each site are compared in Figure 79 and as percentages in Figure 80. There are a number of ways to discuss the results.

One way is to distinguish between the primary particles (those emitted as particles from a source) and secondary particles (those formed by chemical reactions in the atmosphere and by gas-to-particle conversions):

- Primary particles: Fresh sea salt, soil, some vehicle, shipping, wood smoke and industry emissions; and ammonium nitrate at Stockton
- Secondary particles: secondary sulfates and nitrates (such as ammonium sulfate and sodium nitrate), and organic carbon compounds contributed by emissions from combustion sources such as wood heating, vehicles, shipping, and industry. The pollutant-aged sea salt fits best here as it undergoes chemical reactions between source and receptor.

Adding the results for these factors in Figure 79 shows on an annual average basis an approximately 50:50 split between primary and secondary particles at three sites (Newcastle, Beresfield and Mayfield) and a 65:35 split at Stockton because of the significant contribution from the primary ammonium nitrate.

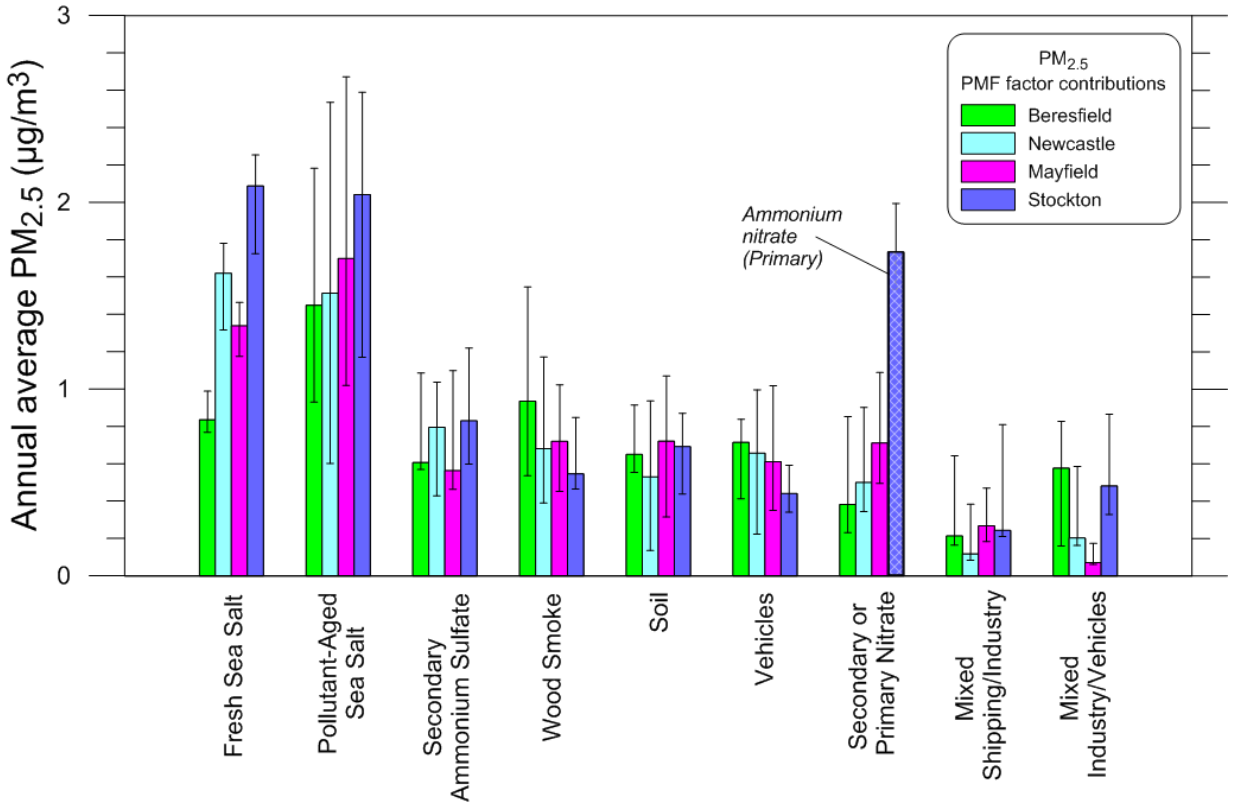

Figure 79: Comparison of the factor contributions at each site to annual average $PM_{2.5}$ mass

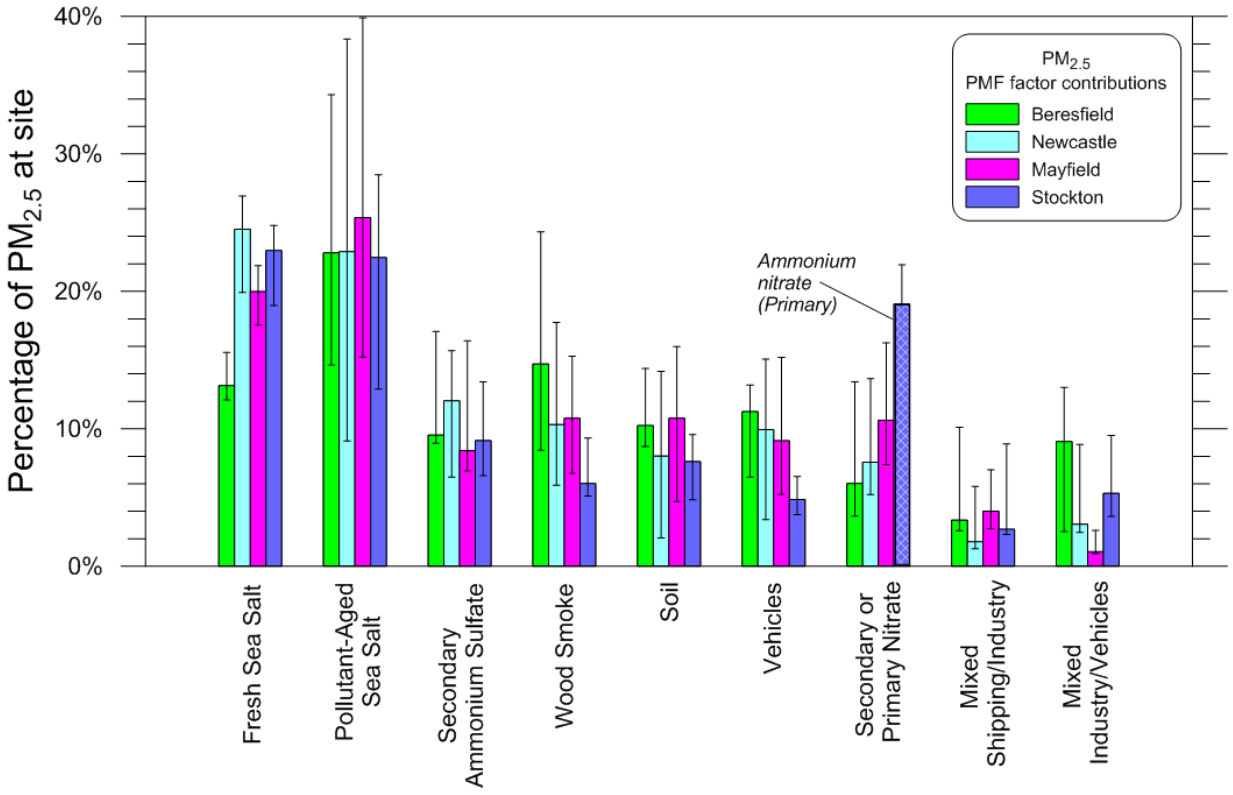

Figure 80: As for Figure 79, but showing values as percentage of annual average $PM_{2.5}$ mass at each site

A second way to analyse the results is comparing the contributions of each factor by site using the percentages shown in Figure 80. As discussed in Section 6.1, the fresh sea salt concentration decreases with distance from the coast, but as percentages of total mass, the three sites nearest the coast are approximately equal with Beresfield about 40% lower. In contrast, the pollutant-aged sea salt and secondary ammonium sulfate contributions are similar across all sites because they are well mixed in the atmosphere. At Stockton, the primary ammonium nitrate contribution is about triple the secondary sodium nitrate contributions at the other sites due to significant nearby emissions from Kooragang Island.

The wood smoke contribution is 50% higher at Beresfield than the all-site average and 50% lower at Stockton, possibly due to the poorer dispersion of wood heater emissions at the most inland site (Beresfield), and the more dispersive conditions at the coastal site (Stockton). In contrast, the vehicle factor is about 40% lower at Stockton than at the other three sites, due both to the much lower local concentration of vehicle emissions and the higher total $PM_{2.5}$ mass at Stockton.

Taking the uncertainties into account, the soil contribution is similar across all sites, consistent with the wind sector analysis (Figure 65) with all sites pointing to the source being to the north-west, up the Hunter Valley.

The last two factors have the largest relative uncertainties, especially at Beresfield and Newcastle. The best fit PMF result for the mixed shipping/industry factor shows the percentage contribution is smallest at Newcastle and similar at the other three sites. As discussed in Section 6.8, a possible explanation for the higher contribution at Beresfield than Newcastle is that the shipping factor at Beresfield includes a larger contribution from sulfate, elemental and organic carbon because of the longer travel time from the emissions source (shipping around the port).

The reason for the higher mixed industry/vehicle factor at Beresfield than the other sites might be that at those sites more of the industry emissions are included with the pollutant-aged sea salt factor because of the higher sea salt concentrations.

7.1 Seasonal variability

The monthly variation in the contributions of each factor at each site are shown in Figure 81 to Figure 84 and discussed in the following sections.

7.1.1 Newcastle

At Newcastle, the annual average $PM_{2.5}$ concentration is 6.6 µg m^{-3} but it ranges between a low of 4.8 µg m^{-3} in February and a high of 9.0 µg m^{-3} in October (Figure 81). On an annual basis the top three factors are fresh sea salt (24%), pollutant-aged sea salt (23%) and secondary ammonium sulfate (12%).

The monthly values are highest in October to December due to the dominant contribution from fresh and pollutant-aged sea salt (50–75% of the total). The largest contributors in late autumn and winter are the wood smoke (30%) and vehicle (16%) factors.

Secondary sulfate and nitrate contributions are greater from September to March, and lowest during winter months. Soil and industry contributions are notably lower in summer when onshore winds prevail (Figure 27). Shipping/industry contributions are evident in spring, summer and early autumn when north-easterly winds are more prevalent, i.e. the port is upwind of the Newcastle site (Figure 73).

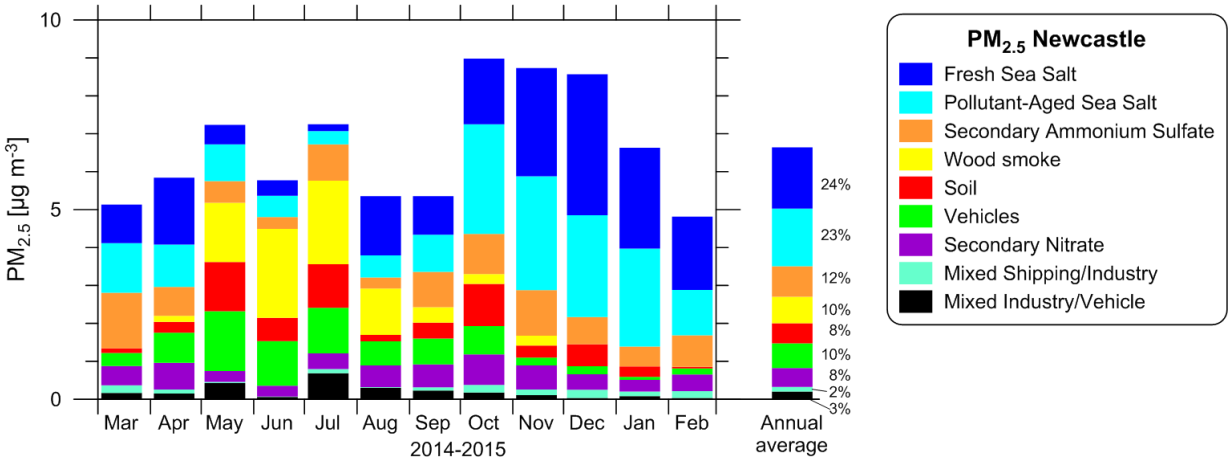

Figure 81: Monthly and annual factor contributions to $PM_{2.5}$ at Newcastle

7.1.2 Beresfield

The overall picture at Beresfield (Figure 82) is similar to that at Newcastle. The annual average $PM_{2.5}$ concentration is 6.4 µg m^{-3} but it ranges between a low of 4.5 µg m^{-3} in February and a high of 9.2 µg m^{-3} in November. On an annual basis the top three factors are pollutant-aged sea salt (23%), wood smoke (15%) and fresh sea salt (13%).

Fresh and pollutant-aged sea salt dominate from November to January with an average 60% contribution. The largest contributors in late autumn and winter are the wood smoke (40%) and industry (15%) factors.

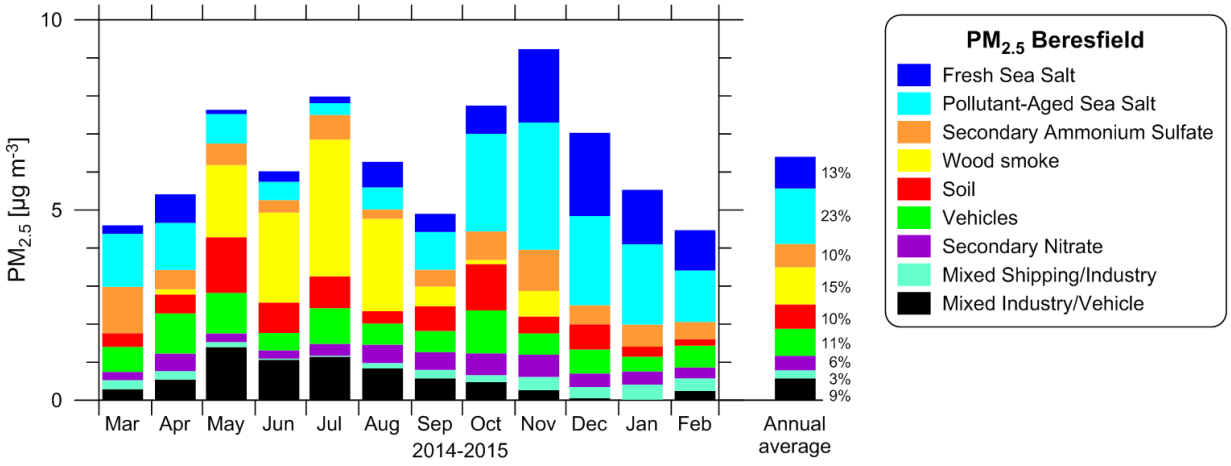

Figure 82: Monthly and annual factor contributions to $PM_{2.5}$ at Beresfield

Unlike at Newcastle, no seasonal trends in the vehicle contribution are apparent. This is likely to be due to vehicle emissions occurring north-east and south-west of the Beresfield site, and transported to the site despite seasonal variations in the wind field (Figure 68).

As at Newcastle, secondary sulfate and nitrate contributions are lower in the winter, soil and industry contributions are lower in the summer, and shipping/industry contributions higher in summer when onshore winds occur.

7.1.3 Mayfield

The annual average $PM_{2.5}$ concentration at Mayfield is 6.7 µg m^{-3} with a range from a low of 4.5 µg m^{-3} in March to a high of 10.1 µg m^{-3} in November. On an annual basis the top three factors are pollutant-aged sea salt (25%), fresh sea salt (20%), with wood smoke and soil both on 11% (Figure 83).

Fresh and pollutant-aged sea salt dominate from October to January with an average 60% contribution. The largest contributors in late autumn and winter are the wood smoke (30%) and vehicle (15%) factors.

Unlike at Beresfield and Newcastle, the soil contribution remains through the summer at Mayfield indicating that local emissions contribute to this factor. Nitrate contributions are greatest during late winter/early spring, with sulfate contributions marginally lower in winter.

Due to the proximity of the Mayfield site to the port, shipping/industry contributions are evident for much of the year but lower during winter when offshore winds prevail (Figure 28, Figure 73).

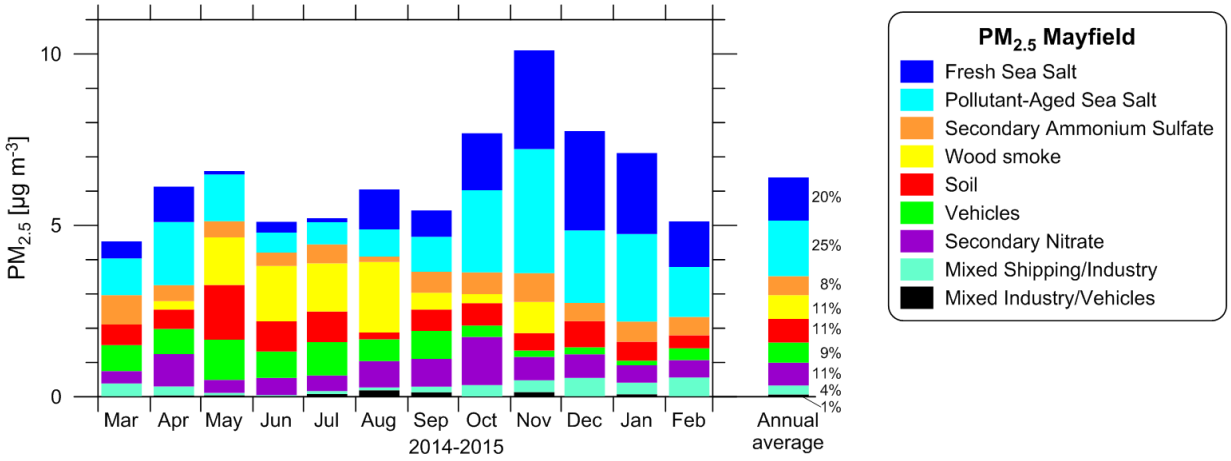

Figure 83: Monthly and annual factor contributions to $PM_{2.5}$ at Mayfield

7.1.4 Stockton

Stockton is significantly different from the other three sites with overall higher $PM_{2.5}$ concentrations and major contributions from ammonium nitrate, sulfate and fresh sea salt (Figure 84). The annual average $PM_{2.5}$ concentration is 9.1 µg m^{-3}, which is 40% higher than the average 6.6±0.2 µg m^{-3} at the other sites. The range of monthly averages at Stockton is from 6.8 µg m^{-3} in February to 13.8 µg m^{-3} in July.

On an annual basis the top three factors are fresh sea salt (23%), pollutant-aged sea salt (22%) and ammonium nitrate (19%).

Ammonium nitrate is the largest contributor during the May to August period. From May to July, the average 5 µg m^{-3} of ammonium nitrate accounts for 40% of the $PM_{2.5}$. As discussed in Section 6.7, this is due to the north-westerly winds at this time of year transporting the emissions from the Orica ammonium nitrate manufacturing facility directly towards the Stockton site. Unlike the trend in sulfate and nitrate contributions at other sites, the highest contributions from these factors occur in winter at the Stockton site.

The next largest contribution is an average 3.8 µg m^{-3} of fresh sea salt from December to February (50% of the $PM_{2.5}$).

Other significant features of Figure 84 are 2.6 µg m^{-3} of soil in May and 2.0 µg m^{-3} of wood smoke in November associated with bushfires/hazard reduction burns.

Mixed industry/vehicle factor contributions are evident throughout the year, with the mixed shipping/industry and vehicle contributions higher in late autumn and winter when north-north-westerlies prevail and shipping and vehicle emissions are directly upwind of the Stockton site (Figure 29, Figure 68, Figure 73).

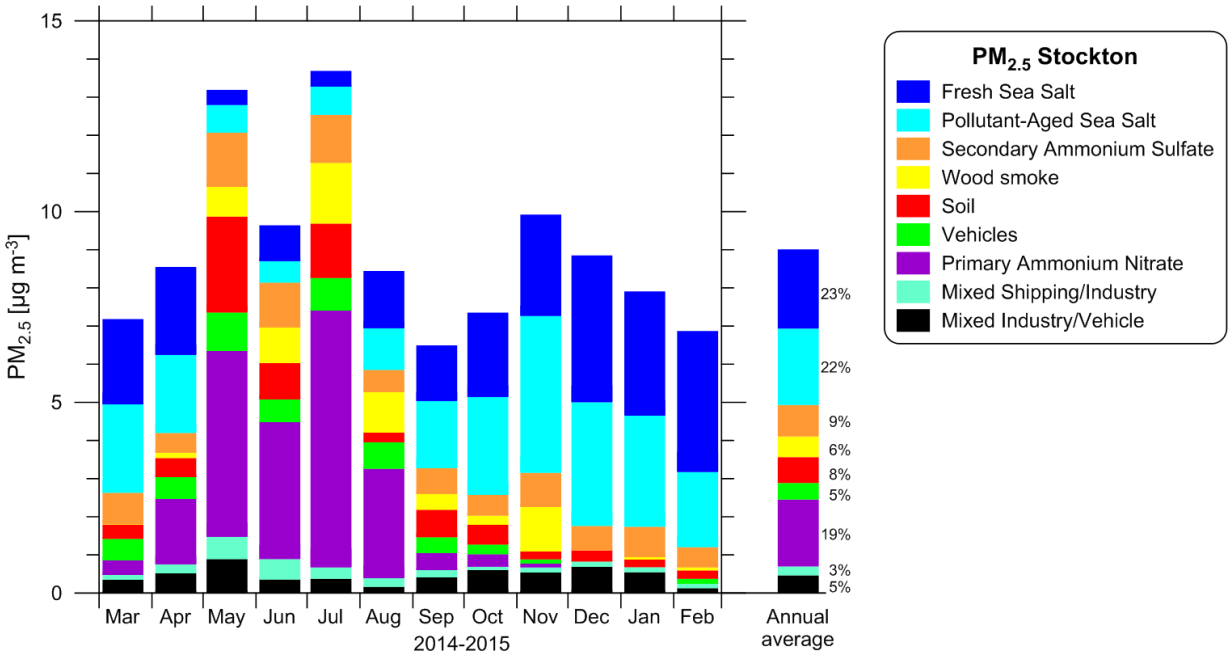

Figure 84: Monthly and annual factor contributions to $PM_{2.5}$ at Stockton

8 Receptor modelling results – $PM_{2.5-10}$ factors

Six factors were identified in the PMF analysis of the $PM_{2.5-10}$ data at each site. These are discussed in detail in the following sections by factor. They are also presented by site in Figure 144 to Figure 147 of Appendix C.

8.1 $PM_{2.5-10}$ Factor 1 – Fresh sea salt

The annual average contribution of this fresh sea salt factor to $PM_{2.5-10}$ is:
Mayfield 3.3 µg m^{-3} (40%); Stockton 13.6 µg m^{-3} (63%).

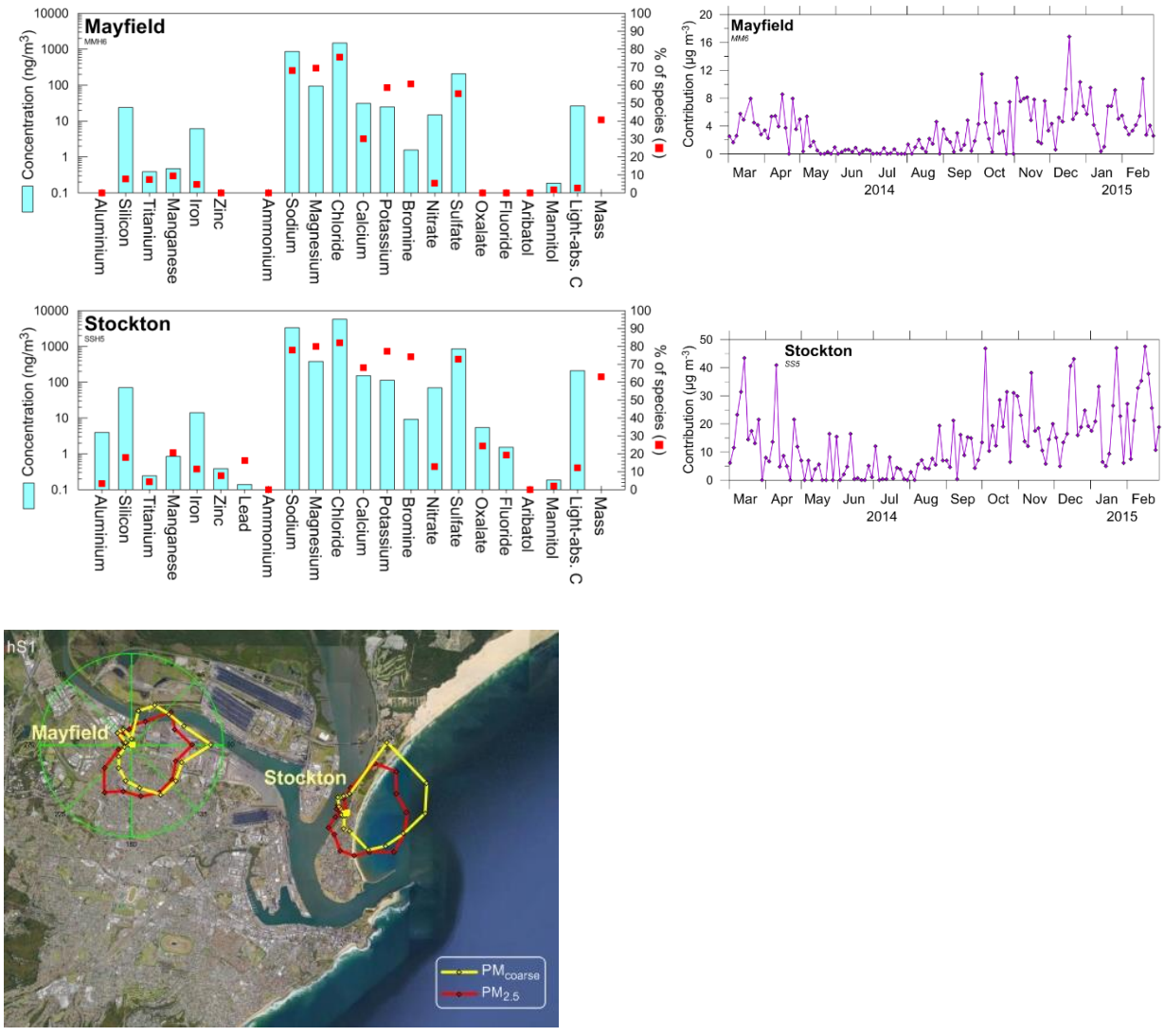

Figure 85: Fingerprints, CPF and time series plots of $PM_{2.5-10}$ Factor 1 (fresh sea salt)

The source of Factor 1 is clearly identifiable as fresh sea salt aerosol because as Figure 85 shows it is dominated by the sea water elements Na, Cl, Mg, and SO_4 and their ratios closely match those for sea water (Table 16), particularly for Na, Cl and SO_4 which are all within 5% of the sea water values. This factor includes about 80% of the chloride, 70–80% of the sodium and magnesium, and 60–75% of the sulfate.

Table 16: Comparison of the constituents of the $PM_{2.5-10}$ fresh sea salt factor with standard sea water

Species ratio to Na	Sea water	Mayfield $PM_{2.5-10}$	Stockton $PM_{2.5-10}$
Cl/Na	**1.80**	1.72	1.75
SO_4/Na	**0.252**	0.248	0.250
Mg/Na	**0.120**	0.110	0.115
Ca/Na	**0.038**	0.039	0.045
K/Na	**0.037**	0.029	0.034

The CPF plots in Figure 85 compare the patterns for this factor with the equivalent CPFs for the $PM_{2.5}$ fresh sea salt factor, and show they are very similar. The $PM_{2.5-10}$ CPF for Mayfield is oriented more towards the coast with a slightly stronger lobe to the east and loss of the $PM_{2.5}$ lobe to the south-west. At Stockton the $PM_{2.5-10}$ CPF is weaker for south to south-westerlies but the north-easterlies contribute more strongly. This is aligned with the coastline to the north-east, so that winds from this direction pick up more of the near-shore wave-generated sea salt aerosol than for more easterly onshore flows.

The time series plots in Figure 85 show that this factor is weakest in winter, corresponding to the absence of onshore winds during this season (Figure 29). As mentioned above, this factor is the dominant contributor to $PM_{2.5-10}$ mass at Stockton. On an annual basis it contributes an average of 13.6 µg m^{-3} (63% of the mass), but in summer this increases to 75% with an average contribution in February of 25.6 µg m^{-3}. On the other hand, in winter this fresh sea salt factor only contributes 3.6 µg m^{-3} (31% of the mass).

At Mayfield, the annual average contribution to the $PM_{2.5-10}$ mass is 3.3 µg m^{-3} (40% of the mass). In summer this increases to 5.6 µg m^{-3} and in winter it drops to 0.7 µg m^{-3}.

Combining the results for the fresh sea salt factor in the fine ($PM_{2.5}$) and coarse ($PM_{2.5-10}$) fractions shows that for standard PM_{10} measurements most of the fresh sea salt aerosol is in the coarse fraction – at Stockton 85% and at Mayfield 75%.

8.2 $PM_{2.5-10}$ Factor 2 – Light-absorbing carbon (LAC)

The annual average contribution of this factor, which contains most of the light-absorbing carbon, to $PM_{2.5-10}$ is: Mayfield 0.8 µg m^{-3} (10%); Stockton 2.2 µg m^{-3} (10%).

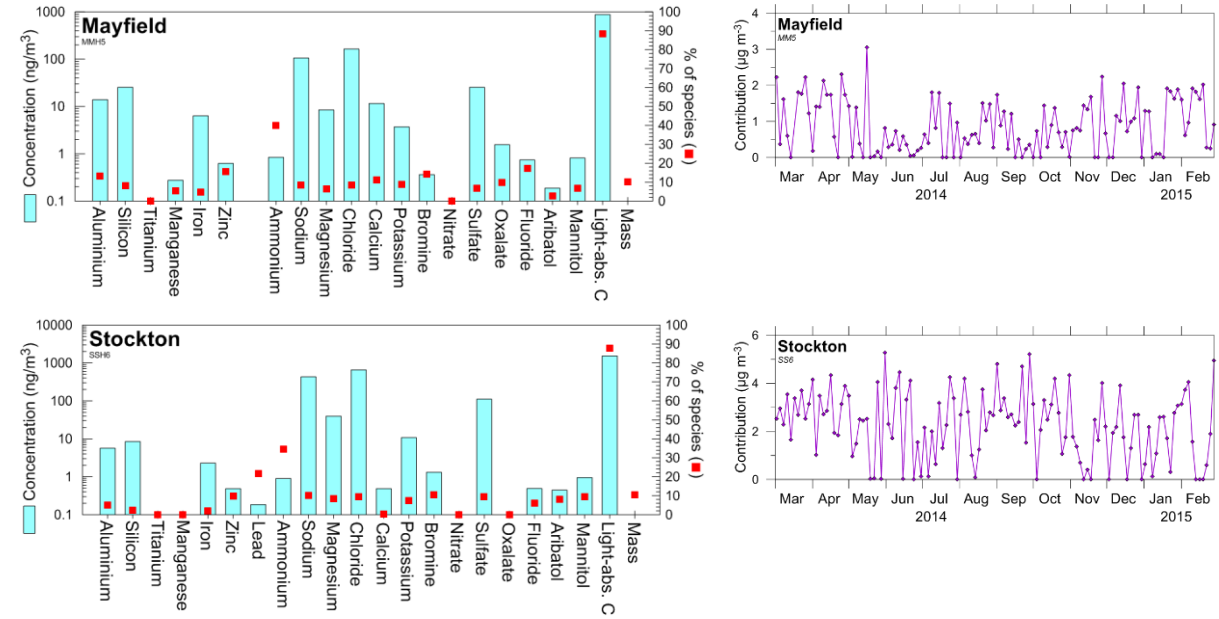

Figure 86: Fingerprints, CPF and time series plots of $PM_{2.5-10}$ Factor 2 (light-absorbing carbon)

The factor includes 90% of the light-absorbing carbon with most of the rest of the factor being slightly aged sea salt – chloride, sodium, magnesium, and sulfate. Table 17 shows there is a small amount of some chloride loss compared to the fresh sea salt factor.

The CPF plots are generally similar to those for fresh sea salt (Figure 85), but the Stockton CPF includes a lobe for west to north-north-westerly winds. The time series do not show any seasonal trends.

Table 17: Comparison of constituents of $PM_{2.5-10}$ Factor 2 with standard sea water

Species / Specie ratios	Sea water	Mayfield	Stockton
Light-absorbing carbon		0.9 µg m^{-3}	1.5 µg m^{-3}
Species ratio to Na			
Mg/Na	**0.120**	0.083	0.092
K/Na	**0.037**	0.035	0.025
Cl/Na	***1.80***	***1.55***	***1.53***
SO_4/Na	***0.252***	***0.25***	***0.26***

Coal particles are conjectured to contribute to this factor. Coal works in the Newcastle region were estimated to emit 90 tonnes/year of $PM_{2.5}$ and 750 tonnes/year of PM_{10} based on the 2008 Greater Metropolitan Region air emissions inventory (EPA 2012). Coal works facilities at the Port of Newcastle are Newcastle Coal Infrastructure Group (NCIG) operations on Kooragang Island, Port Waratah Coal Service Ltd (PWCS) Kooragang Coal Terminal and PWCS Carrington Coal Terminal. Sources of coal dust emissions from coal terminal operations include fugitive emissions from rail receival stations, conveyors and transfer points, wind erosion of stockpiles, stacking and reclaiming, ship loading and dozer and front-end loader operations (Environ 2012). Further analysis is needed to identify whether coal particles could account for the light-absorbing carbon in this factor.

8.3 $PM_{2.5-10}$ Factor 3 – Pollutant-aged sea salt

The annual average contribution of this factor (pollutant-aged sea salt) to $PM_{2.5-10}$ is: Mayfield 1.4 µg m^{-3} (16%); Stockton 1.3 µg m^{-3} (6%).

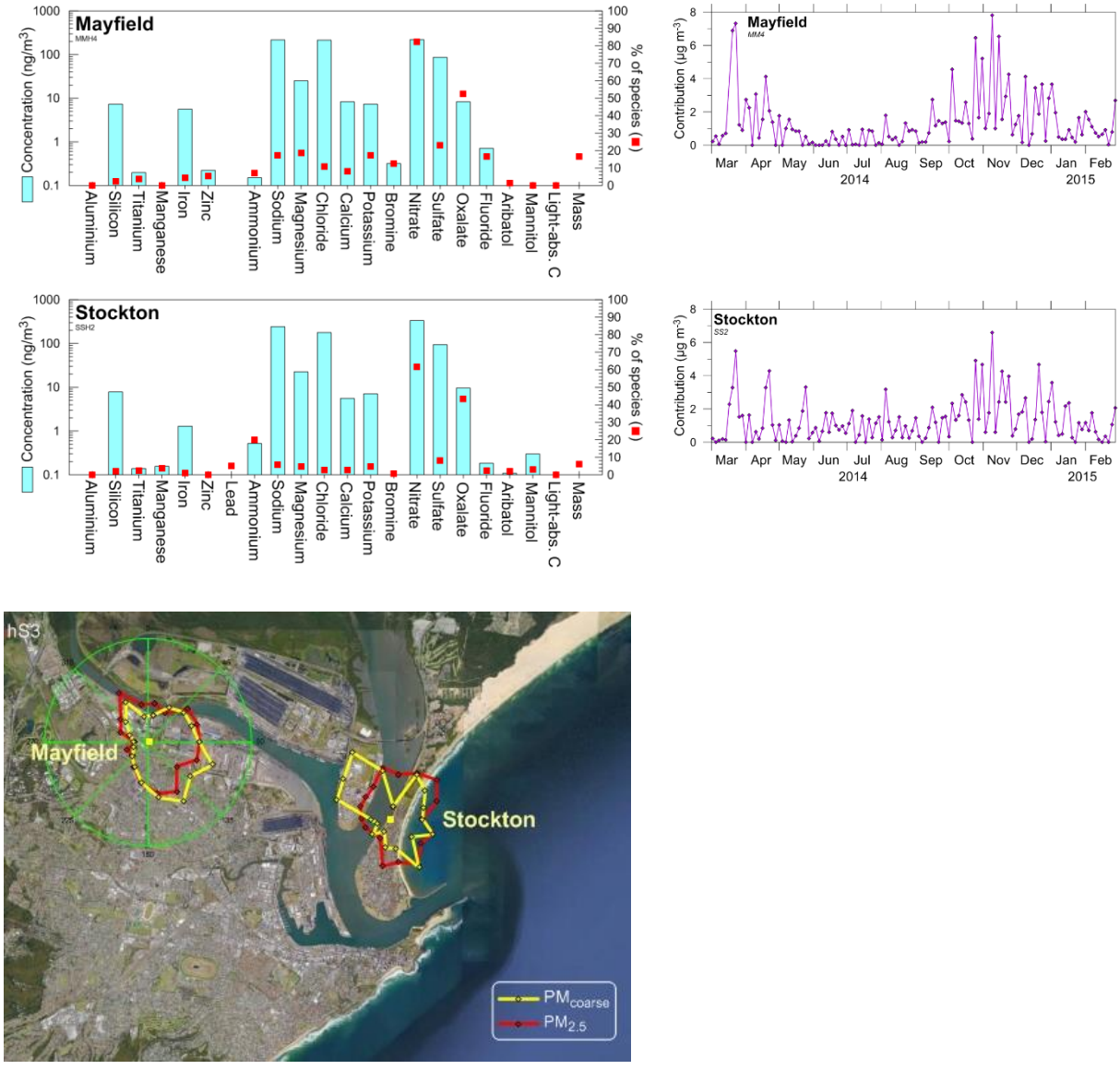

Figure 87: Fingerprints, CPF and time series plots of $PM_{2.5-10}$ Factor 3 (pollutant-aged sea salt)

The factor is identified as pollutant-aged sea salt because it is dominated by sea salt species with a Mg:Na ratio of 0.10 but with 75% of the nitrate and higher sulfate concentrations (i.e. non-sea-salt sulfate) than fresh sea salt. About half the original chloride has been replaced by nitrate and sulfate. The ratios of Mg, Ca, K, Cl, SO_4, NO_3 and C_2O_4 to Na are listed in Table 18 and compared to fresh sea water. This factor is less 'aged' than the corresponding factor for $PM_{2.5}$ (i.e. still retains significant chloride) because the smaller surface-area-to-volume ratio for the coarse particles means the timescale of the reactions replacing the chloride takes longer than for $PM_{2.5}$.

Both the time series (Figure 87) are very similar to those for fresh sea salt (Figure 85) with a peak in spring and minimum in winter although the variation at Stockton is less pronounced than for Factor 1. On the other hand, the CPF plots (yellow) are similar to those for the $PM_{2.5}$

pollutant-aged sea salt factor (shown in red), especially at Mayfield. The Stockton CPF includes a much stronger lobe to the north-west than for $PM_{2.5}$ indicating the significant source of industrial nitrate in this direction, and confirming the naming of this factor.

Table 18: Comparison of constituents of $PM_{2.5-10}$ Factor 3 with standard sea water

Species ratio to Na	Sea water	Mayfield	Stockton
Mg/Na	**0.120**	0.12	0.09
Ca/Na	**0.038**	0.038	0.023
K/Na	**0.037**	0.034	0.029
Cl/Na	***1.80***	***0.99***	***0.74***
SO_4/Na	***0.252***	***0.40***	***0.39***
NO_3/Na		1.01	1.38
C_2O_4/Na		0.044	0.040

8.4 $PM_{2.5-10}$ Factor 4 – Soil

The annual average contribution of this soil factor to $PM_{2.5-10}$ is: Mayfield 1.2 µg m^{-3} (14%); Stockton 2.3 µg m^{-3} (11%).

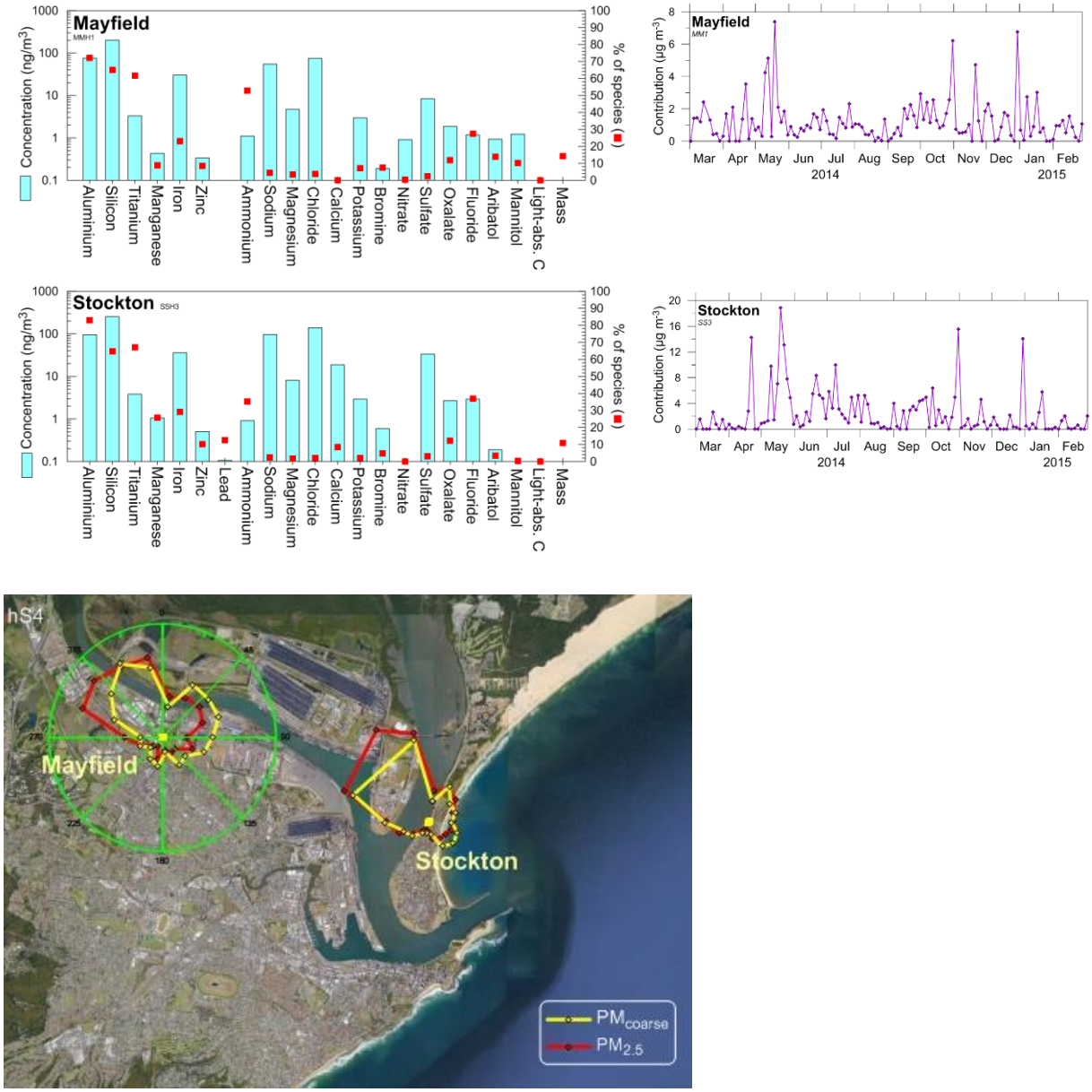

Figure 88: Fingerprints, CPF and time series plots of $PM_{2.5-10}$ Factor 4 (soil)

This factor is identified as soil and is very similar to the soil factor in the $PM_{2.5}$ fraction. It includes the key elements associated with crustal dust – aluminium, silicon, and titanium – and it includes about 65–75% of these elements at both sites. The Al/Ti ratio of 23-25 and Al/Si ratio of 0.38 are close to double those for crustal dust (Table 19) indicating the presence of an additional aluminium source. This factor also includes small amounts of iron, manganese and zinc, so probably includes some road and/or industrial dust. It does not include any black carbon.

The CPF plots (Figure 88) include both the $PM_{2.5-10}$ (yellow) and $PM_{2.5}$ (red) contours, which are very similar. At Mayfield, the coarse fraction is slightly stronger for easterlies and weaker for west-north-westerlies. At Stockton, south-easterlies contribute slightly more for $PM_{2.5-10}$.

The time series is quite spiky. The five days with the highest contributions are the same five days at each site, indicating a more regional source. This is consistent with the north-westerly lobes on the CPF plots.

Disregarding these days with the highest contributions, the time series plots show that winter has the strongest contribution at Stockton but the weakest at Mayfield. At this time of the year, the winds are almost exclusively west-north-westerlies (Figure 29), which means that sources contributing to the factor at these times are most likely to be local and located in the area between the Mayfield and Stockton sites. This corresponds to the CPF lobes pointing to areas on and around Kooragang Island.

Table 19: Comparison of the constituents of the $PM_{2.5-10}$ soil factor with crustal composition (Lide 1997) and some typical Australian dust (Radhi et al. 2010)

Species ratio	Crustal composition (Lide 1997)	Australian dust	Mayfield $PM_{2.5-10}$	Stockton $PM_{2.5-10}$
Al/Ti	**14**	**11.5-15.1**	23	25
Al/Si	**0.29**	**0.27-0.29**	0.38	0.38
Ti/Si	**0.020**	**0.018-0.026**	0.016	0.015
Fe/Si	**0.200**	**0.22-0.23**	0.15	0.14
Ca/Si	**0.15**	**-**	0	0.07

8.5 $PM_{2.5-10}$ Factor 5 – Industry

The annual average contribution of this industry factor to $PM_{2.5-10}$ is: Mayfield 1.0 µg m^{-3} (12%); Stockton 1.1 µg m^{-3} (5%).

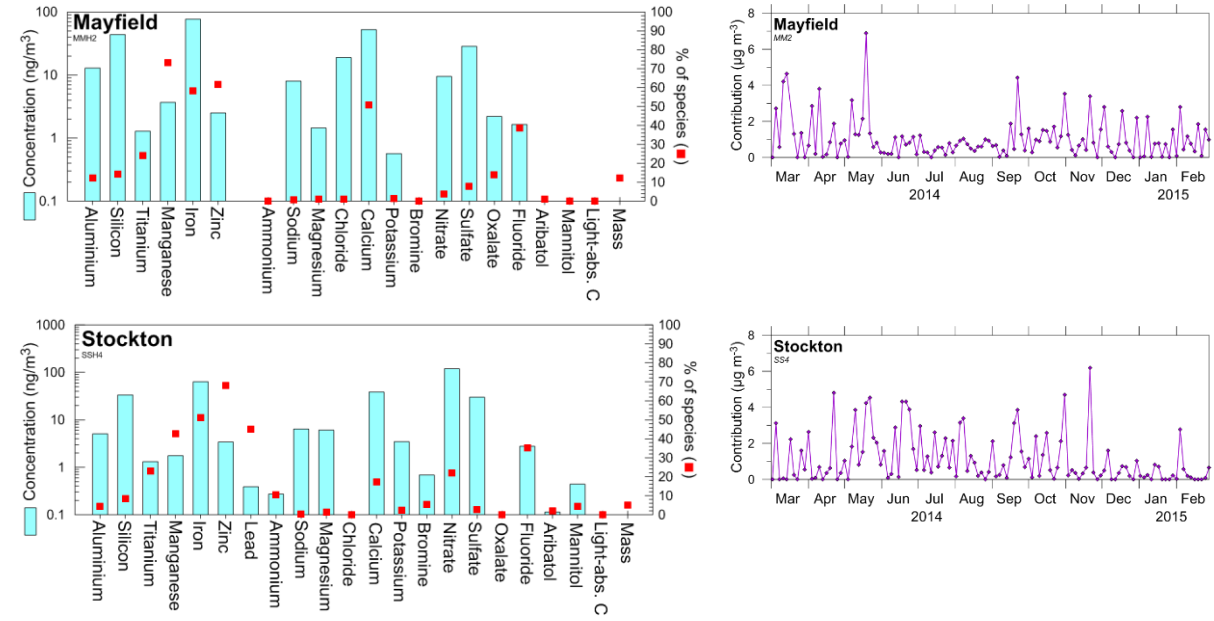

Figure 89: Fingerprints, CPF and time series plots of $PM_{2.5-10}$ Factor 5 (industry)

This factor includes the majority (50–75%) of the zinc, iron and manganese, as well as some calcium and fluoride. There is some aluminium, silicon and titanium present but their ratios are very different from soil, so soil could only be a contributor to this factor.

The time series plots in Figure 89 show that at Mayfield this factor contributes very little in winter, whereas at Stockton this is the case in summer. This factor contributes most in spring to early summer at Mayfield and late autumn to winter at Stockton.

The CPF plots in Figure 89 compare the patterns for this factor with the equivalent CPFs for the $PM_{2.5}$ industry factor, and show there are major differences. A dominant source of $PM_{2.5-10}$ for this factor appears to be located in the vicinity of Kooragang Island. The difference between the fine and coarse CPFs is greatest at Mayfield with a much smaller contribution from the south-west and greater contribution from the east and north-east than for $PM_{2.5}$. Unlike the similarities for the fresh sea salt (Figure 85) and soil fractions (Figure 88), this indicates there are different industry sources for the fine and coarse fractions.

8.6 $PM_{2.5-10}$ Factor 6 – Bioaerosol

The annual average contribution of this bioaerosol factor to $PM_{2.5-10}$ is: Mayfield 0.5 µg m^{-3} (6%); Stockton 1.1 µg m^{-3} (5%).

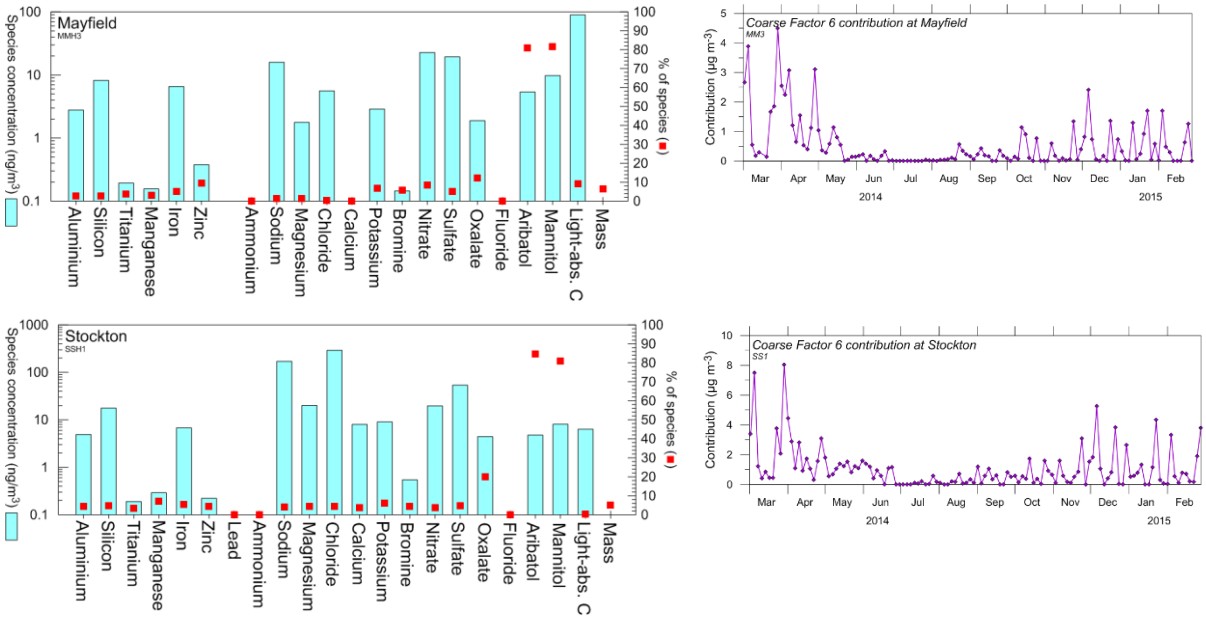

Figure 90: Fingerprints, CPF and time series plots of $PM_{2.5-10}$ Factor 6 (bioaerosol)

This factor includes 80–90% of the arabitol and mannitol, which are biomarkers for fungal spores and they have been used to assess the abundance of bioaerosols in the atmosphere (Bauer et al. 2008; Despres et al. 2012). At Mayfield, the dominant species in the factor is light-absorbing carbon, although the factor includes less than 10% of the total light-absorbing carbon in the filter samples, whereas at Stockton, the LAC concentration is a factor of ten smaller. There is also some nitrate, sulfate and sodium with Table 20 showing that the bioaerosol factor at Mayfield is similar in composition to the pollutant-aged sea salt factor (Factor 3 for $PM_{2.5-10}$) for Mayfield. On the other hand, at Stockton, the sea salt components of

this bioaerosol factor are in ratios extremely close to fresh sea water, indicating very little aging.

The contribution of this factor is greatest in autumn and summer (Figure 90) when fungal spore concentrations peak (Gaskin et al. 2012). Both sites show the same seasonal variation, indicating the factor is driven (determined) by the bioaerosols. Maximum concentrations at Stockton (Mayfield) were 37 ng m^{-3} (50) for arabitol and 71 ng m^{-3} (94) for mannitol. These fall between values reported by Chow et al. (2015) for a central Californian location and a literature survey of previously reported results.

The CPF plots show no preferred direction, which is consistent with many sources for the bioaerosols around the sites. This is a different inference than that made for such CPF plots for $PM_{2.5}$ factors. In those cases, such as for secondary ammonium sulfate, it was taken to indicate that the species were well mixed in the atmosphere. But this does not apply for the larger $PM_{2.5-10}$ factors which have a much shorter lifetime in the atmosphere before being deposited to the surface.

Table 20: Comparison of constituents of $PM_{2.5-10}$ Factor 6 with standard sea water and with $PM_{2.5-10}$ pollutant-aged sea salt Factor 3 at Mayfield

Species ratio to Na	Sea water	$PM_{2.5-10}$ Factor 3 (pollutant-aged sea salt) Mayfield	$PM_{2.5-10}$ Factor 6 (bioaerosol) Mayfield	$PM_{2.5-10}$ Factor 6 (bioaerosol) Stockton
Mg/Na	**0.120**	0.120	0.116	0.118
Ca/Na	**0.038**	0.038	0.040	0.047
K/Na	**0.037**	0.034	0.034	0.053
Cl/Na	***1.80***	***0.99***	***0.99***	***1.71***
SO_4/Na	***0.252***	***0.40***	***0.41***	***0.31***
NO_3/Na		1.01	1.01	0.12
C_2O_4/Na		0.044	0.044	0.026

9 Summary of coarse particle results ($PM_{2.5-10}$)

Table 21 summarises the results for $PM_{2.5-10}$ from the previous section, listing the main species in each factor and the drivers, i.e. those species that are used to identify and name the factor. It also lists the percentage contribution of each factor at each site to total $PM_{2.5-10}$ mass and summarises potential sources.

Table 21: Summary of PMF factors for $PM_{2.5-10}$

Factor	Main species in factor (drivers in bold)	Contribution of the factor to total annual $PM_{2.5-10}$ mass (with uncertainty range) at:		Potential sources
		Mayfield (a)	Stockton	
Factor 1 Fresh sea salt	**Cl^-:Na^+:SO_4^{2-}:Mg^{2+}**	40% (33-45%)	63% (50-66%)	Primary particles. Generated by wave-breaking on ocean
Factor 2 Light-absorbing carbon	**Cl^-:Na^+, BC, SO_4^{2-}, Mg^{2+}**	10% (8-26%)	10% (7-19%)	Light-absorbing carbon (LAC) with some sea salt. Coal particles are conjectured to contribute to this factor.
Factor 3 Pollutant-aged sea salt	**NO_3^-, SO_4^{2-}, Na^+:Mg^{2+}**, Reduced Cl-, enhanced SO_4^{2-} cf. fresh sea salt$^-$	16% (7-17%)	6% (4-11%)	Sea salt reacted with industry emissions, particularly NO_2 and SO_2
Factor 4 Soil	**Si:Al**, Fe, **Ti**, Ca^{2+}, SO_4^{2-}	14% (10-27%)	11% (6-14%)	Primary particles. Soil dust
Factor 5 Industry	**F^-**, Si, **Fe**, Cl^-, Al, **SO_4^{2-}**	12% (3-19%)	5% (3-10%)	Industry
Factor 6 Bioaerosol	Cl^-, SO_4^{2-}, **arabitol, mannitol**, Fe, Mg^{2+}	6% (5-15%)	5% (2-9%)	Bioaerosol such as fungal spores and pollens combined with industrial emissions and sea salt

(a) Factor contributions do not sum to 100% due to rounding of values.

The factor profiles for each site are shown together in Figure 144 to Figure 147 in Appendix C. Also included is the distribution of the species across the factors, which summarises some of the discussion in the previous section in a different presentation format.

The annual contributions of each factor to total $PM_{2.5}$ mass at each site are compared in Figure 91 and as percentages in Figure 92, with uncertainties shown using error bars.

In contrast to the fine particles ($PM_{2.5}$), the coarse particles are all directly emitted as primary particles, just possibly slightly transformed by chemical reactions in the atmosphere.

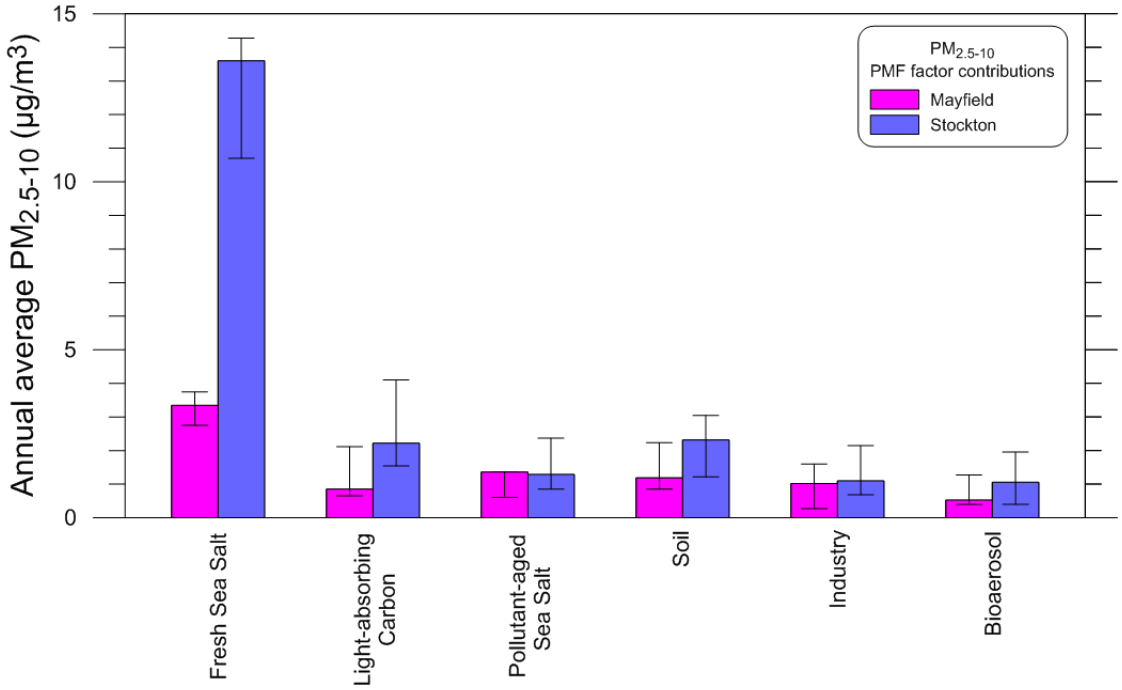

Figure 91: Comparison of the factor contributions at each site to annual average $PM_{2.5-10}$ mass

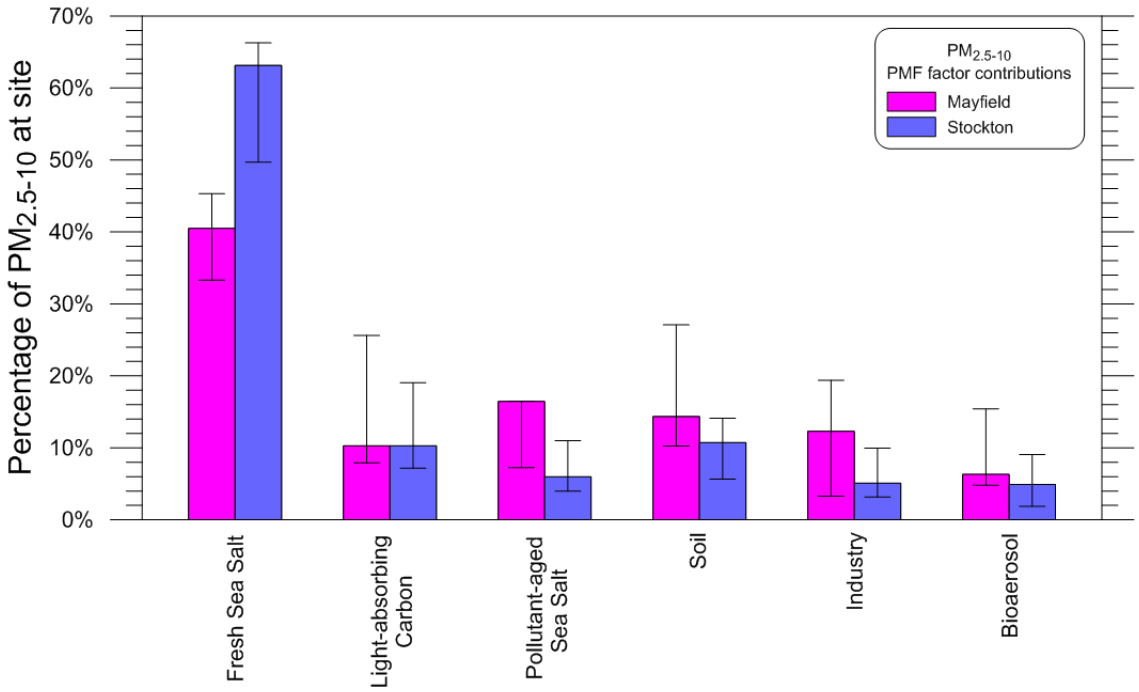

Figure 92: As for Figure 91, but showing values as percentage of annual average $PM_{2.5-10}$ mass at each site

9.1 Seasonal variability

The monthly variation in the contributions of each factor at Mayfield and Stockton are shown in Figure 93 and Figure 94. Both show an approximately bimodal distribution with low concentrations in winter (more precisely May to September) and high concentrations the rest of the year.

9.1.1 Mayfield

At Mayfield, the annual average $PM_{2.5-10}$ concentration is 8.3 µg m^{-3} with monthly averages ranging from a low of 2.4 µg m^{-3} in June and a high of 12.8 µg m^{-3} in December (Figure 93). On an annual basis the top three factors are fresh sea salt (40%), pollutant-aged sea salt (16%) and soil (14%).

The two sea salt factors (factors 1 and 3) dominate $PM_{2.5-10}$ during most of the year, contributing an average of 63% of the mass from August to April. Fresh sea salt contributes an average 5 µg m^{-3} from October to April, being more than 50% of the $PM_{2.5-10}$ from November to February.

Soil is the factor that contributes most consistently during the year with an average of 1.2 µg m^{-3} and a range from 0.6–2.4 µg m^{-3}, followed closely by the light-absorbing carbon factor with an average of 0.8 µg m^{-3} and a range from 0.3-1.3 µg m^{-3}. All other factors show strong seasonal variations. The bioaerosol factor is greatest in autumn and summer when fungal spore concentrations peak. Significantly lower sea salt and marginally lower industry factor contributions are evident during winter when offshore winds prevail.

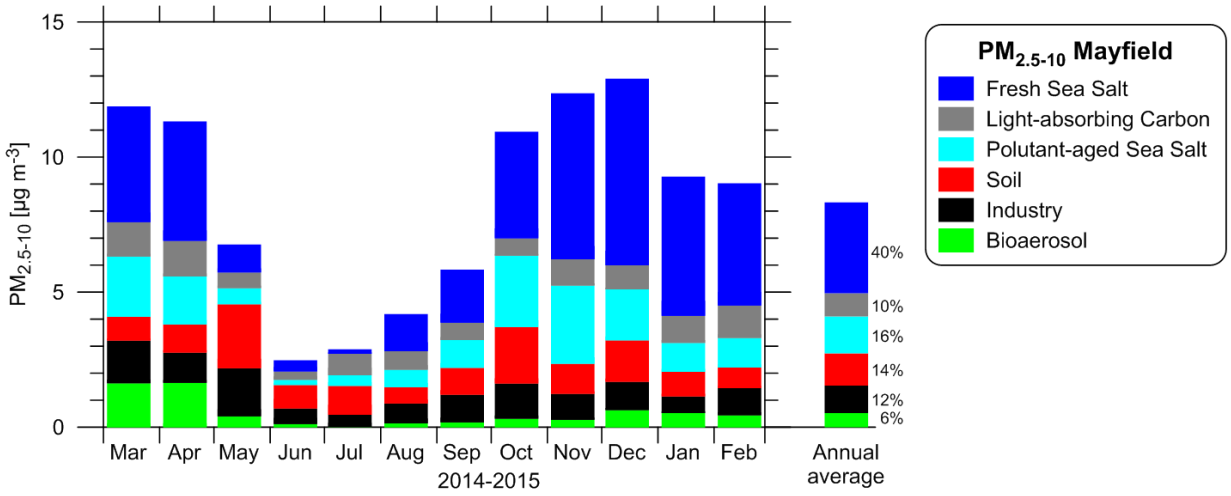

Figure 93: Monthly and annual factor contributions to $PM_{2.5-10}$ at Mayfield

9.1.2 Stockton

At Stockton, the annual average $PM_{2.5-10}$ concentration is 21.5 µg m^{-3} with monthly averages ranging from a low of 11 µg m^{-3} in July and a high of 34 µg m^{-3} in October (Figure 94). On an annual basis the top three factors are fresh sea salt (63%), soil (11%) and light-absorbing carbon (10%).

Fresh sea salt contributes an average 18 µg m^{-3} from October to April, contributing on average 73% of the mass for these months. Adding the pollutant-aged sea salt factor raises this to an average of 79%, demonstrating the dominant role of sea salt at this site on the narrow

Stockton peninsula between the Pacific Ocean and the northern arm of the Hunter River. Soil contributes most in May (6.6 µg m^{-3}) and is elevated from May to October.

The industry factor contribution is greater in late autumn to early spring. The light-absorbing carbon factor does not show any seasonal trends.

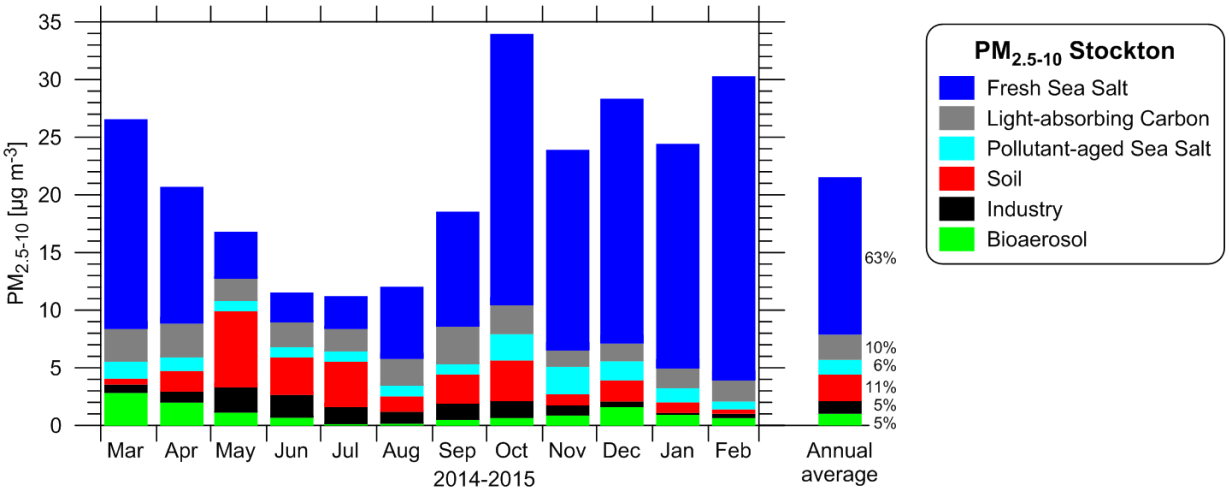

Figure 94: Monthly and annual factor contributions to $PM_{2.5-10}$ at Stockton

10 Modelling results

Case study analysis was undertaken on selected days on which elevated $PM_{2.5}$ concentrations coincided with prevalent PMF factor contributions to support the robustness of the overall study. Reference was made to various data sets, including air quality and meteorological monitoring records from OEH air quality monitoring stations and continuous black carbon measurements undertaken at the Newcastle site, and a range of analytical techniques, such as trajectory analysis, diurnal trend analysis and pollution and wind rose analysis. Further information on trajectory analysis is provided in Appendix E.

10.1 Fresh sea salt case study

Fresh sea salt contributed significantly to fine and coarse particle concentrations on a number of days during the sampling year (refer to Sections 6.1 and 8.1). Two case study days were selected for back trajectory analysis, one autumn day (25 April 2014) and one summer day (18 December 2014).

10.1.1 Friday 25 April 2014

According to PMF analysis, fresh sea salt accounted for 1.8–4.8 µg m^{-3} (40–57%) of the $PM_{2.5}$ mass at study sampling sites on this day, with the contribution being lowest at Beresfield and highest at Stockton. At Stockton, fresh sea salt was found to account for 22 µg m^{-3} (79%) of the coarse $PM_{2.5-10}$ mass, and for 8 µg m^{-3} (62%) of the coarse particle mass at Mayfield.

The back trajectory was initiated at 1900 eastern standard time (EST; 0900 UTC), coinciding with the hour prior to a peak in $PM_{2.5}$ concentrations measured at Beresfield and Newcastle on this day. The 24-hour back trajectory based on the 9km-resolution Weather Research and Forecast (WRF) Model meteorology simulations is illustrated in Figure 95, with the back trajectory using the 3km simulations shown in Figure 96. The prevailing synoptic circulation patterns are discussed based on the mean sea level pressure (MSLP) synoptic charts obtained from the Bureau of Meteorology (Figure 97).

The high pressure located over the Tasman Sea (Figure 97) explains the trajectory path (Figure 95), with the air mass traversing over the ocean for an extended period prior to moving over the study region. The analysis based on the 3km-resolution wind field simulations indicates that the winds were aligned with the coastline to the north-east prior to passing over the sampling sites (Figure 96). Sea salt aerosols form when sea-spray droplets, produced by bubble bursting within the foamy whitecaps and by wind skimming the wave crests, are evaporated. Wave-breaking along the coast may have contributed to the sea salt loading affecting particle concentrations on this day. At Newcastle, moderate south-easterly winds were recorded in the morning on the day, being replaced by north and north-easterly airflow in the afternoon and evening.

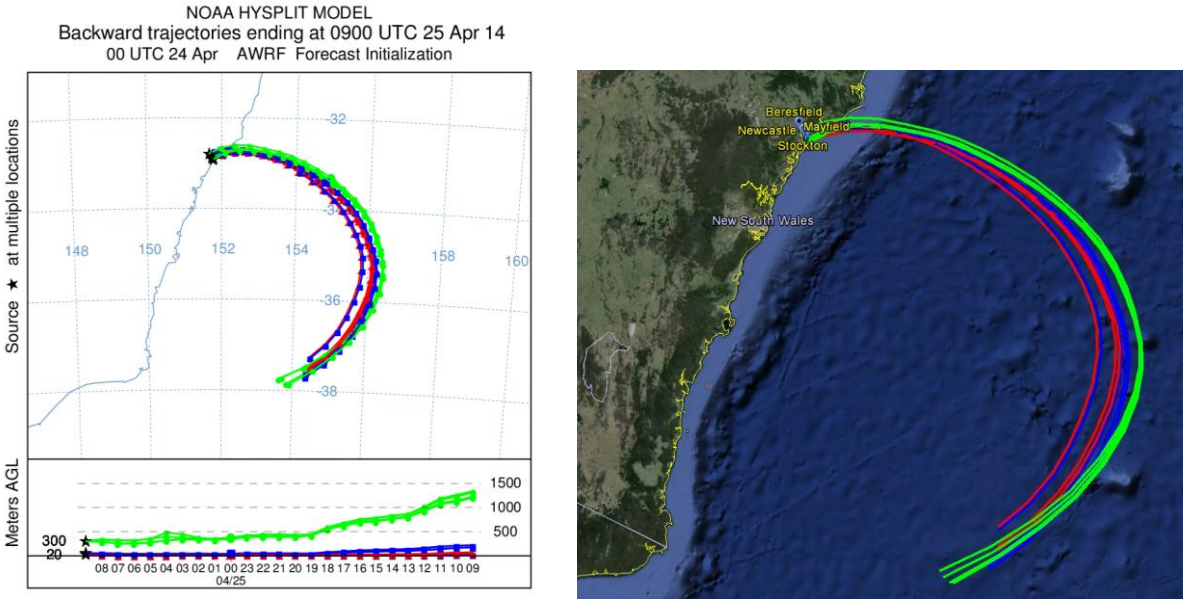

Figure 95: HYSPLIT computed backward trajectories for the 24-hour period ending at 1900 EST (0900 UTC) on 25 April 2014 from Mayfield, Newcastle, Beresfield and Stockton; HYSPLIT initialized with WRF 9km simulations

The red, blue and green lines illustrate the runs initiated from 20m, 50m and 300m above ground level, respectively.

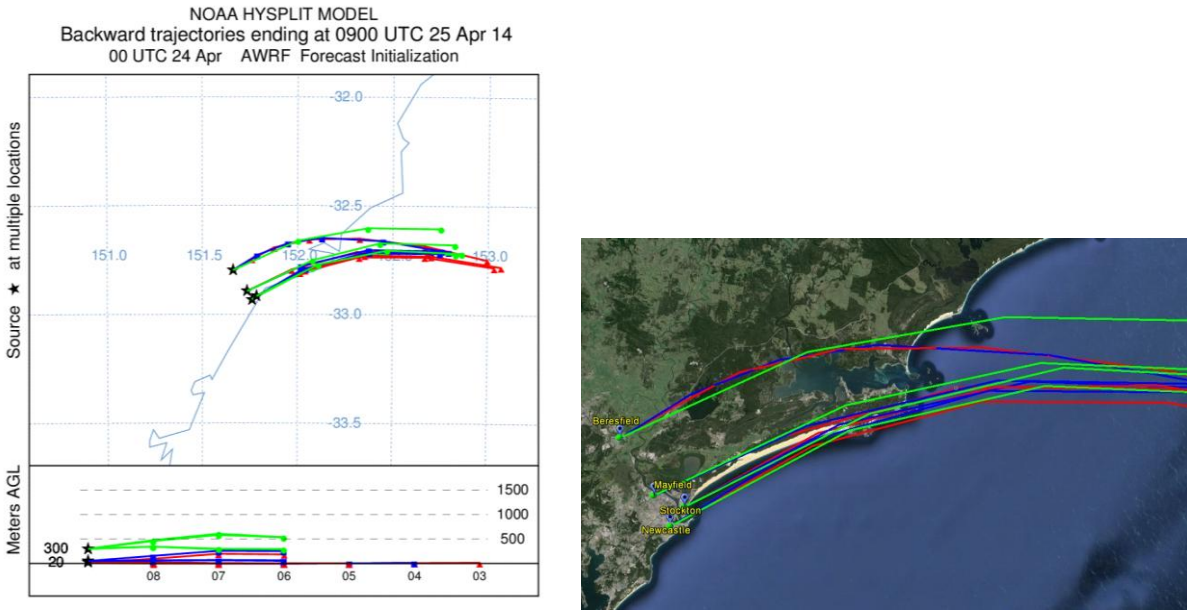

Figure 96: Same as for Figure 95, except HYSPLIT initialised with WRF 3km simulations

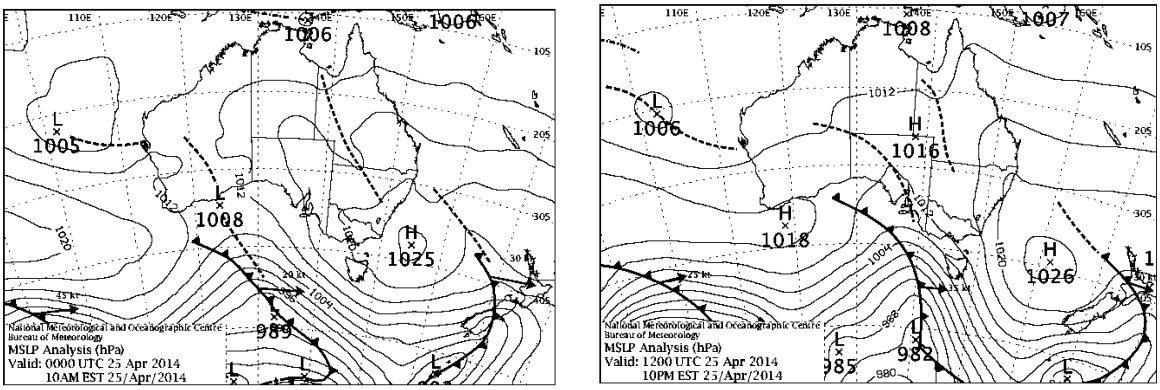

Figure 97: Surface analyses at (a) 1000 EST and (b) 2200 EST on 25 April 2014

Solid lines are contours for surface pressure (hPa).

10.1.2 Thursday 18 December 2014

Fresh sea salt accounted for 6.1–6.4 µg m^{-3} (48–53%) of the $PM_{2.5}$ mass across the four sampling sites on this day. At Stockton, fresh sea salt accounted for 43 µg m^{-3} (89%) of the coarse $PM_{2.5-10}$ mass, and for 17 µg m^{-3} (66%) of the coarse particle mass at Mayfield.

A back trajectory was initiated at 1200 EST, just prior to a peak in $PM_{2.5}$ levels at Stockton. The 24-hour back trajectory based on the 9km-resolution WRF meteorology simulations is illustrated in Figure 98, with the back trajectory using the 3km simulations shown in Figure 99, and synoptic charts for the day given in Figure 100. Similar to the 25 April 2014 case, a high pressure was located over the Tasman Sea on 18 December 2014 with the air mass traversing over the ocean and along the coastline north-east of Newcastle prior to passing over the sampling sites in the afternoon. The high pressure was displaced by a low-pressure system in the late evening with the weaker, offshore winds replacing the afternoon onshore flows and coinciding with a reduction in fine particle concentrations at Stockton, Newcastle and Beresfield.

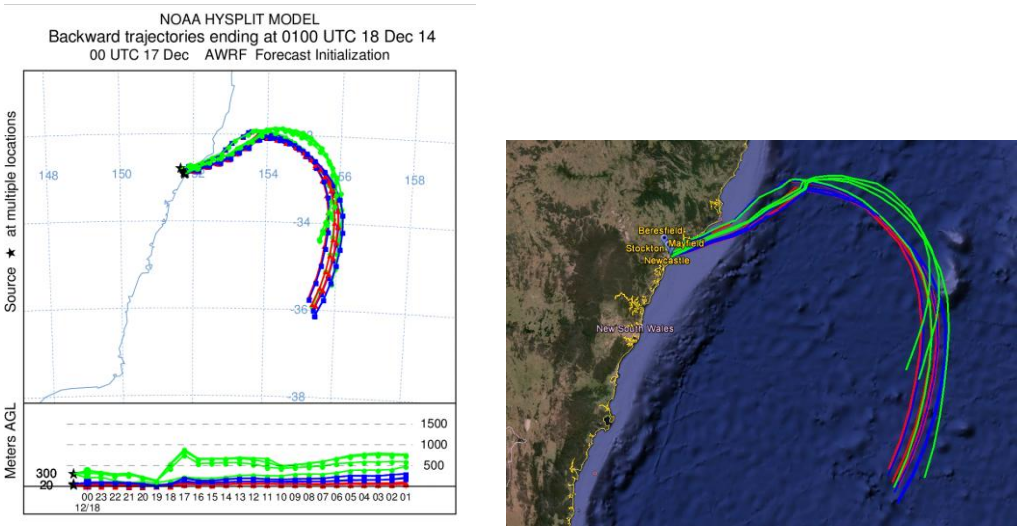

Figure 98: HYSPLIT computed backward trajectories for the 24-hour period ending at 1200 EST (0100 UTC) on 18 December 2014 from Mayfield, Newcastle, Beresfield and Stockton; HYSPLIT initialized with WRF 9km simulations

The red, blue and green lines illustrated the runs initiated from 20m, 50m and 300m above ground level, respectively.

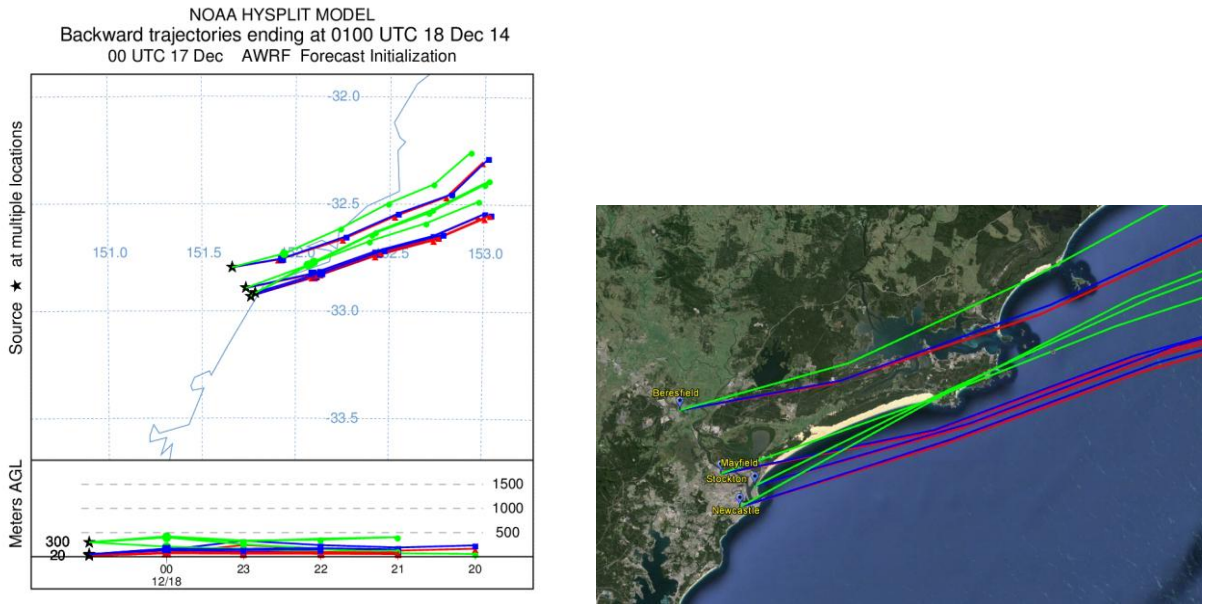

Figure 99: Same as for figure above, except HYSPLIT initialised with WRF 3km simulations

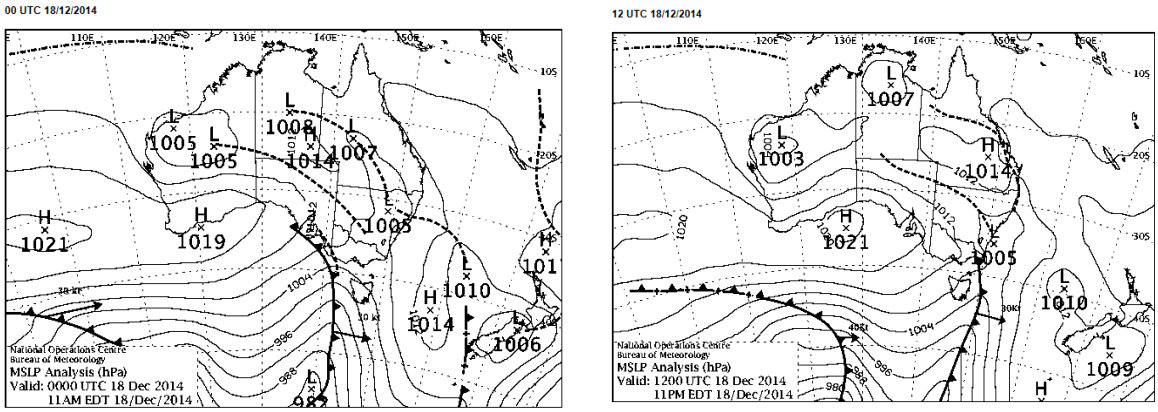

Figure 100: Surface analyses at (a) 1100 EDT and (b) 2300 EDT on 18 December 2014

Solid lines are contours for surface pressure (hPa).

Synoptic charts and prevailing wind were assessed for a further 16 days on which the fresh sea salt contribution at all four sites was determined through PMF analysis to be greater than about 40%. Many of these days, and including days with fresh sea salt contributions of greater than 80% at some or all stations, were characterised by north-easterly gradient winds associated with a high pressure system over the Tasman. The next most prevalent synoptic circulation pattern was the combination of a low pressure system off the east coast and a high pressure system over Tasmania transporting marine aerosol over the region within south-easterly onshore winds.

10.2 Wood smoke (residential wood heating) and ammonium nitrate

Wood smoke has been identified as a significant contributor to $PM_{2.5}$ at all sites during winter months coinciding with residential wood heating and the prevalence of offshore winds (refer to Section 6.4). During winter, the nitrate factor contribution increases substantially at Stockton, occurring as ammonium nitrate (refer to Section 6.7). A case study day is examined coinciding

with high wood smoke contributions at Beresfield, Newcastle and Mayfield and high ammonium nitrate contributions at Stockton.

10.2.1 Sunday 27 July 2014

Based on the PMF analysis, wood smoke accounted for 51% of the $PM_{2.5}$ mass (3.4 µg m^{-3}) at Beresfield and 73% of the $PM_{2.5}$ mass (6.9 µg m^{-3}) at Newcastle on this day, and also contributed to 31% (1.3 µg m^{-3}) of the mass at Mayfield. Smoke was found to contribute 10% (2.2 µg m^{-3}) at Stockton, with ammonium nitrate being the most significant factor contribution at Stockton on this day – accounting for 73% (15.3 µg m^{-3}) of the $PM_{2.5}$ mass.

Hourly $PM_{2.5}$ levels recorded on this day indicate elevated $PM_{2.5}$ levels at Beresfield and Newcastle during the night-time, peaking at 2100 EST. To provide more information reference is made to continuous black carbon measurements undertaken at Newcastle. OEH measured equivalent black carbon (EBC) using an AE33 aethalometer at the Newcastle site during part of the LHPC sampling year (2 June 2014 to 28 February 2015). These instruments support continuous, near real-time, temporally resolved measurements of EBC at seven wavelengths (370, 470, 520, 590, 660, 880 and 950 nm). By simultaneous measuring at multiple wavelengths, black carbon from fossil fuel can be distinguished from biomass combustion. EBC levels measured at 470nm (EBC_470) are more indicative of aromatic compounds related to biomass smoke, whereas concentrations measured at 950nm are more indicative of carbonaceous matter from combustion of fossil fuels. Based on the black carbon measurements for 27 July 2014 it is evident that the 2100 EST peak coincides with black carbon likely to be related to biomass combustion (Figure 101).

Taking into account the diurnal trend in $PM_{2.5}$ concentrations measured at Beresfield and Newcastle, the black carbon measurements at Newcastle, and the absence of vegetation fires in the event log for the region on this day or in the week prior, it is expected that the smoke factor is indicative of residential wood heater emissions. The sharp increase in black carbon at 1900 EST coincides with a distinct shift in the wind field as recorded at the Newcastle site, with the moderate winds with a southerly component prevailing in the afternoon being replaced by weak north-westerly winds in the evening. The trend shown in Figure 101 is indicative of wood smoke, with the transition from black carbon during flaming to brown carbon during smouldering later during the evening evident.

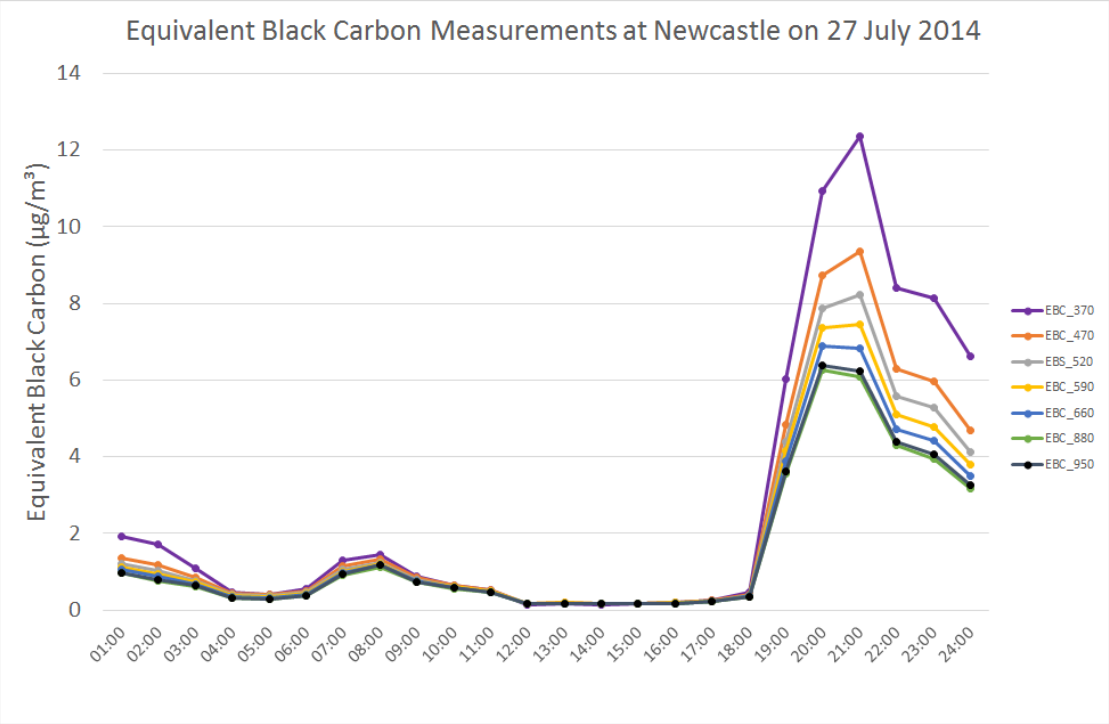

Figure 101: Diurnal variation in equivalent black carbon measured at Newcastle Air Quality Monitoring Station on 27 July 2014 using a seven wavelength aethalometer

As indicated at Stockton, ammonium nitrate was the dominant factor on this day (73%; 15.3 µg m^{-3} of the $PM_{2.5}$ mass). Based on the continuous monitoring data from the Stockton Air Quality Monitoring Station, elevated $PM_{2.5}$ levels were recorded during the early morning, peaking at 0500 EST before decreasing to low levels from noon onwards. The $PM_{2.5}$ peak coincided with a peak in ammonia concentrations being recorded at Stockton Air Quality Monitoring Station (Figure 102). Elevated $PM_{2.5}$ concentrations were associated with west-north-westerly airflow (Figure 103). Given that the ammonium nitrate factor was not prominent at any of the other sites, the source was likely to be local and situated north-west of the Stockton site. The prill tower within the Orica ammonium nitrate manufacturing facility on Kooragang Island is situated west-north-west of the Stockton site and is a source of primary ammonium nitrate $PM_{2.5}$ emissions (refer to Section 11.5).

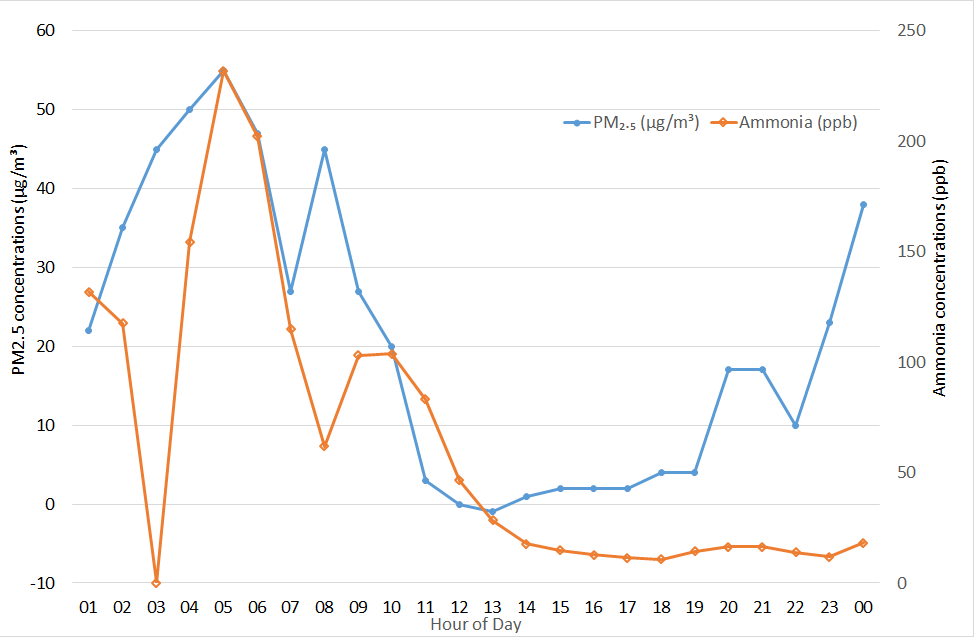

Figure 102: $PM_{2.5}$ and ammonia levels recorded at Stockton Air Quality Monitoring Station on 27 July 2014 (based on data from Orica Australia's Fuller Street Stockton station)

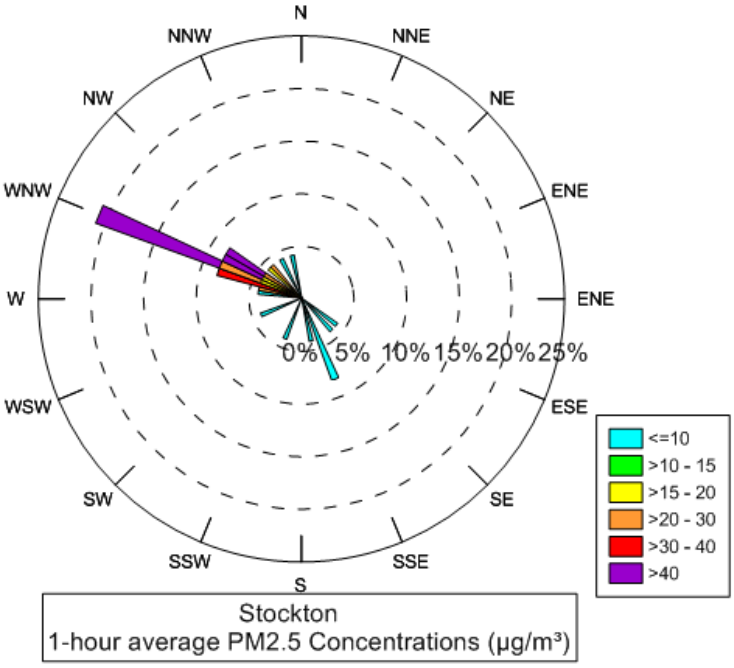

Figure 103: $PM_{2.5}$ rose for Stockton for 27 July 2014

10.3 Wood smoke (vegetation fires)

10.3.1 Monday 3 November 2014

Significant smoke contributions to total $PM_{2.5}$ mass generally only occurred during the late autumn to early spring, and are likely to be due primarily to residential wood heating. Wood smoke contributions on 3 and 9 November 2014 were the exception, with the greatest wood smoke contribution being found on 3 November. On this day wood smoke contributed significantly to the total $PM_{2.5}$ mass at Stockton (50%, 7.4 µg m^{-3}), Beresfield (44%, 6.2 µg m^{-3}) and Mayfield (39%, 4.6 µg m^{-3}). This event is unlikely to be associated with residential wood heating given that it occurred in late spring with overnight air temperatures not being unusually cool.

Notably Newcastle was not as affected by smoke on this day (12%, 0.9 µg m^{-3}), with the total $PM_{2.5}$ mass measured at Newcastle on this day (7.8 µg m^{-3}) being lower than at the other sites (Stockton, 14.8 µg m^{-3}; Beresfield, 14.2 µg m^{-3} and Mayfield, 11.7 µg m^{-3}). Fresh sea salt was the most prominent factor in the $PM_{2.5}$ mass at Newcastle on this day (50%, 3.9 µg m^{-3}) and also contributed significantly to Stockton (25%, 3.7 µg m^{-3}). Fresh sea salt also dominated the coarse particle mass on this day, accounting for 89% (23 µg m^{-3}) of the $PM_{2.5-10}$ mass at Stockton and 74% (11 µg m^{-3}) at Mayfield.

Based on the hourly $PM_{2.5}$ concentration measurements it is evident that $PM_{2.5}$ levels peaked at 0800 EST in the morning at Stockton and Mayfield with a lower but concurrent peak recorded at Newcastle station (Figure 104). $PM_{2.5}$ levels peaked at 1100 EST at Beresfield. Analysis of the wind field indicates that the $PM_{2.5}$ peaks were associated with shifts in the wind field to north-easterly airflow at 0700 EST in the case of Mayfield and Stockton and at 1000 EST in the case of Beresfield, with sharp reductions in $PM_{2.5}$ levels apparent with the onset of south-easterly, onshore winds (Figure 105). There were several large vegetation fires in the region on 2 and 3 November 2014, situated west and north-east of the sampling sites, as shown in Figure 106. It is likely that the transient north-easterlies transported smoke into the region from the vegetation fires situated to the north-east. The persistence of south-easterly winds throughout much of the remainder of the day on 3 November accounts for the prominence of the fresh sea salt factor at the more coastal sites of Stockton and Newcastle.

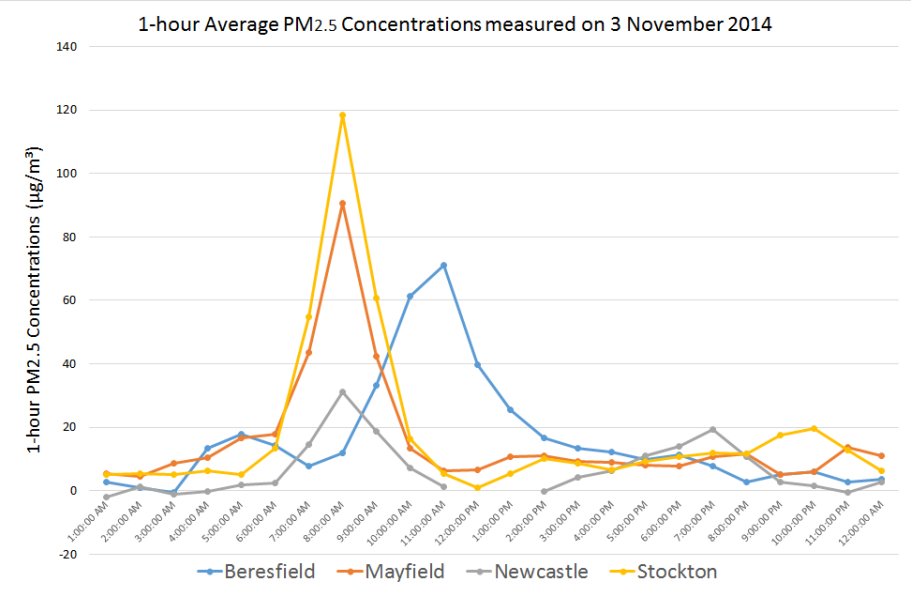

Figure 104: Hourly average $PM_{2.5}$ concentrations measured on 3 November 2014

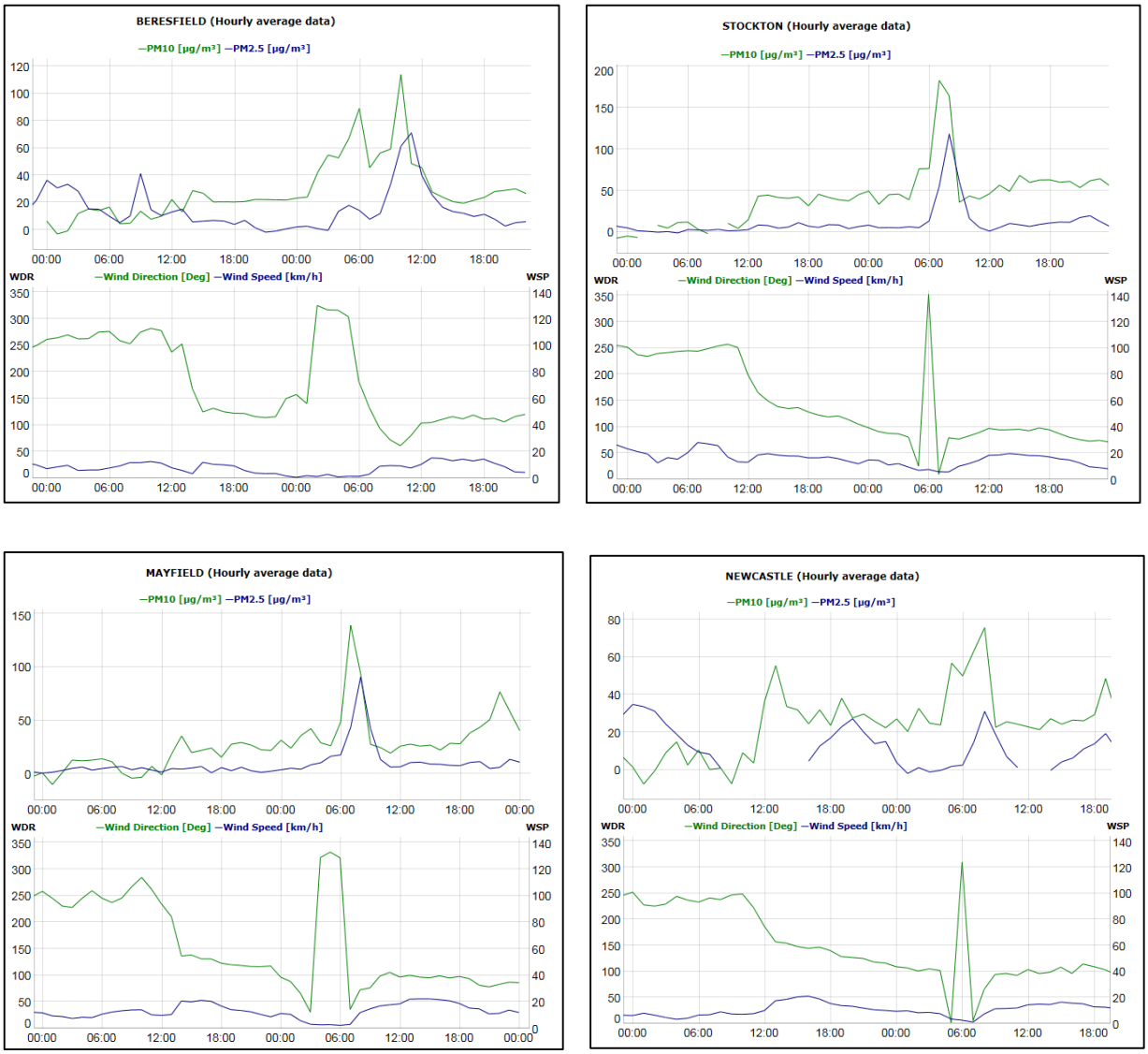

Figure 105: Hourly average wind and $PM_{2.5}$ measured 2 to 3 November 2014 showing the distinct peak in $PM_{2.5}$ (and PM_{10}) levels coinciding with north-easterly winds

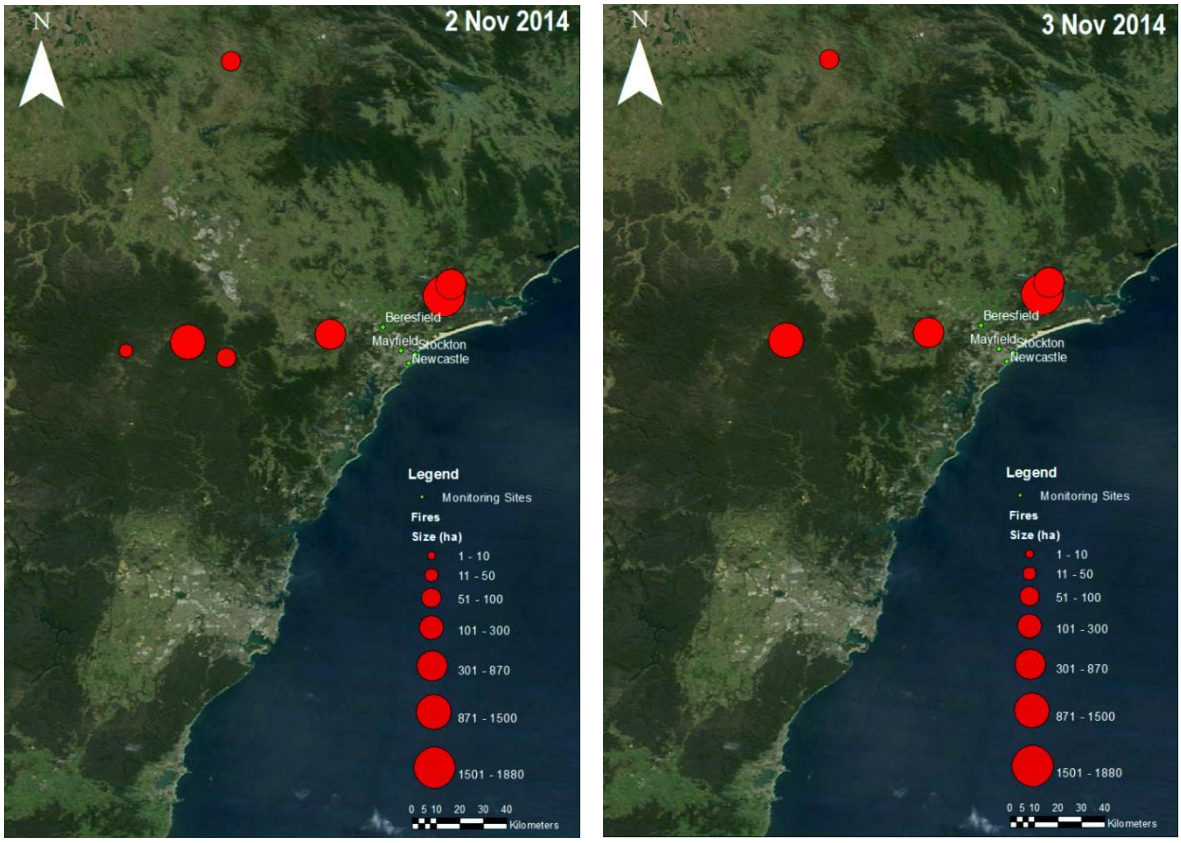

Figure 106: Vegetation fires occurring in the region on 2 and 3 November 2014

10.4 Shipping influence at Beresfield

Although shipping is a minor factor, only accounting for 2–4% of the $PM_{2.5}$ mass in the PMF mixed shipping/industry factor, it appears at all sites including Beresfield (refer to Section 6.8). A case study day is examined on which higher shipping/industry factor contributions occurred at Beresfield to understand more about the relative importance of shipping and industry to this factor and how shipping emissions are transported inland.

10.4.1 Friday 2 January 2015

The mixed shipping/industry factor accounted for 20% (2 µg m^{-3}) at Beresfield on this day. Other significant factor contributions on this day included pollutant-aged sea salt which accounted for 53% (5.4 µg m^{-3}) at Beresfield, 55% (7.1 µg m^{-3}) at Mayfield and 63% (6.8 µg m^{-3}) at Stockton; secondary ammonium sulfate contributions at Stockton (16%, 1.7 µg m^{-3}); and fresh sea salt contributions at Newcastle (23%, 2.7 µg m^{-3}) and Stockton (18%, 2 µg m^{-3}).

The back trajectory was initiated at 1400 EST on 2 January 2015, coinciding with generally elevated $PM_{2.5}$ levels being recorded across sites. The 24-hour back trajectory based on the 9km-resolution WRF meteorology simulations is illustrated in Figure 107, with the back trajectory using the 3km simulations shown in Figure 108. The prevailing synoptic circulation patterns are discussed based on the mean sea level pressure (MSLP) synoptic charts obtained from the Bureau of Meteorology (Figure 109).

The trajectories indicate north to north-easterly airflow over the ocean off the coast associated with the high pressure system located over the Tasman Sea (Figure 109), following which the air mass changes its trajectory and occurs as south-easterly airflow over the study region

(Figure 107), including Beresfield. The south-easterly winds in the region are also evident in the higher resolution trajectory analysis (Figure 108) and in the wind measurements at monitoring stations in the region (Figure 110).

At Newcastle, the contribution of the mixed shipping/industry factor was just 0.3 µg m^{-3} and at Stockton only 0.24 µg m^{-3}. However, it was much higher at 1.8 µg m^{-3} at Mayfield and 2.0 µg m^{-3} at Beresfield. The variation in the direct shipping contribution can be estimated from the vanadium concentrations, which were about 10 ng m^{-3} at Newcastle (10.1 ng m^{-3}) and Stockton (7.8 ng m^{-3}), but double this at Mayfield (20.4 ng m^{-3}) and lower at Beresfield (6.8 ng m^{-3}).

Comparing the shipping variation with the factor variation, it follows that the largest contribution at Beresfield was from industry rather than shipping.

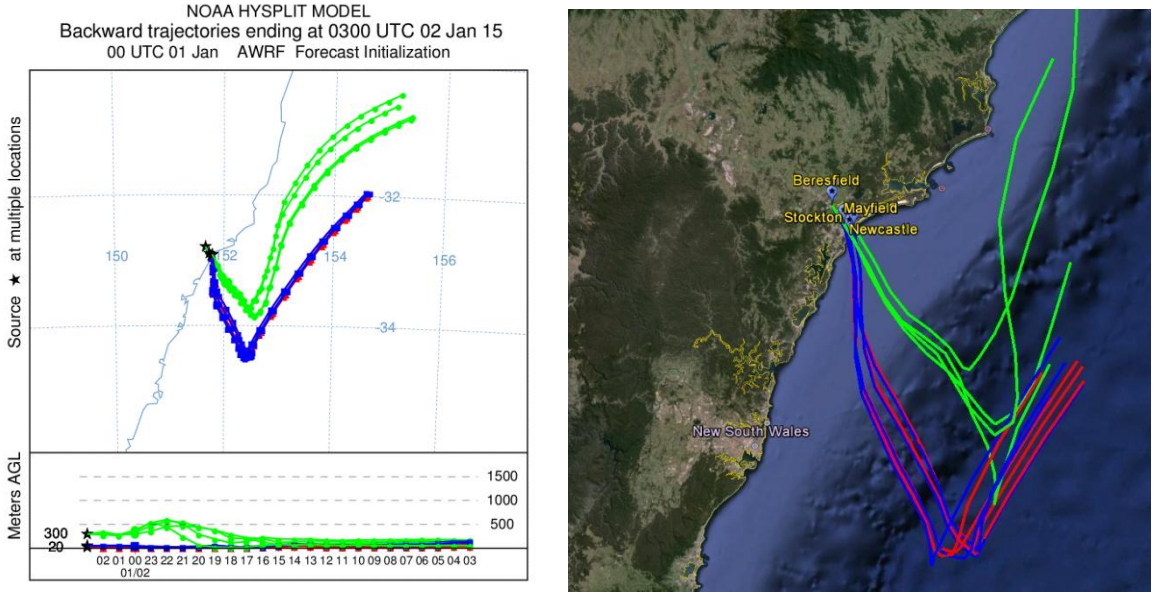

Figure 107: HYSPLIT computed backward trajectories for the 24-hour period ending at 1400 EST (0300 UTC) on 2 January 2015 from Mayfield, Newcastle, Beresfield and Stockton. HYSPLIT initialized with WRF 9km simulations

The red, blue and green lines illustrate the runs initiated from 20m, 50m and 300m above ground level, respectively.

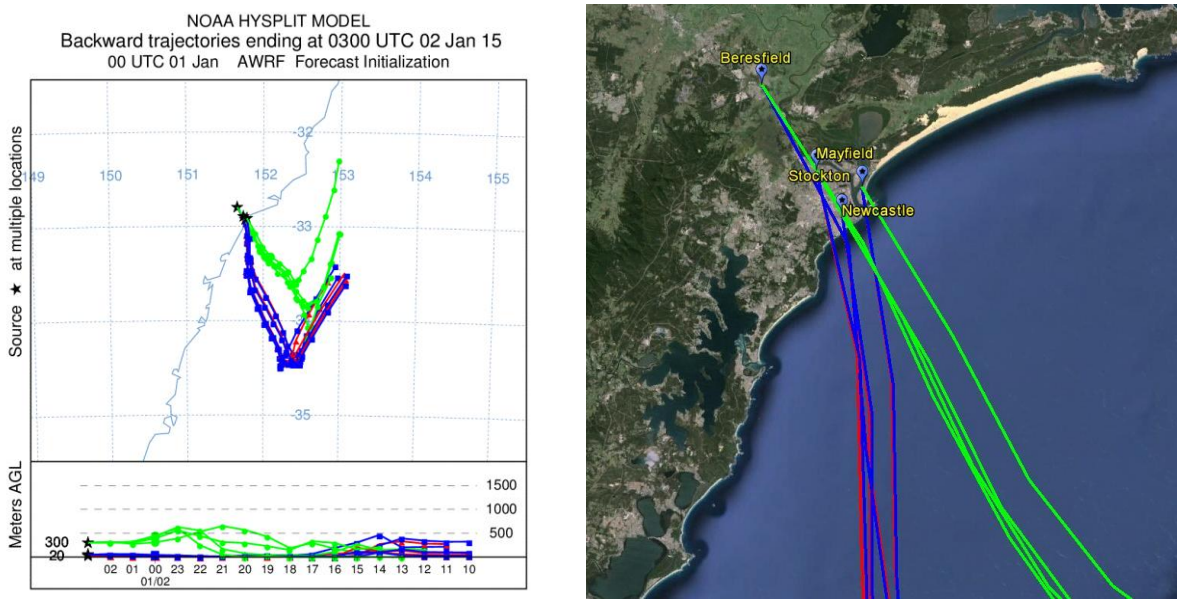

Figure 108: Same as for Figure 107, except HYSPLIT initialised with WRF 3km simulations

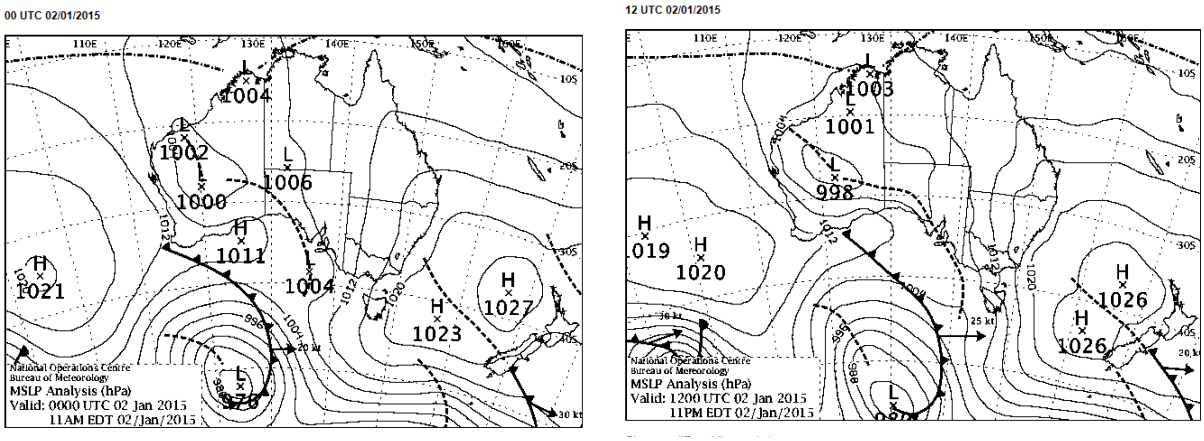

Figure 109: Surface analyses at (a) 1100 EDT and (b) 2300 EDT on 2 January 2015

Solid lines are contours for surface pressure (hPa).

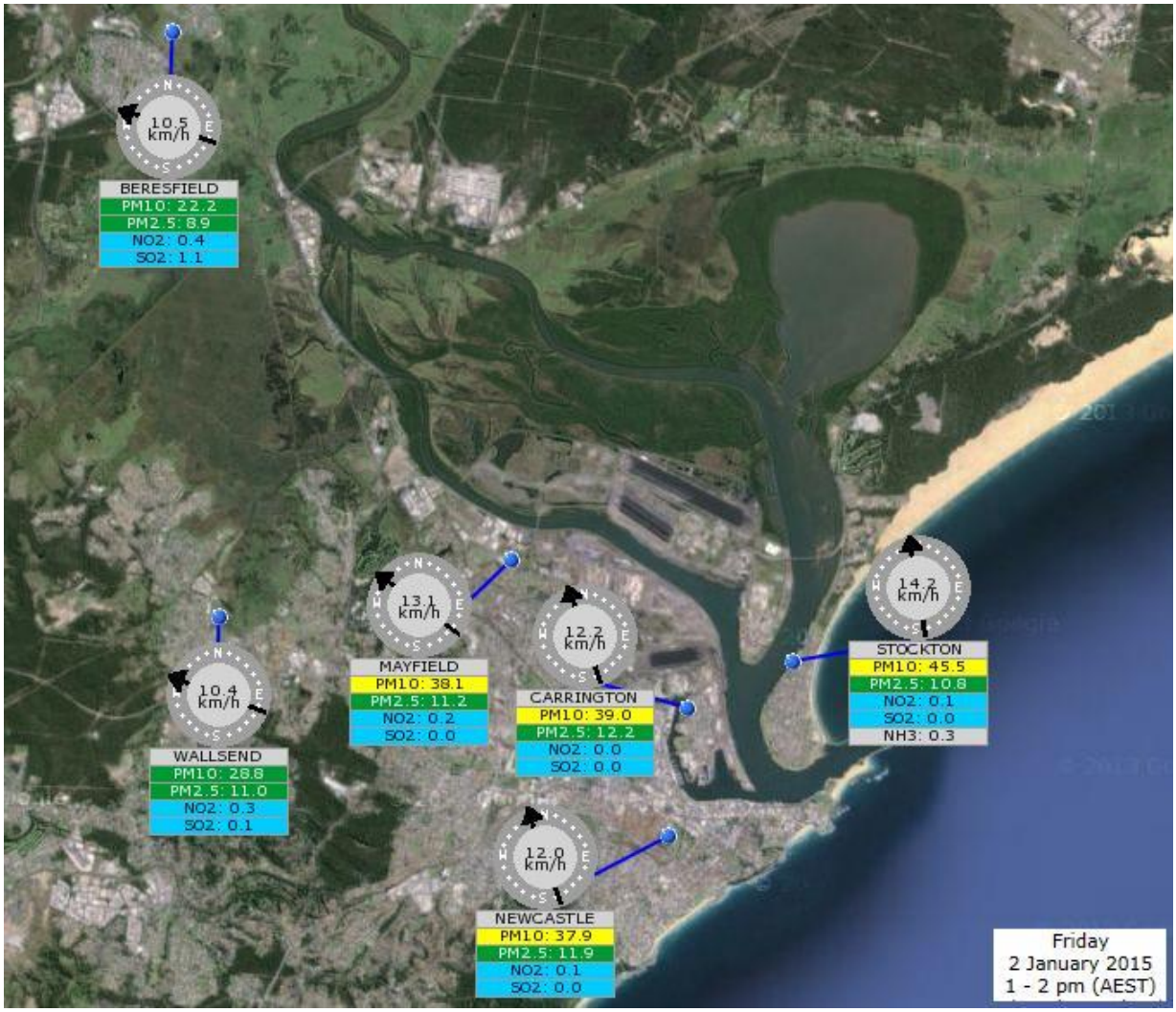

Figure 110: Air quality and wind measurements at Lower Hunter and Newcastle Local air quality monitoring stations at 1300–1400 EST on 2 January 2015

11 Discussion

11.1 General

This study has focused on determining the composition and sources of ambient (airborne) particles in the lower Hunter. Standard results available from air quality monitoring networks are daily concentrations of $PM_{2.5}$ and PM_{10}. The analysis of filter samples collected one-day-in-three for 12 months delivered the composition of elemental species, which using some simple conversions (for soil and organic mass) provided pie charts of the type shown in the left-hand column of Figure 111. Using positive matrix factorisation led to identification of the source factors with a much better understanding of the sources of the particles. The pie charts in the right-hand column of Figure 111 show an example.

There is little direct correspondence between the species (left) and factors (right) because they classify particle composition/sources in different ways. In addition, some of the factors are mixtures of sources or the sources are distributed across more than one factor. However, there is correspondence for soil, with the PMF giving values from 1.0 to 1.5 times those derived directly from the species composition. Wood smoke consists of a range of species and the PMF gives its contribution as 6–9 times that of just levoglucosan (wood smoke tracer species).

Sea salt from the species composition is equal to the sum of the PMF fresh sea salt plus about half the pollutant-aged sea salt, the latter including pollutants and hence a higher mass than fresh sea salt.

The secondary ammonium sulfate proportion is about 4–5 times the species ammonium concentration except at Stockton. Similarly, the secondary nitrate proportion is about double the nitrate proportion.

As discussed earlier, the source factors for $PM_{2.5}$ identified by PMF include both primary and secondary particles.

- Primary particles, such as fresh sea salt, soil, and some wood smoke, vehicle, shipping and industry emissions, are about 50% of the particles at Newcastle, Beresfield and Mayfield, and
- Secondary particles (particles formed by chemical reactions in the atmosphere and by gas-to-particle conversions) such as pollutant-aged sea salt, secondary ammonium sulfate, secondary sodium nitrate, and some wood smoke, vehicle, shipping and industry emissions, together account for about 50% of the particles at Newcastle, Beresfield and Mayfield.
- At Stockton there is about a 20% contribution from directly emitted ammonium nitrate (primary particles), so the primary:secondary split is 65:35.

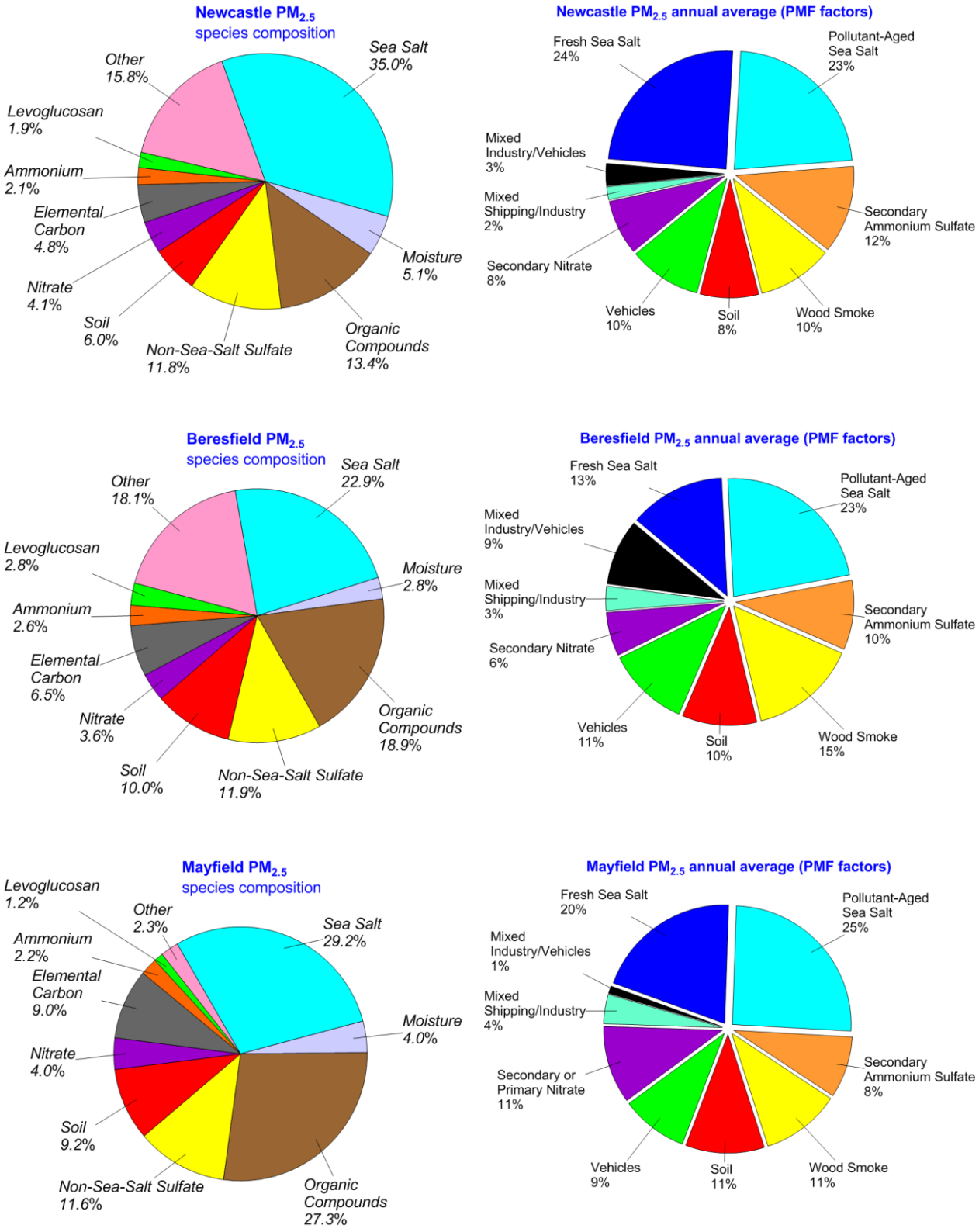

(Figure 111 continued over page)

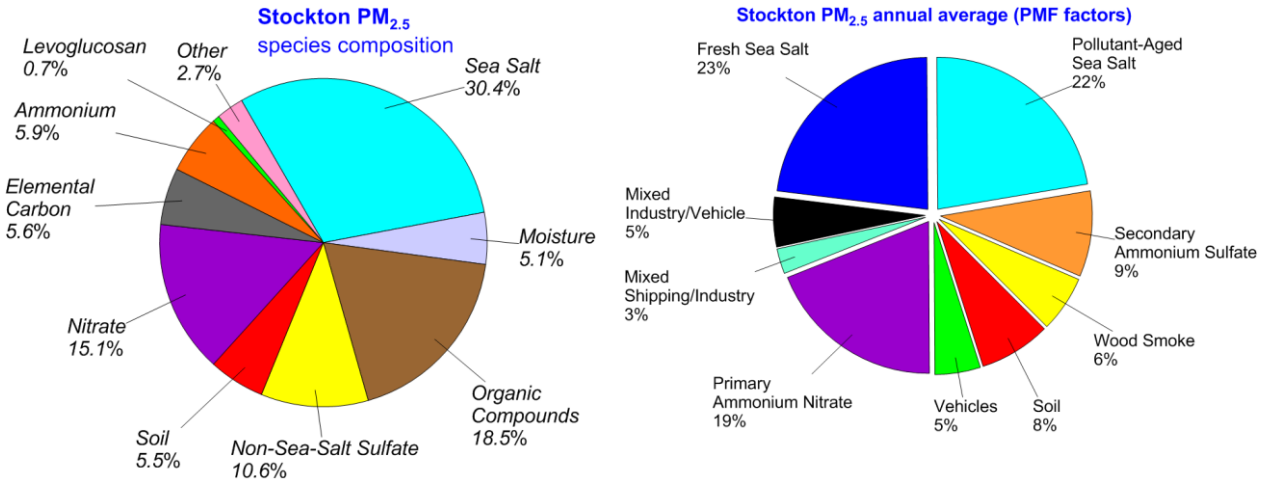

Figure 111: Comparison between (left) species composition and (right) PMF factors in $PM_{2.5}$ at the four sites

Secondary particle formation mainly occurs in the $PM_{2.5}$ fraction but the pollutant-aged sea salt factor in the $PM_{2.5-10}$ fraction (with ~10% contribution to $PM_{2.5}$ mass) is evidence of chemical reactions occurring in this size range too, although the relatively smaller surface area to volume ratio and their shorter lifetime in the atmosphere before being deposited, mean that much less of the chloride is displaced than in $PM_{2.5}$. In this factor, about half the original chloride in fresh sea salt has been replaced by nitrate and sulfate ions. Thus most $PM_{2.5-10}$ particles are primary particles or physical combinations of primary emissions.

The contribution of inter-regional transport to airborne particle concentrations within NSW metropolitan areas has been addressed in several studies (Cope & Ischtwan 1996; Nelson et al. 2002; Cohen et al. 2012; Cope et al. 2014). Given their longer atmospheric residence time and atmospheric chemistry (in the case of secondary particles), fine particles are able to travel far distances, with $PM_{2.5}$ particles being transported 1000 or more kilometres from the sources of their particle or precursor gas emissions (Seinfeld & Pandis 2006).

11.2 Secondary particles

The PMF identified a number of factors that are secondary particles with the key species being non-sea-salt sulfate, ammonium, nitrate and oxalate. Time series of the abundance of these species during the study are shown in Figure 112 for the four sites, except for ammonium and nitrate where the Stockton series is not included because of the local source that dominates the values at that site (see the bottom right-hand panel in Figure 69). Figure 112 shows that on any given day for each species, there is generally close agreement in concentrations across the three or four sites, indicating these species and their associated secondary particles are well-mixed in the atmosphere over the region, at least on a 24-hour average basis, which was the averaging time of the sampling program. The largest deviations are some elevated concentrations (above those at other sites) for non-sea-salt sulfate at Stockton from April to August and similarly for ammonium at Beresfield on a number of occasions throughout the year.

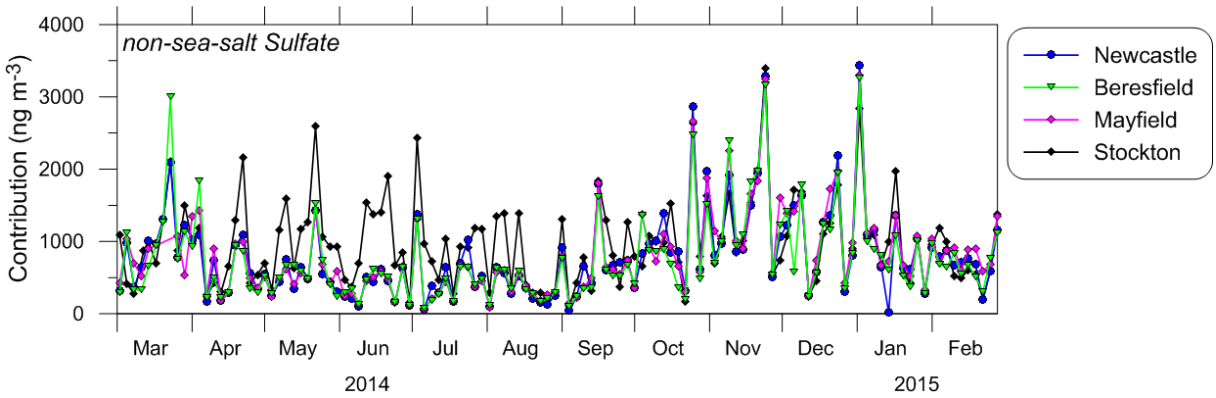

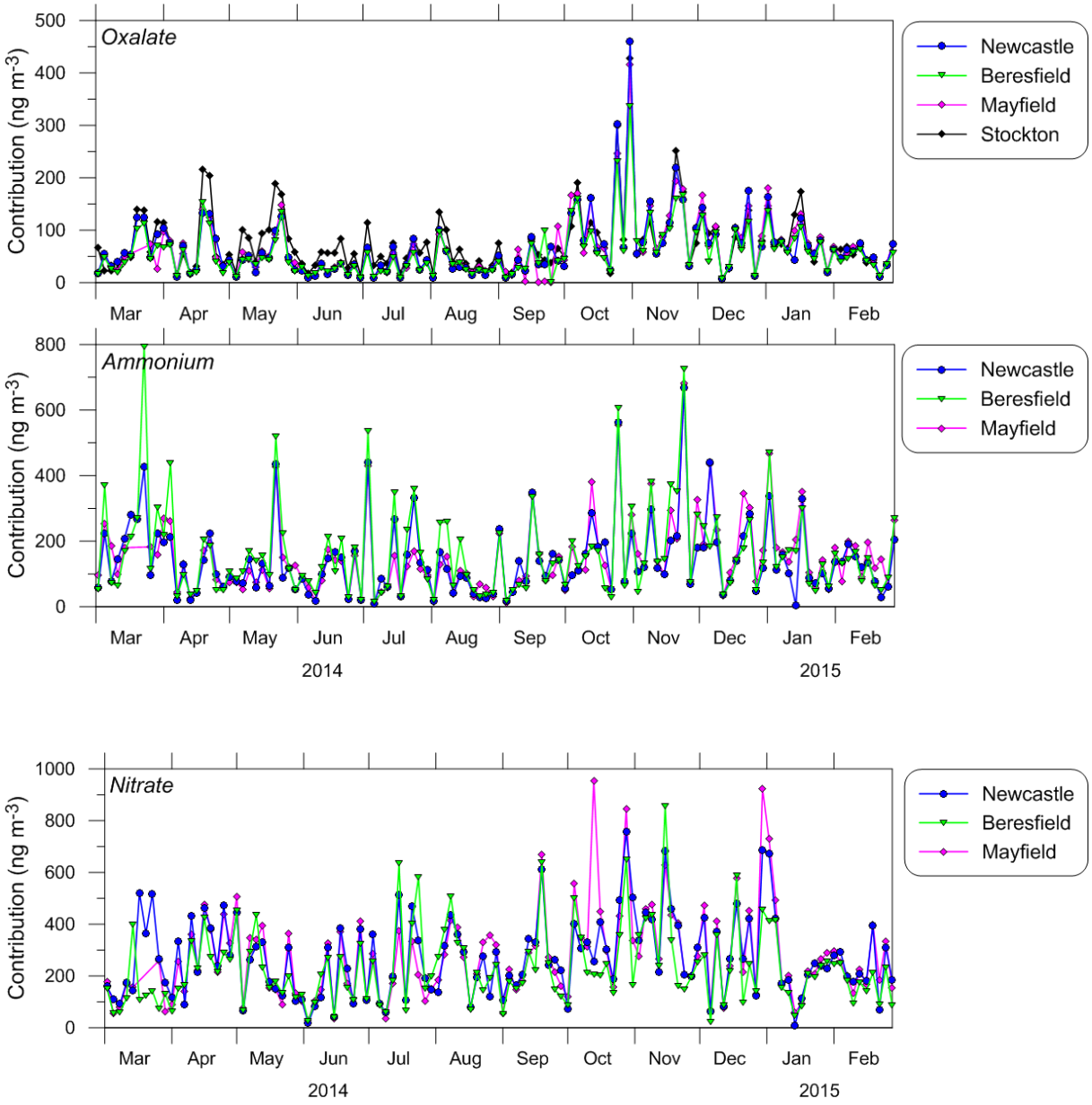

Figure 112: Time series during the study of the abundance of key species involved in secondary particle formation

All sites show generally higher levels during late spring to early summer (October to December) and generally lowest levels during winter, but the seasonal trends are fairly weak and other than for oxalate there are often significant differences from one sampling day to the next. The spikes in the oxalate trace are on 25 and 31 October, which occur a few days before the peaks in the levoglucosan on 3 and 9 November (time series not shown but it is similar to those for the wood smoke factor Figure 61.) The date 25 October corresponds to the start of a fire in the Singleton area on that day but further details about its extent are not currently available.

Precursor pollutant emissions were extracted from the 2008 Greater Metropolitan Region air emissions inventory for the five LGAs of the lower Hunter region shown in Figure 1 to indicate sources potentially contributing to the occurrence of the following secondary particles[8]:

- **Sulfate** – formed from emissions of primary sulfate and the oxidation of sulfur dioxide. Industry and power generation is the largest source of SO_2 emissions in the lower Hunter region (99.7% of SO_2 emissions). Minor sources of SO_2 include off-road mobile sources (includes shipping) (0.09% of emissions), on-road vehicles (0.05%) and bushfires/prescribed burning (0.05%).
- **Ammonium** – the precursor ammonia is released from industrial processes such as animal slaughtering and processing, ammonium nitrate production, waste disposal, chemical production, coal mining and metal processing (64% of lower Hunter emissions), on-road vehicles (11%), natural sources (mainly volatilisation from soils and vegetation burning) (11%), agriculture (mostly from poultry farming) (9%) and residential activities (mainly gas and solid fuel burning) (5%).
- **Nitrate** – industry and power generation is the largest sources of nitrogen oxides (NO_x) (77% of NO_x emissions in the lower Hunter region), followed by on-road vehicles (14%) and off-road mobile sources (6%), with smaller contributions from natural sources (mainly volatilisation from soils) (2%), and domestic and commercial activities (~1%).
- **Oxalate** – produced through the oxidation of volatile organic compounds (VOCs). Significant sources of VOCs in the region include natural sources (biogenic emissions) (59% of total VOC emissions in lower Hunter region), domestic-commercial activities (aerosol and solvent use, painting, lawn mowing, residential wood heating, recreational boating) (19%), on-road vehicles (evaporative and exhaust emissions) (8%), off-road mobile sources (8%), industry (4%) and commercial activities (<3%). Industrial emissions of VOCs are also an important contributor in the Newcastle area.

Further work is needed to reconcile the data in the Greater Metropolitan Region air emissions inventory with the results from this study. This will need to include chemical transport modelling in order to include the processes associated with the formation of secondary particles. Some case study modelling is currently being undertaken and will be reported separately.

11.3 Contribution of human activities to PM levels

To inform air quality management efforts to improve air quality in the region it is useful to provide an approximation of the proportion of airborne fine and coarse particles likely to be due to human activities. For this purpose it is assumed that the following factors are indicative of contributions from human activities:

- $PM_{2.5}$: wood smoke, vehicles, industry, shipping, secondary sulfate and nitrate
- $PM_{2.5\text{-}10}$: industry and light-absorbing carbon

Sea salt is a natural source, with the following factors assumed to be indicative of contributions by both human and natural sources:

[8] Source contributions of precursor gas emissions are discussed here based on emissions for the lower Hunter LGAs without specific reference to emissions from further afield. It is of note that fine particles are able to travel far distances, with $PM_{2.5}$ particles being transported 1000 or more kilometres from the sources of their particle or precursor gas emissions (Seinfeld & Pandis 2006; Cope & Ischtwan 1996; Nelson et al. 2002; Cohen et al. 2012; Cope et al. 2014).

- $PM_{2.5}$: pollutant-aged sea salt and soil
- $PM_{2.5-10}$: pollutant-aged sea salt and soil.

Based on the above assumptions:

- emissions from human activities are estimated to account for 45–54% of the annual $PM_{2.5}$ and 15–22% of the annual $PM_{2.5-10}$
- emissions from mixed human and natural sources for 30–36% of the annual $PM_{2.5}$ and 17–30% of the annual $PM_{2.5-10}$
- fresh sea salt for 13–24% of the annual $PM_{2.5}$ and 46–68% of the annual $PM_{2.5-10}$ across the study sites.

As noted in the previous section, chemical transport modelling can be used to refine these estimates, confirming the contribution of emissions from human activities to sulfate and nitrate and determining their contribution to the pollutant-aged sea salt and soil factors. Such modelling can also be used to assess inter-regional transport of pollution, spatially localised source contributions and determine how reducing specific sources may affect PM concentrations. The usefulness of chemical transport modelling was demonstrated during the study through modelling aerosol components of fine particles ($PM_{2.5}$) for winter and spring case study periods, as documented in the supplementary report (Emmerson et al. 2016).

11.4 Coal particle contributions in $PM_{2.5-10}$

The species analysis of the components of $PM_{2.5-10}$ showed about 10% was light-absorbing carbon (LAC) at both Mayfield and Stockton – 1.0 µg m^{-3} (11.7%) at Mayfield and 1.8 µg m^{-3} (7.9%) at Stockton. As described in Section 3.1.5, this determination from the laser integrated plate method used a value of 0.7 m^2 g^{-1} for the mass absorption coefficient for $PM_{2.5-10}$ based on information provided by Taha et al. (2007) but there is considerable uncertainty surrounding this value. Indeed it could be lower, which would increase the proportion of light-absorbing carbon. A limit on the maximum contribution by LAC is provided by the mass balance for the components in $PM_{2.5-10}$ shown in Figure 42. Attributing all of the 'other' to LAC would increase its contribution to 1.8 µg m^{-3} (21%) at Mayfield and 2.7 µg m^{-3} (12%) at Stockton. These would correspond to a value of 0.4–0.45 m^2 g^{-1} for the mass absorption coefficient.

The time series and CPF plots for this factor in Figure 86 do not show any strong seasonal trends. The scatter plot of the value of this factor at Stockton and Mayfield in Figure 113 shows a lack of correlation between the sites. A third of days with significant concentrations at one site or the other have zero or almost zero concentrations at the other site on that day. This indicates a significant local source, with coal particles from coal handling operations at the port being conjectured to contribute to this factor. The absence of any strong seasonal trends and the lobe for west to north-north-westerly winds evident in the Stockton CPF shown in Figure 86 are as yet unexplained. Further analysis is needed to identify whether coal particles could account for the light-absorbing carbon in this factor.

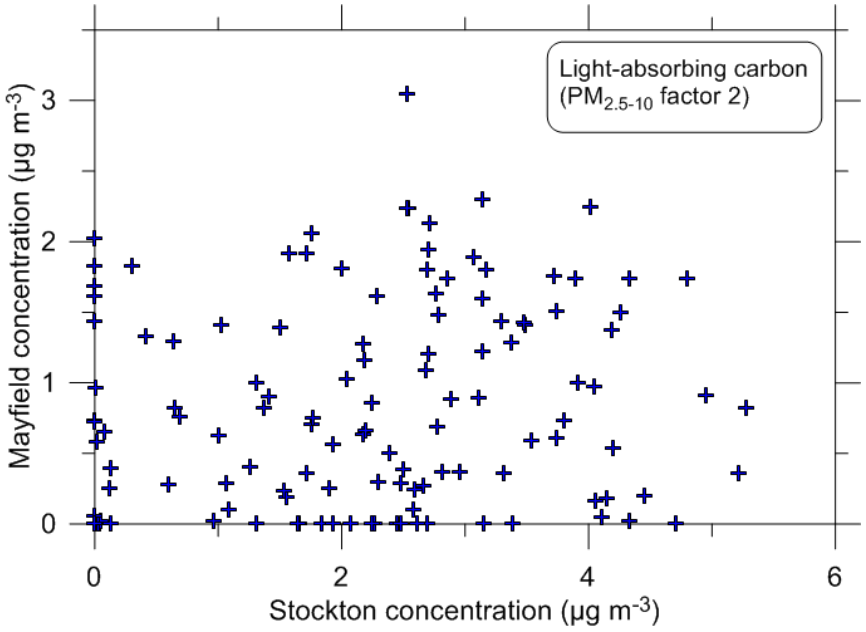

Figure 113: Scatter plot of $PM_{2.5-10}$ Factor 2 (light-absorbing carbon) measured at Stockton and Mayfield

11.5 Ammonium nitrate at Stockton

As discussed in Section 6.7, on average 19% of the $PM_{2.5}$ mass at Stockton is attributed to the ammonium nitrate factor. In winter months, it contributes an average of 5.1 µg m^{-3}, and makes up an average of 41% of total $PM_{2.5}$.

The Stockton site is situated about 700m to the south-east of the Orica Australia Pty Ltd (Orica) ammonia nitrate manufacturing facility on Kooragang Island. Emissions from this facility include particulate matter, ammonia, oxides of nitrogen and nitric acid (AECOM 2009), with particulate matter emissions from ammonium nitrate production (prill tower) largely comprised of $PM_{2.5}$ ammonium nitrate (NH_4NO_3), as reported in monitoring results (Orica Australia Pty Ltd 2014). Prill towers are documented by the US EPA (1995) to comprise mainly small particles, 56% of which are below 2.5 µm ($PM_{2.5}$), 73% below 5 µm and 83% below 10 µm (PM_{10}).

The direction of the source from the monitoring site is clearly indicated by the bivariate pollution rose in Figure 71 (in Section 6.7). The direction is 305° relative to true north, which as shown in Figure 114 points directly towards to Orica's prill tower.

Figure 114: Map showing the bearing of 305° (identified in Figure 71) from the Stockton Air Quality Monitoring Station towards Kooragang Island and Orica's prill tower

The time series at the top of Figure 115 (also Figure 70) shows that at Stockton this factor is only present in the second half of autumn and winter. This corresponds to the part of the year when north-westerly winds prevail at Stockton. A brief investigation of the variation of the factor with wind direction during the year is shown in Figure 115. The year was divided into three periods: (i) before the main contributions (1 March to 15 April 2014), (ii) during the main contribution (20 April to 31 October 2014), and (iii) the rest of the study year (1 November 2014 to 28 February 2015). For each period, the wind rose was calculated as shown in the figure. The middle period, coinciding with a high frequency of north-westerly winds, dominates the occurrence of this factor. The wind roses for both the first and third periods show only occasional north-westerly winds.

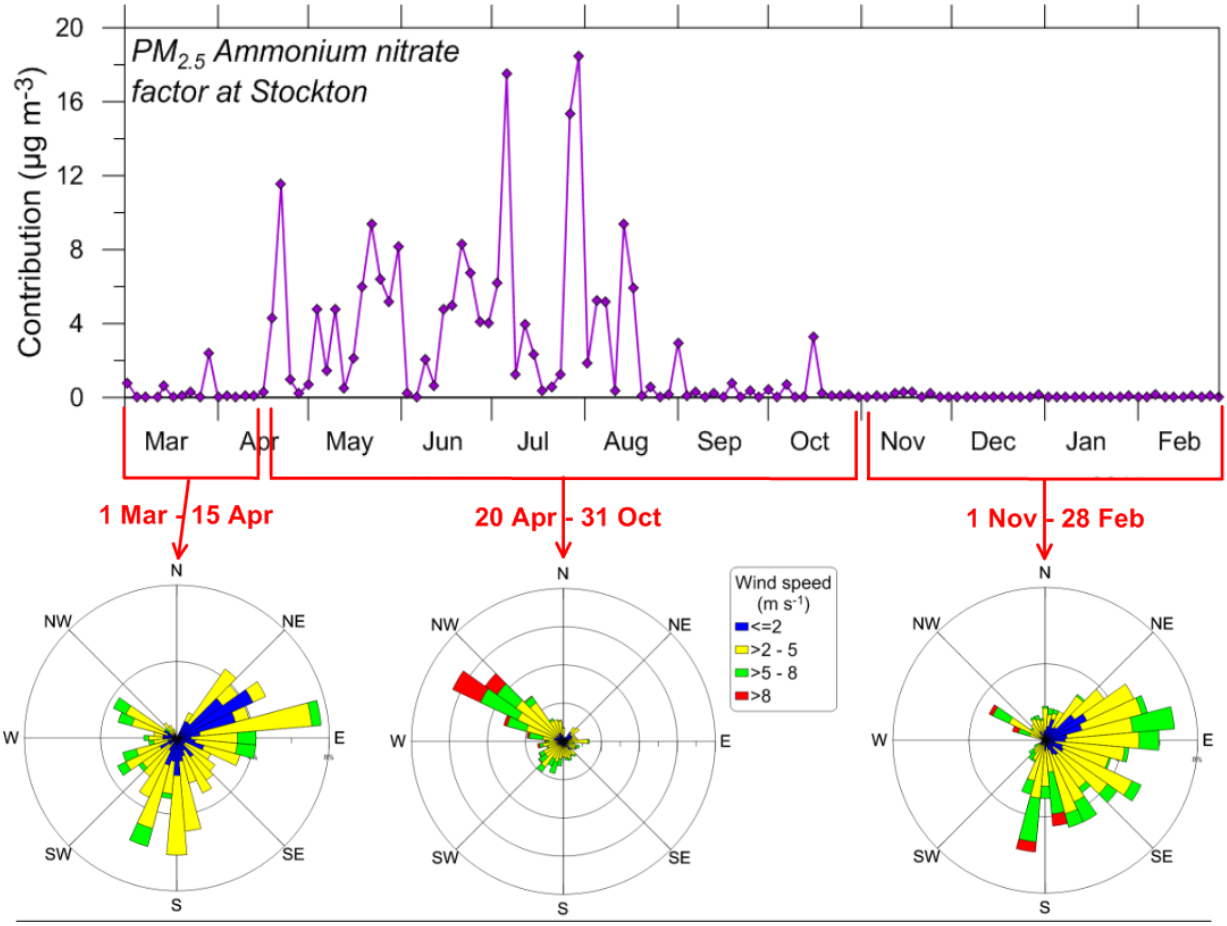

Figure 115: Wind roses at Stockton for three distinct periods identified in the ammonium nitrate factor time series trace at the top of the figure

In 2013, as part of a Pollution Studies and Reduction Program (PRP) associated with its environment protection licence (EPL), Orica characterised particulate emissions from the AN1 prill tower, reviewed options to reduce emissions, and evaluated feasible options to reduce emissions (EPA 2015; Orica 2016). During that study $PM_{2.5}$ and PM_{10} emissions from the prill tower were measured to remain fairly consistent with periodic short-duration spikes in coarser particle emissions found to occur during non-routine operations (e.g. prill head changeovers, plant trips or plant start-ups). The feasibility study concluded that a reduction in particulate emissions larger than PM_{10} from the prill tower would result in a more significant reduction in particulate mass emissions than focusing specifically on fine particles. It is relevant to note that the current study measured negligible amounts of ammonium in the $PM_{2.5\text{-}10}$ fraction (maximum 24-hour average 24 ng m^{-3}) compared to the $PM_{2.5}$ fraction (maximum 3700 ng m^{-3}) at Stockton.

Following a review of options for reducing >PM_{10} particle emissions, Orica initiated a particulate minimisation program as a staged improvement strategy (Orica 2016). Stage 1 of the program started in January 2014 and is reported to have included improvements to monitoring methods, operator awareness and active process monitoring. Stage 2 started in August 2014 and is reported to have comprised changes to the prill production process resulting in a decrease in the potential for particle emissions by reducing fan speed through modifications to prill head design, capping of maximum fan speeds and other process modifications (Orica 2016). The effectiveness of the particulate minimisation program is being

assessed by Orica based on stack measurements and dust deposition sampling to determine reductions in the emissions of coarse particles from AN1 prill tower (Orica 2016).

Orica is also implementing other emission reduction measures including an ammonia management improvement program which comprises construction and operation of three ammonia flares to reduce the facility's emissions by capturing and burning ammonia emissions at safety release points (Orica 2014). As at September 2015 two of the three new ammonia flaring systems were under construction but not yet in operation (Orica 2015).

Ammonium nitrate levels recorded during the LHPCS provide information for any future studies assessing the effectiveness of emission reduction measures at Orica's ammonium nitrate manufacturing facility in reducing fine particle concentrations at Stockton. This study has identified the only suitable time of year to do such an assessment as being during late autumn and winter periods when north-westerly winds prevail. The detailed ammonium nitrate concentrations recorded as part of the LHPCS in autumn/winter 2014 provide a valuable baseline.

11.6 Comparison with earlier PMF results

ANSTO has conducted $PM_{2.5}$ characterisation at Mayfield since 1998, with major source contributions to long-term average $PM_{2.5}$ mass (1998–2013) determined as shown in Figure 116 (Stelcer et al. 2014). Sources identified are: secondary sulfate formed from reactions of SO_2 with ammonium in the atmosphere; motor vehicles; smoke associated with biomass and vegetation burning common in domestic heating, hazard reduction burning and bush fires; fresh sea salt (sea spray); soil dust; and industry. Stelcer et al. (2014) concluded that anthropogenic sources comprising motor vehicles, smoke from biomass burning and secondary sulfate from industrial processes, contributed 70% of ambient $PM_{2.5}$ in the Mayfield local area over the 15-year period, during which there have been major changes in sources with the closure of the major iron and steel works in 1999, phasing out of leaded petrol in 2001, and the closure of a magnesium dioxide production plant in 2008.

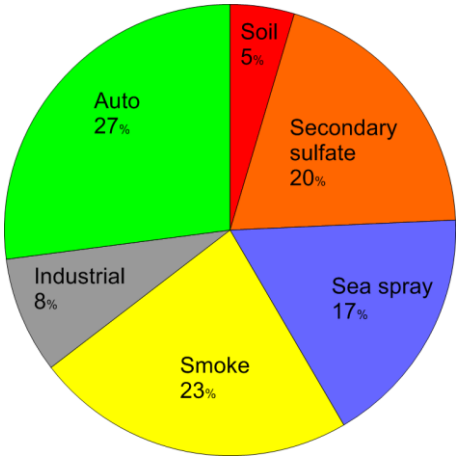

Figure 116: Source contributions to long-term $PM_{2.5}$ concentrations at Mayfield (1998–2013) (after Stelcer et al. 2014)

It would be informative to compare the break-down shown in Figure 116 with results from the current study. However, this is not straightforward for a couple of reasons. Firstly, as described above, there have been significant changes in sources since 1998. Secondly, the ANSTO analysis used the chemical species available from IBA techniques and black carbon, as listed in Section 3.1.2, whereas the current study added a range of species available through ion chromatography (Section 3.1.3) of which nitrate, ammonium, magnesium, levoglucosan and mannosan are particularly significant.

To address these issues, ANSTO undertook a PMF analysis on their IBA and BC data for the five years from 2010–15 finding the best fit with a seven-factor PMF and then determined the contribution of the factors for the period of the current study (1 March 2014 – 28 February 2015). The fingerprints and species contributions to the factors in the seven-factor PMF solution are shown in Figure 117 and Figure 118.

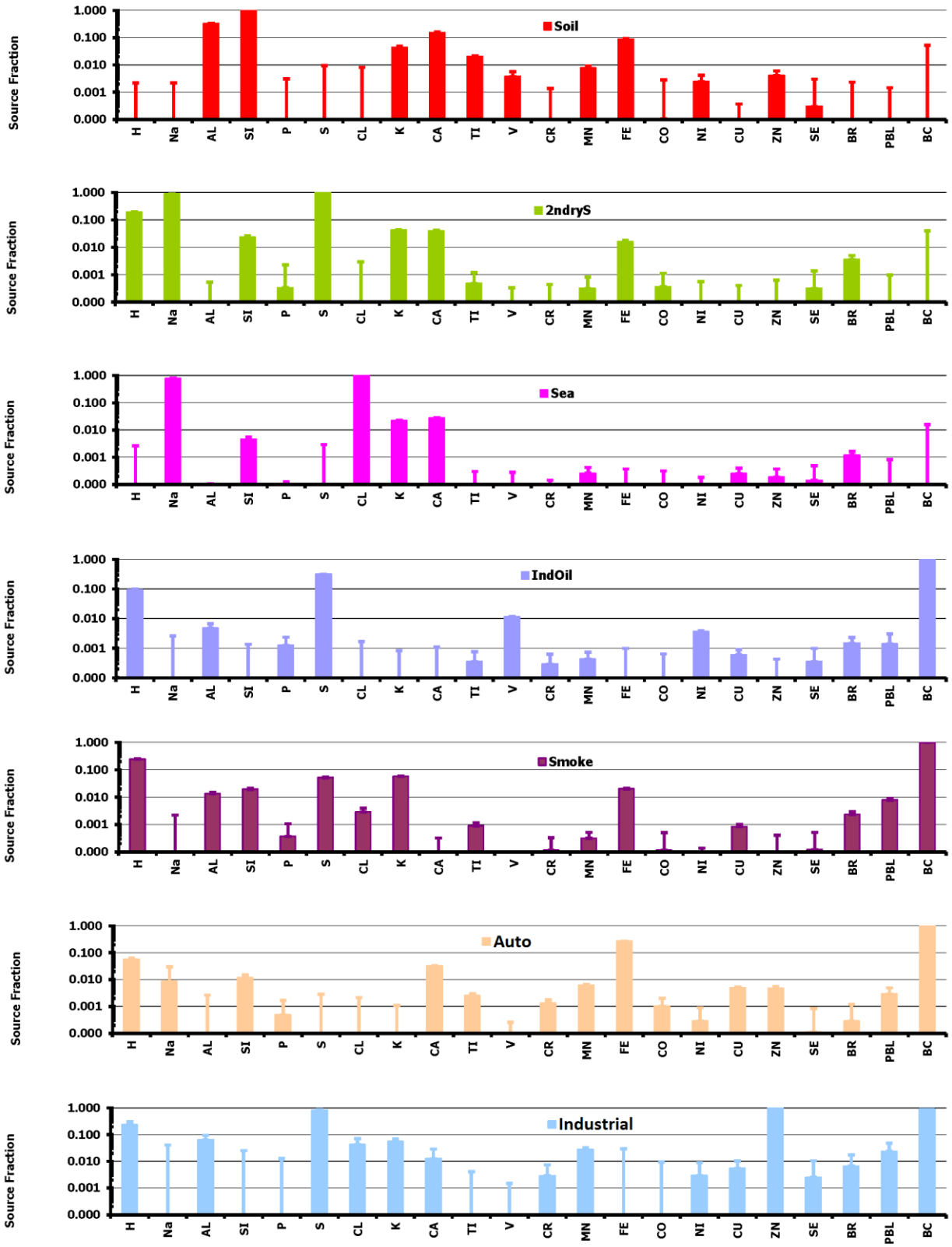

Figure 117: Fingerprints of ANSTO's seven-factor PMF for 2010–15 IBA and BC data showing the contribution of each species to the factor scaled to the largest factor contributing 1.00

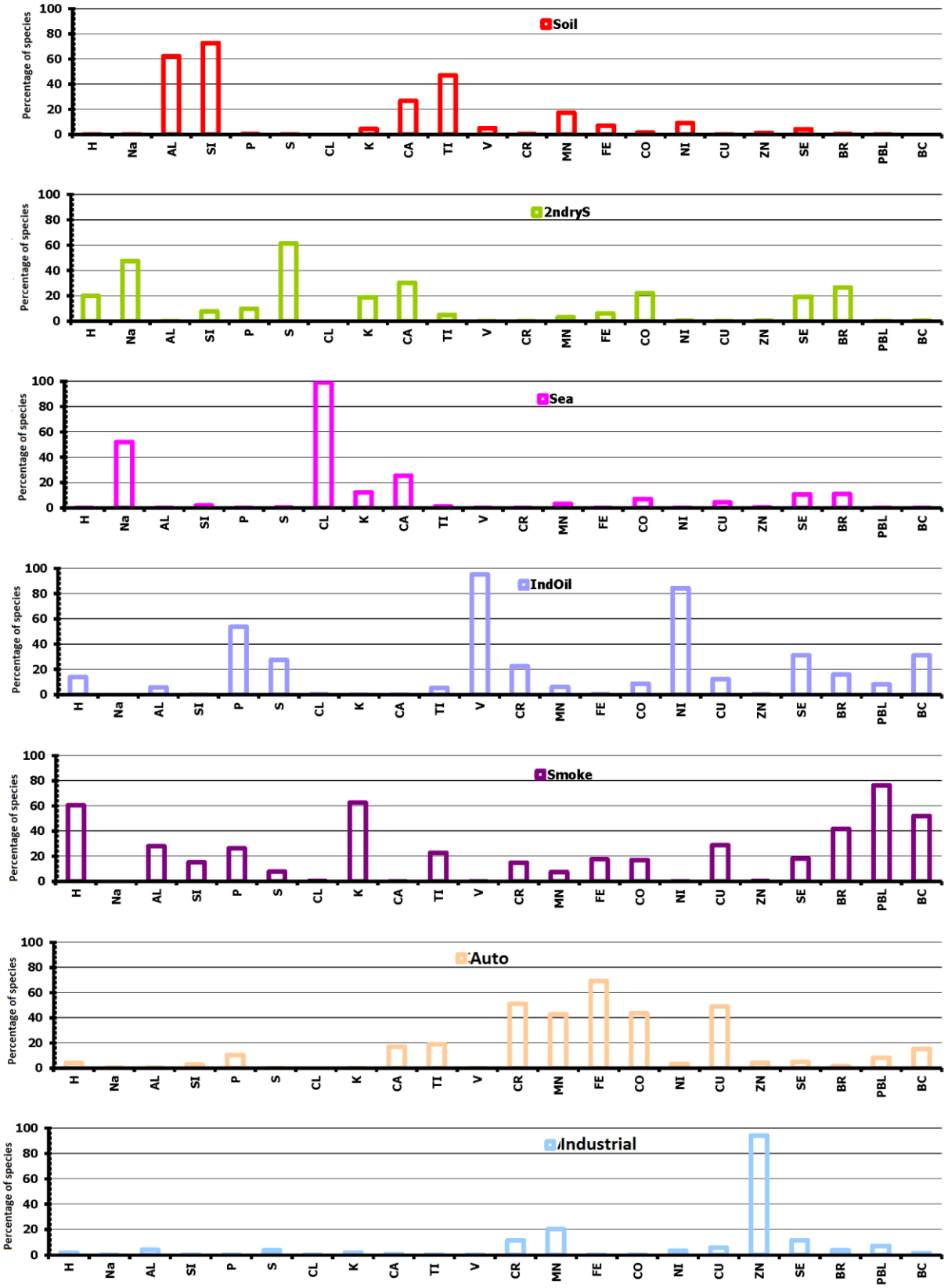

Figure 118: Percentage of each species in the factors in ANSTO's seven-factor PMF for 2010–15 IBA and BC data

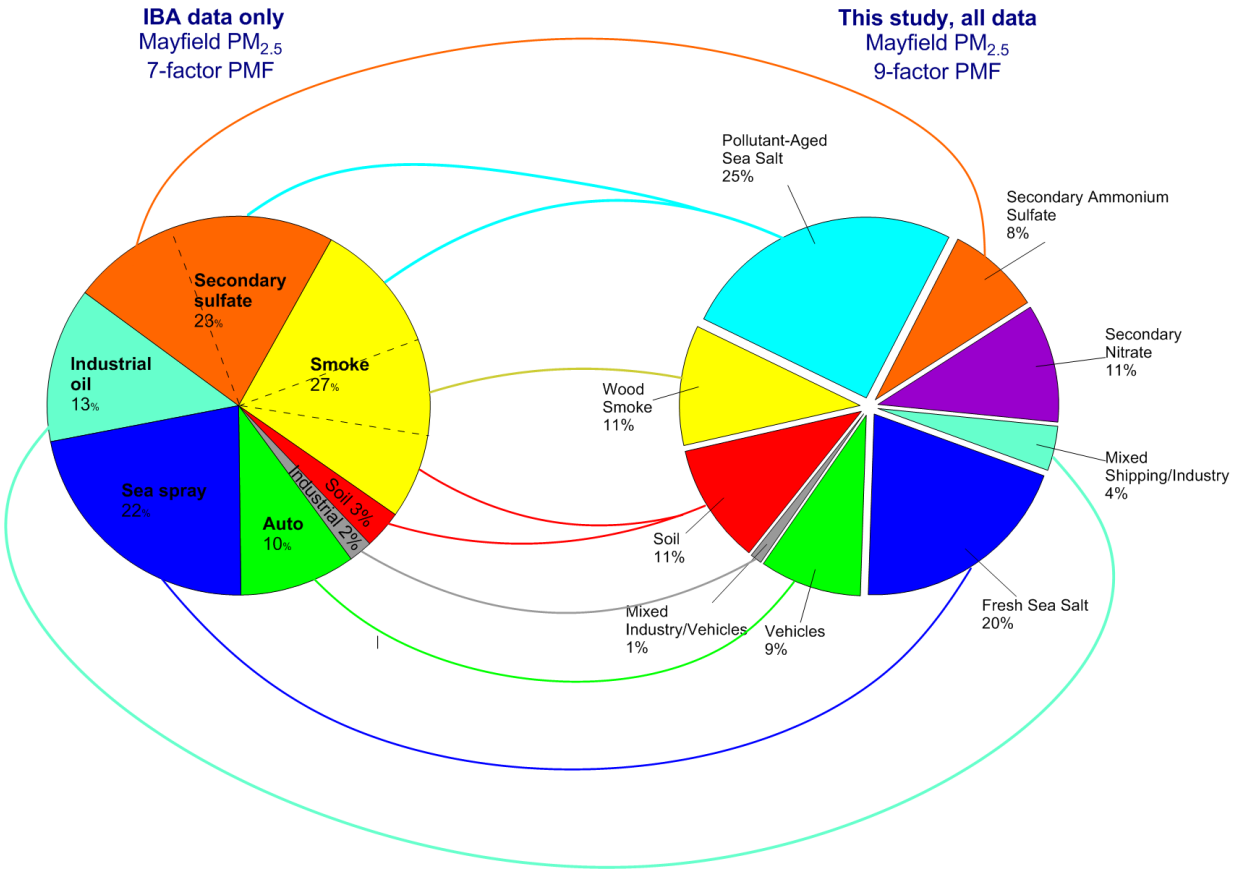

Figure 119: Comparison between (left) the analysis using only the IBA and BC data from the study period and (right) the PMF analysis presented in this report

Note that the same names on left and right do not mean that the species in the corresponding factors are the same. The lines connect the equivalent factors or indicate a possible way to explain the differences.

Figure 119 compares as pie charts (left) the ANSTO seven-factor solution using only the IBA and BC data and (right) the nine-factor PMF analysis presented in this report. It is important to note that use of the same name on the left and right does not mean that the composition of the factors is the same, in fact some are clearly different. The additional information in this study from the IC analysis on the concentration of especially nitrate, ammonium and levoglucosan, influences the PMF and the selection of factors so they are not directly comparable.

Notwithstanding this, there are some directly equivalent factors and the curved lines in Figure 119 connect these as well as indicating a possible way to connect the factors and parts of factors. For example, the additional data in this study on ammonium concentrations allows identification of the specific secondary inorganic aerosol ‘ammonium sulfate’ separately from the more generic secondary sulfate. The nitrate data allows identification of the secondary nitrate (sodium nitrate) as well as the primary source of ammonium nitrate at Stockton discussed in Section 11.5. The levoglucosan data separates out the wood smoke component of the more generic ‘smoke’ factor.

Further work is needed to contextualise the results from this one-year study within the longer term ongoing sampling and analysis at Mayfield and Stockton being undertaken by ANSTO, and to determine how the LHPCS can add value to further analysis at these sites.

11.7 Summary of results from supplementary modelling study

Chemical transport modelling was undertaken to predict aerosol components of fine particles ($PM_{2.5}$) for winter (July 2014) and spring (November 2014) case study periods, as outlined in Section 3.5. Predicted $PM_{2.5}$ component concentrations were compared to the measurements made at the four LHPCS sampling sites (Newcastle, Stockton, Mayfield and Beresfield) to assess model performance. The study method and findings are documented within the supplementary report (Emmerson et al. 2016), with a summary of the main findings presented in this section.

The model generally predicted the measured aerosol components of $PM_{2.5}$ particles reasonably well for the July 2014 case study period, but was unable to replicate the high ammonium nitrate aerosol measured at the Stockton site. The under-prediction of ammonium nitrate at Stockton is anticipated to be due to a local source of direct ammonium nitrate emissions not being represented in the emissions inventory used for the modelling. This source is likely to be the ammonium nitrate manufacturing plant located in close proximity to the Stockton site (refer to Section 11.5).

The spring case study was selected to model a period when onshore winds prevail, transporting sea salt inland. The model predicted the sea salt components well during the November 2014 case study, and also predicted the sulphate and nitrate aerosol concentrations. Organic matter was over-predicted due to the contribution of long-range transport of bushfire smoke from north-west Australia being overestimated.

Modelled spatial distributions of $PM_{2.5}$ for the lower Hunter region showed that the four sampling sites used in the LHPCS generally covered the range of modelled $PM_{2.5}$ and $PM_{2.5}$ component concentrations except for some localised sources of elemental carbon and organic matter.

The model results demonstrate the importance of sea salt transport within onshore airflow in the summer and continental-scale transport of sea salt during the winter in determining inland background concentrations in fine particles.

The measured $PM_{2.5}$ component information from the LHPCS is very useful to refine and validate chemical transport modelling for the region. This modelling in turn has enabled the projection of spatial trends in $PM_{2.5}$ component concentrations across the lower Hunter region, and the projection of $PM_{2.5}$ composition at sites for which measurements were not undertaken, as illustrated in the supplementary report for Maitland and Toronto.

12 Conclusions

The study provides detailed results on the composition and sources of fine ($PM_{2.5}$) and coarse ($PM_{2.5-10}$) particles in the lower Hunter during the one-year sampling program from March 2014 to February 2015.

A fairly consistent picture of the composition emerged for $PM_{2.5}$, as shown by the pie charts in Figure 120. These pie charts show the annual average contribution of the factors identified in the positive matrix factorisation analysis of the results. One major factor was only present at one site – ammonium nitrate at Stockton which contributed on average 19% of the $PM_{2.5}$ mass. This was identified to be very likely due to primary ammonium nitrate emissions from Orica's ammonium nitrate manufacturing facility on Kooragang Island. Emission reduction programs are currently being implemented at this facility (Orica 2014, 2015).

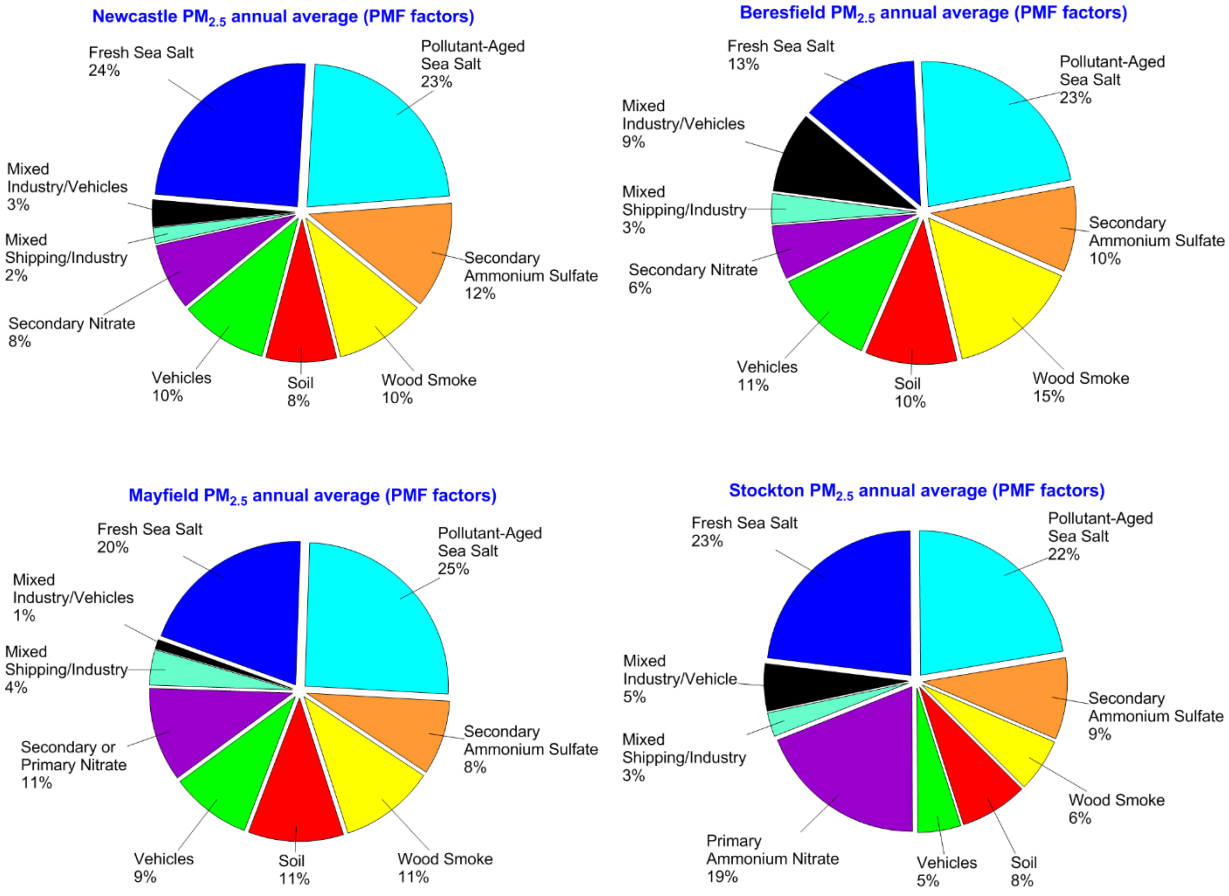

Figure 120: Pie charts of the percentage annual average factor contributions to $PM_{2.5}$ at the study sites.

Annual average $PM_{2.5}$ concentrations were 6.6 µg m^{-3} at Newcastle, 6.4 µg m^{-3} at Beresfield, 6.7 µg m^{-3} at Mayfield and 9.1 µg m^{-3} at Stockton.

The factors that contribute a similar percentage to $PM_{2.5}$ at all sites are:

- pollutant-aged sea salt (~23%)
- secondary ammonium sulfate (~10%)
- soil dust (~10%)
- mixed shipping/industry (~3%).

Those showing significant variations across the sites are:

- fresh sea salt: decreased from 24% at Newcastle to 13% at Beresfield; explained by increasing distance from the source of fresh sea salt, see Figure 55
- wood smoke: increased from 6% at Stockton to 15% at Beresfield; explained by more wind (better dispersion) at Stockton, poorer dispersion at Beresfield, as well as higher local wood smoke emissions at Beresfield than at Stockton
- vehicles: ~10% at three sites but only 5% at Stockton, which can be explained by less traffic in Stockton
- secondary nitrate: increased from 6% at Beresfield to 11% at Mayfield; at Stockton there was 19% of primary ammonium nitrate
- industry: increased from 1% at Mayfield to 9% at Beresfield; combining the contributions from primary and secondary nitrates and industry as generally being from industry, this 'industry' contribution was on average 13% at three of the sites and 24% at Stockton.

While noting the trends across sites listed above, the seasonal variation in the contributions of the various factors at Newcastle, Beresfield and Mayfield can be represented by the results for Mayfield in Figure 83 (repeated below; see also Figure 81 and Figure 82). The most significant features are:

- Fresh sea salt and pollutant-aged sea salt contribute most from October to February. This is due to the predominance of onshore flows during these months whereas during autumn and winter the winds are mostly from the north-west (offshore).
- Wood smoke and vehicles contribute most in the cool months of May to August. There are two reasons for this. One is the meteorology with lower inversion heights and poor dispersion leading to higher concentrations. A second is the higher emissions, such as more cold starts by vehicles, and wood smoke emissions mainly occur during the cooler months (although there were occasional bushfire emissions at other times during the LHPCS).
- Shipping contributes least during winter because most winds are offshore at this time of year.

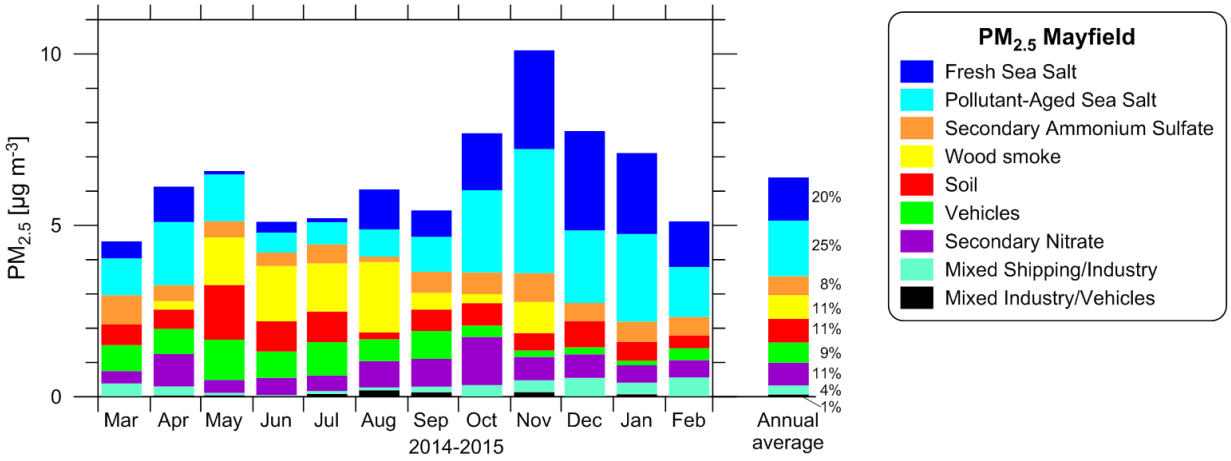

Figure 83: Monthly and annual factor contributions to $PM_{2.5}$ at Mayfield

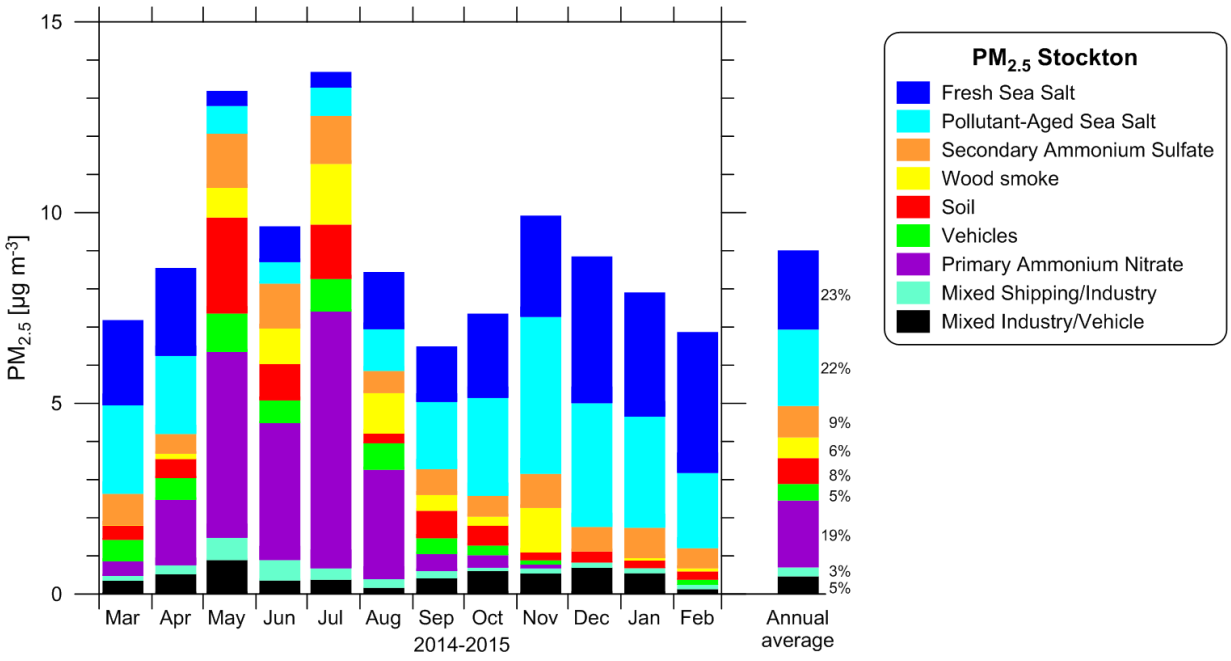

Figure 84: Monthly and annual factor contributions to $PM_{2.5}$ at Stockton

The seasonal $PM_{2.5}$ trends at Stockton are significantly different and are shown in Figure 84 (repeated above). The large contribution from ammonium nitrate of 19% as an annual average is concentrated from May to August making up 40% of the mass from May to July.

For $PM_{2.5\text{-}10}$, the differences between the two sites are more significant, not least because the annual average concentration at Stockton is 2½ times higher than at Mayfield with most of this due to the higher fresh sea salt contribution.

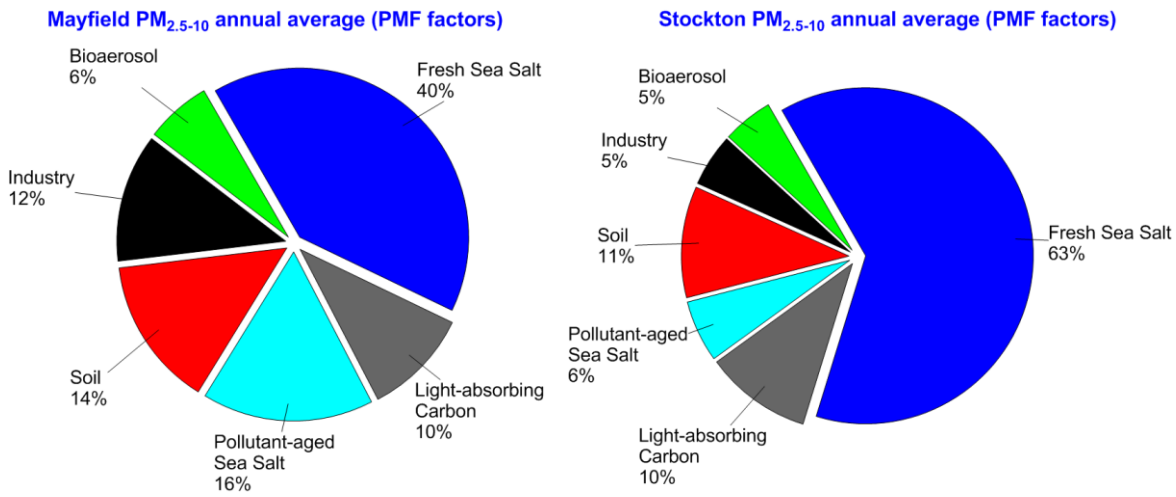

Figure 121: Pie charts of the percentage annual average factor contributions to $PM_{2.5-10}$ at the two study sites

Annual average $PM_{2.5-10}$ concentrations were 8.3 µg m^{-3} at Mayfield and 21.5 µg m^{-3} at Stockton.

Because of the large differences in total $PM_{2.5-10}$ concentrations, it is more useful when comparing the sites to consider the absolute contributions shown in Figure 91 (repeated below). The factors contributing approximately equally are:

- industry and pollutant-aged sea salt (together 2.4 µg m^{-3} at both sites).

Those with a larger contribution at Stockton are:

- fresh sea salt: 13.6 µg m-3 at Stockton vs 3.3 µg m-3 at Mayfield
- light-absorbing carbon: 2.2 µg m-3 at Stockton vs 0.8 µg m-3 at Mayfield
- soil: 2.3 µg m-3 at Stockton vs 1.2 µg m-3 at Mayfield
- bioaerosol: 1.1 µg m-3 at Stockton vs 0.5 µg m-3 at Mayfield.

The seasonal variations in the contributions to $PM_{2.5-10}$ are much larger than for $PM_{2.5}$, as shown for Mayfield in Figure 93 (repeated below). The pattern is similar at Stockton but with larger overall contributions.

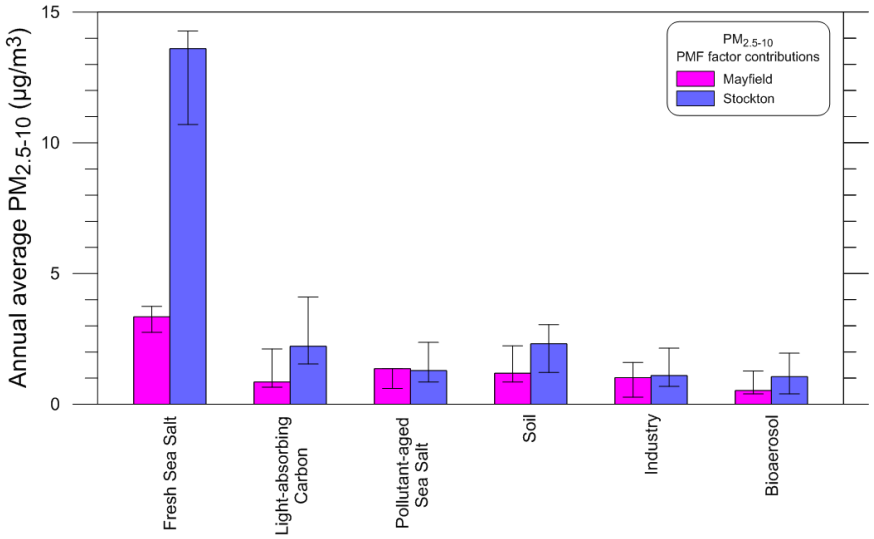

Figure 91: Comparison of the factor contributions at each site to annual average $PM_{2.5-10}$ mass

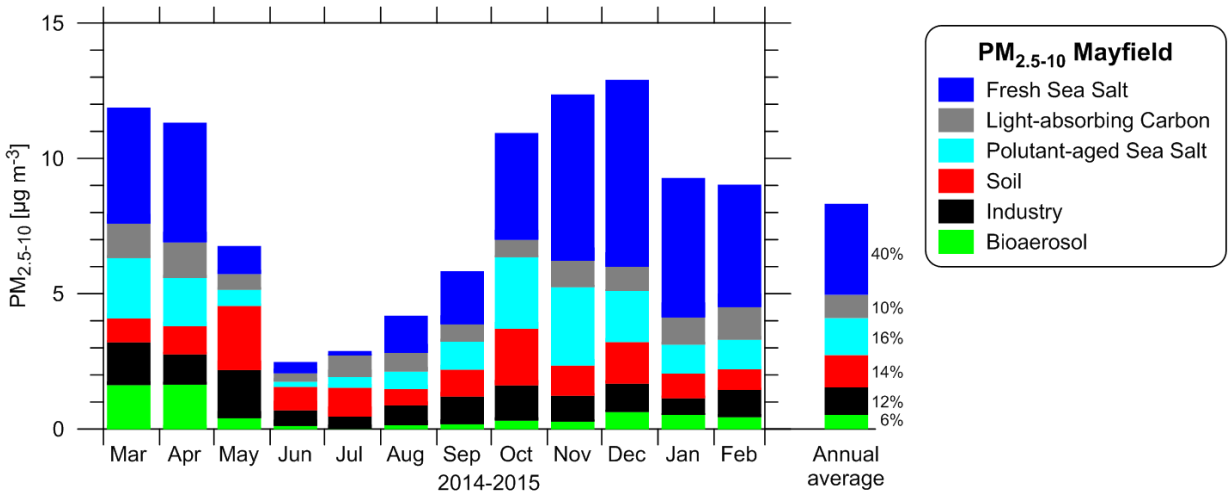

Figure 93: Monthly and annual factor contributions to $PM_{2.5-10}$ at Mayfield

Primary particles emitted directly from sources are estimated to account for about 50% of the annual $PM_{2.5}$ mass at Mayfield, Beresfield and Newcastle with secondary particles (particles formed by chemical reactions in the atmosphere and by gas-to-particle conversions) accounting for the balance. At Stockton there is about a 20% contribution from directly emitted ammonium nitrate (primary particles), so the primary:secondary split is 65:35. Most $PM_{2.5-10}$ particles are primary particles or physical combinations of primary emissions.

The PMF identifies secondary particle factors but does not provide a breakdown of the relative importance of sources to their formation. Based on a first approximation:

- emissions from human activities are estimated to account for 45–54% of the annual $PM_{2.5}$, and 15–22% of the annual $PM_{2.5-10}$
- emission from mixed human and natural sources for 30–36% of the annual $PM_{2.5}$ and 17–30% of the annual $PM_{2.5-10}$
- fresh sea salt for 13–24% of the annual $PM_{2.5}$, and 46–68% of the annual $PM_{2.5-10}$ across the study sites.

Sources associated with human activities which potentially contribute to the factors identified in the study include industrial and commercial sources, vehicles, wood heating, bushfires/hazard reduction burns, non-road diesel equipment and transport (including diesel-electric locomotives), shipping and agriculture as shown in the summary tables for $PM_{2.5}$ and PM_{10}.

In some cases the study identified mixed source factors and secondary particle factors where further evidence is needed to assess the contributions of individual types of sources. Chemical transport modelling accounts for processes associated with the formation of secondary particles and can be used to refine these estimates. Such modelling can confirm the contribution of emissions from human activities to sulfate and nitrate and determine their contribution to the pollutant-aged sea salt and soil factors. Such modelling can also be used to assess inter-regional transport of pollution, spatially localised source contributions and determine how reducing specific sources may affects total PM concentrations.

Black carbon was found through the species analysis of the components of $PM_{2.5-10}$ to account for about 10% of the coarse particle mass at Mayfield and Stockton. Coal particles are conjectured to contribute to this factor. Further analysis is needed to identify whether coal particles could account for the light-absorbing carbon in this factor.

Additional samples were collected after completion of the sampling period for this study for analysis using an optical particle analysis technique to identify whether coal particles could account for the light-absorbing carbon in this factor. The results of this work will be reported separately.

The findings of the LHPCS provide the region's communities and the NSW Government with new information about the chemical composition of fine and coarse particles and insight into sources contributing to particle pollution in the region. Longer term exposure to $PM_{2.5}$ has a larger health effect than short-term exposures and exposures to coarse particles, indicating that strategies that provide long-term reductions in fine particle pollution are likely to produce the greatest health benefit (EPA 2013; US EPA 2011; WHO 2013). Assessing source contributions to average $PM_{2.5}$ concentrations therefore represented a focus of the study. The study also addressed coarse particles in the vicinity of the port to inform assessments of the potential impacts of such particles on the health and well-being of local residents.

Study findings also provide information on sources contributing to periods of elevated particle concentrations at specific sites. At Stockton, by example, sea salt contributed significantly to fine and coarse particles during the spring and summer when onshore winds prevailed with notable contributions of ammonium nitrate to fine particle concentrations during the late autumn and winter.

The results from this research add to the evidence base that the NSW Government relies on to inform policies and programs to improve air quality, public health and the community's understanding of air quality issues in the lower Hunter region.

References

ABS 2015, *3218.0 Regional Population Growth, Australia*, released 31 March 2015, Australian Bureau of Statistics.

AECOM 2009, *Proposed Ammonium Nitrate Facility Expansion, Environmental Assessment, Proposed Ammonium Nitrate Facility Expansion, Greenleaf Road, Kooragang Island, Volume 1 – Main Report*, Report prepared by AECOM for Orica Australia Pty Ltd.

AMC 2013, *Ship Engine Exhaust Emissions and Fuel Consumption in Australian Waters including Ports, Stage 1, 2010/11 Emissions Inventory, Estimations Based on Terrestrial AIS Data, Mapping of Spatial Distribution of Emissions*, Australian Maritime College, University of Tasmania, Launceston.

Bae M-S, Demerjian KL & Schwab JJ 2006, Seasonal estimation of organic mass to organic carbon in $PM_{2.5}$ at rural and urban locations in New York State, *Atmos. Environ*. 40, 7467–7479.

Bauer H, Claeys M, Vermeylen R, Schueller E, Weinke G, Berger A & Puxbaum H 2008, Arabitol and mannitol as tracers for the quantification of airborne fungal spores, *Atmos. Environ.* 42, 588–593.

Behera SN, Sharma M, Aneja VP & Balasubramanian R 2013, Ammonia in the atmosphere: a review on emission sources, atmospheric chemistry and deposition on terrestrial bodies, *Environ. Sci. Pollut. Res.* 20, 8092–8131.

Carlton AG, Turpin BJ, Altieri KE, Seitzinger S, Reff A, Lim H-J & Ervens B 2007, Atmospheric oxalic acid and SOA production from glyoxal: Results of aqueous photooxidation experiments, *Atmos. Environ*. 41, 7588–7602.

Chan YC, Cohen DD, Hawas O, Stelcer E, Simpson R, Denison L, Wong N, Hodge M, Comino E & Carswell S 2008, Apportionment of sources of fine and coarse particles in four major Australian cities by positive matrix factorisation, *Atmospheric Environment* 42(2), 374–389.

Cheung KL, Ntziachristos L, Tzamkiozis T, Schauer JJ, Samaras Z, Moore KF & Sioutas C 2010, Emissions of Particulate Trace Elements, Metals and Organic Species from Gasoline, Diesel, and Biodiesel Passenger Vehicles and Their Relation to Oxidative Potential, *Aerosol Science and Technology* 44(7), 500–513.

Chow JC, Watson JG, Chen LWA, Chang MCO, Robinson NF, Trimble D & Kohl S 2007, The IMPROVE-A temperature protocol for thermal/optical carbon analysis: maintaining consistency with a long-term database, *Journal of the Air & Waste Management Association* 57(9), 1014–1023.

Chow JC, Yang XF, Wang XL, Kohl SD & Watson JG 2015, Characterization of ambient PM_{10} bioaerosols in a California agricultural town, *Aerosol & Air Qual. Res.* 15, 1433–1447.

Cohen DD 1993, Applications of simultaneous IBA techniques to aerosol analysis, *Nuclear instruments & methods in physics research, Section B, Beam interactions with materials and atoms* 79(1-4), 385–388.

Cohen DD 1996, Elemental analysis by PIXE and other IBA techniques and their application to source fingerprinting of atmospheric fine particle pollution, *Nuclear instruments & methods in physics research, Section B, Beam interactions with materials and atoms* 109–110, 218–226.

Cohen DD 1998, Characterisation of atmospheric fine particles using IBA techniques, *Nuclear instruments & methods in physics research, Section B, Beam interactions with materials and atoms* 136–138: 14–22.

Cohen DD, Bailey GM & Kondepudi R 1996, Elemental analysis by PIXE and other IBA techniques and their application to source fingerprinting of atmospheric fine particle pollution, *Nuclear Instruments and Methods in Physics Research, Section B, Beam Interactions with Materials and Atoms*, 109–110, 218–226.

Cohen DD, Crawford J, Stelcer E & Antanacio AJ 2012, Application of positive matrix factorisation, multi-linear engine and back trajectory techniques to the quantification on coal-fired power station pollution in metropolitan Sydney, *Atmospheric Environment* 61, 204–2011.

Cohen DD, Taha G, Stelcer E, Garton D & Box G 2000, The measurement and sources of fine particle elemental carbon at several key sites in NSW over the past eight years, *13th Internat. Clean Air & Environ. Conf*. 27–30 November, 485–490.

Cohen DD, Garton D, Stelcer E, Hawas O, Wang T, Poon S, Kim J, Choi BC, Oh SN, Shin H-J, Young Ko M & Uematsu M 2004, Multielemental analysis and characterization of fine aerosols at several key ACE-Asia sites, *Journal of Geophysical Research*, 109, D19S12.

Cohen DD, Gulson BL, Davis JM, Stelcer E, Garton D, Hawas O & Taylor A 2005, Fine-particle Mn and other metals linked to the introduction of MMT into gasoline in Sydney, Australia: Results of a natural experiment, *Atmos. Environ*. 39, 6885–6896.

Cohen DD, Stelcer E, Garton D & Crawford J 2011, Fine particle characterisation, source apportionment and long-range dust transport into the Sydney Basin: a long term study between 1998 and 2009, *Atmospheric Pollution Research* 2(2), 182–189.

Cohen DD, Crawford J, Stelcer E & Atanacio AJ 2012, Application of positive matrix factorization, multi-linear engine and back trajectory techniques to the quantification of coal-fired power station pollution in metropolitan Sydney, *Atmospheric Environment* 61, 204–211.

Cope ME & Ischtwan J 1996, Airshed Modelling component from the *Metropolitan Air Quality Study* (MAQS), Environment Protection Authority, Victoria.

Cope M Cope ME, Keywood M, Emmerson K, Galbally I, Boast K, Chambers S, Cheng M, Crumeyrolle S, Dunne E, Fedele R, Gillett R, Griffiths A, Harnwell J, Katzfey J, Hess D, Lawson S, Mijevic B, Molloy S, Powell J, Reisen F, Ristovski Z, Selleck P, Ward J, Zhang C and Zeng J 2014, *Sydney Particle Study – Stage-II*, Study undertaken by the Centre for Australian Weather and Climate Research (CAWCR) on behalf of the NSW Office of Environment and Heritage, June 2014.

Cope ME, Hess GD, Lee S, Tory K, Azzi M, Carras J, Lilley W, Manins PC, Nelson P, Ng L, Puri K, Wong N, Walsh S & Young M 2004, The Australian Air Quality Forecasting System. Part I: Project description and early outcomes, *J. Appl. Meteorol*. 43, 649–662, Doi 10.1175/2093.1.

Despres VR, Huffman JA, Burrows SM, Hoose C, Safatov AS, Buryak G, Frohlich-Nowoisky J, Elbert W, Andreae MO, Poschl U & Jaenicke R 2012, Primary biological aerosol particles in the atmosphere: a review, *Tellus B: Chemical and Physical Meteorology*, 64, 15598, DOI: 10.3402/tellusb.v64i0.15598.

DNV 2015, *NSW Ship Emissions Study, Emissions from ships operating in the Greater Metropolitan Area*, Report for NSW Environment Protection Authority, Det Norske Veritas (Australia) Pty Ltd, www.epa.nsw.gov.au/resources/air/gma-ship-emissions.pdf.

Draxler RR & Rolph GD 2015, HYSPLIT, Hybrid Single Particle Lagrangian Integrated Trajectory Model, access via NOAA ARL READY website, http://ready.arl.noaa.gov/HYSPLIT.php, NOAA Air Resources Laboratory, Silver Spring, MD.

EEA 2013, *Status of black carbon monitoring in ambient air in Europe*, Technical report No. 18/2013, European Environment Agency, www.eea.europa.eu/publications/status-of-black-carbon-monitoring.

Environ 2012, *Port Waratah Coal Services Terminal 4 Environmental Assessment Appendix M – Air Quality Assessment for the Terminal 4 Project,* http://majorprojects.planning.nsw.gov.au/index.pl?action=view_job&job_id=4399

Emmerson KM, Cope ME, Hibberd MF, Selleck PW & Thatcher M 2016, *Lower Hunter Particle Characterisation Study Supplementary Report – Chemical Transport Modelling Case Studies*, Report to NSW Office of Environment and Heritage, CSIRO, Australia.

EPA 1999, *Environmental Guidelines for Selecting, Installing and Operating Domestic Solid Fuel Heaters*, NSW Environment Protection Authority, Sydney, www.epa.nsw.gov.au/resources/woodsmoke/woodguide.pdf.

EPA 2012, *Air Emissions Inventory for the Greater Metropolitan Region in New South Wales: 2008 Calendar Year*, NSW Environment Protection Authority, Sydney, www.epa.nsw.gov.au/air/airinventory2008.htm.

EPA 2013, *Managing particles and improving air quality in NSW*, NSW Environment Protection Authority, Sydney, www.epa.nsw.gov.au/resources/air/130784AirPartStr.pdf.

EPA 2015, Environment Protection Licence No. 828 (Orica Australia Pty Ltd), version dated 23 September 2015, NSW Environment Protection Authority, Sydney.

Fujita EM, Campbell DE, Arnott WP, Chow JC & Zielinska B 2007, Evaluations of the chemical mass balance method for determining contributions of gasoline and diesel exhaust to ambient carbonaceous aerosols, *J. Air Waste Manag. Assoc.* 57, 721–740.

Gaskin S, Taylor M, Bentham R & Pisaniello D 2012, *Understanding and managing risks associated with fungal contamination in indoor environments*, University of Adelaide, www.adelaide.edu.au/oeh/research/fungal.pdf.

Goldsworthy L & Goldsworthy B 2015, Modelling of ship engine exhaust emissions in ports and extensive coastal waters based on terrestrial AIS data – An Australian case study, *Environmental Modelling & Software* 63, doi:10.1016/j.envsoft.2014.09.009

Goncalves C, Alves C, Evtyugina M, Mirante F, Pio C, Caseiro A, Schmidl C, Bauer H & Carvalho F 2010, Characterisation of PM_{10} emissions from woodstove combustion of common woods grown in Portugal, *Atmospheric Environment* 44(35), 4474–4480.

Gupta D, Kim H, Park G, Li X, Eom HJ & Ro CU 2015, Hygroscopic properties of NaCl and $NaNO_3$ mixture particles as reacted inorganic sea-salt aerosol surrogates, *Atmos. Chem. Phys.* 15, 3379–3393.

Hibberd M, Selleck P, Keywood M, Cohen D, Stelcer E & Atanacio A 2013, *Upper Hunter Fine Particle Characterisation Study*, Final report, prepared for the NSW Office of Environment and Heritage and the NSW Department of Health, www.environment.nsw.gov.au/aqms/uhaqmnfpcs.htm.

Hopke PK, Xie Y, Raunemaa T, Biegalski S, Landsberger S, Maenhaut W, Artaxo P & Cohen D 1997, Characterization of the Gent stacked filter unit PM_{10} sampler, *Aerosol Science and Technology*, 27, 726–735.

Iinuma Y, Brüggemann E, Gnauk T, Müller K, Andreae MO, Helas G, Parmar R & Herrmann H 2007, Source characterization of biomass burning particles: The combustion of selected European conifers, African hardwood, savanna grass, and German and Indonesian peat, *Journal of Geophysical Research: Atmospheres* 112(D8), D08209.

John W & Reischl G 1980, A cyclone for size-selective sampling of ambient air, *JAPCA* 30, 872–876.

John W, Hering SV, Reischl G, Sasaki GV & Goren S 1983, Anomalous filtration of solid particles by Nuclepore filters, *Atmos. Environ*. 17, 373–373.

Joly A, Lambert J, Gagnon C, Kennedy G, Mergler D, Adam-Poupart A & Zayed J 2011, Reduced Atmospheric Manganese in Montreal Following Removal of Methylcyclopentadienyl Manganese Tricarbonyl (MMT), *Water Air and Soil Pollution* 219(1-4), 263–270.

Kim E & Hopke PK 2004, Comparison between conditional probability function and nonparametric regression for fine particle source directions, *Atmospheric Environment* 38(28), 4667–4673.

Kristensen LJ, Taylor MP, Odigie KO, Hibdon SA & Flegal AR 2014, Lead isotopic compositions of ash sourced from Australian bushfires, *Environ. Pollution* 190, 159–165.

Lide DR (Ed.) 1997, *CRC Handbook of Chemistry and Physics*, 78th edition, CRC Press, Boca Raton, FL, USA.

Malm WC, Sisler JF, Huffman D, Eldred RA & Cahill TA 1994, Spatial and seasonal trends in particle concentration and optical extinction in the United-States, *Journal of Geophysical Research-Atmospheres* 99(D1), 1347–1370.

McInnes LM, Quinn PK, Covert DS & Anderson TL 1996, Gravimetric analysis, ionic composition, and associated water mass of the marine aerosol, *Atmos. Environ*. 30, 869–884.

Millero FJ, Feistel R, Wright DG & McDougall TJ 2008, The composition of Standard Seawater and the definition of the Reference-Composition Salinity Scale, *Deep-Sea Research* 55, 50–72.

Nelson PF, Azzi M, Cope M, Lilley W, Carras JN, Hurley PJ & Hyde R 2002, *Interregional Transport of Air Pollutants Study* (IRTAPS), CSIRO Energy Technology, NSW.

NICNAS 2003, *Methylcyclopentadienyl Manganese Tricarbonyl (MMT): Priority Existing Chemical Assessment Report No. 24*, Commonwealth of Australia.

Norris G & Duvall R 2014, *EPA Positive Matrix Factorization (PMF) 5.0 Fundamentals and User Guide*, US Environmental Protection Agency, Office of Research and Development, EPA/600/R-14/108.

NPI 2014, *National Pollutant Inventory*, www.npi.gov.au.

OEH 2012, *Lower Hunter Ambient Air Quality Review of Available Data*, Office of Environment and Heritage, Sydney, www.environment.nsw.gov.au/resources/NCCCE/120281LHunterAirMonitoring.pdf.

OEH 2014, *New South Wales Air Quality Statement 2013*, Office of Environment and Heritage, Sydney, www.environment.nsw.gov.au/aqms/140057nswairqual13.htm.

OEH 2015, *New South Wales Air Quality Statement 2014*, Office of Environment and Heritage, Sydney, www.environment.nsw.gov.au/aqms/150004nswairqual14.htm.

Orica Australia Pty Ltd 2014, Orica Kooragang Island Annual Environmental Management Report, December 2014, www.orica.com/ArticleDocuments/493/Annual%20Environmental%20Management%20Report_December%202014_Final.pdf.aspx.

Orica Australia Pty Ltd 2015, Testing to begin on new flaring systems, media release, www.orica.com/locations/asia-pacific/australia/kooragang-island/news---media/testing-to-begin-on-new-flaring-systems#.VmlbdoY8bCQ.

Orica Australia Pty Ltd 2016, AN1 Prill Tower Particle Minimisation Program, brief summary of program progress provided to Office of Environment and Heritage on 5 February 2016.

Paatero P 1997, Least squares formulation of robust non-negative factor analysis, *Chemometrics and Intelligent Laboratory Systems* 37(1), 23–35.

Paatero P, Eberly S, Brown SG & Norris GA 2014, Methods for estimating uncertainty in factor analytic solutions, *Atmos. Meas. Tech*. 7, 781–797.

Petzold A, Ogren JA, Fiebig M, Laj P, Li S-M, Baltensperger U, Holzer-Popp T, Kinne S, Pappalardo G, Sugimoto N, Wehrli C, Wiedensohler A & Zhang X-Y 2013, Recommendations for reporting 'black carbon' measurements, *Atmos. Chem. Phys*. 13, 8365–8379, doi:10.5194/acp-13-8365-2013.

Radhi M, Box MA, Box GP, Mitchell RM, Cohen DD, Stelcer E & Keywood MD 2010, Optical, physical and chemical characteristics of Australian continental aerosols: results from a field experiment, *Atmos. Chem. Phys.* 10, 5925–5942.

Rinaldi M, Decesari S, Finessi E et al. 2010, Primary and Secondary Organic Marine Aerosol and Oceanic Biological Activity: Recent Results and New Perspectives for Future Studies, *Advances in Meteorology*, Article ID 310682, 10 pp, doi:10.1155/2010/310682.

Russell LM 2003, Aerosol organic-mass-to-organic-carbon ratio measurements, *Environmental Science & Technology* 37(13), 2982–2987.

Santoso M, Hopke PK, Hidayat A & Dwiana DL 2008, Source identification of the atmospheric aerosol at urban and suburban sites in Indonesia by positive matrix factorization, *Science of the Total Environment*, 397(1-3), 229–37.

Seinfeld JH & Pandis SN 2006, *Atmospheric chemistry and physics: from air pollution to climate change*, 2nd edition, Wiley, 1232 pp.

Skamarock WC and co-authors 2008, A description of the advanced research WRF version 3, *NCAR Tech Note NCAR/TN-475+STR*, 125 pp.

Stelcer E, Cohen DD & Atanacio AJ 2014, Long term $PM_{2.5}$ trends in the Australian industrial city of Newcastle: a 15-year study from 1998 to 2013, *Environ. Chem.* 11, 644–652.

Taha G, Box GP, Cohen DD & Stelcer E 2007, Black carbon measurement using laser integrating plate method, *Aerosol Science and Technology* 41(3), 266–276.

US EPA 1995, AP 42, Fifth Edition Compilation of Air Pollutant Emission Factors, Volume 1: Stationary Point and Area Sources, Chapter 8 Inorganic Chemical Industry, Section 8.3 Ammonium Nitrate, Research Triangle Park, United States Environmental Protection Agency, North Carolina, http://www3.epa.gov/ttnchie1/ap42/.

US EPA 2009, *Integrated Science Assessment for Particulate Matter*, United States Environmental Protection Agency National Center for Environmental Assessment – RTP Division, North Carolina.

US EPA 2011, Policy Assessment for the Review of the Particulate Matter National Ambient Air Quality Standards, United States Environmental Protection Agency, EPA 452/R-11-003, Washington DC, USA.

US EPA 2012, Report to Congress on Black Carbon, Appendix 1: Ambient and Emissions Measurements of Black Carbon, United States Environmental Protection Agency.

Viana M, Amato F, Alastuey A, Querol X, Moreno T, Garcìa Dos Santos S, Herce MD & Fernaìndez-Patier R 2009, Chemical Tracers of Particulate Emissions from Commercial Shipping, *Environ. Sci. Technol*., 43, 7472–7477, doi:10.1021/es901558t.

Viana M, Hammingh P, Colette A, Querol X, Degraeuwe B, de Vlieger I & van Aardenne J 2014, Impact of maritime transport emissions on coastal air quality in Europe, *Atmospheric Environment* 90, 96–105, doi:10.1016/j.atmosenv.2014.03.046.

Visser S, Slowik JG, Furger M et al. 2015, Advanced source apportionment of size-resolved trace elements at multiple sites in London during winter, *Atmos. Chem. Phys.* 15, 11291–11309, doi:10.5194/acp-15-11291-2015.

Warneck P 2003, In-cloud chemistry opens pathway to the formation of oxalic acid in the marine atmosphere, *Atmospheric Environment* 37, 2423–2427.

Watson JG, Chow JC, Lowenthal DH, Pritchett LC, Frazier CA, Neuroth GR & Robbins R 1994, Differences in the carbon composition of source profiles for diesel-powered and gasoline-powered vehicles, *Atmospheric Environment* 28, 2493–2505.

WHO 2013, *Review of evidence on health aspects of air pollution – REVIHAAP Project*, WHO European Centre for Environmental and Health, Bonn.

Yu JZ, Huang XF, Xu JH & Hu M 2005, When aerosol sulfate goes up, so does oxalate: Implication for the formation mechanisms of oxalate, *Environ. Sci. Technol*. 39, 128–133.

List of tables

Table S1: Summary of PMF factors for $PM_{2.5}$ listing main species, contributions and potential sources xx

Table S2: Summary of PMF factors for $PM_{2.5-10}$ listing main species present, contributions and potential sources xxi

Table 1: LHPCS monitoring sites, equipment, filter types and sampling schedule 8

Table 2: Key statistics of the 2013 and 2014 PM_{10} and $PM_{2.5}$ OEH monitoring results. 20

Table 3: Overall annual sample collection rate for the one-year study 23

Table 4: Species excluded from the PMF analysis 53

Table 5: Species included in PMF analysis of $PM_{2.5}$ data listing PMF category, and the median concentration and signal-to-noise ratio calculated by EPA PMF at each site 54

Table 6: Species included in PMF analysis of $PM_{2.5-10}$ data listing PMF category, and the median concentration and signal-to-noise ratio calculated by EPA PMF at each site 55

Table 7: Comparison of the constituents of the fresh sea salt factor with standard sea water (Millero et al. 2008) 67

Table 8: Comparison of constituents of Factor 2 with standard sea water 71

Table 9: Analysis of possible contribution of bushfire/hazard reduction burning to the wood smoke factor 79

Table 10: Comparison of the constituents of the soil factor with crustal composition (Lide 1997) and some typical Australian dust (Radhi et al. 2010) 82

Table 11: Ratios of key species in the industry/vehicle factor 85

Table 12: Ratios of key species in Factor 7 for all sites except Stockton 89

Table 13: Ratios of key species at Stockton (ammonium nitrate) 90

Table 14: Ratios of key species in the mixed shipping/industry factor 94

Table 15: Summary of PMF factors for $PM_{2.5}$ listing main species present, contributions of these factors at each site, and potential sources 99

Table 16: Comparison of the constituents of the $PM_{2.5-10}$ fresh sea salt factor with standard sea water 107

Table 17: Comparison of constituents of $PM_{2.5-10}$ Factor 2 with standard sea water ... 109

Table 18: Comparison of constituents of $PM_{2.5-10}$ Factor 3 with standard sea water ... 111

Table 19: Comparison of the constituents of the $PM_{2.5-10}$ soil factor with crustal composition (Lide 1997) and some typical Australian dust (Radhi et al. 2010) . 113

Table 20: Comparison of constituents of $PM_{2.5-10}$ Factor 6 with standard sea water and with $PM_{2.5-10}$ pollutant-aged sea salt Factor 3 at Mayfield 117

Table 21: Summary of PMF factors for $PM_{2.5-10}$ 118

List of figures

Figure S1: Sampling sites for Lower Hunter Particle Characterisation Study xvi

Figure S2: Percentage annual average contributions to total $PM_{2.5}$ mass at the four study sites during the study xix

Figure S3: Percentage annual average contributions to total $PM_{2.5\text{-}10}$ mass at Mayfield and Stockton during the study xxi

Figure S4: Monthly and annual factor contributions to $PM_{2.5}$ at the four study sites ... xxiii

Figure S5: Monthly and annual factor contributions to $PM_{2.5\text{-}10}$ at Mayfield and Stockton xxiv

Figure 1: The lower Hunter region of New South Wales 2

Figure 2: 24-hour average $PM_{2.5}$ and PM_{10} concentrations measured at Lower Hunter and Newcastle Local AQMN stations (maximum, minimum, median, 90th and 10th percentile) 3

Figure 3: The Lower Hunter Air Quality Monitoring Network and Newcastle Local Air Quality Monitoring Network 4

Figure 4: Spatial distribution of primary $PM_{2.5}$ emissions for the 2008 calendar year 5

Figure 5: Spatial distribution of primary PM_{10} emissions for the 2008 calendar year 5

Figure 6: Sampling sites for the Lower Hunter Particle Characterisation Study 7

Figure 7: Newcastle Air Quality Monitoring Station during the site visit from the project team 10

Figure 8: A 360° panorama from the roof of the Newcastle Air Quality Monitoring Station located next to an athletics field (vertically stretched to aid identification of features) 10

Figure 9: Beresfield Air Quality Monitoring Station located adjacent to Francis Greenway High School 11

Figure 10: A 360° panorama from the roof of the Beresfield Air Quality Monitoring Station (vertically stretched to aid identification of features) 11

Figure 11: The location of the Beresfield site with respect to the railway line (indicated by dashed black line) 11

Figure 12: Mayfield Air Quality Monitoring Station located in the grounds of the CSIRO Energy Park 12

Figure 13: A 270° panorama in the vicinity of the Mayfield Air Quality Monitoring Station 12

Figure 14: View from the Stockton Air Quality Monitoring Station looking west, across the river to Kooragang Island 13

Figure 15: A 360° panorama from the roof of the Stockton Air Quality Monitoring Station (vertically stretched to aid identification of features; residences are located to the east and south of the site) 13

Figure 16: ASP samplers (Teflon filters on left and quartz filters on right) installed at the OEH Newcastle Air Quality Monitoring Station 15

Figure 17: Details of the ASP Sampler at the Newcastle site being inspected by David Cohen 15

Figure 18: Identification of ASP and GENT samplers and inlets of OEH's continuous particle monitoring instruments on the roof of the Stockton Air Quality Monitoring Station....16

Figure 19: Details of the GENT sampler at the Stockton site being inspected by Peter Crabbe....16

Figure 20: Long-term (Oct 2012 – Oct 2015) time series of 24-hour average PM_{10} (TEOM) concentrations recorded at the OEH lower Hunter monitoring stations....18

Figure 21: Long-term (Oct 2012 – Oct 2015) time series of 24-hour average $PM_{2.5}$ (BAM) concentrations recorded at the OEH lower Hunter monitoring stations....19

Figure 22: Long-term time series of $PM_{2.5}/PM_{10}$ ratio (31-day running average) recorded at OEH and Newcastle local air quality monitoring stations (Oct 2012 – Oct 2015)....20

Figure 23: Time series of 24-hour average $PM_{2.5}$ concentrations measured at the Newcastle, Beresfield, Mayfield and Stockton sites using the standard BAM equipment....21

Figure 24: Time series of 24-hour average PM_{10} concentrations measured at the Newcastle, Beresfield, Mayfield, and Stockton sites using the standard TEOM equipment....22

Figure 25: Annual wind roses from the study sites including data from the sample days only....23

Figure 26: Seasonal wind roses from the Beresfield site (including wind data from the study sample days only)....24

Figure 27: Seasonal wind roses from the Newcastle site (including wind data from the study sample days only)....25

Figure 28: Seasonal wind roses from the Mayfield site (including wind data from the sample days only; data available for the second half of the study period only)....26

Figure 29: Seasonal wind roses from the Stockton site (including wind data from the sample days only)....26

Figure 30: Comparison of rainfall recorded during the study period (March 2014 to February 2015) with rainfall statistics for the January 2001 to December 2015 period, as recorded at the Bureau of Meteorology's Newcastle University station28

Figure 31: PM_{10} pollution roses for $PM_{10} > 20$ µg m^{-3} for the study period at Newcastle, Beresfield and Stockton showing close agreement between all days (left-hand side) and the 1-day-in-3 sampling days (right-hand side)....29

Figure 32: $PM_{2.5}$ pollution roses for $PM_{2.5} > 10$ µg m^{-3} for the study period at Newcastle, Beresfield and Stockton showing close agreement between all days (left-hand side) and the 1-day-in-3 sampling days (right-hand side)....30

Figure 33: Size distribution measured at Liverpool in Sydney during the Australian Fine Particle Study (Keywood, pers. comm.) with size-selective inlet cut-offs for $PM_{2.5}$ and PM_{10}....33

Figure 34: Mass absorption coefficient, ε, as a function of particle diameter at wavelength of 630nm (adapted from Taha et al. 2007). See text for description 37

Figure 35: Time series of 24-hour average $PM_{2.5}$ concentrations from gravimetric analysis of LHPCS samples....41

Figure 36: Time series of 24-hour average $PM_{2.5-10}$ levels from gravimetric analysis of LHPCS samples at Stockton and Mayfield 42

Figure 37: Comparison of $PM_{2.5}$ concentrations measured on the LHPCS filters with the regular results from the OEH Air Quality Monitoring Network using BAM instruments 43

Figure 38: Comparison of PM_{10} concentrations measured on the LHPCS filters with the regular results from the OEH Air Quality Monitoring Network using TEOM instruments 44

Figure 39: Box and whisker plot of the $PM_{2.5}$ species concentrations measured in the year of filter samples from Newcastle 46

Figure 40: Box and whisker plot of the $PM_{2.5-10}$ species concentrations measured in the year of filter samples from Stockton 48

Figure 41: Main components of $PM_{2.5}$ based on the chemical speciation (annual averages) 50

Figure 42: Main components of $PM_{2.5-10}$ based on the chemical speciation (annual averages) 51

Figure 43: Scatter plot of daily $PM_{2.5}$ concentrations from the gravimetric mass determination and the reconstructed mass from the PMF solution 57

Figure 44: Scatter plot of daily $PM_{2.5-10}$ concentrations from the gravimetric mass determination and the reconstructed mass from the PMF solution 58

Figure 45: Scatter plot showing the strong linear relationship between magnesium and sodium concentrations in the LHPCS dataset 59

Figure 46: Scatter plot for $PM_{2.5}$ showing that for a given sodium concentration, the observed chloride concentrations are always lower than for fresh sea salt (Cl^-/Na^+ = 1.80) due to the presence of 'aged' sea salt in the atmosphere for these 24-hour averages 60

Figure 47: Scatter plot for $PM_{2.5-10}$ showing that, unlike for $PM_{2.5}$, there is a strong correlation between chloride and sodium concentration with the ratio (Cl^-/Na^+ = 1.80) matching that for fresh sea salt 60

Figure 48: Scatter plot of sulfate versus sodium in fine and coarse fractions 61

Figure 49: Scatter plot of mannosan versus levoglucosan in the $PM_{2.5}$ measured during the study 62

Figure 50: Scatter plot of titanium versus aluminium in $PM_{2.5}$ and $PM_{2.5-10}$ 63

Figure 51: Scatter plot of silicon versus aluminium in $PM_{2.5}$ and $PM_{2.5-10}$ 63

Figure 52: Scatter plot of nickel versus vanadium in $PM_{2.5}$. 64

Figure 53: Fingerprints and time series plots of $PM_{2.5}$ Factor 1 (fresh sea salt) at the four study sites 66

Figure 54: CPF of $PM_{2.5}$ Factor 1 (fresh sea salt) at the four study sites 67

Figure 55: Variation in annual average $PM_{2.5}$ fresh sea salt concentration with distance from coast 68

Figure 56: Fingerprints and time series plots of $PM_{2.5}$ Factor 2 (pollutant-aged sea salt) for each of the four study sites 69

Figure 57: CPF of $PM_{2.5}$ Factor 2 (pollutant-aged sea salt) at the four study sites 70

Figure 58: Fingerprints and time series plots of $PM_{2.5}$ Factor 3 (secondary ammonium sulfate) at the four study sites....72

Figure 59: CPF of $PM_{2.5}$ Factor 3 (secondary ammonium sulfate) at the four study sites 73

Figure 60: Scatter plot of ammonium versus total sulfate in all $PM_{2.5}$ and $PM_{2.5\text{-}10}$ samples 75

Figure 61: Fingerprints and time series plots of $PM_{2.5}$ Factor 4 (wood smoke) at the four study sites....76

Figure 62: CPF of $PM_{2.5}$ Factor 4 (wood smoke) at the four study sites overlaid on the annual domestic wood heater $PM_{2.5}$ emissions from the Greater Metropolitan Region air emissions inventory for the 2008 calendar year (EPA 2012) 77

Figure 63: Time series of total lead concentrations in samples (not just in this factor) .78

Figure 64: Fingerprints and time series plots of $PM_{2.5}$ Factor 5 (soil) at the four study sites 81

Figure 65: CPF of $PM_{2.5}$ Factor 5 (soil) at the four study sites 82

Figure 66: Fingerprints and time series plots of $PM_{2.5}$ Factor 6 (vehicle) at the four study sites 84

Figure 67: Monthly average nitric oxide (NO) concentrations (top) and seasonal average diurnal trends in NO concentrations (bottom) as measured at Newcastle Air Quality Monitoring Station during the study period 86

Figure 68: CPF of $PM_{2.5}$ Factor 6 (vehicle) at the four study sites overlaid on contour of $PM_{2.5}$ vehicle emissions from the Greater Metropolitan Region air emissions inventory (EPA 2012) 87

Figure 69: Fingerprints and time series plots of $PM_{2.5}$ Factor 7 (secondary sodium nitrate at three sites, primary ammonium nitrate at Stockton)....88

Figure 70: CPF of $PM_{2.5}$ Factor 7 (secondary sodium nitrate at three sites, primary ammonium nitrate at Stockton)....89

Figure 71: Bivariate pollution rose of Factor 7 (ammonium nitrate) contributions (colour scale units µg m^{-3}) versus wind direction and speed (m s^{-1}) for the LHPCS study period....91

Figure 72: Fingerprints and time series plots of $PM_{2.5}$ Factor 8 (mixed shipping/industry) at the four study sites....92

Figure 73: CPF of $PM_{2.5}$ Factor 8 (mixed shipping/industry) at the four study sites....93

Figure 74: CPF contours overlaid on a map of the region with an inset of the geographical distribution of shipping fuel consumed in Newcastle (DNV 2015)..94

Figure 75: Annual $PM_{2.5}$ emissions from shipping for 2010–11 (given in tonnes per 1km grid cell) for the region near Newcastle (provided by Brett Goldsworthy)....95

Figure 76: Fingerprints and time series plots of $PM_{2.5}$ Factor 9 (mixed industry/vehicle) at the four study sites....96

Figure 77: CPF of $PM_{2.5}$ Factor 9 (mixed industry/vehicle) at the four study sites....97

Figure 78: CPF contours overlaid on contour of $PM_{2.5}$ industrial emissions from the Greater Metropolitan Region air emissions inventory 98

Figure 79: Comparison of the factor contributions at each site to annual average $PM_{2.5}$ mass....101

Figure 80: As for Figure 79, but showing values as percentage of annual average $PM_{2.5}$ mass at each site 101

Figure 81: Monthly and annual factor contributions to $PM_{2.5}$ at Newcastle 103

Figure 82: Monthly and annual factor contributions to $PM_{2.5}$ at Beresfield 103

Figure 83: Monthly and annual factor contributions to $PM_{2.5}$ at Mayfield 104

Figure 84: Monthly and annual factor contributions to $PM_{2.5}$ at Stockton 105

Figure 85: Fingerprints, CPF and time series plots of $PM_{2.5\text{-}10}$ Factor 1 (fresh sea salt) 106

Figure 86: Fingerprints, CPF and time series plots of $PM_{2.5\text{-}10}$ Factor 2 (light-absorbing carbon) 108

Figure 87: Fingerprints, CPF and time series plots of $PM_{2.5\text{-}10}$ Factor 3 (pollutant-aged sea salt) 110

Figure 88: Fingerprints, CPF and time series plots of $PM_{2.5\text{-}10}$ Factor 4 (soil) 112

Figure 89: Fingerprints, CPF and time series plots of $PM_{2.5\text{-}10}$ Factor 5 (industry) 114

Figure 90: Fingerprints, CPF and time series plots of $PM_{2.5\text{-}10}$ Factor 6 (bioaerosol) 116

Figure 91: Comparison of the factor contributions at each site to annual average $PM_{2.5\text{-}10}$ mass 119

Figure 92: As for Figure 91, but showing values as percentage of annual average $PM_{2.5\text{-}10}$ mass at each site 119

Figure 93: Monthly and annual factor contributions to $PM_{2.5\text{-}10}$ at Mayfield 120

Figure 94: Monthly and annual factor contributions to $PM_{2.5\text{-}10}$ at Stockton 121

Figure 95: HYSPLIT computed backward trajectories for the 24-hour period ending at 1900 EST (0900 UTC) on 25 April 2014 from Mayfield, Newcastle, Beresfield and Stockton; HYSPLIT initialized with WRF 9km simulations 123

Figure 96: Same as for Figure 95, except HYSPLIT initialised with WRF 3km simulations 123

Figure 97: Surface analyses at (a) 1000 EST and (b) 2200 EST on 25 April 2014 124

Figure 98: HYSPLIT computed backward trajectories for the 24-hour period ending at 1200 EST (0100 UTC) on 18 December 2014 from Mayfield, Newcastle, Beresfield and Stockton; HYSPLIT initialized with WRF 9km simulations 124

Figure 99: Same as for figure above, except HYSPLIT initialised with WRF 3km simulations 125

Figure 100: Surface analyses at (a) 1100 EDT and (b) 2300 EDT on 18 December 2014 125

Figure 101: Diurnal variation in equivalent black carbon measured at Newcastle Air Quality Monitoring Station on 27 July 2014 using a seven wavelength aethalometer 127

Figure 102: $PM_{2.5}$ and ammonia levels recorded at Stockton Air Quality Monitoring Station on 27 July 2014 (based on data from Orica Australia's Fuller Street Stockton station) 128

Figure 103: $PM_{2.5}$ rose for Stockton for 27 July 2014 128

Figure 104: Hourly average $PM_{2.5}$ concentrations measured on 3 November 2014 129

Figure 105: Hourly average wind and $PM_{2.5}$ measured 2 to 3 November 2014 showing the distinct peak in $PM_{2.5}$ (and PM_{10}) levels coinciding with north-easterly winds130

Figure 106: Vegetation fires occurring in the region on 2 and 3 November 2014.....131

Figure 107: HYSPLIT computed backward trajectories for the 24-hour period ending at 1400 EST (0300 UTC) on 2 January 2015 from Mayfield, Newcastle, Beresfield and Stockton. HYSPLIT initialized with WRF 9km simulations 132

Figure 108: Same as for Figure 107, except HYSPLIT initialised with WRF 3km simulations.....133

Figure 109: Surface analyses at (a) 1100 EDT and (b) 2300 EDT on 2 January 2015133

Figure 110: Air quality and wind measurements at Lower Hunter and Newcastle Local air quality monitoring stations at 1300–1400 EST on 2 January 2015 134

Figure 111: Comparison between (left) species composition and (right) PMF factors in $PM_{2.5}$ at the four sites.....137

Figure 112: Time series during the study of the abundance of key species involved in secondary particle formation 139

Figure 113: Scatter plot of $PM_{2.5\text{-}10}$ Factor 2 (light-absorbing carbon) measured at Stockton and Mayfield.....142

Figure 114: Map showing the bearing of 305° (identified in Figure 71) from the Stockton Air Quality Monitoring Station towards Kooragang Island and Orica's prill tower143

Figure 115: Wind roses at Stockton for three distinct periods identified in the ammonium nitrate factor time series trace at the top of the figure.....144

Figure 116: Source contributions to long-term $PM_{2.5}$ concentrations at Mayfield (1998–2013) (after Stelcer et al. 2014).....145

Figure 117: Fingerprints of ANSTO's seven-factor PMF for 2010–15 IBA and BC data showing the contribution of each species to the factor scaled to the largest factor contributing 1.00 147

Figure 118: Percentage of each species in the factors in ANSTO's seven-factor PMF for 2010–15 IBA and BC data.....148

Figure 119: Comparison between (left) the analysis using only the IBA and BC data from the study period and (right) the PMF analysis presented in this report 149

Figure 120: Pie charts of the percentage annual average factor contributions to $PM_{2.5}$ at the study sites. 151

Figure 121: Pie charts of the percentage annual average factor contributions to $PM_{2.5\text{-}10}$ at the two study sites.....154